

SARAH PAULIN



Impact of epicatechin gallate on the structural integrity of the PBP2/PBP2a complex in methicillin resistant *Staphylococcus aureus*

Thesis submitted in accordance with the requirements of the School of Pharmacy, University College London for the degree of Doctor of Philosophy.

Microbiology Group, Department of Pharmaceutics
School of Pharmacy, University College London

June 2014

PLAGIARISM STATEMENT

I, Sarah Paulin confirm that the work presented in this thesis is my own. Where information has been derived from other sources, I confirm that this has been indicated in the thesis.

Signature

Date

ABSTRACT

Introduction: The selective pressure imposed by the misuse and overuse of antibiotics has led to the emergence and dissemination of methicillin resistant *Staphylococcus aureus* (MRSA), forcing a re-evaluation of therapeutic approaches to the treatment of MRSA infections. Epicatechin gallate (ECg), a constituent of the tea plant *Camellia sinensis*, has the capacity to abrogate the resistance of MRSA to β -lactam antibiotics and may be useful as an adjunct to conventional chemotherapy. Current evidence suggests that ECg sensitises resistant strains to β -lactam agents by disruption of the penicillin binding protein (PBP) complex PBP2/PBP2a at the septal site of cell division following its intercalation into the cytoplasmic membrane (CM) bilayer.

Methods: Styrene maleic acid lipid co-polymer (SMALP) was used to solubilise and extract PBP2/PBP2a membrane complexes from the CM of EMRSA-16 and ECg-exposed cells. Cell walls were partially digested and membrane proteins excised and solubilised with hydrolysed styrene maleic acid (SMA). SMALP particles were visualised by TEM and size distribution determined by dynamic light scattering. Membrane protein complexes were cross-linked within SMALPs, protein complexes recovered by co-immunoprecipitation and the constituents determined by Western blotting and flow cytometry.

Results: PBP2/PBP2a complexes were identified in both ECg-exposed and control EMRSA-16 cells when SMALPs were pulled down with anti-PBP2 and anti-PBP2a antibodies. Fewer complexes were recovered from ECg exposed cells. Co-immunoprecipitation of SMALPs with antibody against the division scaffold protein FtsZ led to the identification of FtsZ/PBP2/PBP2a complexes. ECg displaced PBP2a from this complex. The PBP2/PBP4 complex was also identified, however there was no difference observed following ECg exposure.

Conclusion: Intercalation of ECg into the MRSA phospholipid palisade led to partial disruption of PBP2a from PBP2/PBP2a and FtsZ/PBP2/PBP2a complexes. The data suggest that ECg-mediated conversion of MRSA to β -lactam susceptibility may in part be related to loss of functional integrity of the cellular replication machinery. The therapeutic approach with the use of antibiotic resistance modifying agent, such as ECg, in combination with a previously ineffective β -lactam antibiotic, presents a novel therapy to combat antibiotic resistance in MRSA.

ACKNOWLEDGMENTS

I would like to start by thanking my principle supervisor Professor Peter W. Taylor for his supervision and guidance throughout the PhD process and for providing me with the opportunity to undertake this research. I would also like to thank him for all of his help with my thesis writing process. I would also like to thank my second supervisor Professor Stephen Neidle. Next I would like to thank my collaborators, Professor Tim Dafforn, Dr. Mohammed Jamshad, Professor Simon Foster for their support and input throughout the process. I would especially like to thank Mohammed for his help with all parts pertaining to the SMALPs methodology.

I would also like to thank David McCarthy for his help with electron microscopy and all of the rest of the support staff at the UCL School of Pharmacy. Next I would like to send a special thank you to everyone in the Microbiology Lab 218, past and present, for their support, problem solving, teamwork and above all their friendship. This includes Lucia, Christina, Joao, George, Dave, Fatosh, Luci, Alex and all of our Erasmus and Masters Students. And a special thank you goes to Dr. Helena Rosado for her continued help, input and support throughout the process. Without you I would have never ventured into the world of flow cytometry. Obrigada! And I would also like to thank all of my colleagues at the UCL School of Pharmacy and a special thank you to Basma for her amazing friendship and for keeping me sane throughout the PhD process.

And finally I would like to thank my friends and family near and far. To my nearest and dearests: Sally, Aparna, Dani, Nina, Laila, Evi, Najada, Isra, Oriel and Lilla, muchas gracias. And a very special thank you goes to my parents who have supported me throughout my endeavors and who have always believed in me. I would not have made it this far without you. Vielen Dank für eure Unterstützung und Liebe. And of course a big Dankeschön to my siblings Simon and Edda, thank you for everything.

Thank you, Dankeschön, gracias, obrigada!

Sarah Paulin

TABLE OF CONTENTS

1. GENERAL INTRODUCTION	23
1.1 Beginning of the golden era of antimicrobial chemotherapy.....	24
1.2 Antibacterial agents.....	27
1.2.1 Inhibitors of cell wall synthesis	27
1.2.1.1 β -lactams	28
1.2.1.2 Glycopeptides.....	30
1.2.2 Inhibitors of protein synthesis	30
1.2.3 Inhibitors of nucleic acid synthesis	32
1.2.4 Inhibitors of cell membrane function.....	33
1.2.5 Mechanisms of antibiotic resistance	33
1.3 MRSA	35
1.3.1 Epidemiology	36
1.3.2 Infections caused by MRSA.....	38
1.3.3 Pathogenesis.....	39
1.3.4 Cell Division	41
1.3.4.1 PG structure.....	42

1.3.4.2 Division machinery	44
1.3.4.3 PBPs	46
1.3.5 MRSA resistance determinants	48
1.4 Plant-derived alternative therapeutics	50
1.4.1 Green tea and its components	51
1.4.2 Health benefits of green tea.....	52
1.4.2.1 Antioxidant effect of catechins	52
1.4.2.2 Effects on cardiovascular diseases	53
1.4.2.3 Anti-carcinogenic effects of catechins	53
1.4.2.4 Antimicrobial effects of catechins	54
1.5 Effect of ECg on MRSA	54
1.5.1 Effect of ECg on MRSA division proteins	56
1.6 Membrane proteins.....	57
1.6.1 Surfactant-mediated protein extraction	57
1.6.2 Bicelles	58
1.6.3 Amphipols	59

1.6.4 Nanodiscs	59
1.7 Use of SMALPs to solubilise membrane proteins	61
1.8 Aims and Objectives	63
2. ANTIBIOTIC SUSCEPTIBILITY, CELL MORPHOLOGY AND SURFACTANT PROTEIN EXTRACTION	64
2.2 Introduction	65
2.2.1 The PBP2/PBP2a complex.....	65
2.2.2 Use of surfactant to probe for the PBP2/PBP2a complex.....	66
2.3 Material and methods	66
2.3.1 Bacterial strains and reagents.....	66
2.3.2 Growth requirements.....	67
2.3.3 MIC	67
2.3.4 Morphology.....	68
2.3.5 Nascent PG investigation	68
2.3.6 Expression of recombinant PBP2 in <i>E. coli</i> for Ab generation	69
2.3.7 Membrane protein solubilisation with Triton X-100	71
2.3.8 PBP analysis.....	72

2.3.8.1 Cross-linking with 3,3'Dithiobis [sulfosuccinimidylpropionate] (DTSSP) and 1% formaldehyde	72
2.3.8.2 Probing for the PBP2/PBP2a complex.....	73
2.3.9 Detection of proteins with 1D gel electrophoresis.....	74
2.3.10 Western blot	75
2.4 Results	77
2.4.1 Effect of ECg on MRSA	77
2.4.1.1 Sensitisation of MRSA to oxacillin with ECg	77
2.4.1.2 Antibiotic treatment optimisation	78
2.4.1.3 The effect of oxacillin on MRSA morphology	79
2.4.1.4 Impact of ECg on nascent PG synthesis	80
2.4.2 Probing for the PBP2/PBP2a complexes	81
2.4.2.1 Anti-PBP2 and PBP2a Abs	81
2.4.2.2 Surfactant membrane protein solubilisation for detection of PBP2/PBP2a complexes.....	82
2.5 Discussion	84
3. SMALPS: METHOD DEVELOPMENT	88
3.1 Introduction	89

3.1.1 Membrane protein solubilisation	89
3.1.2 Solubilisation of membrane proteins with SMA co-polymer.....	90
3.2 Material and methods	94
3.2.1 Bacterial strains and reagents	94
3.2.2 Cell preparation	94
3.2.2.1 Membranes	94
3.2.2.2 Whole cells.....	94
3.2.2.3 Preparation of hydrolysed SMA.....	95
3.2.2.4 SMALP solubilisation of DMPC lipids	95
3.2.3 Solubilisation of membrane proteins from membranes	95
3.2.4 Solubilisation of membrane proteins from whole cells.....	95
3.2.5 Optimisation steps of SMALPs solubilisation method	96
3.2.6 Optimised SMALPs method	96
3.2.6.1 Tricine SDS-PAGE	96
3.2.7 Imaging of SMALPs	97
3.2.7.1 Transmission electron microscopy (TEM).....	97

3.2.7.2 Scanning electron microscopy	98
3.2.7.3 Confocal fluorescence microscopy	98
3.2.8 Size distribution of SMALPs	98
3.2.8.1 Dynamic light scattering	98
3.2.8.2 Flow cytometry	99
3.3 Results	100
3.3.1 Membrane proteins from protoplasts solubilised in SMALPs	100
3.3.2 Solubilisation of membrane proteins from intact cells	103
3.3.2.1 Enzymatic disruption of the cell wall	104
3.3.2.2 Overnight incubation of SMALPs	110
3.3.2.3 Sonication.....	112
3.3.2.4 The effect of temperature on SMALP development	113
3.3.3 Optimal SMALP conditions.....	116
3.3.3.1 TEM	117
3.3.3.2 Size distribution of SMALPs	119
3.3.3.3 Co-localisation of PBPs	124

3.4 Discussion	126
4. EFFECT OF EXPOSURE TO ECG ON THE PBP2/PBP2A COMPLEX	130
4.1 Introduction	131
4.2 Materials and methods	135
4.2.1 Bacterial strains and reagents	135
4.2.2 Anti-PBP2a polyclonal Ab affinity purification	135
4.2.3 Cross-linking of proteins in SMALPs	135
4.2.4 Protein pull down assays for complex identification	135
4.2.4.1 Ab affinity chromatography	136
4.2.4.2 Co-immunoprecipitation	136
4.2.5 Identification of protein complexes	137
4.2.5.1 1D SDS-PAGE	137
4.2.5.2 Western blotting	138
4.2.5.3 2D gel electrophoresis	138
4.2.5.4 Flow cytometry	139
4.3 Results	140

4.3.1 Protein complexes	141
4.3.1.1 FtsZ/PBP2/PBP2a	141
4.3.1.2 PBP2/PBP2a complexes.....	142
4.3.2 Complex detection by flow cytometry	148
4.4 Discussion	153
5. EFFECT OF EXPOSURE TO ECG ON OTHER PBPS	158
5.1 Introduction	159
5.2 Materials and methods	161
5.2.1 Bacterial strains and reagents.....	161
5.2.2 MICs of PBP inhibition by β -lactam agents	161
5.2.3 Detection of PBP2/PBP4 complexes	161
5.2.4 Analysis of protein complexes with 1D Tricine-SDS-PAGE and Western blotting.....	161
5.3 Results	162
5.4 Discussion	165
6. GENERAL DISCUSSION	167
LIST OF PUBLICATIONS, PRESENTATIONS AND AWARDS	177

Publications	177
Presentations	177
Awards	178
REFERENCES.....	179

LIST OF FIGURES

Figure 1-1 Important milestones in the discovery and development of antibiotics and the emergence of resistance that encompassed the golden era of antibiotic development: focus on <i>S. aureus</i>	25
Figure 1-2 The formation of bacterial cell wall PG showing the sites of cell wall synthesis and the steps inhibited by glycopeptide and β -lactam antibiotics	28
Figure 1-3 Chemical structure of the β -lactam ring and general structure of penicillins, carbapenem and cephalosporins.....	29
Figure 1-4 Inhibitors of protein synthesis	31
Figure 1-5 Gram-positive and Gram-negative cell envelopes	34
Figure 1-6 Virulence factors associated with <i>S. aureus</i> , surface and secreted proteins involved in virulence. A cross section of the envelope shows PBPs involved in replication and antibiotic resistance and β -lactamase (Morell and Balkin, 2010).	39
Figure 1-7 Division in multiple planes; (A) three proscribed planes as seen in <i>S. aureus</i> , leading to clusters of bacteria and (B) two proscribed planes leading to tetrads in <i>Pediococcus</i> (Turner <i>et al.</i> , 2010)	41
Figure 1-8 PG cross-linking in <i>S. aureus</i> . Alternating subunits of GlcNAc (G) and MurNAc (M) cross-linked through a pentaglycine cross-bridge linking stem peptides (Schneider <i>et al.</i> , 2004)	42
Figure 1-9 The cell wall and cytoplasmic membrane of <i>S. aureus</i> that maintain cell integrity	43
Figure 1-10 Proposed proteins of the divisome recruited to the division septum of MRSA during cell division (representation)	44
Figure 1-11 Role of PBPs in cell wall synthesis where they display TGase and TPase activity (Zapun <i>et al.</i> , 2008).....	47
Figure 1-12 Antibiotic resistance mechanisms in MRSA. (A) Decreased binding affinity of PBP2a for β -lactam antibiotics and (B) β -lactamases that hydrolyse antibiotics to an inactive form.....	49
Figure 1-13 Structure of EC, EGC, ECg and EGCg	52

Figure 1-14 (a and b) SEM and (c and d) TEM of control (a and c) EMRSA-16 and (b and d) EMRSA-16 exposed to 12.5 mg/L ECg. EMRSA-16 were grown to mid-logarithmic phase (from Bernal <i>et al.</i> , 2009)	56
Figure 1-15 Protein encapsulation methods produce: (A) bicelles, (B) amphipols and (C) nanodiscs. Lipids bilayer in blue with bicelles, amphipols and nanodisc membrane scaffold proteins in red (from Jamshad <i>et al.</i> , 2011).....	58
Figure 1-16 Styrene/maleic acid co-polymer (Tonge, 2006)	61
Figure 2-1 Cooperative function of PBP2 and PBP2a in the presence of oxacillin. Oxacillin binds to the active site of PBP2 and inhibits TPase activity; PBP2a, with a low affinity for oxacillin, cooperates with the TGase domain of PBP2 to allow continued cell replication	65
Figure 2-2 U-shaped 96 well plate for MIC determination of test antibiotic oxacillin (OXA). In the first column, medium control: 200 μ L MHB was added, control of OXA: 200 μ L of OXA with no bacteria, and in control for bacteria: 100 μ L bacterial solution with 100 μ L of antibiotic at a concentration known to kill the bacteria	67
Figure 2-3 Gene map of plasmid pGL600 with the AmpR resistance gene and PBP2 gene	70
Figure 2-4 Electrophoretic transfer	76
Figure 2-5 Growth of MSSA (BB255) and EMRSA-16 in MHB containing 12.5 mg/L ECg.....	77
Figure 2-6 Viability of mid-logarithmic phase EMRSA-16 after exposure to 4 mg/L oxacillin after 4 hours of growth. Bacteria were either grown in MHB or MHB supplemented with 12.5 mg/L ECg. The red circle indicates the optimal time point for recovery of cells (10 min post-induction)	78
Figure 2-7 SEM of EMRSA-16 cells grown to mid-logarithmic phase (A and B) in the absence or (C and D) presence of 12.5 mg/L ECg either in the (A and C) absence or (B and D) presence of 4 mg/L oxacillin.....	79
Figure 2-8 Localisation of nascent PG (D-Ala-D-Ala) in (A) control and (B) ECg-exposed EMRSA-16 following Van-FL labelling and fluorescence microscopy. Scale bar: 2 μ m	80
Figure 2-9 SDS-PAGE of the first and second elution of PBP2 recovered from <i>E. coli</i> BL21. Positive control of total EMRSA-16 membrane proteins solubilised with triton X-100	81

Figure 2-10 Western blots of MSSA (BB255) and EMRSA-16 total membrane proteins using (A) Bioserv anti-PBP2 Ab or (B) commercially available anti-PBP2a Ab.....	82
Figure 2-11 Anti-PBP2 Ab co-immunoprecipitation of cross-linked EMRSA-16 membrane proteins solubilised with surfactant Triton X-100. Enriched proteins were separated by SDS-PAGE and Western blots probed with (A) anti-PBP2 and (B) anti-PBP2a antiserum. PBP2a was not found complexed with PBP2.....	83
Figure 2-12 SEM of (a) EMRSA-16 and (b) ECg-exposed EMRSA-16 cells grown to mid-log phase (from Bernal <i>et al.</i> , 2009).....	85
Figure 2-13 Fluorescence imaging of GFP-PBP2 localising PBP2 during cell division in RNpPBP2-31. Initially, (A) two spots are visible corresponding to localisation of PBP2 to the ring surrounding the future division site and (B) a border at mid-cell that appears as the septum closes across the disc containing co-localised PBP2; (C) the process continues as daughter cells are formed. Scale bar: 2 μ M (from Pinho and Errington, 2005).....	86
Figure 3-1 Formation of SMALP nanostructure around an integral membrane protein and associated lipids in an environment above pH 6.5	91
Figure 3-2 Cells and/or particles analysed by flow cytometry. Particles pass through the beam of light emitted by the laser and are scattered according to cell size (forward scatter (FSC)) or complexity (side scatter (SSC)). A second parameter, the addition of fluorescent signals, can be detected. Two-parameter dot plots of FSC vs. SSC or fluorescent signal vs. light-scattering parameters can be created from the data. Adapted from abcam, flow cytometry guide	92
Figure 3-3 SDS-PAGE of membrane proteins stained with (A) Coomassie brilliant blue or (B) silver stain. MSSA and EMRSA-16 surfactant-solubilised proteins were separated in the gels along with SMALP-solubilised membrane proteins from EMRSA-16 and ECg-exposed EMRSA-16	100
Figure 3-4 EMRSA-16 and ECg-exposed EMRSA-16 membrane proteins solubilised in SMALPs. Samples were concentrated using 10,000 molecular weight cut-off Vivaspinn columns to 25 mg/mL, samples run on a 0.75 mm and 1.00 mm 10% SDS-PAGE and stained with silver stain.....	101
Figure 3-5 (A) Tricine-SDS-PAGE and (B) Western blot using anti-PBP2 Ab of EMRSA-16 and ECg-exposed EMRSA-16 membrane proteins extracted from protoplasts with SMA. A protein-enriched EMRSA-16 SMALP sample was also examined	102
Figure 3-6 Western blot with (A) anti-PBP2a and (B) anti-FtsZ antiserum of EMRSA-16 and ECg-exposed SMALPs. Arrows indicate proteins of interest. Triton X-100 solubilised EMRSA-16 membrane proteins are also shown.....	103

Figure 3-7 Distribution of the hydrodynamic diameter determined by DLS of SMALPs from (red) EMRSA-16 and (green) ECg-exposed EMRSA-16 SMALPs. Lysostaphin was not employed for this experiment; SMALPs collected by centrifugation**Error! Bookmark not defined.**104

Figure 3-8 (A) Coomassie brilliant blue-stained Tricine-SDS-PAGE of total protein of EMRSA-16 and ECg exposed EMRSA-16 solubilised in SMALPs. Washed cell pellets were suspended in digestion buffer and SMA for 1 h at 37 °C, no lysostaphin. SMALPs were then sonicated and incubated overnight at 37 °C. (B) SMA with and without digestion buffer; Tricine-SDS-PAGE gel stained with Coomassie brilliant blue..... 105

Figure 3-9 Hydrodynamic diameter of SMALPs from (red) EMRSA-16 and (green) ECg-exposed EMRSA-16 determined by DLS; lysostaphin was added to the preparations for 10 min followed by addition of SMA for 50 min..... 106

Figure 3-10 TEM of A-C: low magnification and D-F: high magnification, of (A, D) EMRSA-16 in digestion buffer, (B, E) digested with lysostaphin for 10 min, and (C, F) 50 min after addition of SMA 107

Figure 3-11 TEM (930000x magnification) of an EMRSA-16 cells after 10 min exposure to lysostaphin 107

Figure 3-12 TEM of A-C: low magnification and D-F: high magnification, of ECg-exposed EMRSA-16 cells in (A, D) digestion buffer, (B, E) digested with lysostaphin for 10 min, and (C, F) after addition of SMA and incubation for 50 min 108

Figure 3-13 TEM of A-C: low magnification and D-F: high magnification, of COL (A, D) in digestion buffer, (B, E) digested with lysostaphin for 10 min, and (C, F) after addition of SMA and incubation for 50 min 108

Figure 3-14 TEM (65000x magnification) of an EMRSA-16 after 10 min lysostaphin digestion followed by addition of SMA and incubation for 50 min. Two SMALPs (37.9 nm and 32.8 nm) can be seen 109**Error! Bookmark not defined.**

Figure 3-15 Hydrodynamic diameter, determined by DLS, of SMALPs from EMRSA-16 following (red) concomitant addition of SMA, lysostaphin and DNase1 and incubation for 60 min in comparison to (green) SMALPs obtained by addition of lysostaphin and DNase1 (10 min) followed by addition of SMA and incubation for a further 50 min..... 109

Figure 3-16 Hydrodynamic diameter of EMRSA-16 SMALPs with the (red) presence or (green) absence of 14 - 16 h incubation of SMALPs at 37 °C with agitation prior to collection, measured by DLS 100

Figure 3-17 Hydrodynamic diameter of ECg-exposed EMRSA-16 SMALPs (red) with or (green) without 14-16 h incubation at 37 °C with agitation prior to collection as measured by DLS	111
Figure 3-18 Tricine-SDS-PAGE of total protein from EMRSA-16 and ECg-exposed cells solubilised in SMALPs. Lysostaphin and SMA were added and bacteria incubated for 1 h at 37 °C. SMALPs were then sonicated and either (a) incubated overnight (14 - 16 h) at 37 °C or (b) processed without overnight incubation.....	111
Figure 3-19 Size distribution (hydrodynamic diameter) of EMRSA-16 SMALPs (red) after sonication prior to collection by ultracentrifugation, or (green) without sonication; measured by DLS	112
Figure 3-20 Tricine-SDS-PAGE of total membrane proteins from EMRSA-16 solubilised in SMALPs. Washed cell pellets were suspended in digestion buffer and digested with lysostaphin (10 min) prior to addition of SMA (50 min). Subsequently SMALPs were sonicated or not.....	113
Figure 3-21 The hydrodynamic diameter of EMRSA-16 SMALPs formed at (red) 4 °C and (green) 37 °C before sonication and ultracentrifugation as determined by DLS ...	115
Figure 3-22 Tricine SDS-PAGE of EMRSA-16 and SH1000 membrane proteins solubilised with Triton X-100 or SMA. Proteins were resolved in a 10% Tricine-SDS-PAGE gel	116
Figure 3-23 TEM images of (A) DMPC lipids solubilised within SMALPs and (B) SH1000 (C) EMRSA-16 and (D) ECg exposed EMRSA-16 membrane proteins solubilised in SMALPs	117
Figure 3-24 TEM size distribution of SMALPs of (A) EMRSA-16 membrane protein SMALPs and (B) ECg exposed EMRSA-16 membrane protein SMALPs	118
Figure 3-25 Hydrodynamic diameter of (red) EMRSA-16 and (green) ECg-exposed EMRSA-16 SMALPs; (blue) digestion buffer and (black) SMA, measured by DLS .	119
Figure 3-26 Size distribution (hydrodynamic diameter) of (red) EMRSA-16 and (green) ECg-exposed EMRSA-16 SMALPs; (blue) MRSA COL; (black) ECg-exposed COL determined by DLS. EMRSA-16 and COL SMALPs overlap in a size range from 15 to 45 nm and ECg-exposed SMALPs from 10 to 40 nm	120
Figure 3-27 Size distribution of SMALPs and impact of growth in ECg	120
Figure 3-28 Hydrodynamic diameter of (red) EMRSA-16 and (green) SH1000 SMALPs determined by DLS	121

Figure 3-39 Fluorescence intensity of (red and green) 60 μ M Nile Red-staining for lipids in SMALPs compared to (black) non-fluorescence SMALPs. AU, arbitrary units	122
Figure 3-30 Flow cytometry of (A) EMRSA-16 and (B) ECg-exposed EMRSA-16 SMALPs (labelled with 60 μ M Nile Red); by size (FSC-A) and complexity (SSC-A)122	
Figure 3-31 Change in FSC and SSC values determined by flow cytometry of EMRSA-16 SMALPs following exposure to ECg and incubation with 60 μ M Nile Red for 30 min	123
Figure 3-32 Single parameter histogram of light measurements of SMALP particles by flow cytometry stained with 60 μ M Nile Red. (A) FSC-A and (B) SSC-A measurements of EMRSA-16, EMRSA-16 exposed to ECg and DMPC. (C) FSC-A of EMRSA-16, COL and ECg exposed SMALPs	124
Figure 3-33 Confocal fluorescence microscopy of EMRSA-16 SMALPs labelled with (A and D) bocillin FL and (B and C) Nile Red detecting PBPs and lipid SMALPs. C and F are merged confocal images	125
Figure 3-34 TEM of uranyl acetate stained preparations of (A) DMPC SMALPs (also termed lipodisqs) from Orwick <i>et al.</i> (2012) and (B) SMALPs containing PagP or bR with the insert showing a single SMALP particle (Knowles <i>et al.</i> , 2009)	128
Figure 4-1 Co-immunoprecipitation for protein-protein interactions	132
Figure 4-2 Gel mapping of PBP2, PBP2a, PBP2/PBP2a complexes and multi-protein complexes.....	133
Figure 4-3 Predicted Western blots for individual or complexed proteins captured by SMALPs and purified by co-immunoprecipitation.....	134
Figure 4-4 Detection in SMALPs of PBP2a and PBP2 from EMRSA-16 after growth in ECg.....	140
Figure 4-5 (A) Western blot and (B) schematic of the anti-FtsZ affinity chromatography eluent showing the presence of FtsZ/PBP2/PBP2a and FtsZ/PBP2 complexes in EMRSA-16 and ECg exposed SMALPs	141
Figure 4-6 (A) Tricine-SDS-PAGE (silver stain) and (B) anti-FtsZ Ab Western blot of purified FtsZ from EMRSA-16 SMALPs; chemical cross-linking is compared to the conventional methodology	142

Figure 4-7 Western blot detection of PBP2 and PBP2a interacting proteins following affinity chromatography with (A) anti-PBP2 and (B) anti-PBP2a Ab. The PBP2/PBP2a complexes were detected in EMRSA-16 SMALPs 143

Figure 4-8 Western blot of affinity chromatography eluents from assays utilising (A) anti-PBP2 and (B) -PBP2a Ab. PBP2/PBP2a complexes were observed in EMRSA-16 SMALPs..... 144

Figure 4-9 Detection of PBP2 in Western blots from co-immunoprecipitation eluents with anti-PBP2 Ab (A) super signal West pico chemiluminescence or (B) TMB detection 144**Error! Bookmark not defined.**

Figure 4-10 Western blots employing (A) anti-PBP2a and (B) anti PBP2 Ab of co-immunoprecipitation eluents from SMALPs recovered with anti-PBP2 and -PBP2 Abs. Protein bands detected by chemiluminescence 145

Figure 4-11 Detection of PBP2 and PBP2a in EMRSA-16 and ECg-exposed EMRSA-16 SMALPs following co-immunoprecipitation with anti-PBP2 and -PBP2a Ab. Protein bands detected by chemiluminescence..... 146

Figure 4-12 Western blots with anti- (A) PBP2 and (B) PBP2a Ab of SMALPs from COL and ECg-exposed COL co-immunoprecipitation eluents using anti-PBP2 and anti-PBP2a Ab. Samples were run on a Tricine-SDS-PAGE under native conditions. The PBP2/PBP2a complex was detected in COL and ECg-exposed COL SMALPs 147

Figure 4-13 Western blots with polyclonal (A) anti-PBP2a and (B) anti-PBP2 Ab of co-immunoprecipitation eluents from EMRSA-16 SMALPs. Protein bands detected with chemiluminescence 148

Figure 4-14 Flow cytometry for detection of PBP2/PBP2a complexes after co-immunoprecipitation of SMALPs with (A) anti-PBP2a or (B) anti-PBP2 Abs. Eluent was labelled with (A) anti-PBP2 or (B) anti-PBP2 Ab and a fluorescent secondary Ab. The eluent was gated for 20,000 Nile Red events and the fluorescence intensity of the secondary Ab conjugated to FITC measured (AU)..... 149

Figure 4-15 Co-immunoprecipitation eluents of SMALPs obtained from (A) EMRSA-16 and (C) ECg-exposed EMRSA-16 by precipitation with anti-PBP2a Ab were gated for 20,000 Nile Red events and (E) the FSC change determined. After fluorescence labelling of the partner protein in the complex (PBP2) with secondary FITC conjugated Ab, the fluorescence intensity was determined for SMALPs from (B) EMRSA-16 and (D) ECg-exposed EMRSA-16. Changes in fluorescence intensity are shown (G & H). F shows the fluorescence intensity of Nile Red labelled SMALPs. Values in AU..... 150

Figure 4-16 Co-immunoprecipitation eluents of SMALPs from (A) EMRSA-16 and (C) ECg-exposed EMRSA-16 SMALPs after purification with anti-PBP2 Ab were gated for 20,000 Nile Red events and (E) FSC changes determined. After fluorescence labelling

of the partner protein in the complex (PBP2a) with secondary FITC conjugated Ab, the fluorescence intensity of FITC was determined for (B) EMRSA-16 and (D) ECg-exposed EMRSA-16. Changes in fluorescence intensity are shown (G & H). F shows the fluorescence intensity of Nile Red labelled SMALPs. Values in AU..... 151

Figure 5-1 Western blot of protein expression of (A) PBP2 and (B) PBP4 by EMRSA-16 and ECg-exposed cells 163

Figure 5-2 Detection of PBP2/PBP4 complexes by Western blot with (A) anti-PBP2 and (B) anti-PBP4 Ab using co-immunoprecipitation (affinity ligand: anti-PBP2 Ab) eluent of EMRSA-16 and ECg SMALPs. Proteins detected by chemiluminescence... 164

Figure 6-1 Proportion of MRSA cases in EU/EEU countries in 2012 surveyed by the European Antimicrobial Resistance Surveillance Network (EARS-Net)..... 171

Figure 6-2 Modulation of bacterial resistance phenotype by natural products. A) Classic scenario selecting for antibiotic resistant bacteria as a consequence of treatment with antibiotics. B) Novel therapeutic approach using natural products to modulate the resistance phenotype, resulting in ‘less fit’ bacteria that are cleared by the host or become susceptible to previously ineffective antibiotics..... 173

Figure 6-3 Structures of (-)-ECg, (-)-EGCg and analogues 1-6 synthesised by Anderson *et al.* (2011) 175

LIST OF TABLES

Table 1-1 Advantages and disadvantages of membrane protein solubilisation studies .	60
Table 2-1 MICs of oxacillin against EMRSA-16 ^a	78
Table 3-1 Components of Tricine-SDS-PAGE for one gel.....	97
Table 3-2 Optimisation of the SMALPs procedure for solubilisation of MRSA membrane proteins	115
Table 4-1 Changes in fluorescence intensity (AU) of PBP2 and PBP2a after exposure of EMRSA-16 to ECg, co-immunoprecipitation and flow cytometry.....	152
Table 5-1 EMRSA-16 MICs of four β -lactam agents with selective binding to PBPs 1-4	162

ABBREVIATIONS

~	approximate
°C	degree Celsius
µg	microgram
µL	microliter
µM	micromolar
<i>agr</i>	accessory gene regulator
ATCC	American type culture collection
bR	bacteriodopsin
BCA	Bicinchoninic acid
BSA	bovine serum albumine
<i>B. subtilis</i>	<i>Bacillus subtilis</i>
CA-MRSA	community acquired methicillin resistant <i>Staphylococcus aureus</i>
CC	clonal complex
CDC	Centre for Disease Control and Prevention
CFU	colony forming units
Cg	catechin gallate
CHAPS	3-[(3-Cholamidopropyl)dimethylammonio]-1-propanesulfonate
Clf	clumping factor
CMC	critical micelle concentration
CNA	collagen-binding protein
D-Ala	D-Alanine
D-Lac	D-Lactate
DLS	dynamic light scattering
DMPC	1,2-dimyristoyl-sn-glycero-3-phosphocholine
DNA	deoxyribonucleic acid
DTSSP	3,3'-dithiobis [sulfosuccinimidylpropionate]
DSP	dithiobis [succinimidylpropionate]
EARS-Net	European Antimicrobial Resistance Surveillance Network
EC	epicatechin
ECDC	European Centre for Disease Control
ECg	epicatechin gallate
ECM	extra cellular matrix
<i>E. coli</i>	<i>Escherichia coli</i>

EDTA	ethylenediamine tetraacetic acid
EEA	European Economic Union
EGC	epigallocatechin
EGCg	epigallocatechin gallate
EM	electron microscope
EMRSA	epidemic methicillin resistant <i>Staphylococcus aureus</i>
EU	European Union
FITC	fluorescein-isothiocyanate
FL	fluorescent
FnBP	fibronectin-binding protein
FY	fiscal year
<i>g</i>	gravitational force
GBP	Great British Pound
GCg	gallocatechin gallate
GlcNAc	<i>N</i> -acetylglucosamine
Gly	glycine
h	hour
HA-MRSA	hospital acquired methicillin resistant <i>Staphylococcus aureus</i>
HMW	high molecular weight
HRP	horseradish peroxidase
I	current
IPTG	isopropyl- β -D-thiogalactopyranoside
L	litre
L-Ala	L-Alanine
LMW	low molecular weight
M	molar
MDR	multidrug resistant
MHA	Mueller-Hinton agar
MHB	Mueller-Hinton broth
MIC	minimum inhibitory concentration
min	minute
mL	millilitre
mM	millimolar
MLST	multilocus sequence type
MPS	membrane scaffold protein

mRNA	messenger ribonucleic acid
MRSA	methicillin resistant <i>Staphylococcus aureus</i>
MSCRAMM	microbial surface components recognizing adhesive matrix molecule
MSF	membrane scaffold protein
MSSA	methicillin sensitive <i>Staphylococcus aureus</i>
<i>M. tuberculosis</i>	<i>Mycobacterium tuberculosis</i>
MurNAc	N-acetylmuramic acid
mW	molecular weight
NaCl	sodium chloride
NAG	N-acetylglucosamine
NAM	N-acetylmuramic acid
nm	nanometre
NMR	nuclear magnetic resonance
NTCC	national collection of type culture
OD	optical density
OXA	oxacillin
PBP	penicillin binding protein
PBS	phosphate buffered saline
PFGE	pulsed-field gel electrophoresis
PG	peptidoglycan
PVDF	polyvinylidene difluoride
PVL	Paton-Valentine leukocidin
R	resistance
RFUCMS	Royal Free University College Medical School
RNA	ribonucleic acid
rpm	rounds per minute
rRNA	ribosomal ribonucleic acid
RT	room temperature
s	second
SAg	superantigen
<i>S. aureus</i>	<i>Staphylococcus aureus</i>
<i>S. epidermidis</i>	<i>Staphylococcus epidermidis</i>
<i>S. sciuri</i>	<i>Staphylococcus sciuri</i>
SCCmec	staphylococcal cassette chromosome <i>mec</i>
SDS-PAGE	sodium dodecyl sulphate-polyacrylamide gel electrophoresis

SEM	scanning electron microscopy
SERAM	secretable expanded repertoire adhesive molecule
SMA	styrene maleic acid
SMALP	styrene maleic acid lipid co-polymer
spA	<i>Staphylococcus aureus</i> protein A
ST	sequence type
TBST	tris buffered saline with tween 20
TEM	transmission electron microscopy
TGase	transglycosylase
TMB	3,3',5,5'-tetramethylbenzidine
TPase	transpeptidase
tRNA	transfer ribonucleic acid
TSST-1	toxic shock syndrome toxin-1
UDP	uridine diphosphate
UK	United Kingdom
USA	United States of America
V	volt
Vo	voltage
VISA	vancomycin intermediate <i>Staphylococcus aureus</i>
VRSA	vancomycin resistant <i>Staphylococcus aureus</i>
WHO	World Health Organization
WTA	wall teichoic acid

CHAPTER ONE

1. GENERAL INTRODUCTION

Bacteria have existed for over 3.8 billion years. Over this time they have been involved in an evolutionary arms race with other forms of life in order to compete for the resources which they require to survive and replicate (Bush *et al.*, 2011). The development of resistance mechanisms that allow bacteria to survive the effects of bioactive molecules produced by fungi, plants and other microorganisms is an important aspect of this evolutionary process. For approximately seventy years, mankind has been playing a direct role in this process through the widespread use of antimicrobial chemotherapy. This has dramatically reduced the burden of bacterial disease in the human population; however, many clinically important bacterial species have adapted to this selective pressure by evolving resistance to antimicrobial agents. Understanding the mechanisms that underpin this resistance and finding new ways to overcome them is crucial if we are to maintain our ability to combat bacterial disease.

1.1 Beginning of the golden era of antimicrobial chemotherapy

The antimicrobial era began in 1904 with Paul Ehrlich who discovered that a dye, trypan red, was effective in the treatment of mice infected with African trypanosomes however resistance quickly developed (Ehrlich and Shiga, 1904). In 1905 he moved onto aminophenyl arscenic acid with the commercial name of atoxyl as a therapeutic agent against the parasite *Trypanosoma brucei*, which causes African sleeping sickness. In 1908 Ehrlich, together with the Japanese scientist Sahachiro Hata, successfully tested the arsenic-containing substance arsphenamine against syphilis. This became known as the ‘magic bullet’ for the treatment of syphilis under the trade name Salvarsan (Abraham, 1948). It was not until the 1920s that the first naturally occurring antibiotic was discovered.

Antibiotics, translated from Greek to mean ‘against life’, are naturally occurring low-molecular weight microbial products that are able to inhibit the growth of susceptible bacteria at low concentrations (Lancini *et al.*, 1995; Willey *et al.*, 2008). Alexander Fleming discovered penicillin, a naturally occurring antibiotic produced by the fungus *Penicillium notatum*, in 1928 (Fleming, 1929). Fleming noticed a zone of inhibition on an old Petri dish of *Staphylococcus aureus* (*S. aureus*) caused by the accidental growth of the fungus on the plate and concluded that the substance had antibacterial properties,

however he was not able to purify the active substance (Fleming, 1929). More than ten years later a research group at Oxford University headed by Howard Florey and Ernst Chain successfully purified penicillin with the help of the biochemist Norman Heatley (Abraham and Chain, 1940; Abraham *et al.*, 1941). In 1945 Florey, Chain and Fleming won the Nobel Prize for the discovery of penicillin (Nobelprize.org, 2013). These findings, together with the discovery of sulphonamides by Gerhard Domagk from a red dye synthesised by Bayer AG and streptomycin from *Streptomyces griseus* by Selman Waksman, began the golden age of antibiotics along with the subsequent rise in antibiotic resistance (Clardy *et al.*, 2009).

A chronology of the introduction of new antibiotic classes in the golden era and the emergence of resistance is depicted in figure 1-1. Following the development of the early antibiotics, the 1950s saw a surge in the discovery and clinical application of antibacterial agents. Tetracyclines, chloramphenicol, aminoglycosides (neomycin and kanamycin), erythromycin, vancomycin, cephalosporin and rifamycin were all produced during this period (Hopwood, 2007). Unfortunately, the rate of discovery of new antibiotics did not continue into the 1960s; for example, carbapenems were not discovered until the 1970s (Kahan *et al.*, 1979).

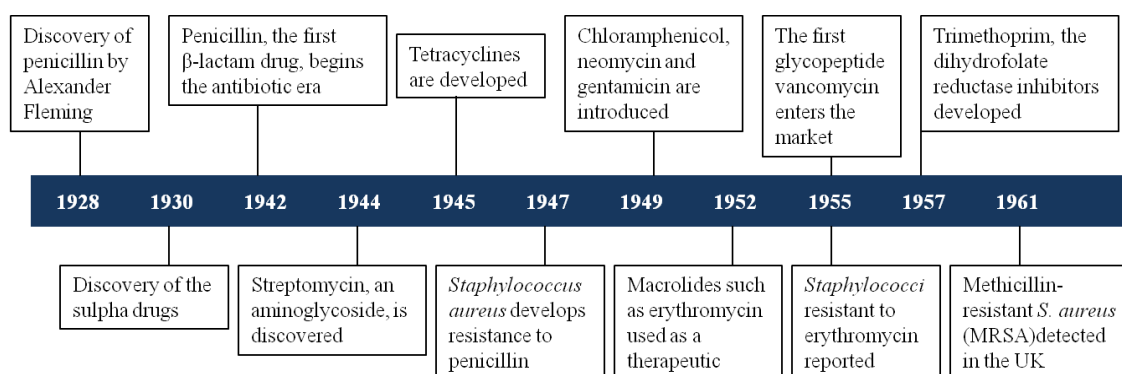


Figure 1-1 Important milestones in the discovery and development of antibiotics and the emergence of resistance that encompassed the golden era of antibiotic development: focus on *S. aureus*

Following these discoveries, new antibiotics brought to market were primarily semi-synthetic derivatives of previous antibiotics as well as the introduction of wholly synthetic quinolones in 1962 (Leshner *et al.*). During more recent phases of antibacterial drug discovery, pharmaceutical companies diverted their efforts from natural product

screening to synthetic chemistry and target driven screening with a relatively poor output compared to the golden years (Hopwood, 2007).

The discovery and use of antibiotics and antibacterial agents went hand in hand with the development and rise in bacterial resistance mechanisms to the major classes of antibiotics. In 1940, prior to the introduction of penicillin as a therapeutic agent, a bacterial enzyme able to degrade penicillin (penicillinase) was identified (Abraham and Chain, 1940). The discovery of this resistance determinant before the therapeutic application of antibiotics set the scene for the subsequent co-evolution of antibiotics and the bacterial resistance mechanisms (Davies and Davies, 2010). Resistance of *S. aureus* to penicillin was observed in 1947 and later to erythromycin in 1955 following the introduction of erythromycin only three years earlier (Spink and Ferris, 1947; Maccabe and Gould, 1956). Similar trends were seen with other bacteria-drug combinations, such as the spread of penicillin resistant *Neisseria gonorrhoea* that began in 1967 and with penicillin-resistant *Enterococcus faecium* from 1983 onwards. The spread of drug-resistant pathogens has accelerated over time with essential medicines failing to treat basic infections and the pool of effective therapeutics rapidly shrinking. Today, many epidemic-associated human bacterial pathogens have become multidrug resistant (MDR), for example MDR *Mycobacterium tuberculosis* and methicillin resistant *S. aureus* (MRSA), due to the widespread use and misuse of antibiotics (Davies and Davies, 2010). In 2011, the importance of addressing antibiotic resistance was highlighted by the World Health Organization (WHO), with World Health Day focusing on combating drug resistance (WHO, 2011). The organization emphasised that the production of new antibiotics has failed to keep up with the spread of resistance and the world may be heading towards a post-antibiotic era.

“At the time of multiple calamities in the world, we cannot allow the loss of essential medicines – essential cures for many millions of people – to become the next global crisis” (WHO, 2011).

The importance and value of antibiotics cannot be underestimated: there is an urgent need to control the spread of antibiotic resistance and find new methods of treatment. These include the development of new antibiotics and the robust evaluation of new therapeutic modalities such as the application of agents that reduce the capacity of

pathogens to express antibiotic resistance genes or virulence effectors during the course of infection. In order for this to happen we must first understand the basic mechanisms of action behind conventional antibiotics as well as bacterial resistance mechanisms.

1.2 Antibacterial agents

Antibacterial agents can be classified into five classes dependent on their primary site of action; cell wall synthesis, protein synthesis, nucleic acid synthesis, metabolic pathways and cell membrane function (Goering *et al.*, 2013). Bacterial susceptibility to low antibiotic concentrations is governed by a limited number of factors. Firstly, the target must be essential for bacterial viability or replication. Secondly, the target must be accessible to the antibiotic molecule. Lastly, the antibiotic must be able to reach the target without being inactivated or degraded. Resistance occurs when one or more of these factors is compromised (Goering *et al.*, 2013).

1.2.1 Inhibitors of cell wall synthesis

The bacterial cell wall represents an ideal target for antibacterial drugs by interfering with cell wall biosynthesis or integrity. The peptidoglycan (PG) of bacterial cell walls are unique structures and thus drugs acting against this macromolecule can exhibit a high target specificity and favourable therapeutic index (Bush, 2013). PG is composed of covalently cross-linked units of N-acetylglucosamine (NAM) and N-acetylmuramic acid (NAG) (Figure 1-2) (Worke, 1957). The synthesis of PG involves multiple steps from synthesis of cell wall precursors in the cytoplasm to the production of new cell wall subunits attached to lipid carriers in the cytoplasmic membrane and finally the attachment of the new cell wall units to the growing PG chain (Goering *et al.*, 2013). The two major classes of cell wall synthesis inhibitors are β -lactams agents and glycopeptides which act on different steps of PG synthesis (Goering *et al.*, 2013). β -lactams are able to acylate the transpeptidase (TPase) (cross-linking) site of the enzymes that catalyse the links between the PG precursor subunits whereas glycopeptides bind to the D-Alanine-D-Alanine (D-Ala-D-Ala) terminus of the PG precursors, preventing incorporation of further PG subunits (Figure 1-2).

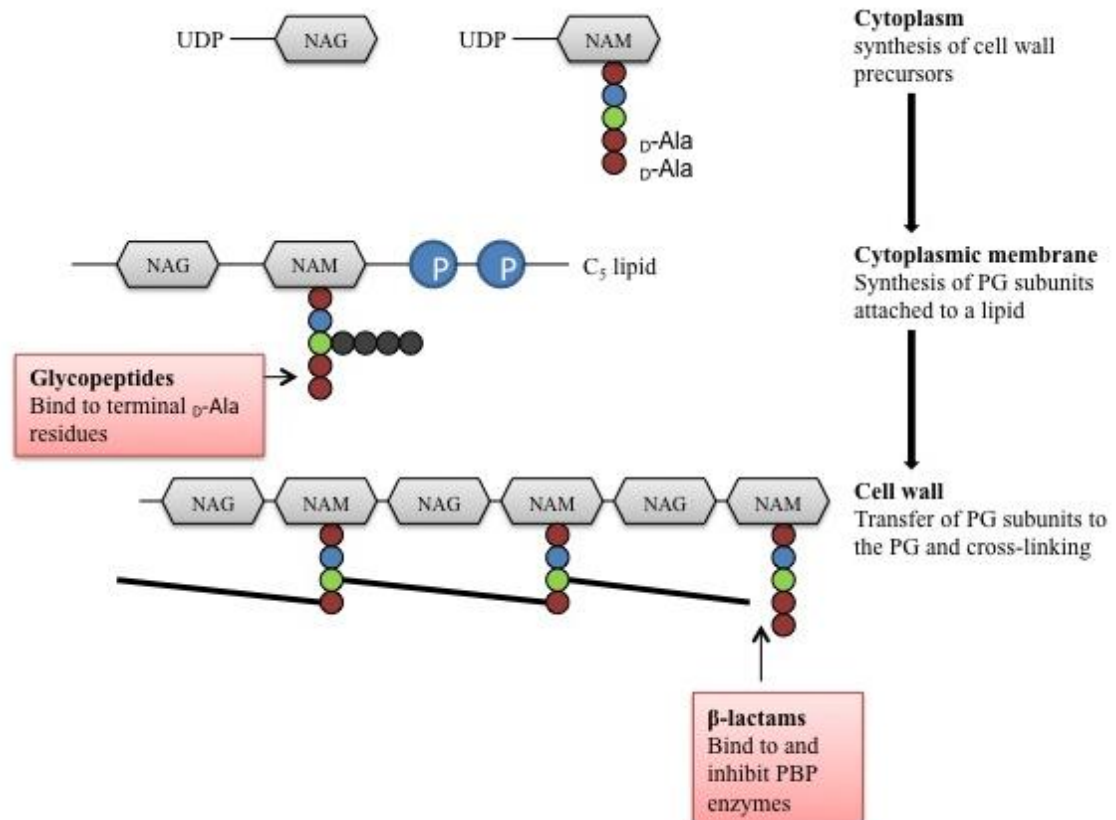


Figure 1-2 The formation of bacterial cell wall PG showing the sites of cell wall synthesis and the steps inhibited by glycopeptide and β-lactam antibiotics

1.2.1.1 β-lactams

The β-lactam antibiotic class consists of a range of natural, semi-synthetic and synthetic molecules that have been developed over the last 40 to 60 years (Llarrull *et al.*, 2010). They consist primarily of penicillins, cephalosporins, and carbapenems that target the penicillin binding proteins (PBPs) that control the final step of PG synthesis (Drawz and Bonomo, 2010). β-lactam antibacterial activity stems from their structural analogy to D-Ala-D-Ala, the natural substrate of the PBPs (Chambers, 2003). β-lactams such as penicillin, oxacillin and methicillin acylate the TPase active site of the PBPs, blocking their interaction with D-Ala-D-Ala (Goffin and Ghuysen, 1998). Initially, the β-lactam antibiotic (or D-Ala-D-Ala) associates non-covalently with the PBPs to form a Michaelis complex (Chambers, 2003). Subsequently, the complex can either dissociate or go through an irreversible acylation reaction where the PBP covalently binds to the β-lactam antibiotic, causing cleavage of the cyclic amide bond in the β-lactam ring and causing rapid deacylation of the cell wall substrate (Goffin and Ghuysen, 1998; Reynolds, 1989). Penicillins, cephalosporins, and carbapenems all feature a β-lactam

ring (Figure 1-3), which is a cyclic amide formed of a four atom ring (Greenwood *et al.*, 2007b).

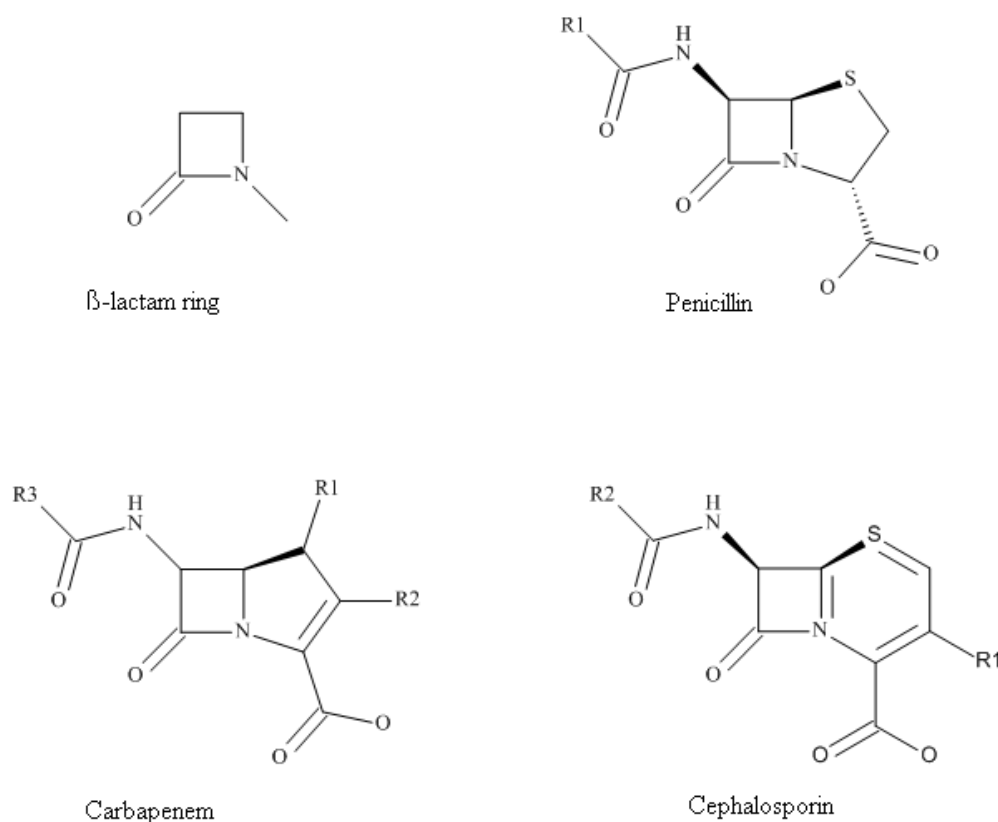


Figure 1-3 Chemical structure of the β -lactam ring and general structure of penicillins, carbapenem and cephalosporins

Penicillins and carbapenems can be distinguished from cephalosporins by the ring attached to the β -lactam ring. This is a five-atom ring in penicillins and carbapenems and a six-atom ring in cephalosporins. Most derivatives of β -lactam agents currently in use were obtained by chemical modification of the lateral chain at position 6 of penicillins and position 7 of cephalosporins (Lancini *et al.*, 1995). The first β -lactams developed, typified by penicillin G, were limited to the treatment of infections caused by Gram-positive bacteria; however, later semi-synthetic penicillins and cephalosporins such as cephalosporin C were designed to be active against Gram-negative bacteria, including *Enterobacter* and *Klebsiella* strains (Lancini *et al.*, 1995; Goering *et al.*, 2013). Cephalosporins in general have a broader spectrum of activity than penicillins but they lack activity against enterococci. Clavulanic acid, a naturally occurring β -lactam with no intrinsic antibacterial activity from *Streptomyces clavuligerus*, can be given in combination with β -lactams to render β -lactam antibiotics to be effective

against some β -lactamase producing bacteria due to its capacity to acylate the TPase active site (Wise *et al.*, 1978); β -lactamases are enzymes that inactivate β -lactam antibiotics by hydrolysing the β -lactam ring (Kelly *et al.*, 1986). Novel β -lactams including cabapenems such as ampicillin exhibit broad spectrum activity against both Gram-positive and Gram-negative bacteria as well as being relatively stable to most β -lactamases (Sutherland and Rolinson, 1964; Greenwood *et al.*, 2007a).

1.2.1.2 Glycopeptides

In contrast to β -lactam agents, glycopeptide antibiotics bind with high affinity to the D-Ala-D-Ala terminus of the extracellular precursor PG (Figure 1-2), resulting in steric hindrance of the PBP-substrate reaction (Reynolds, 1989). This activity inhibits transglycosylation and prevents incorporation of new PG subunits (Goering *et al.*, 2013). The principal glycopeptides vancomycin and teicoplanin are large, complex structures that are mainly active against Gram-positive bacteria, as their large size restricts their capacity to penetrate the outer membrane of most Gram-negative bacteria (Denyer *et al.*, 2011). Vancomycin was introduced in 1959 and is still widely used to treat MRSA infections as well as exhibiting activity against other Gram-positive bacterial species such as *S. epidermidis*, *Clostridium difficile* and *Enterococcus faecalis* (Geraci and Hermans, 1983). Teicoplanin was introduced into the market in the early 1990s and differs from vancomycin in that it possesses additional fatty acid side chains resulting in a more hydrophobic nature and thus able to penetrate tissue further compared to vancomycin (Williams and Grüneberg, 1984).

1.2.2 Inhibitors of protein synthesis

Selective toxicity of antibacterial agents that target protein synthesis is possible due to structural differences between eukaryotic (80S) and prokaryotic (70S) ribosomes (Goering *et al.*, 2013). Mechanisms of action include binding to the 30S (small) or 50S (large) ribosomal subunit as well as inhibition of some critical stages of protein synthesis, such as amino-acyl transfer ribonucleic acid (tRNA) binding, peptide bond formation, messenger RNA (mRNA) translation and translocation (Figure 1-4).

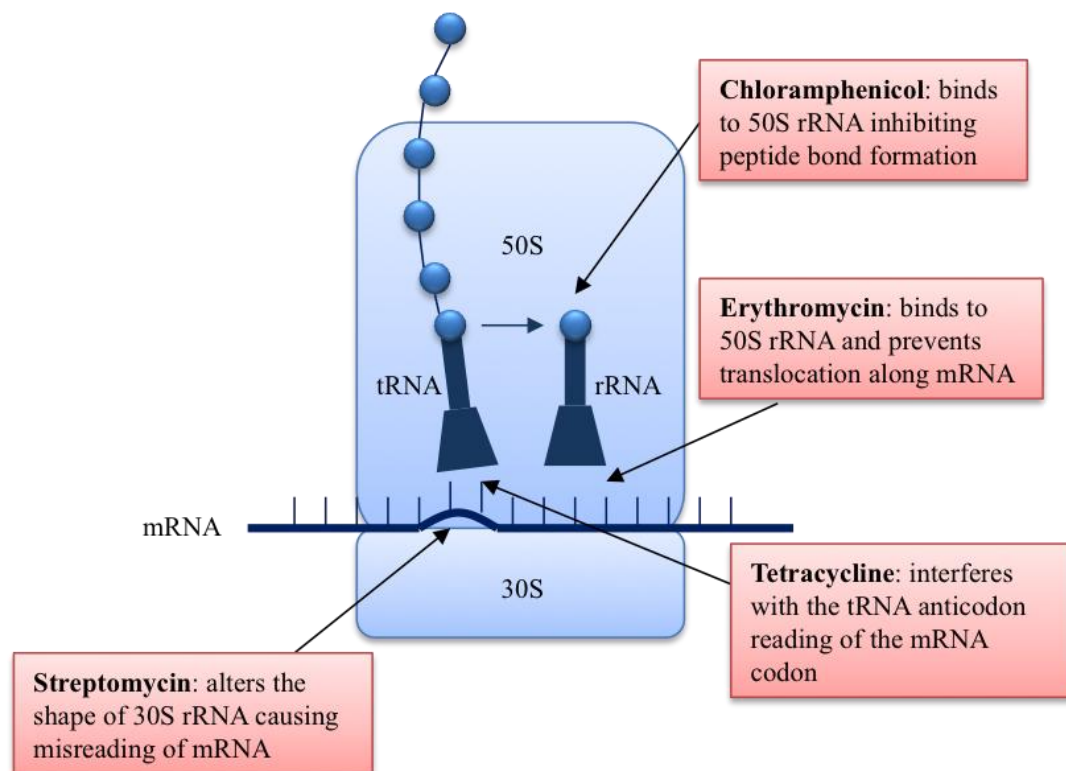


Figure 1-4 Inhibitors of protein synthesis

The main inhibitors of proteins synthesis include aminoglycosides, chloramphenicol, tetracyclines, lincosamides, macrolides, streptogramins, oxazolidinones, mupirocin and fusidic acid (Greenwood *et al.*, 2007a). The first aminoglycoside discovered was streptomycin in 1943 and in general aminoglycosides are potent, broad spectrum bactericidal agents that have activity against most Gram-negative bacilli and staphylococci (Schatz *et al.*, 1944). They inhibit the formation of the ribosomal initiation complex by altering the shape of the 30S ribosomal ribonucleic acid (rRNA) as well as causing misreading of the mRNA (Luzzatto *et al.*, 1968). Tetracyclines have broad spectrum bacteriostatic activity against most Gram-positive and Gram-negative bacteria by preventing the binding of tRNA to the ribosome (Figure 1-4) (Chopra, 1985).

Chloramphenicol is the sole member of a third group of protein synthesis inhibitors and possess broad spectrum bactericidal activity against Gram-positive and Gram-negative bacteria (Greenwood *et al.*, 2007a). This antibiotic inhibits peptidyl transferase activity, preventing peptide bond formation (Hahn *et al.*, 1954). The first macrolide (represented by erythromycin) was discovered in 1952; they were initially reserved for treatment of staphylococcal infections when resistance to penicillin was increasing (Hobson, 1954,

Greenwood *et al.*, 2007a). Macrolides inhibit the binding of rRNA to the ribosome preventing translocation and have strong activity against staphylococci and streptococci (Schmid, 1971).

1.2.3 Inhibitors of nucleic acid synthesis

Another class of antibacterial agents, comprised mainly of synthetic compounds, inhibit nucleic acid synthesis, either indirectly by interruption of metabolic pathways leading to nucleic acid synthesis or directly by inhibition of deoxyribonucleic acid (DNA) or RNA synthesis by interfering with the action of DNA polymerase, DNA helicase or RNA polymerase (Greenwood *et al.*, 2007b). Sulphonamides and diaminopyrimidines affect DNA synthesis by inhibiting folic acid metabolism, which is essential for the one-carbon transfers involved in nucleotide synthesis. Sulphonamides directly block an early stage of folate synthesis leading to a failure to synthesise purine nucleotides (adenine and guanine) and thymidine (McCullough and Maren, 1973; Willey *et al.*, 2008). They are broad spectrum, primarily bacteriostatic agents that inhibit growth slowly because they gradually deplete folate (Greenwood *et al.*, 2007a). Diaminopyrimidines inhibit dihydrofolate reductase, an enzyme that reduces dihydrofolate to tetrahydrofolate (Baccanari and Kuyper, 1993). Sulphonamides and trimethoprim, the most important diaminopyrimidine, are often given in combination as they act at different points of the same metabolic pathway (Reeves, 1982). Another family of antibacterial agents that inhibit nucleic acid synthesis are the quinolones. The first quinolone, nalidixic acid, was introduced in 1962 for use in treating uncomplicated urinary tract infections (Leshner *et al.*, 1962). Quinolones are bactericidal and act by inhibiting bacterial DNA gyrase and topoisomerase II, two enzymes involved in maintaining the integrity of the supercoiled DNA helix during replication and transcription (Hooper, 1993). DNA gyrase introduces a negative twist in the DNA helix to effect separation of the strands and the topoisomerase II untangles DNA further during replication (Willey *et al.*, 2008). Other nucleic acid inhibitors include nitroimidazoles, which causes DNA strand breakage (Edwards, 1980), novobycin, which acts on the β subunit of the DNA gyrase (Sugino *et al.*, 1978), and rifamycins, which inhibit transcription from RNA to DNA by binding to the β subunit of RNA polymerase (Floss and Yu, 2005). Inhibitors of nucleic acid synthesis are not as selective as previous antibiotic groups due to the fact that prokaryotes and eukaryotes do not differ in their nucleic acid synthesis pathways

however they are still selective due to the difference in the subunit structure of the RNA polymerase (Willey *et al.*, 2008)

1.2.4 Inhibitors of cell membrane function

Cell membrane integrity is vital for cell survival and thus inhibitors of cell membrane function are highly toxic. Polymyxins act as cationic detergents by binding to the cell membrane to elicit disruption of the phospholipid cell membrane and consequent leakage of cytoplasmic contents (Newton, 1956). Polymyxin B and polymyxin E (colistin) show potent activity against Gram-negative bacteria and are primarily used to treat pseudomonas infections (Tam *et al.*, 2005; Michalopoulos and Falagas, 2008). Another class of semi-synthetic compounds that inhibit membrane function are the bactericidal lipopeptides. One example is daptomycin which is used in the treatment of MDR Gram-positive cocci such as vancomycin resistant *Enterococcus faecalis* and *E. faecium* as well as MRSA and *S. epidermidis* (Carpenter and Chambers, 2004). The bactericidal effect of daptomycin is thought to be due to the insertion of lipophilic daptomycin tails into the membrane causing membrane depolarisation and potassium ion efflux. This eventually results in the inhibition of DNA, RNA and protein synthesis leading to cell death (Steenbergen *et al.*, 2005).

The important factors for antibiotic susceptibility are a vital and accessible target for the antibacterial agent to be effective at low concentration without being inactivated prior to reaching the target. Antibiotic resistance occurs when one or more of these factors are compromised (Greenwood *et al.*, 2007a). Some bacteria, such as MRSA, have become resistant to multiple classes of antibacterial agents and are classified as MDR; treatment of infections due to these pathogens is a major cause for concern (Tenover, 2006).

1.2.5 Mechanisms of antibiotic resistance

Bacterial resistance to any antibiotic is partly determined by the structure of the bacterial cell envelope. The dual membrane structure of the Gram-negative cell envelope is more complex than the envelope of Gram-positive bacteria (Figure 1-5) (Glauert and Thornley, 1969).

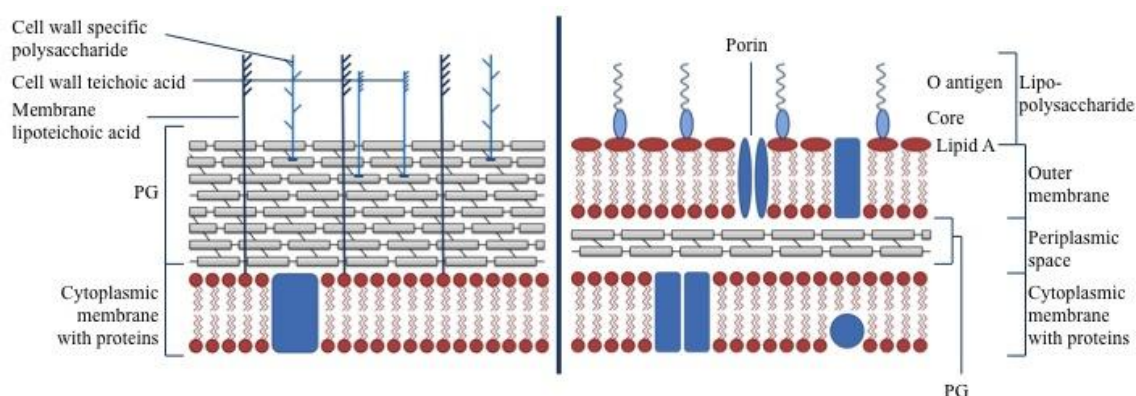


Figure 1-5 Gram-positive and Gram-negative cell envelopes

The Gram-negative outer membrane limits accessibility of antibiotics such as penicillins, glycopeptides and macrolides to the periplasmic PG and inner membrane. Antibiotic resistance mechanisms unrelated to cell envelope structure can be broadly grouped into three functional categories: 1) inactivation of the antibiotic before reaching its target; 2) exclusion of the antibiotic from the target by efflux or other mechanisms; 3) modification of the target (McCallum *et al.*, 2010).

Inactivation of the antibiotic is the most common mechanism of resistance to penicillins, cephalosporins and other β -lactam agents (Greenwood *et al.*, 2007a). Bacteria can produce several enzymes that can inactivate or degrade the antibacterial agent. These include β -lactamases, aminoglycoside-modifying enzymes and chloramphenicol acetyl transferase (Willey *et al.*, 2008). β -lactamases inactivate β -lactam antibiotics by hydrolysis of the β -lactam ring (Waley, 1988). To date, more than 200 β -lactamases have been identified. They are generally plasmid-encoded and are more frequently associated with Gram-negative bacteria (Bush, 1989; Greenwood *et al.*, 2007a).

Exclusion of an antibiotic from its target may be mediated by efflux pumps, which actively transport the drug from the bacterium, or by modifying the permeability of the cell wall to the antibiotic molecule (Willey *et al.*, 2008). These mechanisms are an important cause of resistance to tetracyclines, β -lactam agents and quinolones (Greenwood *et al.*, 2007a). Tetracycline resistance is mediated by efflux pumps in both Gram-negative and Gram-positive bacteria (Schnappinger and Hillen, 1996). On the other hand, resistance to β -lactam agents is primarily due to reduction in the internal diameter of the porin channel, preventing the antibiotic from penetrating the cell

envelope (Heesemann, 1993). Both overexpression of efflux pumps and impermeability of the membrane also govern quinolone resistance (Ruiz, 2003)

Target modification is another common mechanism of antibiotic resistance. This form of resistance can result from a mutation in the gene encoding the target, resulting in lower affinity for the antibiotic. Alternatively, bacteria may acquire the ability to produce a molecule which performs the same function as the target but is not susceptible to the antibiotic (Tenover, 2006). Drugs that are primarily affected by this resistance mechanism are β -lactams, rifampicin and quinolones (Greenwood *et al.*, 2007a). Specific examples of both forms of this resistance mechanism have been observed in the β -lactam target proteins, the PBPs. These include modification of the pneumococcal PBP2b and acquisition of an alternative PBP (PBP2a) by MRSA (McManus, 1997).

Bacterial antibiotic resistance mechanisms may be acquired by chromosomal mutation and selection (vertical mutation) or by transfer of genetic material from another resistant organism (horizontal mutation) by conjugation, transduction and transformation (Tenover, 2006). Natural selection ensures that resistance determinants are maintained and expanded within bacterial populations in response to the selective pressure of widespread antibiotic use (Tenover, 2006). This has clearly been the case with the evolution of MRSA, which has become a significant medical problem both in hospital and community settings.

1.3 MRSA

S. aureus is a Gram-positive, facultative anaerobe, approximately 0.5 – 1.0 μm in size with an ideal growth temperature of 35 °C that forms grape-like clusters of cocci (Foster, 1996; Anderson *et al.*, 2005b). It has a low G + C content and is a member of the *Bacillus-Lactobacillus-Streptococcus* phylogenetic cluster (Foster, 1996). Antibiotic pressure and a strong tendency to accumulate antibiotic resistance genes has aided the rapid vertical spread of resistance within *S. aureus* populations, resulting in the widespread rise in MRSA isolates (Anderson *et al.*, 2005b). Methicillin resistance is due to the addition of the *mecA* gene, which may have originated from *Staphylococcus sciuri* (*S. sciuri*), which encodes for an additional 78-kDa PBP, designated PBP2a, that

confers resistance to β -lactam agents (Gordon and Lowy, 2008). MRSA is resistant to a wide spectrum of β -lactam antibiotics, including methicillin, oxacillin and flucloxacillin (Anderson *et al.*, 2005b).

1.3.1 Epidemiology

Penicillin resistance was first observed in *S. aureus* only seven years after the commercialisation of penicillin as a therapeutic in the 1940s (Figure 1-1) (Hopwood, 2007). The first three cases of MRSA were reported in 1961, two years after the introduction of methicillin into clinical practice; the minimum inhibitory concentration (MIC) of methicillin ranged from 3.1 to 25 $\mu\text{g/ml}$ (Chambers, 1988). The first isolate came from a patient with eczema, the second from the infected finger of a nurse and the third from a surgical wound of one of the nurse's patients (Chambers, 1988). In 1963, the first epidemic involving an MRSA strain was described, followed by further outbreaks in the United States and Europe in the 60s and 70s (Chambers, 1988). The first MRSA strain isolated in the United Kingdom (UK) was in 1960 (Deurenberg and Stobberingh, 2008). In the late 1970s, gentamicin-resistant MRSA emerged and persisted in several countries until the 1980s (Johnson, 2011). The prevalence of MRSA greatly increased in the 1990s and included the emergence of epidemic MRSA strains (EMRSA), primarily EMRSA-15 and EMRSA-16 (Johnson, 2011). These two strains were predominantly resistant to erythromycin and ciprofloxacin in addition to β -lactam antibiotics (Johnson, 2011).

The two most common EMRSA clones in the UK are EMRSA-15 of multi-locus sequence type (MLST) clonal complex (CC) 22 and sequence type (ST) 22, and EMRSA-16 of CC30, (ST36) (Johnson *et al.*, 2001). In 1999-2000, these two strains accounted for 95.6% of all cases of MRSA bacteraemia in the UK, with EMRSA-15 accounting for a higher percentage than EMRSA-16 (60.2% and 35.4% respectively) (Johnson *et al.*, 2001). EMRSA-15 and EMRSA-16 were first isolated in the UK; however, EMRSA-15 eventually became widespread in Europe, Australia, the Middle East and Asia, whereas EMRSA-16 was mostly restricted to the UK (Ellington *et al.*, 2010). In a study of 374 MRSA cases in the UK between 2001 and 2007, approximately 90% were either EMRSA-15 or EMRSA-16, with EMRSA-15 the more dominant MRSA lineage over this period (Ellington *et al.*, 2010). The majority of these isolates were resistant to macrolides and fluoroquinolones, but had low resistance to gentamicin

(EMRSA-15: 3 %, EMRSA-16: 24%) and tetracyclines (3% for both) (Ellington *et al.*, 2010). MRSA accounted for 2% of *S. aureus* infections in hospital intensive care units in 1974, rising to 22% in 1995 and 64% in 2004 (Chambers and DeLeo, 2009). In 2005, it was one of the leading cause associated with death in the UK from a single pathogen and was associated with approximately 19,000 deaths (Chambers and DeLeo, 2009). There was also a significant rise in MRSA cases in the USA, with 60% of hospital-acquired *S. aureus* infections and 30-62% of bloodstream infections attributed in 2002 (Boyce *et al.*, 2005). Additionally, in 2005 *S. aureus* (primarily MRSA) was reported as the most significant cause of serious infection in the USA, causing 90,000 invasive infections (Schlievert *et al.*, 2010).

At the same time as hospital-acquired MRSA (HA-MRSA) infections were on the rise, the late 1990s saw the emergence of community-acquired MRSA (CA-MRSA) (Carleton *et al.*, 2004). The first isolation of CA-MRSA was recognised in Western Australia (Chambers, 1988). CA-MRSA and HA-MRSA differ both phenotypically and genetically. Pulsed-field gel electrophoresis (PFGE) and MLST analyses indicated that isolates from both groups comprised two distinct lineages (Deurenberg and Stobberingh, 2008). Genetic analysis of CA-MRSA isolates revealed acquisition of a unique *mec* element (primarily type IV, V or VII) and expression of the Paton-Valentine leukocidin (PVL) virulence factor encoded by the *lukS-lukF* genes (Chambers, 1988). PVL is a *S. aureus*-specific leukocidin exotoxin that creates pores in host cell membranes. Infections with PVL-positive strains often present as severe skin and soft tissue infections ranging from furuncles to necrotising fasciitis and pneumonia (Deurenberg and Stobberingh, 2008; Köck *et al.*, 2010). The most successful CA-MRSA strain in the USA is PFGE profile USA300 (MLST ST8) which expresses PVL (Köck *et al.*, 2010). This strain is also prevalent in European countries, along with CA-MRSA strain ST80 (Deurenberg *et al.*, 2007).

European health services have taken significant steps towards the control of MRSA infections. Target-driven measures in England resulted in a 62% reduction in cases of bacteraemia due to MRSA from Fiscal Year (FY) 2003-2004 to 2008-2009 (HPA, Sept 2009). France saw a 30% reduction in surgical site MRSA infections and a 20% decrease in MRSA bacteraemia as a result of implementation of additional infection control measures (Köck *et al.*, 2010). In the UK, the incidence of MRSA bacteraemia has been reduced further, with a 22% decrease from Fiscal Year (FY) 2009/2010 (1989

cases) to FY 2010/2011 (1481 cases) (HPA, June 2011). However, MRSA is still isolated from approximately five percent of healthcare-associated infections in the UK and the National Audit Office estimates the cost of MRSA infections to total one billion Great British Pounds (GBP) per year (WHO, 2011). In the USA the cost of MRSA infections was higher, at eight billion dollars per year (Zeller *et al.*, 2007). Although the global incidence of MRSA infections is falling, there remains a need for alternative treatments, as the pathogen continues to be a health threat.

1.3.2 Infections caused by MRSA

MRSA has become the most common cause of nosocomial infections worldwide and was previously believed to be solely an opportunistic agent. MRSA now accounts for a large proportion of CA-MRSA infections, which present distinct clinical symptoms compared to HA-MRSA (Memmi *et al.*, 2008; Watkins *et al.*, 2012). The primary site of colonisation of *S. aureus* in humans is the anterior nares, with approximately 20% of individuals colonised at any given time (Berger-Bachi, 2002). Other sites of frequent colonisation include the armpit, groin and gastrointestinal tract (Gordon and Lowy, 2008). Colonisation can be commensal or pathogenic in character. Once established the bacterium is most likely to cause overt infection when host defences are breached and the bacterium is able to enter the body through open wounds, cuts and medical devices such as indwelling catheters (Gordon and Lowy, 2008). Diseases caused by *S. aureus* include superficial infections such as skin abscesses and impetigo or more serious invasive infections including endocarditis, septic arthritis and osteomyelitis (Morell and Balkin, 2010). A study by Von Eiff *et al.* (2001) showed that 80% of all patients with MRSA bacteraemia had the same blood and nasal isolate, indicating that most infections were caused by the same colonising strain. In hospitalised patients, HA-MRSA infections commonly occur in patients who have undergone surgery or have a suppressed immune system (Gordon and Lowy, 2008). These infections are most commonly associated with pneumonia, bacteraemia, and invasive infections, including septic arthritis (Watkins *et al.*, 2012). On the other hand, infections caused by CA-MRSA primarily consist of skin and soft tissue infections (90%) as well as more severe infections such as necrotising pneumonia, sepsis, osteomyelitis and necrotising fasciitis (Foster, 2005; Watkins *et al.*, 2012).

1.3.3 Pathogenesis

The pathogenicity of MRSA is multi-factorial and, as stated above, the bacterium is both a pathogen and a commensal (Berger-Bachi, 2002; Gordon and Lowy, 2008). The primary mode of transmission is human to human *via* skin contact with a colonised source or fomite (Morell and Balkin, 2010). A weakened immune system or break in the skin barrier is a predisposition for infection of a colonised host (Morell and Balkin, 2010). The bacterium is able to adhere to host tissue structures such as mucus, epithelial cells, plasma proteins, endothelial cells and the extracellular matrix (ECM) as well as to prosthetic devices. Adherence is mediated through strain-specific microbial surface components that recognise adhesive matrix molecules (MSCRAMMs) (Figure 1-6) (Speziale *et al.*, 2009; Morell and Balkin, 2010). MSCRAMMs are able to bind to the majority of ECM and blood plasma proteins including collagen, fibronectin and fibrinogen (Gordon and Lowy, 2008). The most common members of the MSCRAMM family are protein A (SpA), fibronectin-binding proteins (FnBP) A and B, collagen-binding protein (CNA) and clumping factors (Clf) A and B (Figure 1-6) (Speziale *et al.*, 2009).

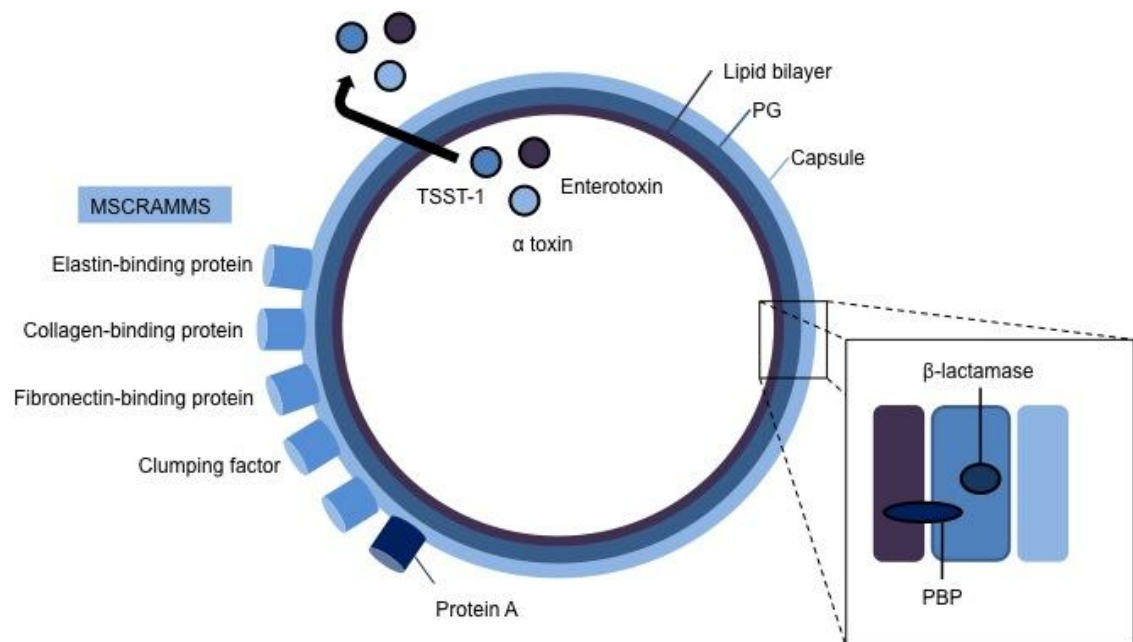


Figure 1-6 Virulence factors associated with *S. aureus*, surface and secreted proteins involved in virulence. A cross section of the envelope shows PBPs involved in replication and antibiotic resistance and β -lactamase (Morell and Balkin, 2010).

Protein A binds to the Fc region of IgG and plays a role in the evasion of phagocytosis by the host's immune system (Foster, 2005). Clumping factors A and B bind to

fibrinogen and fibrinogen-coated substances respectively, causing coagulation of blood plasma and other solutions containing fibrinogen (Speziale *et al.*, 2009). The adhesins FnBP A and B bind to fibrinogen, elastin and fibronectin which play a key role in attachment to, and colonisation of, host tissues (Speziale *et al.*, 2009). Lastly, CNA is required for collagen attachment and is expressed in over 90% of *S. aureus* strains isolated from patients with bone and joint infections (Speziale *et al.*, 2009).

Another set of adherence-related proteins are the secretable expanded repertoire adhesive molecules (SERAMs) that effect colonisation of host tissue (Speziale *et al.*, 2009). Other cell-surface virulence factors include the capsular polysaccharide that forms a protective layer during systemic invasion; it has antiphagocytic properties and plays a role in biofilm formation (Speziale *et al.*, 2009). Others include iron-regulator proteins and polysaccharide intercellular adhesins (Schlievert *et al.*, 2010). The bacterium is able to secrete a number of exoenzymes that include proteases, hyaluronidase, lipase and nuclease that elicit tissue destruction and enable bacterial dissemination (Foster, 2005). Secreted enzymes also include inflammatory cytolytins (e.g. PVL and α , β , γ and δ toxins), exfoliative toxins A and B (leading to scalded skin syndrome) and superantigens (SAGs). PVL is a two-component cytolytic toxin, which has a high affinity for human leukocytes and is often associated with severe skin infections and necrotising pneumonia caused primarily by CA-MRSA (Bohach and Foster, 1999; Gillet *et al.*, 2002). An additional toxin, toxic shock syndrome toxin-1 (TSST-1), is associated with hypotension, desquamation, septic shock and multiple organ failure (Foster, 2005; Schlievert *et al.*, 2010).

The regulation of virulence genes is controlled by two component systems (Gordon and Lowy, 2008). In general, MSCRAMMs are produced primarily in the logarithmic phase and secreted proteins in the stationary phase (Gordon and Lowy, 2008). Regulators of these virulence factors include the accessory gene regulator (*agr*), a quorum sensor primarily involved in reduction of expression of cell surface proteins and secretion of virulence factors during progression from late exponential to stationary phase (Yarwood and Schlievert, 2003). Other virulence regulators include ArlR and ArlS (Cheung *et al.*, 1994), SaeRS (Liang *et al.*, 2006), Rot (Saïd-Salim *et al.*, 2003) and *mgr* (Luong *et al.*, 2003).

S. aureus both attacks and evades the host immune response mechanisms. Cytolytic toxins target components of the innate immune system such as neutrophils (Voyich *et al.*, 2005). The bacterium secretes immunomodulatory proteins that induce a humoral and cell-mediated host response. However, antibody (Ab) levels in the host are usually too low to combat a secondary infection and repeated infections are common (Foster, 2005). Other host immune evasion mechanisms include bacterial resistance to killing by antimicrobial peptides and lysozyme as well as the capacity for survival in phagosomes following engulfment by neutrophils and macrophages (Sieprawska-Lupa *et al.*, 2004, Bera *et al.*, 2005). As a primary infection may fail to protect against subsequent infections as the bacterium is able to prevent the host from mounting a strong Ab response, this restricts preventative treatment (Foster, 2005). Instead we must look towards understanding the replication machinery of MRSA in order to determine alternative treatment options that could include modulation of the bacterial replication and resistance machinery.

1.3.4 Cell Division

S. aureus replication is dependent on the formation of a division septum that separates the nascent daughter cells (Margolin, 2009). During growth and cell separation, the cocci form clusters (or packets) because the division plane alternates from generation to generation, resulting in cell division on orthogonal planes in three dimensions (Margolin, 2009; Turner *et al.*, 2010). As *S. aureus* divides in three proscribed planes, this produces clusters of cells often described as bunches of grapes. This contrasts with bacteria that divide on two proscribed planes such as *Pediococcus* (Figure 1-7) (Turner *et al.*, 2010).

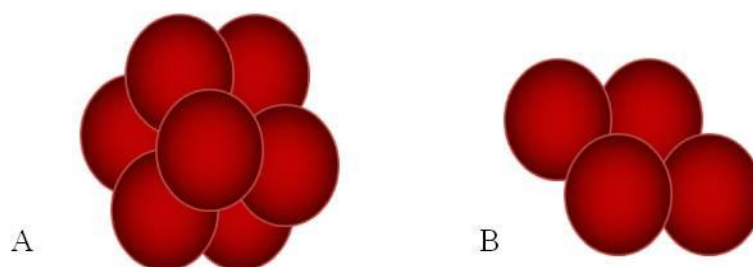


Figure 1-7 Division in multiple planes; (A) three proscribed planes as seen in *S. aureus*, leading to clusters of bacteria and (B) two proscribed planes leading to tetrads in *Pediococcus* (Turner *et al.*, 2010)

As *S. aureus* cells divide, they form a ring of nascent PG at the septum followed by hemispherical split of the two daughter cells in X and Y conformation; however, a partial attachment remains between daughter cells, creating cell clusters (Tzagoloff and Novick, 1977). The next division plane is created in orthogonal fashion to the previous two, resulting in three planar division (Turner *et al.*, 2010). *S. aureus* does not undergo an elongation phase, as is the case with rod shaped bacteria such as *Bacillus subtilis* (*B. subtilis*), as nascent PG synthesis occurs solely at the septum (Errington *et al.*, 2003; Pinho and Errington, 2003; Steele *et al.*, 2011). During cell division new septa are formed perpendicular to completed septa with the cells remaining predominantly spherical or elliptical until the formation of a completely transverse septum (Tzagoloff and Novick, 1977). The septum, once cleaved, becomes the nascent hemispherical poles of the two daughter cells (Steele *et al.*, 2011).

1.3.4.1 PG structure

S. aureus cellular integrity, shape and ability to replicate are dependent on a functional cell wall of more than 20 linear glycan chains in which the sugar residues N-acetylglucosamine (GlcNAc) and N-acetylmuramic acid (MurNAc) alternate. Chains are cross-linked by flexible pentaglycine cross-bridges (Figure 1-8) (Schneider *et al.*, 2004).

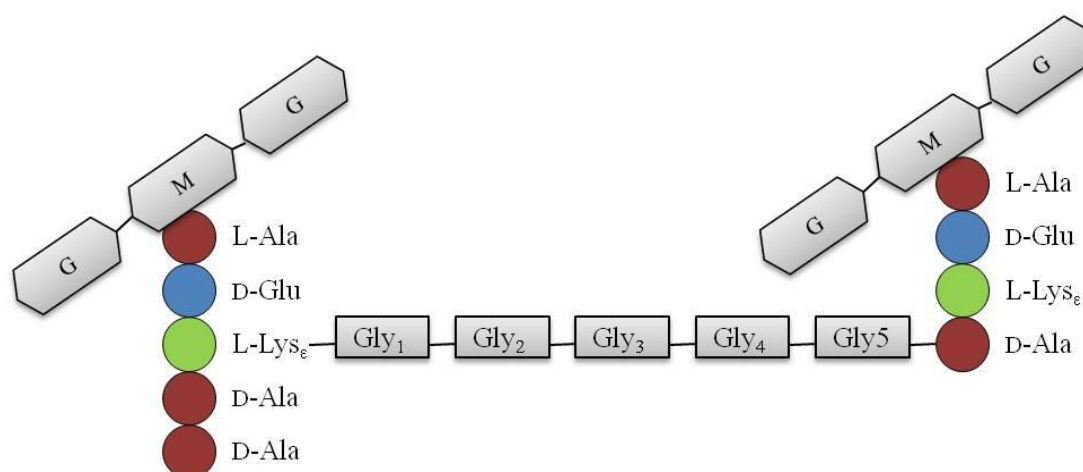


Figure 1-8 PG cross-linking in *S. aureus*. Alternating subunits of GlcNAc (G) and MurNAc (M) cross-linked through a pentaglycine cross-bridge linking stem peptides (Schneider *et al.*, 2004)

The pentaglycine cross-bridges that connect PG strands connect stem peptides from adjacent PG layers, allowing a high degree of cross-linking (up to 90%) (Wilkinson,

1997). Initially GlmS/M/U convert fructose-6-P to uridine diphosphate (UDP)-GlcNac, which is further converted to UDP-MurNac through MurA/Z/B enzymes. UDP-MurNac is linked to the active undecaprenyl-phosphate, C55-P, lipid carrier by the translocase MraY, resulting in lipid I, which is then sequentially linked to UDP-GlcNac by MurG to form lipid II (Münch *et al.*, 2012). For cross-linking to occur between glycan strands the MurNac glycan chain is substituted for a stem peptide consisting of L-Alanine (L-Ala)- D-Glutamate (D-Glu)- L-Lysine (L-Lys)- D-Ala-D-Ala. A pentaglycine bridge is formed between the ϵ -amino group of the L-Lys of one stem peptide and the D-Ala at the fourth position of another MurNac stem peptide (Schneider *et al.*, 2004). The nonribosomal peptidyl transferase family FemABX synthesises the pentaglycine interpeptide utilising glycyl-tRNA as a glycine donor (Hubscher *et al.*, 2007). FemX is responsible for the addition of the first glycine (Gly) (essential for cell viability) followed by Gly_{2,3} and Gly_{4,5} synthesised by FemA and FemB respectively (Maidhof *et al.*, 1991; Strandén *et al.*, 1997; Rohrer *et al.*, 1999). Modified lipid II with the interpeptide bridge is translocated across the cytoplasmic membrane by FtsW and the glycan strands are then cross-linked by the PBPs (Mohammadi *et al.*, 2011). The stem peptides that are not cross-linked carry an additional D-Ala, which is cleaved during cross-linking (Giesbrecht *et al.*, 1998). The resulting PG allows for a strong, but elastic structure that protects the cytoplasmic membrane, shown in figure 1-9 from lysis due to high internal osmotic pressure (Scheffers and Pinho, 2005).

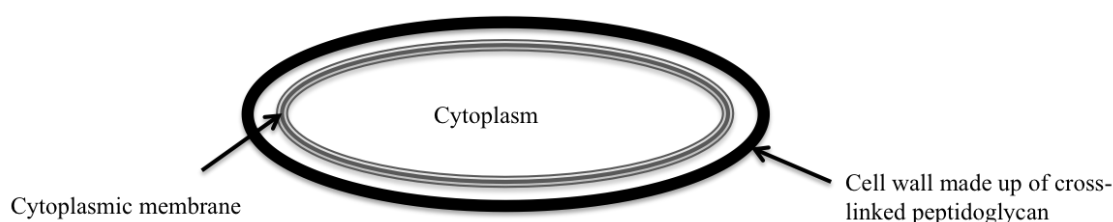


Figure 1-9 The cell wall and cytoplasmic membrane of *S. aureus* that maintain cell integrity

The thick cell wall (approximately 20 to 40 nm) of *S. aureus* and other Gram-positive bacteria contains covalently linked charged polymers that include wall teichoic acid (WTA) and cell membrane associated lipoteichoic acids (LTAs) as well proteins anchored to the cell wall (Giesbrecht *et al.*, 1998; Scheffers and Pinho, 2005). WTAs constitute 50% of the total cell wall mass and are covalently linked to the muramic acid of the cell wall by phosphodiester bonds (Atilano *et al.*, 2010). The typical cell membrane of *S. aureus* is comprised of three major phospholipids: negatively charged

established experimentally or predicted by observation of the function of homologous components in related bacteria, notably *B. subtilis*.

Cell division is initiated by polymerisation of the cytosolic tubulin homologue protein FtsZ, a self activating guanosine triphosphatase (Adams and Errington, 2009). To enable subsequent cell division, FtsZ first polymerises into a filamentous Z-ring structure at a mid-cellular location (Errington *et al.*, 2003). FtsZ is a scaffold protein for the divisome machinery, which is tethered to the Z-ring by a second cytoplasmic protein, FtsA that helps to stabilise initial Z-ring formation (Adams and Errington, 2009). Another cytoplasmic protein, SepF, has an overlapping role with FtsA as it is required for correct septum morphology and acts as a “molecular tape measure” by forming ring polymers that organise FtsZ protofilaments into higher order structures (Adams and Errington, 2009; Gündoğdu *et al.*, 2011). A second scaffold protein important for cell division is the membrane counterpart of FtsZ, EzrA (Singh *et al.*, 2007). Although EzrA is not directly involved in PG synthesis it is proposed to negatively regulate FtsZ and also acts as a secondary divisome scaffold protein (Kirkpatrick and Viollier, 2011). Steele *et al.* (2011) showed that depletion of EzrA resulted in delocalisation of the division machinery from the septum and delocalisation of GpsB, a protein required for transition between the division and elongation phases of division in Gram negative bacteria.

FtsZ subsequently recruits further divisome proteins to the septum. In methicillin sensitive *S. aureus* (MSSA), this includes PBP2 which is either directly or indirectly anchored to the cell division machinery by FtsZ (Pinho and Errington, 2003). Other proteins directly associated with the C-terminal peptide of FtsZ are ClpX and MinC, which regulate the Z-ring in *B. subtilis* (Erickson *et al.*, 2010). ClpX helps to maintain the cytoplasmic pool of FtsZ, where as MinC is a negative regulator of FtsZ recruited by MinD (Erickson *et al.*, 2010). Following initial recruitment of these proteins, membrane proteins are recruited to advance the division process. These include DivIC/DivIB/FtsL and the PBPs (PBP1/PBP2/PBP3/PBP4) as well as PBP2a in the case of MRSA (Tan *et al.*, 2012). It has been suggested that FtsL helps to stabilise the divisome at the septum in *S. aureus*, as it does in *B. subtilis*, as well as interacting directly with EzrA (Kawai and Ogasawara, 2006; Steele *et al.*, 2011). Following assembly of the divisome, cross-linked PG is undertaken by membrane bound PBPs, which catalyse the terminal reactions of PG (Llarrull *et al.*, 2009).

1.3.4.3 PBPs

The PBPs are conveniently grouped into either low molecular weight (LMW) or high molecular weight (HMW) PBPs (Ghuysen, 1991). LMW PBPs have only a penicillin binding domain whereas HMW PBPs are multi-domain proteins that are grouped into classes A and B. HMW Class A PBPs are bi-functional enzymes that possess an N-terminal domain that catalyses transglycosylase (TGase) reactions and a C-terminal penicillin binding domain that catalyses TPase reactions (Ghuysen, 1991; Goffin and Ghuysen, 1998). Class B HMW PBPs contain a functional C-terminal TPase domain, but lack the N-terminal TGase-associated motif (Goffin and Ghuysen, 1998). In *S. aureus* the PBPs are localised at the outer surface of the cytoplasmic membrane *via* membrane anchors (FtsZ and EzrA) and catalyse both TGase and TPase activity (Llarrull *et al.*, 2009). In *S. aureus* there are four PBPs involved in PG replication; PBP1, PBP2, PBP3 and PBP4, with an additional PBP, PBP2a, in MRSA (Pinho and Errington, 2005). The numbering system of the PBPs arose historically from their migration during sodium dodecyl sulphate-polyacrylamide gel electrophoresis (SDS-PAGE) separation (Yoshida *et al.*, 2010). The three HMW PBPs (PBP1, PBP2, PBP3) are essential whereas the LMW PBP (PBP4) is less important; however, it is responsible for the unusually high cross-linking found in *S. aureus* (Navratna *et al.*, 2010).

The penicillin binding domain of the PBPs has one of three unique motifs (SXXK, (S/Y) XN and (K/H) (S/T) G) that characterise the active site for the serine penicillin-recognising enzyme family (Zapun *et al.*, 2008). The SXXK motif enables the catalytic activity involved in cross-linking the stem peptides of two glycan strands. The serine of the SXXK motif attacks the penultimate D-Ala of the stem peptide, causing the release of the terminal D-Ala to form a covalent acyl-enzyme complex (Figure 1-11) (Zapun *et al.*, 2008). This complex is sequentially attacked in the TPase step by a primary amine, which is itself linked to the third residue of another stem peptide, forming a peptide bridge between the two peptide stems as depicted in figure 1-11 (Zapun *et al.*, 2008). β -lactam antibiotics are able to irreversibly acylate the catalytic serine in the TPase active site of PBPs and impair their function by forming a covalent acyl-enzyme complex that is hydrolysed very slowly, preventing further PG synthesis (Zapun *et al.*, 2008).

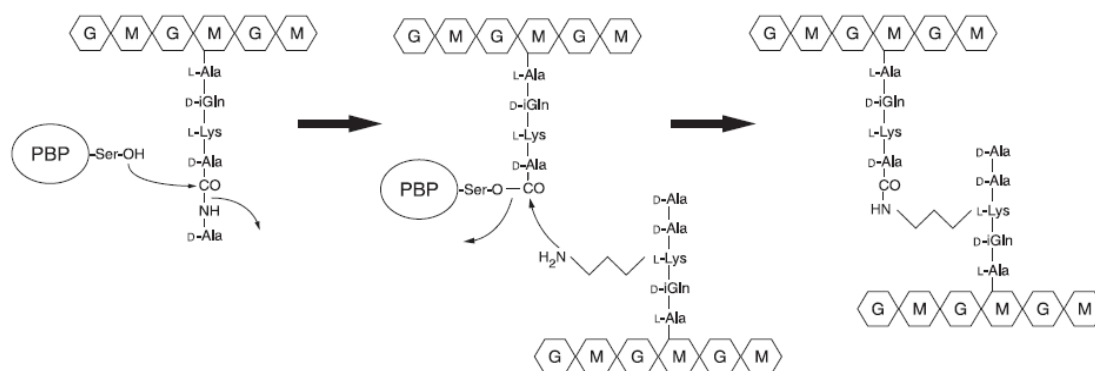


Figure 1-11 Role of PBPs in cell wall synthesis where they display TGase and TPase activity (Zapun *et al.*, 2008)

The four PBPs in MSSA are present in the following approximate proportions: PBP1 (17.1%), PBP2 (42.8%), PBP3 (13.7%) and PBP4 (26.4%) (Pucci and Dougherty, 2002). Pucci and Dougherty (2002) found a re-shuffling of these proportions in MRSA strain RN450M, with the additional PBP2a making up a large proportion of PBP molecules (42.6%), followed by PBP2 (23.3%), PBP3 (10.2%), PBP4 (15.4%) and finally PBP1 (8.6%) .

PBP1 is a native, mono-functional enzyme with regard to PG synthesis that belongs to HMW class B and is essential for staphylococcal growth. It possesses TPase function and is involved in septum formation and cell separation at the end of the division cycle (Pereira *et al.*, 2007; Atilano *et al.*, 2010). PBP1 is recruited to the septum by the GspB cytoplasmic protein (Claessen *et al.*, 2008). Pereira *et al.* (2007) showed that, in the absence of PBP1, an incomplete septum was formed during division, producing cells of increased size and envelope thickness. It is speculated that both PBP1 and PBP2 are essential for cellular division in MSSA strains; however, in MRSA, division is dependent primarily on PBP2 and, in the presence of β -lactam agents, PBP2a (Pereira *et al.*, 2009).

PBP2 is a HMW class A bi-functional PBP with spatially well separated TGase and TPase domains (Llarrull *et al.*, 2009). The TGase domain is responsible for catalysing the polymerization of the carbohydrate chain of PG and the TPase domain drives the PG cross-linking reaction (Llarrull *et al.*, 2009). It is an essential PBP localised to the septum in a substrate-dependent manner, as it recognises the D-Ala-D-Ala terminus of translocated PG muropeptides (Atilano *et al.*, 2010). At the septum, PBP2 interacts with

the division anchors FtsZ and EzrA as well as with PBP4 (Leski and Tomasz, 2005; Pinho and Errington, 2005; Steele *et al.*, 2011). In the absence of PBP2, two monofunctional transglycosylases (MGT and SgtA) can normally take over the TGase function. MGT, but not SgtA, is essential for cell viability, as only MGT acts in isolation (Lovering *et al.*, 2007). However, in MRSA cells exposed to a β -lactam antibiotic, MGT cannot replace the PBP2 TGase activity; thus, the PBP2 TGase function is essential for expression of the resistant phenotype of MRSA (Lovering *et al.*, 2007).

PBP3 and PBP4 are not essential for MSSA cell viability and division (Atilano *et al.*, 2010). There is a lack of information on the functionality of the class B PBP3 in *S. aureus*; however, it has been shown to have 44% homology with PBP2a from *B. subtilis* where it is involved in cell elongation (Murray *et al.*, 1997; Pinho *et al.*, 2000). Deletion of PBP3 in MRSA cells produced abnormal growth in the absence of β -lactams, the presence of septation defects and an increase in resistance to methicillin (Pinho *et al.*, 2000). PBP4 on the other hand is a LMW class B PBP (Atilano *et al.*, 2010). It is the only type-5 PBP that is not a strict DD-carboxypeptidase and is able to catalyse TPase reactions, producing the unusually high cross-linking seen in the PG of *S. aureus* (Matsushashi *et al.*, 1979). It has been speculated that PBP4 restricts the availability of pentapeptides from MurNAc strands for PG synthesis, removes the terminal D-Ala from the stem peptide and cross-links glycan chains through terminal D-Ala-D-Ala moieties (Sauvage *et al.*, 2008). A study by Sieradzki *et al.* (1999) established that loss of PBP4 leads to distortion of PG, resulting in increased chain length of glycan strands as well as decreased susceptibility to the PG hydrolase, lysostaphin. PBP2a is a fifth PBP found in MRSA and participates in one of two resistance mechanisms with respect to β -lactam antibiotics.

1.3.5 MRSA resistance determinants

Resistance of MRSA to β -lactam antibiotics is mediated primarily through a low-affinity PBP, PBP2a, as well as through the expression of a β -lactamase with the capacity to hydrolyse methicillin and other β -lactam agents; there is also a lowering of affinity of endogenous PBPs for β -lactams (Figure 1-12) (Stapleton and Taylor, 2002).

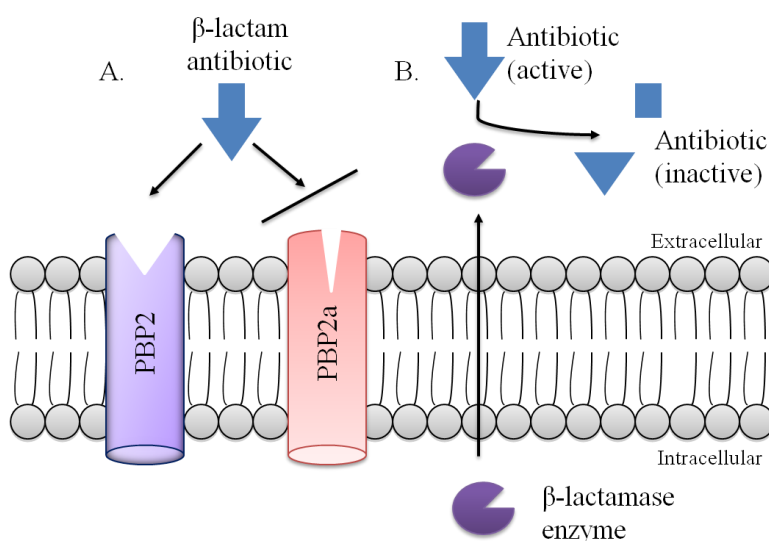


Figure 1-12 Antibiotic resistance mechanisms in MRSA. (A) Decreased binding affinity of PBP2a for β -lactam antibiotics and (B) β -lactamases that hydrolyse antibiotics to an inactive form

Staphylococci produce plasmid-encoded exo-enzymes that hydrolyse benzylpenicillin, ampicillin and the majority of other penicillins (Greenwood *et al.*, 2007a). However, for MRSA, β -lactam resistance is primarily due to PBP2a; this protein is encoded by an exogenous DNA element staphylococcal cassette chromosome *mec* (SCC*mec*) containing the *mecA* operon (Berger-Bächli and Rohrer, 2002). A *mecA* homologue, *mecC*, has recently also been identified in MRSA isolates (Harrison *et al.*, 2013). It has been suggested that the *mecA*-containing operon originated from *S. sciuri*, as a close homologue of PBP2a has been found in the species (Pinho *et al.*, 2001b). The *mecA*-containing operon is found within SCC, a large mobile element, which is able to integrate rapidly into the *S. aureus* chromosome in a site-specific manner at a location near the origin of replication (Llarrull *et al.*, 2009). *mecA* is highly conserved in MRSA (>90 %) and PBP2a has less than 21% sequence homology with endogenous PBPs in *S. aureus* (Lim and Strynadka, 2002). β -lactam antibiotics acylate PBP2a at a rate one to three orders of magnitude slower than comparable acylation rates in native PBPs and it is this difference that confers β -lactam resistance (Pinho *et al.*, 2001b). Elucidation of the crystal structure of PBP2a has provided an indication of a higher acylation efficiency (K_D) for the non-covalent β -lactam-PBP2a complex and a lower rate of serine acylation following binding of members of this antibiotic class (Llarrull *et al.*, 2009). A higher K_D reflects a reduction in the accessibility of the PBP2a active site to β -lactam agents due to the blocking action of a loop (Llarrull *et al.*, 2009). Another factor that

contributes to PBP2a resistance is a serine residue 403 in the protein's narrow groove active site leading to the formation of an acyl intermediate, which in turn makes irreversible acylation reaction less favourable (Chambers, 2003). PBP2a lacks TGase activity and must functionally cooperate with PBP2 to continue PG synthesis in the presence of β -lactam antibiotics (Pinho *et al.*, 2001b).

Vancomycin has for a long time been the drug of last resort for the treatment of MRSA infections. However, both vancomycin intermediate (VISA) and vancomycin resistant (VRSA) *S. aureus* isolates have emerged in recent years, which has increased the need to develop novel therapeutic options (CDC, 2002). VRSA (MIC 16 mg/L) is associated with the expression of *vanA* resulting in reduced susceptibility to vancomycin and teicoplanin (Moubareck *et al.*, 2009). This gene was most likely acquired from an enterococcus and it catalyses the synthesis of PG precursors terminating in D-Ala-D-Lactate (D-Ala-D-Lac) rather than D-Ala-D-Ala, the target for vancomycin (Moubareck *et al.*, 2009).

Other treatment options for MRSA include linezolid and daptomycin (Liu *et al.*, 2011), however resistance to both antibiotics has emerged. Linezolid resistance is associated with both a mutation in the 23S rRNA and a plasmid-mediated rRNA methyltransferase (Ziglam *et al.*, 2005). Daptomycin is used primarily for the treatment of severe skin and soft tissue infections caused by MRSA; resistance has developed in some MRSA clinical isolates (Hayden *et al.*, 2005). Daptomycin non-susceptible MRSA (MIC > 1 mg/L) exhibit thicker cell walls, increased positive surface charge and altered membrane function, resulting in reduced surface binding of daptomycin (Hayden *et al.*, 2005). Additional treatment options include clindamycin and trimethoprim-sulfamethoxazole; however, clinical data is lacking for these treatment options and clindamycin resistance has been detected (Liu *et al.*, 2011). These resistance scenarios highlight the need for a re-evaluation of therapeutic approaches for the treatment of MRSA infections.

1.4 Plant-derived alternative therapeutics

With a decrease in recent screening for novel drug targets and drug discovery (Sams-Dodd, 2005), an increased interest in the potential of plant derived products with

antimicrobial activity has been observed (Gibbons, 2004; Saleem *et al.*, 2010). For over 100 years chemical compounds have been isolated from medicinal plants as well as plant-derived medicines used to treat a variety of medical conditions (Shaw, 1998), including bacterial (Dixon, 2001) and parasitic infections (Paddon *et al.*, 2013). However, the MICs of most plant derived extracts against bacteria remains high (>100 mg/L) (Naz *et al.*, 2012; Mohamed *et al.*, 2013). Thus, attention has shifted to the study of synergism between antibacterial drugs and plant extracts and the ability of plant extracts to modify bacterial phenotypes (Betoni *et al.*, 2006). One such plant extract, epicatechin gallate (ECg), a constituent of the green tea plant *Camellia sinensis* (*C. sinensis*), has the capacity to abrogate the resistance of MRSA to β -lactam antibiotics and may be useful as an adjunct to conventional chemotherapy (Stapleton *et al.*, 2004).

1.4.1 Green tea and its components

C. sinensis was first cultivated in China and Japan and spread to the west by European traders in the 15th and 16th century (Forrest, 1985). A study conducted in 1985 indicated that tea was the most widely consumed beverage in the world after water (Graham, 1992). Green tea and black tea stem from the same plant; however, unlike black tea, green tea is non-fermented and contains a higher concentration of pharmacologically active components (Lin *et al.*, 2003). Green tea contains polyphenols that include flavanoids such as flavanols (e.g. catechins) and phenolic acids (Wang and Ho, 2009). Catechins, phenol-derived flavanoids, make up approximately 30% of the dry weight of green tea. Many health benefits have been associated with these compounds including antioxidative, anticarcinogenic and antimicrobial benefits (Graham, 1992; Taylor *et al.*, 2005).

The main polyphenolic catechins in green tea are (+)-catechin, (+)-gallocatechin, (-)-epicatechin, (EC) and (-)-epigallocatechin (EGC). Galloyl catechins present in the green tea leaf include (-)-epicatechin gallate (ECg), (-)-epigallocatechin gallate (EGCg), (-)-catechin gallate (Cg) and (-)-gallocatechin gallate (GCg) (Taylor *et al.*, 2005). The core structure of these catechins consists of two phenolic aromatic rings (designated A and B) substituted with hydroxyl groups (Figure 1-13). Structural variation is due to the presence or absence of a galloyl moiety and the number of hydroxyl groups on the B-ring (Minoda *et al.*, 2010). The A-ring is the site of carbonyl trapping, whereas the B-ring is the preferred site of oxidation (Wang and Ho, 2009).

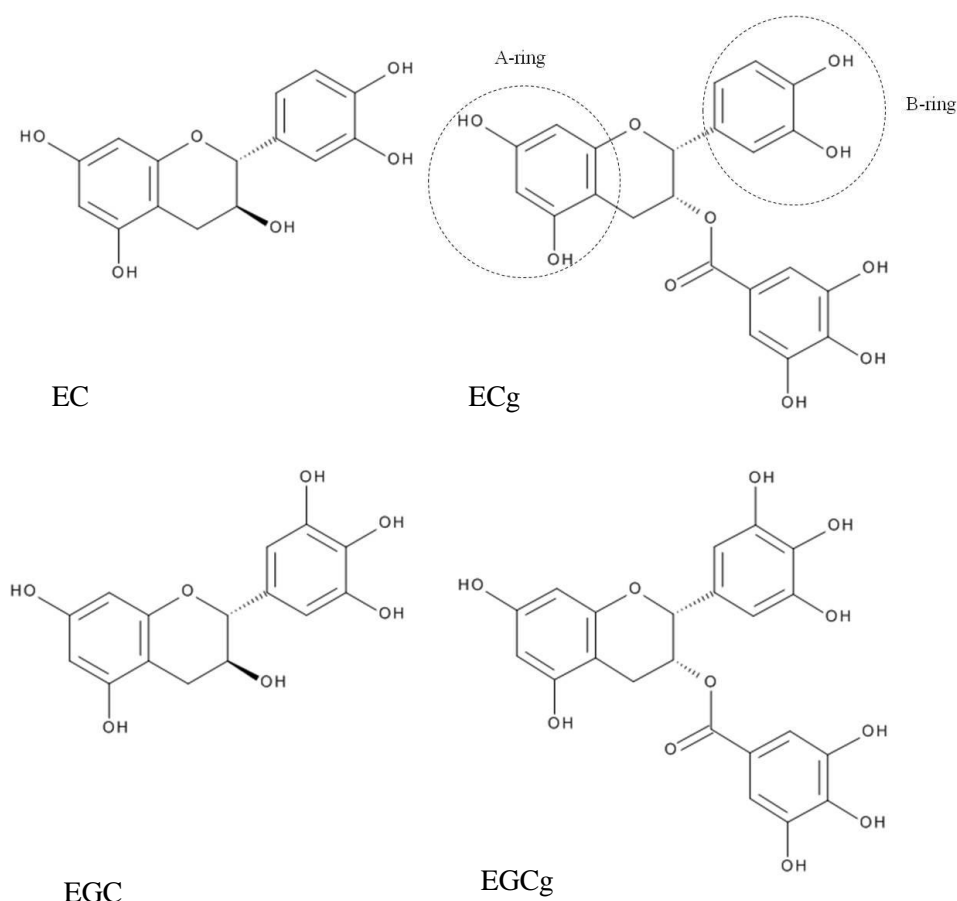


Figure 1-13 Structure of EC, EGC, ECg and EGCg

There is good evidence that EC, EGC, ECg and EGCg are absorbed intestinally, as catechins ingested by rats were found to be concentrated in the portal vein (Okushio *et al.*, 1996). Following absorption, catechins are rapidly metabolised. In rats, EGCg and ECg are excreted primarily in bile, whereas EGC and EC are excreted in both bile and urine (Chen *et al.*, 1997). Overall, catechins have poor oral bioavailability due, in part, to the rapid degradation of the compounds caused by protonation of hydroxyl groups, release of the galloyl group by hydrolysis and further modifications including methylation and sulfonation (Chen *et al.*, 2001; Lu *et al.*, 2003; Manach and Donovan, 2004). There are, however, health benefits associated with the consumption of green tea.

1.4.2 Health benefits of green tea

1.4.2.1 Antioxidant effect of catechins

Green tea flavanoids protect cells and tissues from oxidative stress by a combination of iron chelation and free radical scavenging (Salah *et al.*, 1995). Cellular oxidative stress is due to increased production of free radicals, leading to an imbalance between

oxidants and antioxidants that may result in cell damage and, in severe cases, apoptosis (Sies, 1991). Reactive oxygen species (ROS) are a common form of intracellular free radical. Catechins act as hydrogen donors, reducing ROS such as superoxide, peroxy radicals and singlet oxygen (Guo *et al.*, 1999). They also chelate metal ions such as copper and iron, preventing transition redox-active metals from catalysing free radical formation (Rice-Evans and Miller, 1996). Sung *et al* showed a significant increase in plasma antioxidant levels in patients who drank 300 mL of green tea containing 5 g of dry tea leaves (2000). Further, Langley-Evans (2000) showed that green tea possessed a 2.5 fold greater antioxidant activity than black tea and both possessed higher antioxidant activity against peroxy radicals than vegetables such as spinach and garlic. EGCg and ECg have the highest radical scavenging activity (Henning *et al.*, 2003).

1.4.2.2 Effects on cardiovascular diseases

Green tea may have a beneficial impact on cardiovascular diseases (CVDs). CVDs are a major cause of morbidity and mortality worldwide and are often associated with obesity (WHO, 2013). A study in 2000 revealed that green tea consumption significantly reduced the risk of CVD-related mortality; especially within the male study cohort (Nakachi *et al.*, 2000). A more recent study in Japan quantified the green tea effect on CVDs in a population of 40,530 adults and showed that consumption of five or more cups of green tea daily reduced CVDs by 26%, with the strongest reduction in the occurrence of strokes (-37%), particularly cerebral infarctions (-51%) (Kuriyama *et al.*, 2006). The inverse relationship between green tea consumption and CVDs remained as significant after adjustment for age, physical activity, diet, education and job status (Kuriyama *et al.*, 2006).

1.4.2.3 Anti-carcinogenic effects of catechins

Another potential health benefit associated with green tea resides in the capacity of catechins to suppress tumour cell growth *in vitro* and *in vivo*. Treatment of carcinoma cell lines with EGCg has shown that exposure initiates apoptosis and cell cycle arrest in the G0/G1 phase (Gupta *et al.*, 2000). Furthermore, EGCg inhibits protein kinase C- α , inhibiting cell proliferation. It also inhibits transcription factors such as nuclear factor- κ B and suppresses vascular endothelial growth factors, leading to inhibition of angiogenesis (Livneh and Fishman, 1997; Gupta *et al.*, 2000; Adhami *et al.*, 2003).

Tumor cell suppression by catechins has been demonstrated in prostate (Adhami *et al.*, 2003), esophageal (Gao *et al.*, 1994), stomach (Vainio and Hemminki, 1989), skin (Meeran *et al.*, 2009), breast (Bigelow and Cardelli, 2006), ovarian (Spinella *et al.*, 2006), lung (Lu *et al.*, 2008) and pancreatic cancers (Qanungo *et al.*, 2005).

1.4.2.4 Antimicrobial effects of catechins

Catechins possess antibacterial, antiviral and antifungal activities. Weak antibacterial properties of catechins, in particular, EC, ECg, EGC and EGCg have been demonstrated against Gram-positive and Gram-negative bacteria (Hamilton-Miller, 1995; McKay and Blumberg, 2002; Cho *et al.*, 2008). For example, weak *in vitro* activity (MIC₅₀ 8-16 mg/L) against *Helicobacter pylori* (Stoicov *et al.*, 2009) and the inhibition of *Pseudomonas aeruginosa* growth by EGCg has also been observed. Catechins have also been investigated for potential synergy with antibiotics for the treatment of MRSA infections (Zhao *et al.*, 2001; Liu *et al.*, 2013). ECg sensitise MRSA to β -lactam antibiotics by disruption of the resistance machinery (Bernal *et al.*, 2010).

The antiviral effect of catechins has been explored in human immunodeficiency virus (HIV) and influenza virus infections. Fassina *et al.* (2002) demonstrated that EGCg caused inhibition of HIV infection and viral replication by inactivation of casein kinase II, which is responsible for the phosphorylation and activation of HIV-1 reverse transcriptase. A combination of EGCg and ECg inhibits replication of influenza virus by suppression of RNA synthesis (Song *et al.*, 2005). In addition, catechins possess activity against the yeast *Candida albicans* and sensitise resistant fungi to amphotericin B (Hirasawa and Takada, 2004).

1.5 Effect of ECg on MRSA

Yam *et al.* (1998) analysed the capacity of green tea extracts to sensitise MRSA to β -lactam antibiotics and observed that the extracts were able to reverse methicillin resistance. The study suggested that the synergistic effect of the green tea extracts and β -lactam agents is due to catechin-mediated inhibition of PBP2a synthesis and β -lactamase secretion. However, later studies indicated that ECg has a more complex and multi-factoral effect on MRSA (Stapleton *et al.*, 2007; Bernal *et al.*, 2010).

12.5 mg/L of ECg reduces the oxacillin MIC of MRSA strains, including EMRSA-16, to below the therapeutic breakpoint (Stapleton *et al.*, 2006). This is in contrast to non-galloylated catechins that do not reduce the MIC as significantly, which may be explained by the difference in ability to penetrate the staphylococcal membrane. ECg along with EGCg intercalate deep into the cytoplasmic membrane with ECg penetrating deeper into the membrane than EGCg (Hashimoto *et al.*, 1999). On the other hand non-galloylated catechins, such as EC, remain at a superficial location within the membrane bilayer (Stapleton *et al.*, 2006). The affinity of catechins for the MRSA membrane is dependent on the galloyl moiety and the number of hydroxyls on the B-ring, with fewer hydroxyl groups resulting in a more lipophilic compound facilitating deeper intercalation into the membrane (Minoda *et al.*, 2010). The binding capacity of ECg to the MRSA membrane can be enhanced by the presence of EC; however EC exposure alone had no effect on the bacterium (Caturla *et al.*, 2002; Stapleton *et al.*, 2006).

Exposure of MRSA cells to ECg has a significant impact on the cellular morphology of MRSA. The cells are transformed from round, loosely clumped cocci with a smooth surface to larger, clumped cells with a rougher exterior surface (Figure 1-14) (Bernal *et al.*, 2009). A further study with radiolabelled ECg, showed that 58% of the label was associated with the cytoplasmic membrane and 31% with the cell wall. Membrane intercalation of ECg produced an initial decrease in membrane fluidity followed by an increase in fluidity as the cells overcompensated (Bernal *et al.*, 2009). Intercalation also led to tighter acyl chain packing and a reorganisation of the cell membrane with a reduction in lysophosphatidyl glycerol (6.5% to 1.5%) and an increase in branched chain fatty acid moieties of the membrane phospholipids (Bernal *et al.*, 2010).

Further effects of ECg on EMRSA-16 cell wall composition include a 5-10% reduction in PG cross-linking as well as and a 50% decrease in D-Ala substitution of WTA (Stapleton *et al.*, 2007; Bernal *et al.*, 2009). Furthermore, ECg reduced the net positive charge of the cells, leading to inhibition of biofilm formation as a consequence of electrostatic repulsion (Stapleton *et al.*, 2007) as well as an increased retention of autolysins in the cell wall (Bernal *et al.*, 2010).

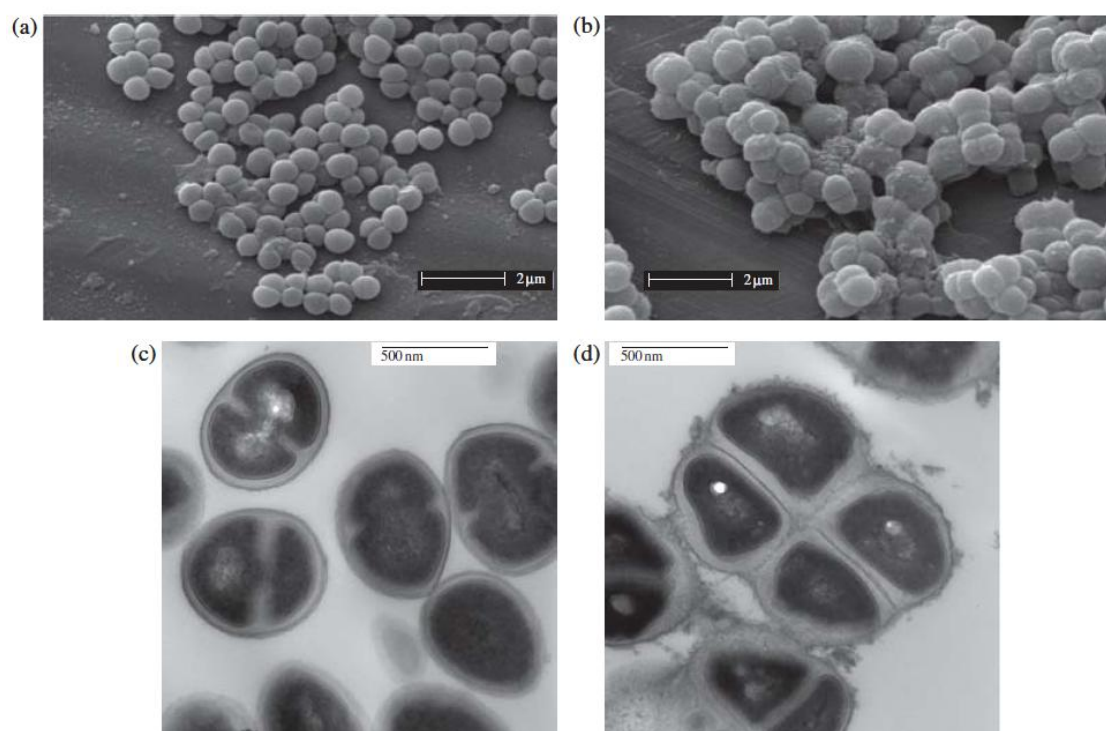


Figure 1-14 (a and b) SEM and (c and d) TEM of control (a and c) EMRSA-16 and (b and d) EMRSA-16 exposed to 12.5 mg/L ECg. EMRSA-16 were grown to mid-logarithmic phase (from Bernal *et al.*, 2009)

MRSA responds to ECg exposure by attempting to preserve or repair the cell wall and membrane. Up-regulation of 103 genes and down-regulation of a further 166 genes following bilayer intercalation of ECg has been noted (Bernal *et al.*, 2010). Up-regulated genes included those for cation transport and binding, electron transport, β -lactamase expression, shape determination and pathogenesis proteins. Additionally, ECg induced expression of genes belonging to the general cell wall stress stimulon governed by *vraR/vraS*. Furthermore, genes encoding osmotic shock proteins, membrane export proteins, ion transport proteins, lipoproteins and multiple pathogenesis associated proteins were down regulated (Bernal *et al.*, 2010).

1.5.1 Effect of ECg on MRSA division proteins

Intercalation of ECg into the staphylococcal cytoplasmic membrane alters the lipid environment in which the divisome proteins reside. ECg does not bind to PBPs; however, it elicits indirect effects on these proteins (Bernal *et al.*, 2010). There is a small reduction in the expression of PBP1 and PBP3 and delocalisation of PBP2 (Bernal *et al.*, 2010). Previous studies revealed that PBP2a expression is still detected when

MRSA cells are sensitised to β -lactams with ECg. It has therefore been hypothesised that this reversal of resistance is due to either displacement of PBP2a, along with PBP2, from the division septum or that there is a functional disruption of the PBP2/PBP2a resistance complex (Stapleton *et al.*, 2004; Bernal *et al.*, 2010).

1.6 Membrane proteins

In order to study the effect of ECg on the functional integrity of the PBP2/PBP2a resistance complex, the membrane protein complexes first need to be isolated and detected. PBP2/PBP2a is a theoretical, highly unstable and transient complex. Current methods to solubilise membrane proteins primarily involve surfactants that are not ideal for solubilising membrane proteins in a functional state.

Membrane proteins make up 30% of the total cell protein content and account for more than 50% of current drug targets (Hong *et al.*, 2011). A frequent obstacle encountered when working with membrane proteins is the difficulty in solubilising the protein in a functional state. Most membrane proteins possess highly hydrophobic exterior domains that are associated with lipids and hydrophilic interior domains that often act as ion channels and transporters (Jamshad *et al.*, 2011). The relative hydrophobicity of the different domains regulates correct protein folding, function and stability by controlling the interactions of the protein with the aqueous membrane exterior, the hydrophobic membrane interior and the charged membrane lipid head groups (Jamshad *et al.*, 2011). However, this property also means that membrane proteins do not stay in a functional monomeric form in aqueous buffer due to the tendency of hydrophobic moieties to minimise the number of water molecules associated with the hydrophobic domains, leading to protein aggregation and precipitation (Popot, 2010).

1.6.1 Surfactant-mediated protein extraction

Surfactants are amphipathic substances with a hydrophilic head group and a hydrophobic tail that disintegrate the lipid bilayer while incorporating the proteins into surfactant micelles (Helenius and Simons, 1975). In order for this to occur, protein-lipid and protein-protein interactions that anchor membrane proteins to the membrane are disrupted and replaced with surfactant molecules that disrupt membrane protein complexes (Popot, 2010). Surfactants accomplish this disruption by stressing the

membrane-water interface, leading to the planar membrane structure becoming unfavourable and subsequently dispersing the membrane constituents into multiple micelles (Popot, 2010).

The major problem with the use of surfactants for membrane protein solubilisation is the large difference between the conformation of the protein in micellar environments as opposed to their native membrane environment (Rajesh *et al.*, 2011). Small changes in the nature of head groups and acyl chains within phospholipid bilayer have significant effects on the physical properties of the membrane, which directly affect the embedded proteins and their functional interactions (Debnath *et al.*, 2011). Individual membrane proteins are normally associated with specific lipids in the membrane for maintenance of correct folding and function (Lee, 2005). In a surfactant micellar environment, the absence of normally bound lipids as well as a diminished lateral pressure, may affect the stability and functionality of membrane proteins leading, to rapid inactivation (Zhou *et al.*, 2001).

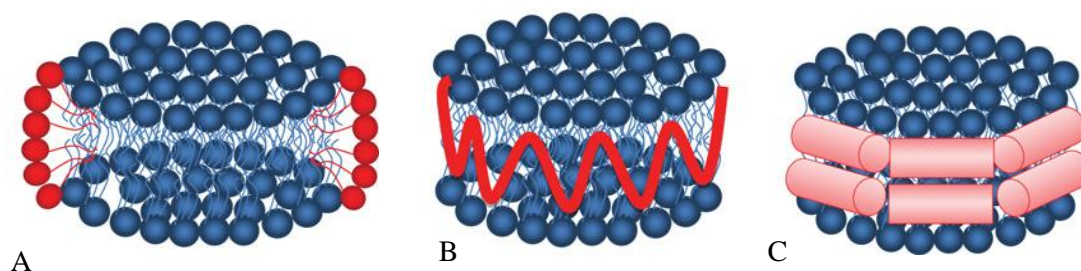


Figure 1-15 Protein encapsulation methods produce: (A) bicelles, (B) amphipols and (C) nanodiscs. Lipids bilayer in blue with bicelles, amphipols and nanodisc membrane scaffold proteins in red (from Jamshad *et al.*, 2011)

As a consequence, alternative methods have been developed to create a less destabilising environment after surfactant extraction; these include adopting procedures to decrease the concentration of surfactant or transfer of membrane proteins to less aggressive environments, including bicelles, amphipols and nanodiscs, depicted in figure 1-15.

1.6.2 Bicelles

Bicelles are a mix of surfactants such as DMPC or CHAPS with short chain lipids that form highly curved discoidal structures (Sanders and Prosser, 1998). At optimised lipid

to surfactant ratios, disc-like structures form with a lamella lipid layer surrounded by non-bilayer forming lipids as depicted in figure 1-15 (Jamshad *et al.*, 2011). The drawback to this method of extraction is that it is not possible to form bicelles directly from biological membranes; instead, a surfactant extraction step is necessary prior to bicelle formation (Jamshad *et al.*, 2011).

1.6.3 Amphipols

A second encapsulation method for membrane proteins are amphipols: amphipathic polymers containing hydrophobic side chains with a hydrophilic backbone (Popot, 2010). Amphipols are milder than surfactants and proteins are usually in a more stable form after encapsulation in an amphipol compared to surfactant solutions; however, surfactant extraction is still required before encapsulation in most cases (Popot, 2010). The method is highly dependent on precise concentrations and very small errors can result in amphipol aggregation and thus insufficient protein solubilisation (Picard *et al.*, 2006). A second problem concerning amphipols is that they can cause functional inhibition of proteins as demonstrated by Picard *et al.* (2006); they demonstrated that amphipols interfered with the intrinsic ATPase activity of the eukaryotic sarcoplasmic reticulum Ca^{2+} -ATPase protein.

1.6.4 Nanodiscs

Nanodiscs have been used to stabilise membrane proteins after surfactant removal (Bayburt and Sligar, 2002). Nanodiscs are discoidal nanometer-sized phospholipid bilayers encircled by an engineered amphipathic, helical membrane scaffold protein (Figure 1-15), which self-assembles to reconstitute membrane proteins within a semi-native membrane (Bayburt and Sligar, 2002; Borch and Hamann, 2009). The nanodisc membrane environment is believed to better reflect that of complex biological membranes, allowing easier integration of membrane proteins and maintenance of the folded structure (Shaw *et al.*, 2004). Further advantages of nanodiscs over other methods are that they have a more monodisperse and consistent size and are more stable over time due to the presence of the protein belt (Shaw *et al.*, 2004). However, nanodiscs are expensive to produce, membrane proteins must first be solubilised with surfactants and once the membrane proteins are captured it is difficult to remove them

for experimentation (Jamshad *et al.*, 2011). The major advantages and disadvantages of membrane protein solubilisation methods described are listed below in table 1-1.

Table 1-1 Advantages and disadvantages of membrane protein solubilisation studies

Solubilisation method	Advantage	Disadvantage
Surfactants	Size homogeneity	Causes for decrease in lateral pressure Can lead to inactivation of membrane proteins Associated lipids are disrupted Concentrations below CMC results in membrane protein aggregation
Bicelles	Suitable for many biophysical studies	Surfactant solubilisation needed prior to membrane protein insertion Limited choice of lipid combinations
Amphipols	Size homogeneity Maintains membrane protein lateral pressure	Surfactant solubilisation needed prior to insertion of membrane proteins
Nanodiscs	Size homogeneity Native lipid environment Maintains membrane protein lateral pressure	Membrane scaffold protein (MSP) can interfere with functional studies of membrane proteins Surfactant solubilisation needed prior to formation

Despite the above listed drawbacks, these methods have greatly improved the field of membrane protein research; however, a method that both extracts and solubilises membrane proteins in a semi-native state for downstream analysis is yet to be widely available. A recent development that addresses this issue is the use of styrene maleic acid lipid co-polymer or ‘SMALPs’ (Knowles *et al.*, 2009)

1.7 Use of SMALPs to solubilise membrane proteins

Poly (styrene-co-maleic acid) (SMA) (Figure 1-16) has been used widely in the engineering of plastic film coverings and has received limited use in cosmetic products such as UV radiation protection and anti-aging products (Tonge, 2006; Pompe *et al.*, 2003). However, in recent years the use of low molecular weight SMA for membrane solubilisation has been adopted (Tonge and Tighe, 2001; Tonge, 2006; Knowles *et al.*, 2009).

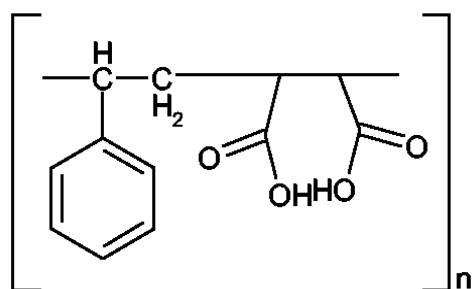


Figure 1-16 Styrene/maleic acid co-polymer (Tonge, 2006)

SMA is an amphipathic polymer composed of alternating maleic acid (hydrophilic) and styrene (hydrophobic) moieties that are soluble in water at neutral and alkaline pH but insoluble at a lower pH due to protonation of the maleic acid moiety (Tonge, 2006; Jamshad *et al.*, 2011). Thus, SMA is a hypercoiling polymer that is sensitive to environmental pH (on/off switch) due to the balance between charge repulsion and hydrophobic interaction, enabling the polymer to transition from a charged extended state at low pH to a collapsed uncharged coil structure at neutral or higher pH (Tonge and Tighe, 2001). These properties enable SMA to auto-assemble at neutral or alkaline pH into a biological membrane to form discoidal structures around membrane proteins and their associated lipids (Tonge, 2006). Abundant membrane proteins including bacteriorhodopsin (bR) and PagP, have been successfully solubilised in SMA to produce SMALPs containing membrane proteins (Knowles *et al.*, 2009). The solubilised membrane proteins exhibited native function and correct folding as determined by circular dichroism, analytical ultracentrifugation and differential scanning calorimetry (Knowles *et al.*, 2009).

The SMALPs method is superior to previous membrane protein solubilising procedures as it effects solubilisation of membrane proteins and protein complexes in a semi-native

state together with associated lipids to maintain correct folding and function without the use of surfactants. The method is still in early development with very few proteins (primarily from Gram-negative bacteria) solubilised thus far. However, it has great potential for solubilising single membrane proteins and may have potential for the extraction of functional membrane protein complexes such as the transient PBP2/PBP2a complex in MRSA.

1.8 Aims and Objectives

MRSA infections remain a significant health concern, both in hospital and community settings. The development of truly novel antibiotics has slowed significantly over the last half-century and we should consider alternative treatment strategies in order to overcome bacterial resistance to antibiotics. The use of compounds such as ECg to sensitise resistant organisms, including MRSA, to existing antibiotics is a strategy that is worthy of investigation. A deeper understanding of the mode of action of ECg with respect to its capacity to abrogate β -lactam resistance will underpin efforts to develop this molecule, or one of its bioactive analogues (Anderson *et al.*, 2011) as a ‘modifier’ to be used in combination with a conventional antibiotic. At present, it is not possible to fully account for the ECg-induced MRSA phenotype, in particular the restoration of full β -lactam susceptibility. For this profound change to occur, it is assumed that the cell replication machinery is directly compromised. In the presence of oxacillin, MRSA replication continues through the cooperative action of PBP2 and PBP2a which, it has been speculated, forms part of a multi-enzyme complex (Bernal *et al.*, 2009; Bernal *et al.*, 2010). The intercalation of ECg into the cell membrane of MRSA may disrupt PBP2/PBP2a functionality and disperse the protein complex. Bernal *et al.* (2010) showed that ECg does not interfere with PBP2a directly but partially delocalises PBP2 from the site of replication. The native membrane environment is altered by intercalation of ECg, inducing changes in the lipid composition of the cell membrane, and thus may provide an incompatible environment for the maintenance of the multi-enzyme replication machinery. If the PBP2/PBP2a complex is disrupted this could, at least in part, account for the sensitisation of MRSA to oxacillin by ECg.

The overall aim of this study was to increase understanding of the mechanism of MRSA sensitisation to β -lactams by ECg. The objectives of this work were to: 1) develop a method utilising SMA to probe and capture the PBP2/PBP2a complex in a semi-native state inside SMALPs; 2) investigate if ECg disrupts the functionality of the complex and other relevant proteins involved at the site of division that may be involved in ECg-mediated MRSA sensitisation to oxacillin.

CHAPTER TWO

2. ANTIBIOTIC SUSCEPTIBILITY, CELL MORPHOLOGY AND SURFACTANT PROTEIN EXTRACTION

2.2 Introduction

Yam *et al.* (1998) noted the sensitisation of MRSA to β -lactams by aqueous extracts of green tea, demonstrating a decrease in the MIC of β -lactam antibiotics. MRSA cells show significant morphological change after exposure to ECg, as described in section 1.4; failure of daughter cells to separate normally after cell division may be indicative of changes to the environment within the membrane surrounding the division proteins. Markedly reduced β -lactam resistance may also indicate alterations in PBP2a function to confer β -lactam resistance on strains bearing this protein. Bernal *et al.* (2010) demonstrated partial displacement of PBP2 from the division septum after sensitisation by ECg. These data suggest that ECg physically disrupts the PBP2/PBP2a component of the PG biosynthetic machinery and forms the basis of current hypotheses to account for the action of ECg.

2.2.1 The PBP2/PBP2a complex

Induction with a β -lactam antibiotic such as oxacillin may be necessary to ensure full functional expression of the PBP2/PBP2a complex (Bernal *et al.*, 2010). In the presence of oxacillin, PBP2 and PBP2a functionally cooperate to continue replication after the active site of the TPase domain of PBP2 has been acylated by the antibiotic (Pinho and Errington, 2005).

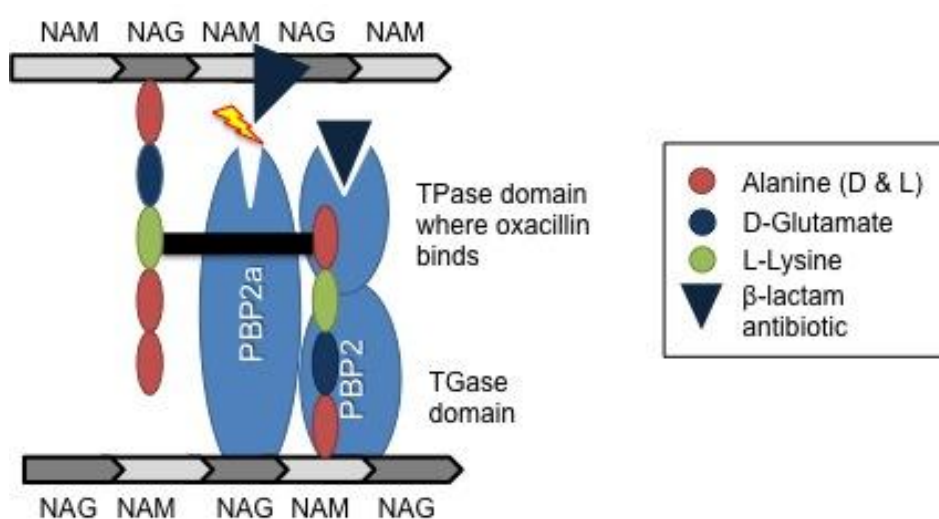


Figure 2-1 Cooperative function of PBP2 and PBP2a in the presence of oxacillin. Oxacillin binds to the active site of PBP2 and inhibits TPase activity; PBP2a, with a low affinity for oxacillin, cooperates with the TGase domain of PBP2 to allow continued cell replication

As described in section 1.2.5, PBP2a has low affinity for β -lactam antibiotics due to structural features around the active site that include a groove and a loop that cover the active site as shown in figure 2-1, allowing TPase activity to continue in the presence of β -lactam agents (Pinho and Errington, 2005). In the absence of β -lactam agents, PBP2 alone can provide TPase and TGase activity for cell replication (Pinho and Errington, 2005). This chapter describes the optimisation of oxacillin treatment of MRSA in order to observe PBP2/PBP2a complex formation.

2.2.2 Use of surfactant to probe for the PBP2/PBP2a complex

Surfactants provide inexpensive and widely available reagents for protein solubilisation to study membrane proteins, including PBP2 and PBP2a (see 1.5.1). Surfactants possess both hydrophobic and hydrophilic groups and enable solubilisation of membrane proteins; however, they have a higher degree of hydrophilicity compared to biological membranes (Helenius and Simons, 1975). Triton X-100 (octylphenol ethylene oxide condensate) is an inexpensive, nonionic, surfactant widely used in protein solubilisation; it has a critical micelle concentration (CMC) of 0.3 (Smith, 2011). Below the CMC, detergent penetrates into the lipid bilayer but cannot form micelles; above the CMC the detergent disrupts the bilayer to form mixed micelles (Luckey, 2008). In order to rule out the use of simple surfactants for the capture of the PBP2/PBP2a complex, Triton X-100-induced membrane protein solubilisation was undertaken.

2.3 Material and methods

2.3.1 Bacterial strains and reagents

EMRSA-16 was provided by Jeremy Hamilton-Miller of the Royal Free University College London Medical School (RFUCMS). CA-MRSA strain USA-300 (ATCC BAA-1556) was purchased from the American Type Culture Collection and MSSA strain BB255 from the National Collection of Type Cultures (NCTC 8325). *E. coli* BL21 over-expressing his₆-tagged PBP2 was a gift from Simon Foster (University of Sheffield, UK) and ECg was a gift from Mitsui Norin (Tokyo, Japan). Anti-PBP2a Ab was purchased from My Biosource (San Diego, CA, USA).

2.3.2 Growth requirements

The bacteria were grown in Mueller-Hinton Broth (MHB) (Oxoid Ltd., Basingstoke, UK) with aeration and constant agitation at 37 °C. ECg was dissolved in 50% ethanol and added to MHB to a final concentration of 6.25, 12.5 or 25 mg/L, depending on the application.

2.3.3 MIC

The microbroth dilution protocol from the Clinical and Laboratory Standards Institute (CLSI) guidelines (CLSI, 2008) was used for susceptibility testing. The microbroth dilution assay was favoured over the macrodilution procedure: it is undertaken in U-shaped 96-well plates and requires smaller volumes of test compound. Broth microdilutions were performed in 96-well U microtitre plates (Bibby Sterlin Ltd., Stone, UK) and the plates incubated overnight at 37 °C. All stock concentrations of antibiotics were sterilised with a 0.22 µm syringe filter (Millipore Corporation, Billerica, MA, USA).

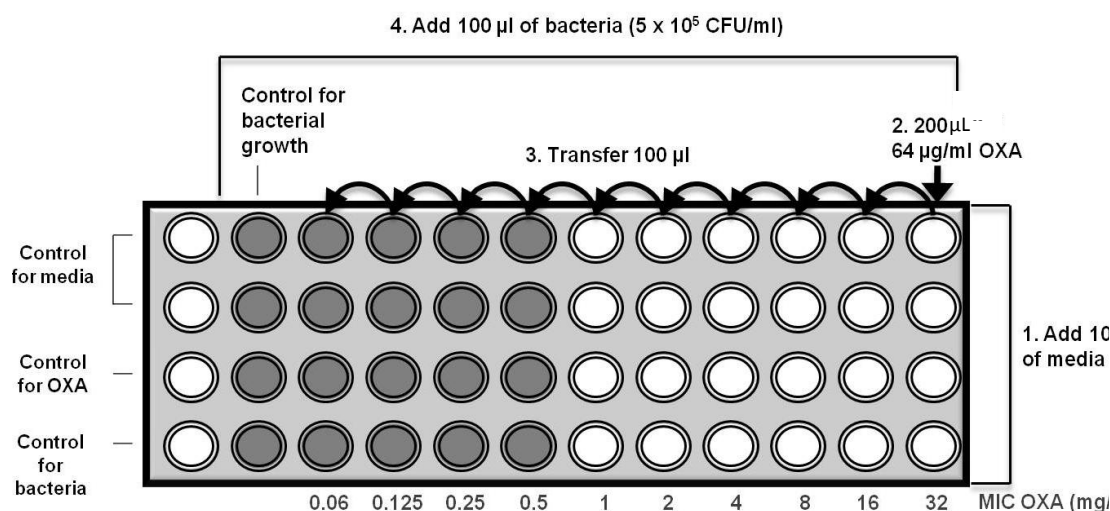


Figure 2-2 U-shaped 96 well plate for MIC determination of test antibiotic oxacillin (OXA). In the first column, medium control: 200 µL MHB was added, control of OXA: 200 µL of OXA with no bacteria, and in control for bacteria: 100 µL bacterial solution with 100 µL of antibiotic at a concentration known to kill the bacteria

For each experiment, stock solutions of antibiotics or catechins were diluted to the required concentration (double the starting MIC in the twelfth column as indicated in

(Figure 2-2) in MHB supplemented with 2% NaCl to enhance expression of β -lactam resistance: 200 μ L of the desired concentration of antibiotic or ECg was dispersed into column twelve (Figure 2-2). One hundred microlitres of MHB was added to the remaining wells in columns two to eleven. Two-fold serial dilutions of oxacillin or ECg were prepared over the ranges 1 - 1024 mg/L or 0.0625 - 32 mg/L.

Bacterial suspensions were grown to an optical density equivalent to 0.5 McFarland (BioMerieux SA, Marcy l'Etoile, France) at 37 °C as outlined in the CLSI guidelines. The inoculum was diluted to a final density of approximately 5×10^5 CFU/mL and 100 μ L added to the wells (final volume of 200 μ L). The plates were sealed with a plastic lid and incubated overnight at 37 °C. The final inoculum density (CFU/mL) was verified by culture of serial dilutions on MH agar (MHA) plates with overnight incubation at 37 °C.

The MIC was determined as the lowest concentration of compound that prevented visible bacterial growth after 16 - 20 h (Swenson and Ferraro, 2008). Various concentrations of ECg and salt (1 - 2% NaCl) were tested and experiments were performed in triplicate.

2.3.4 Morphology

For electron microscopy (EM), bacteria from 50 mL mid-logarithmic phase cultures were collected by centrifugation (5,000 g, 10 min, 4 °C), washed twice with PBS, fixed with 1.5% glutaraldehyde (VWR, Leicestershire, UK) and incubated at RT for 2 h. Samples were washed with 1 mL of 70% ethanol followed by 1 mL 100% ethanol then 500 μ L of 100% ethanol. Cells were gold-coated and examined with a FEI XL30 scanning electron microscope (SEM) (Philips Electron Optics, Eindhoven, Netherlands). EM was undertaken with guidance and advice from Mr David McCarthy (UCL School of Pharmacy, London).

2.3.5 Nascent PG investigation

To examine septal cell wall synthesis in EMRSA-16, fluorescent (FL) labelled vancomycin was used to label the nascent cell wall. In Gram-positive cocci, cell wall synthesis occurs only at the septum, and once the septum is formed, it is subsequently

cleaved to establish the new hemispherical poles of the daughter cells (Pinho and Errington, 2003). There is evidence that ECg alters the division of EMRSA-16 cells and this assay was designed to investigate alterations to the site of division.

FL vancomycin (Bodipy FL) preferentially labels nascent cell wall by binding to D-Ala-D-Ala residues at the carboxy terminus of the PG precursor (Pinho and Errington, 2003). The problem with using Bodipy FL is that the *S. aureus* cell wall contains a large number of D-Ala-D-Ala residues in the mature cells, resulting in fluorescent labelling of the entire cell wall and septum of exponential *S. aureus*, confounding identification of nascent PG. EMRSA-16 nascent PG was labelled according to Pinho and Errington (2003) as follows: bacteria were grown in MHB containing 0.125 M D-serine (Sigma, Dorset, UK) in order to replace the carboxy terminal D-Ala residue of PG precursors with D-serine. This procedure does not alter the mucopeptide composition of PG, except for a decrease in the level of highly-linked oligomerised peptides, which has little effect on cell growth (Pinho and Errington, 2003).

Fifty millilitres of this growth medium were inoculated from an overnight culture; in some experiments, 12.5 mg/L ECg was added. Cells were grown at 37 °C with constant agitation until the OD₆₀₀ reached 0.6, harvested by centrifugation (5000 x g, 10 min, 4 °C) and suspended in fresh MHB without D-serine, allowing incorporation of D-Ala into the cell wall and enabling identification of nascent PG with Bodipy FL. Cells were incubated for 30 min at room temperature (RT) and 1 mL of culture incubated in the dark with 0.15 mg/L Bodipy FL vancomycin (Sigma) for 10 min at 37 °C. Cells were washed twice with MHB, suspended in 100 µL MHB and vortexed to ensure homogeneous distribution of cells; 2 µL was then injected into a drop of 1% overlay agarose (Bio-Rad, Hercules, CA, USA) on a polylysine slide (VWR), a coverslip placed over the suspension and bacteria examined with a Zeiss Axio Observer fluorescent microscope (Zeiss, Oberkochen, Germany). Images were analysed with AxioVision software (Zeiss).

2.3.6 Expression of recombinant PBP2 in *E. coli* for Ab generation

As a commercial PBP2 Ab is not available, purified PBP2 protein was produced from anti-serum against this protein in a rabbit. *E. coli* BL21 cells, containing a his₆-tagged

PBP2 construct (plasmid pGL600) (figure 2-3), were grown to mid-log phase in MHB containing 50 mg/L ampicillin at 37°C with constant aeration.

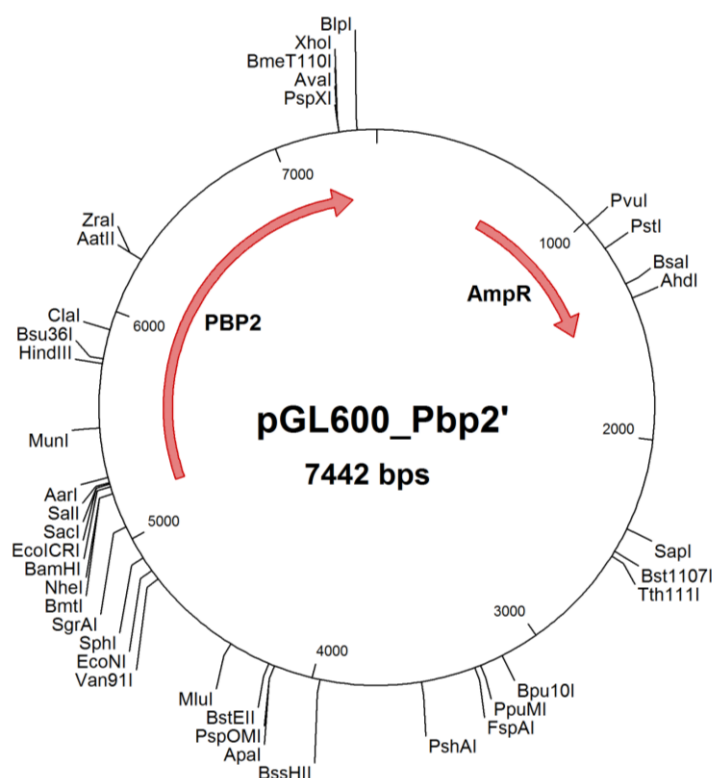


Figure 2-3 Gene map of plasmid pGL600 with the AmpR resistance gene and PBP2 gene

PBP2 expression was induced by addition of isopropyl- β -D-thiogalactopyranoside (IPTG) (Melford, Suffolk, UK), a synthetic analogue of lactose that inactivates the *lac* repressor on the operator and induces expression of his₆-tagged PBP2. IPTG was added to a final concentration of 1 mM and the mixture incubated for 4 h at 37°C. Cells were harvested by centrifugation (5000 g, 10 min) at 4 °C. The pellet was frozen and subsequently suspended in Buffer A (20 mM Na₂-PO₄, 300 mM NaCl pH 7.4), sonicated (3 x 10 sec) and centrifuged at 18,000 rpm for 25 min (Beckman JA20 rotor, Beckman Coulter, High Wycombe, UK). The pellet was suspended in Buffer A containing 8 M urea and, following centrifugation (12000 rpm, 4 °C, 30 min), the supernatant (cell lysate) was sterilised with a 0.22 μ m syringe filter (Millipore Corporation, Billerica, MA, USA) and subjected to IMAC midi purification (Pro-Chem Inc, MA, USA) following manufacturer's instructions.

Pre-packed Ni-imidazole resin midi plug was inserted into the Proteus spin column barrel and the columns equilibrated with 10 mL binding buffer (50 mM Na₂-PO₄, 300 mM NaCl, 10 mM imidazole, 8M urea, pH 7.4) by centrifugation (500 g, 4 °C, 3 min) (Beckman Coulter). Twenty millilitres of the filtered cell lysate was dispensed into the spin column, which was centrifuged (150 g, 4 °C, 30 min). The column was washed three times with 10 mL wash buffer (50 mM Na₂-PO₄, 300 mM NaCl, 30 mM imidazole, 8M urea, pH 7.4) by centrifugation (500 g, 4 °C, 3 min) to remove non-tagged proteins that lack affinity for the immobilized Ni-imidazole metal resin. His₆-tagged PBP2 was eluted from the resin into a new centrifuge tube with 10 mL elution buffer (50 mM Na-PO₄, 300 mM NaCl, 300 mM imidazole, 8M urea, pH 7.4) by centrifugation (500 g, 4 °C, 3 min). Elution was performed twice for each column. Elution buffer containing the protein was filtered through a 3,000 mw 20 mL viva spin column (Sartorius AG, Göttingen, Germany) at 3000 g for intervals of 15 min at 4 °C with the addition of 50 mM Na₂-PO₄ buffer containing 300 mM NaCl at pH 7.4 to remove imidazole and any residual metal ions that may cause irreversible precipitation of the protein when stored at -20 °C. Finally, the solution was concentrated to 1 mL by centrifugation and the purity of purified PBP2 confirmed by SDS-PAGE. This procedure was repeated until a 2 mg/mL solution of PBP2 was attained. Antiserum against the purified PBP2 was commercially generated by Bioserv Ltd (University of Scheffield, UK) using 2 mg/mL protein concentration per rabbit for the production of anti-serum.

2.3.7 Membrane protein solubilisation with Triton X-100

Steps were taken to minimise deleterious effects to the proteins. As membrane proteins have a low abundance, relatively large volumes of bacterial culture are required to obtain adequate amounts of protein (Van Jagow *et al.*, 1994). Due to their hydrophobic nature, aggregation of membrane proteins is likely to occur and relatively high concentrations of surfactants, usually in the range 0.5 - 5% (v/v), are required (Schimerlik, 2001). Further, following protein solubilisation, membrane proteins are prone to protease degradation. Addition of metal chelators such as ethylenediamine tetraacetic acid (EDTA), an inactivator of metalloproteases (protease enzymes with catalytic activity dependent on the presence of metals) through the removal of zinc that is essential for their activity, will aid minimisation of protein degradation. Another protease inhibitor, phenylmethyl sulfonyl fluoride, an inhibitor of serine proteases,

may also be employed. Purification at 4 °C and addition of sodium azide to minimise proteolysis as a result of microbial growth will also aid recovery of intact membrane proteins (Smith, 2011).

One litre of EMRSA-16 was grown to late exponential phase ($OD_{600} \sim 0.8$) in MHB at 37 °C with constant shaking and aeration. For PBP complex analysis, 4 mg/L of oxacillin was added to the culture for 10 min once the desired OD_{600} was reached in order to induce the resistance complex. Cells were collected by centrifugation (5,000 g, 10 min, 4 °C), washed once with PBS (Oxoid Ltd) and suspended in 1 - 4 mL of ice-cold distilled water. The cells were disrupted using a fast prep cell distribution system FP120 (Thermo Fischer Scientific) (40 s, power setting 6) and cell wall debris removed by centrifugation (5000 rpm, 10 min, 4 °C). The cytoplasmic membrane fraction was recovered by ultracentrifugation (Beckman Optima MAX ultracentrifuge) of the supernatant at 130,000 g for 1 h at 4 °C and the pellet suspended in 200-1000 μ L of 10 mM Tris-HCl, pH 7 containing 2% (v/v) Triton X-100 (Sigma), depending on the size of the starting culture, to release membrane proteins. Protein concentration was determined using the Bradford Protein Assay (Bio-Rad). Briefly, Bradford reagent was diluted 1:5 in water and bovine serum albumin (BSA) standards prepared over the concentration range 0.1 - 1 mg/mL. Samples (20 μ L) were added to 1 mL of diluted Bradford reagent and mixed twice by inversion. After five min at RT, absorbance was determined at 595 nm and protein concentration calculated from the BSA standard curve.

2.3.8 PBP analysis

2.3.8.1 Cross-linking with 3,3'Dithiobis [sulfosuccinimidylpropionate] (DTSSP) and 1% formaldehyde

Two cross-linkers, DTSSP (Thermo Fischer Scientific) and formaldehyde (BDH Laboratory Supplies, Poole, UK), were used in attempts to recover PBP2/PBP2a complexes from EMRSA-16. DTSSP is a reversible homo-functional thiol-cleavable cross-linker that reacts with primary amines, forming bonds that result in the release of N-hydroxysuccinimide (Vollmer, 2006). The advantage of DTSSP over the functionally related cross-linker dithiobis (succinimidylpropionate) is its water solubility (Vollmer, 2006). DTSSP cross-links closely associated proteins by virtue of a 12 Å spacer arm

and establishes an internal disulfide bond between two proteins in proximity of less than 1.2 nm. The cross-linker is cleavable with 5% β -mercaptoethanol (Sigma). Cell membrane proteins prepared as described in section 2.3.7 were cross-linked with DTSSP prior to protein-protein pull down assays. DTSSP was dissolved to a final concentration of 10 mM in 200 μ l of protein solution (\sim 1.0 mg/mL protein) and incubated at 4 °C for 30 min. The cross-linking reaction was quenched by addition of 2.5 μ L of 1 M Tris, pH 7.5 and the mixture incubated for 15 min at 4 °C (Bennett *et al.*, 2000). Prior to loading the protein sample for SDS-PAGE, the cross-linker was cleaved by addition of 5% β -mercaptoethanol in sample buffer.

The low molecular mass of formaldehyde allows rapid penetration of the membrane and subsequent fixation of membrane proteins. Cross-linking is also reversible, allowing separation of protein complexes by boiling prior to SDS-PAGE (Müller *et al.*, 2011). The procedure described in section 2.3.7 was used with minor alterations; 1 L cultures of EMRSA-16 were grown to $OD_{600} = 0.6$ at 37 °C with constant agitation and aeration and then exposed to 4 mg/L oxacillin for 10 min to induce the resistance complex. At this point, 1% formaldehyde was added to the culture and the cells incubated for 5 - 20 min at 37 °C to enable cross-linking of proteins. Cross-linking was arrested by addition of 0.05 M glycine followed by incubation for 5 min at RT. Cells were harvested and membrane proteins collected as described in section 2.3.7.

2.3.8.2 Probing for the PBP2/PBP2a complex

To probe for protein complexes, a Dynabeads co-immunoprecipitation kit (Life Technologies Ltd. Paisley, UK) was used: Dynabeads M-270 epoxy (10 mg) were washed with 1 mL of C1 buffer followed by coupling of 10 μ g of Ab (anti-PBP2) to the Dynabeads in C1 (500 μ L/ 1 μ L of Ab) and C2 (500 μ l) buffer to a total volume of 1 mL. Ab coupling was performed overnight on a roller at 37 °C and the coupled Dynabead-Ab washed with HB buffer followed by LB buffer and two short washes with SB. Finally, the Dynabeads were washed with SB at RT for 15 min on a roller and the beads suspended in fresh SB buffer to give a final bead-Ab concentration of 10 mg/mL. Protein samples were centrifuged; \sim 0.05 g of cross-linked membrane proteins extracted with Triton X-100 were suspended in 0.45 mL immune precipitation (IP) buffer (PBS, 100 mM NaCl, pH 7.0) and added to the beads prior to incubation on a roller at 4 °C for 30 min. Subsequently, beads were washed three times with IP buffer and once with

LWB. The protein complexes were eluted from the dynabeads with 60 μ L EB (0.1 M citrate pH 2.0 - 3.0). Protein content of the eluents was determined using the Bradford assay and protein complexes investigated by SDS-PAGE and Western blotting.

2.3.9 Detection of proteins with 1D gel electrophoresis

Total membrane protein or protein complexes were investigated by SDS-PAGE on a 10% (w/v) acrylamide/bis-acrylamide gel matrix. Under denaturing conditions that dissociate the proteins into individual polypeptide subunits, proteins may be separated on a polyacrylamide gel (Shapiro *et al.*, 1967). SDS is bound to proteins, resulting in protein unfolding to generate random rod-like chains and masking the intrinsic charge of the proteins (Gallagher, 2006). Denatured polypeptides are bound by SDS in proportion to the molecular weight of the polypeptide, resulting in negatively-charged SDS-protein complexes with a charge to mass ratio inversely proportional to molecular weight. The resolution of the polyacrylamide gel is governed by the polyacrylamide concentration and the degree of bisacrylamide-dependent cross-linking. The size of the gel pores is inversely dependent on the bisacrylamide: acrylamide ratio, with a ratio of 1:29 able to resolve polypeptides with size differences below 3% (Gallagher, 2006).

Membrane samples were adjusted to 20 μ g of protein in 10 μ L volume with PBS and combined with an equal amount of 2x Laemmli sample buffer (4% (w/v) SDS, 20% (v/v) glycerol, 10% (v/v) β -mercaptoethanol, 0.0004% (w/v) bromophenol blue, 0.125 M Tris-HCl, pH 6.8), followed by protein denaturation at 95 °C for 5 min; samples were then loaded onto the gel. Gels were run at 100 Volts (V) constant V until the bromophenol blue dye reached the bottom of the gel. Proteins were visualised with Coomassie brilliant blue (Sigma) or silver stain (Invitrogen Ltd., Paisley, UK) with a limit of detection of 0.2 μ g and 0.002 μ g protein respectively. Coomassie brilliant blue (3 g/L Coomassie brilliant blue R250: 10% acetic acid: 40% methanol) was added to distilled water-washed gels for 1 h, followed by de-staining for 2 h with 10% Acetic Acid: 40 % methanol. For silver staining, gels were washed with ultrapure water for 10 min followed by fixation in 30% ethanol: 10% acetic acid overnight at 4 °C. Gels were washed twice in 10% ethanol for 5 min. Gels were then incubated in sensitizer working solution (1 part silver stain sensitizer: 500 part ultrapure water) from the kit for 1 min followed by two washes in ultrapure water for 1 min. Subsequently, gels were incubated in stain working solution (1 part silver stain enhancer: 50 part silver stain) for 30 min

followed by two 20 s washes in water. Developer working solution (1 part silver stain enhancer: 50 parts silver stain developer) was added until protein bands appeared and 5% acetic acid solution added to terminate the development.

2.3.10 Western blot

Proteins were identified by Western blotting (Towbin *et al.*, 1979). The immunodetection of proteins by Western blotting is a powerful tool for the study of individual proteins and is highly compatible with proteins of low abundance. Proteins are electrophoretically transferred from a post-electrophoresis SDS-PAGE gel to an adsorbent polyvinylidene membrane and proteins bound to the membrane detected with Ab probes (Kurien and Scofield, 2006).

Proteins were transferred to polyvinylidene flouride (PVDF) microporous membranes (Millipore) with a uniform pore structure of 0.45 μ M pores to enable a high binding capacity of proteins with a molecular mass greater than 10 kDA. Migration of proteins is dependent on Ohm's law $V = I \times R$; V is generated across the electrodes is equal to the current (I) applied to the system multiplied by the resistance (R) generated by the transfer buffer, filter papers, gel and membrane.

The electrophoretic transfer was performed as a wet transfer utilizing a Mini Trans-Blot cell (Bio-Rad) with a blotting area of 10 x 7.5 cm. Prior to transfer, the membrane was prepared by soaking in 100 % methanol for 15 s, followed by 2 min in de-ionized water and a minimum of five min in transfer buffer (25 mM Tris, 192 mM glycine, pH 8.3). The gel and membrane sandwich was put in place (Figure 2-4), held together by a gel holder cassette and inserted into the buffer tank together with an ice block to avoid over heating of the membrane leading to protein degradation and insufficient transfer.

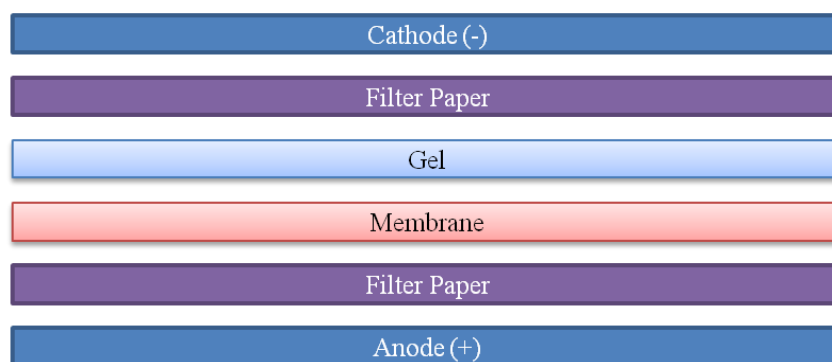


Figure 2-4 *Electrophoretic transfer*

After complete submersion of the membrane sandwich in transfer buffer, a standard stir bar was added to maintain even buffer temperature and ion distribution. Transfer was performed at 100 V (Constant V) for 1 h at RT followed by membrane blocking for 1 h at RT with 40 mL Western blotting solution (TBST) (20 mM Tris pH 7.4, 0.15 M NaCl, 0.1% Tween, 1% skimmed milk powder) on a shaker. Membranes were then incubated with the appropriate primary Ab (anti-PBP2 and -PBP2a) in 30 mL Western blotting solution at optimised concentration and incubated overnight at 4 °C on a shaker. Membranes were washed four times for five minutes with 40 mL TBST followed by incubation of membranes with an appropriate volume of monoclonal secondary Ab conjugated to horseradish peroxidase (HRP) in 20 mL Western blotting solution for one hour at RT on a shaker. After four washes of five minutes with TBST, protein bands were detected with 3,3',5,5'-tetramethylbenzidine (TMB) (Bio-Rad), a solution containing a peroxide substrate. The protein bands were scanned using the Molecular Imager FX (Bio-rad) and examined using Quantity One Advanced software.

2.4 Results

2.4.1 Effect of ECg on MRSA

2.4.1.1 Sensitisation of MRSA to oxacillin with ECg

The growth of MSSA (BB255) and EMRSA-16 was examined in the presence and absence of 12.5 mg/L ECg to determine if exposure altered bacterial growth kinetics. OD₆₀₀ was determined over 24 h as shown in figure 2-5. No differences observed in the growth of either strain when cells were exposed to ECg.

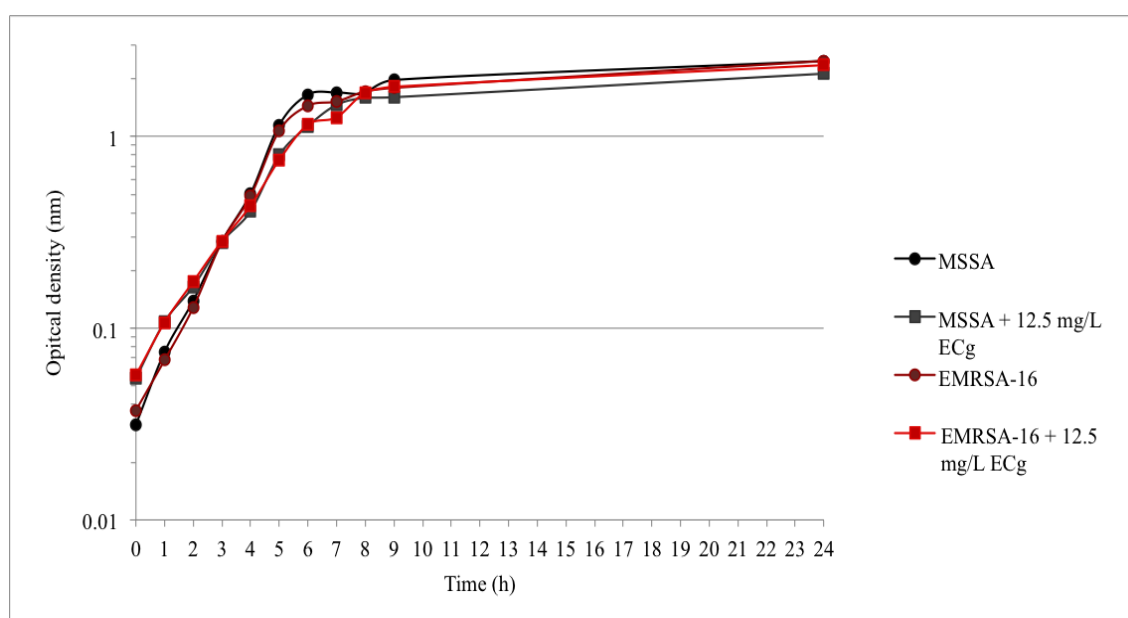


Figure 2-5 Growth of MSSA (BB255) and EMRSA-16 in MHB containing 12.5 mg/L ECg

To investigate the capacity of ECg to sensitise MRSA to β -lactam agents, the MIC for oxacillin was determined in the presence of various concentrations of ECg (0, 6.25, 12.5 and 25 mg/L) in 1 and 2% NaCl. Oxacillin MICs for EMRSA-16 are shown in table 2-1. The MIC of oxacillin for EMRSA-16 is 512 mg/L. Increasing concentrations of ECg reduced the MIC; NaCl enhanced this sensitisation and 12.5 and 25 mg/L ECg reduced the MIC to levels below 1 mg/L.

Table 2-1 MICs of oxacillin against EMRSA-16^a

NaCl concentration in MHB	Oxacillin MIC (mg/L)			
	ECg (mg/L)			
	0	6.25	12.5	25
1%	512	16	1	0.125
2%	512	4	0.5	<0.06

^a Assays were performed in triplicate; no variation was noted

2.4.1.2 Antibiotic treatment optimisation

Pinho and Errington (2005) proposed that PBP2 and PBP2a cooperate only in the presence of β -lactam agents. ECg sensitises MRSA to β -lactams; therefore, conditions allowing maximum recovery of intact bacterial cells after ECg and β -lactam exposure were investigated. Control and ECg-exposed EMRSA-16 cells were grown to mid-logarithmic phase and exposed to 4 mg/L of oxacillin. CFU/mL was determined at 10 min intervals for 1 h following addition of the antibiotic as seen in figure 2-6.

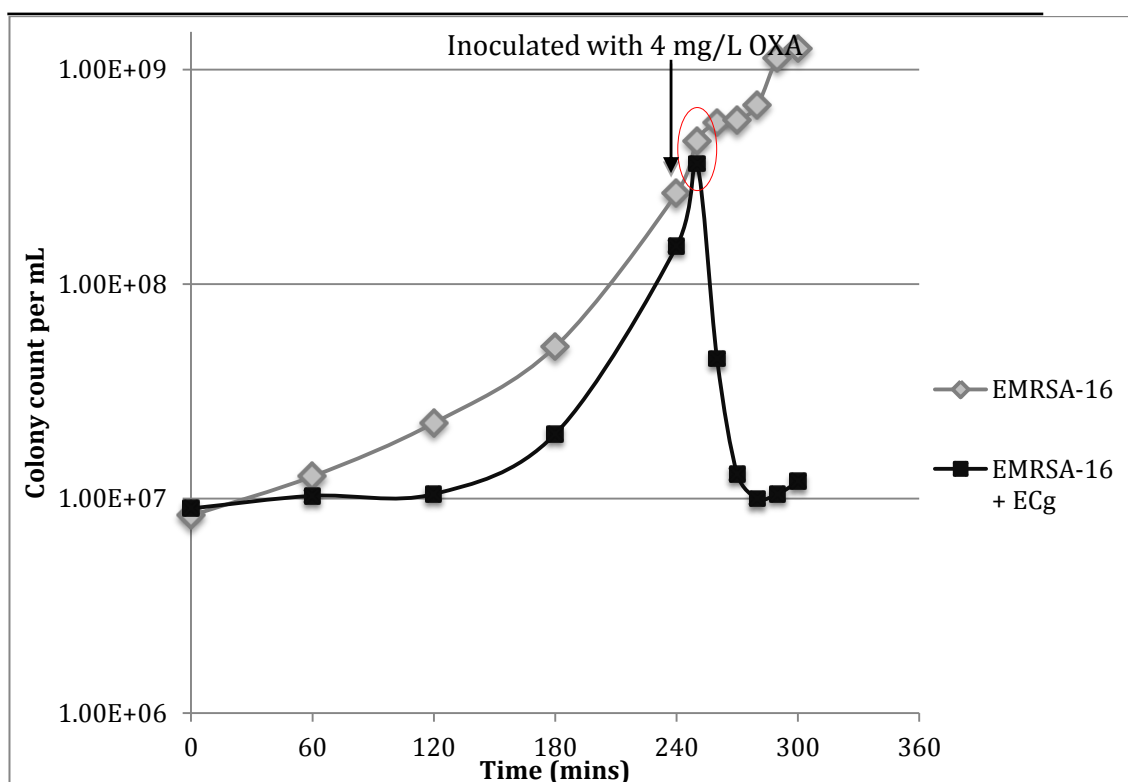


Figure 2-6 Viability of mid-logarithmic phase EMRSA-16 after exposure to 4 mg/L oxacillin after 4 hours of growth. Bacteria were either grown in MHB or MHB supplemented with 12.5 mg/L ECg. The red circle indicates the optimal time point for recovery of cells (10 min post-induction)

The optimum length of exposure to the antibiotic prior to cell collection was determined to be 10 min; after this time point, viable cell numbers were substantially reduced, also seen microscopically. Exposure of EMRSA-16 cells to 12.5 mg/L of ECg caused a delay in the lag phase of growth.

2.4.1.3 The effect of oxacillin on MRSA morphology

The morphology of 12.5 mg/L ECg-grown and control cells after 10 min of 4 mg/L oxacillin induction was examined by SEM (Figure 2-7).

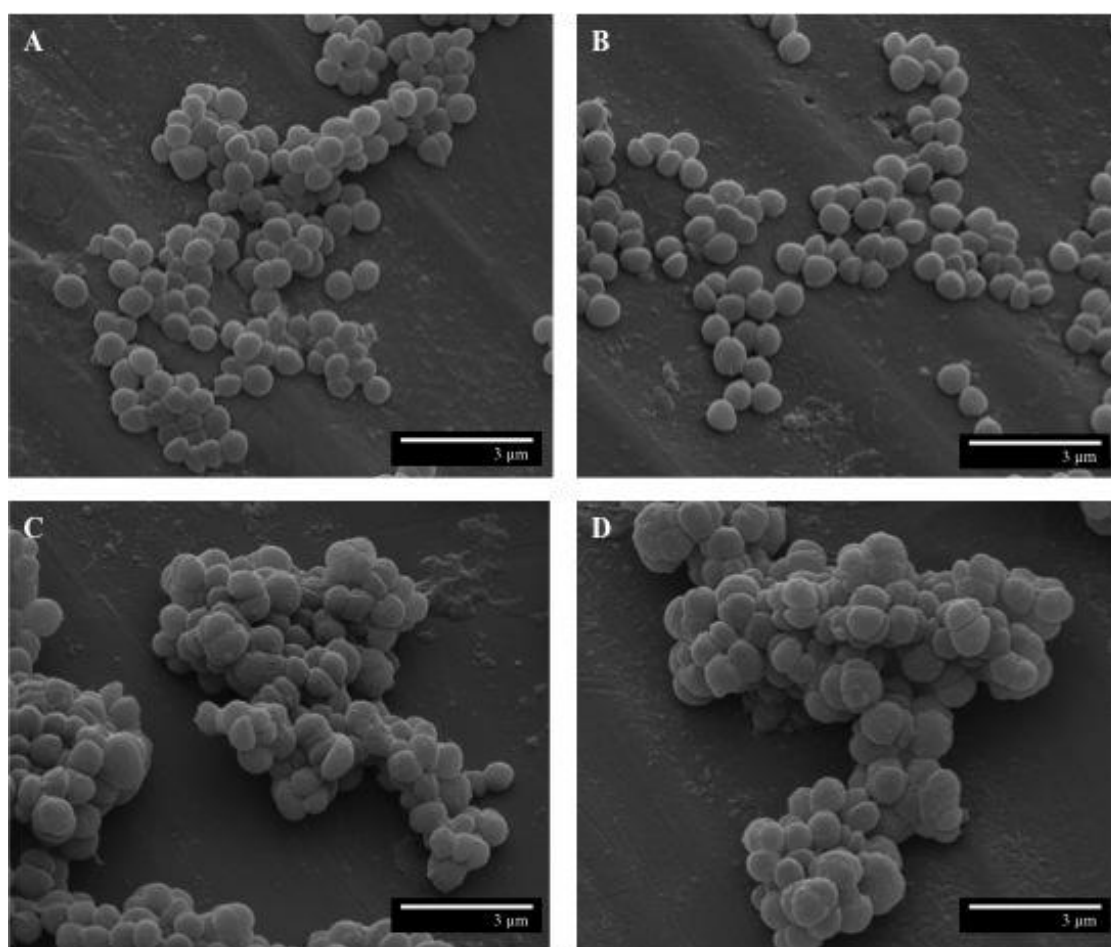


Figure 2-7 SEM of EMRSA-16 cells grown to mid-logarithmic phase (A and B) in the absence or (C and D) presence of 12.5 mg/L ECg either in the (A and C) absence or (B and D) presence of 4 mg/L oxacillin

There were no obvious differences in the morphology of bacteria exposed to ECg, aside from a glossy coating of the cell exterior following oxacillin exposure.

2.4.1.4 Impact of ECg on nascent PG synthesis

The effect of ECg on PG synthesis at the division septum was analysed by visualisation of newly incorporated D-Ala-D-Ala residues by the labelling with Van-FL (Figure 2-8) according to Pinho and Errington (2003).

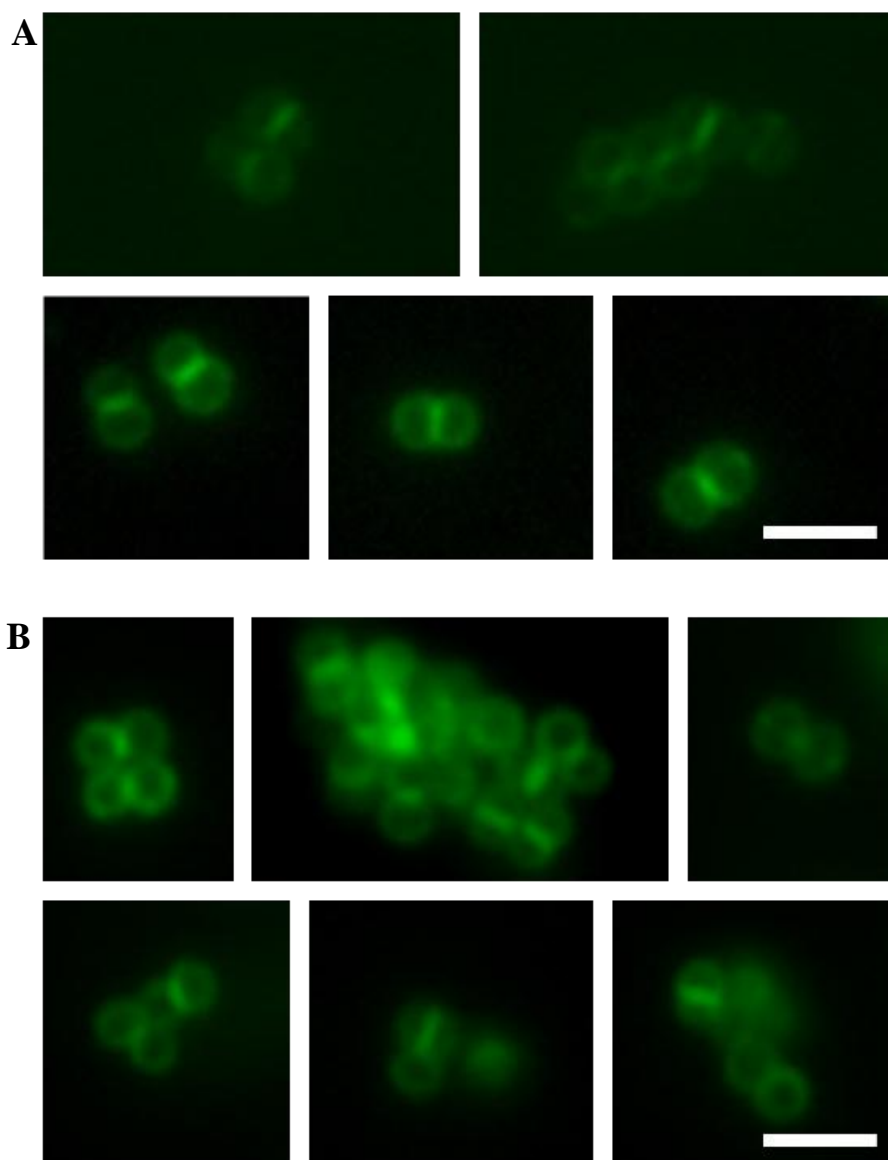


Figure 2-8 Localisation of nascent PG (D-Ala-D-Ala) in (A) control and (B) ECg-exposed EMRSA-16 following Van-FL labelling and fluorescence microscopy. Scale bar: 2 μ m

There was no discernible difference observed for nascent PG between EMRSA-16 grown in the presence of ECg and control cells. Nascent PG was found primarily at the division septum or in a ring structure in both instances. The only difference observed was an increase in clumping of cells following exposure to ECg.

2.4.2 Probing for the PBP2/PBP2a complexes

2.4.2.1 Anti-PBP2 and PBP2a Abs

In order to generate anti-PBP2 antiserum, recombinant PBP2 was expressed in, and purified from, *E.coli* BL21.

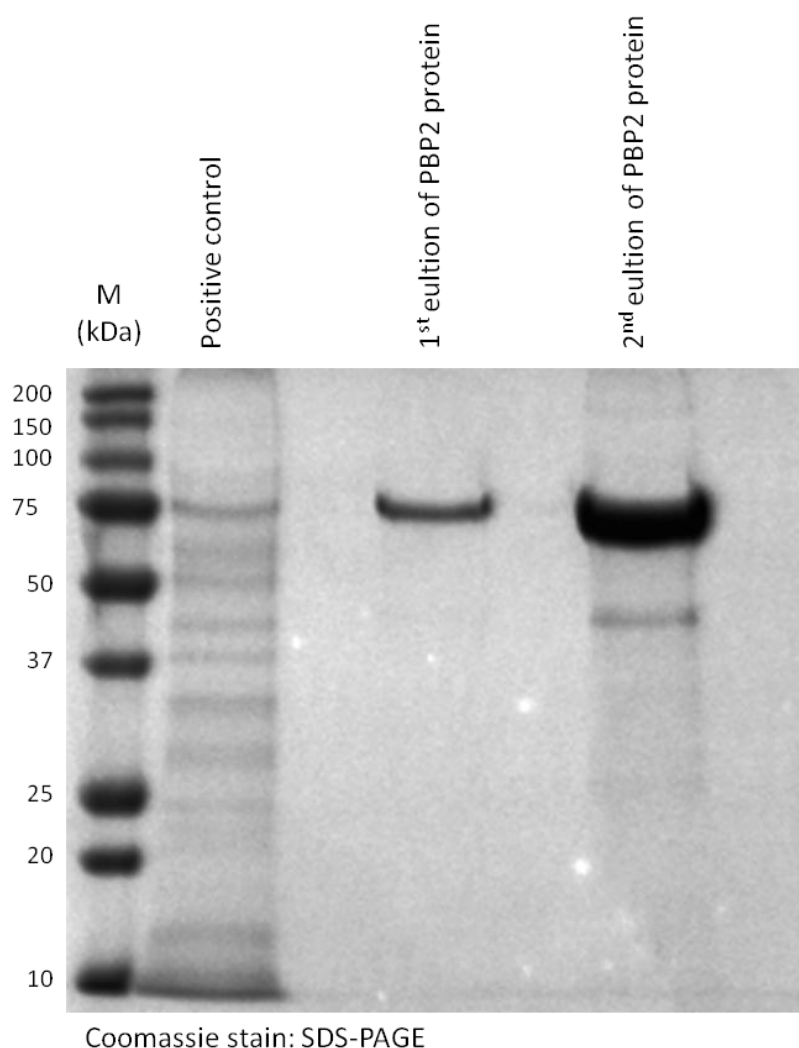


Figure 2-9 SDS-PAGE of the first and second elution of PBP2 recovered from *E. coli* BL21. Positive control of total EMRSA-16 membrane proteins solubilised with triton X-100

Purified protein was assessed by SDS-PAGE (Figure 2-9). Eluents were pooled to a final protein concentration of 2 mg/L and sent to Bioserv for commercial rabbit anti-serum production. Specificity of the Bioserv PBP2 Ab and the commercially available anti-PBP2a Ab was examined against MSSA (BB255) and EMRSA-16 membrane proteins with SDS-PAGE and Western blotting as shown in figure 2-10.

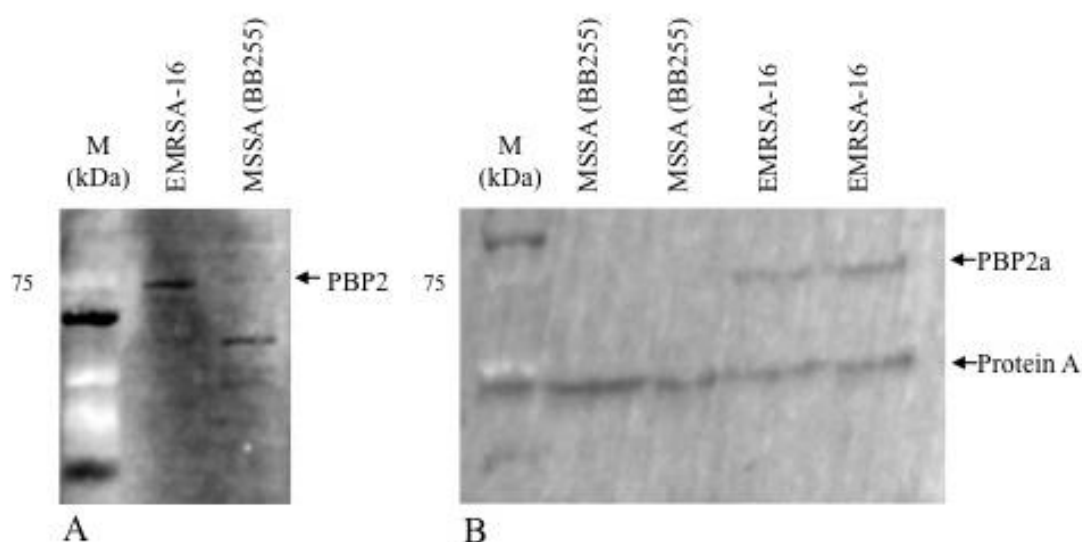


Figure 2-10 Western blots of MSSA (BB255) and EMRSA-16 total membrane proteins using (A) Bioserv anti-PBP2 Ab or (B) commercially available anti-PBP2a Ab

PBP2 was detected in EMRSA-16 and MSSA membrane preparations at the expected molecular weight of approximately 78 kDa. PBP2a was detected in EMRSA-16 but not in MSSA cells. However, an additional band at approximately 50 kDa was also found in all preparations, suggesting a degree of non-specific binding. The molecular mass of the non-specific band was that expected for protein A, a secreted *S. aureus* protein that binds to the Fc region of Abs.

2.4.2.2 Surfactant membrane protein solubilisation for detection of PBP2/PBP2a complexes

Subsequently, the capacity of surfactant Triton X-100 to solubilise intact PBP2/PBP2a complexes was assessed by co-immunoprecipitation. Solubilised membrane proteins were cross-linked with 1% formaldehyde (5 or 20 min) or DTSSP (30 min) and subjected to immunoprecipitation using columns coated with anti-PBP2 Ab through affinity attachment. Immunoprecipitation eluents were separated by SDS-PAGE and probed by Western blotting with PBP2 and PBP2a Abs. PBP2 was detected in all three samples; PBP2a was not found (Figure 2-11) indicating that PBP2/PBP2a complexes could not be detected by Triton X-100 solubilisation. It was not possible to co-purify PBP2/PBP2a complexes with the detergent used.

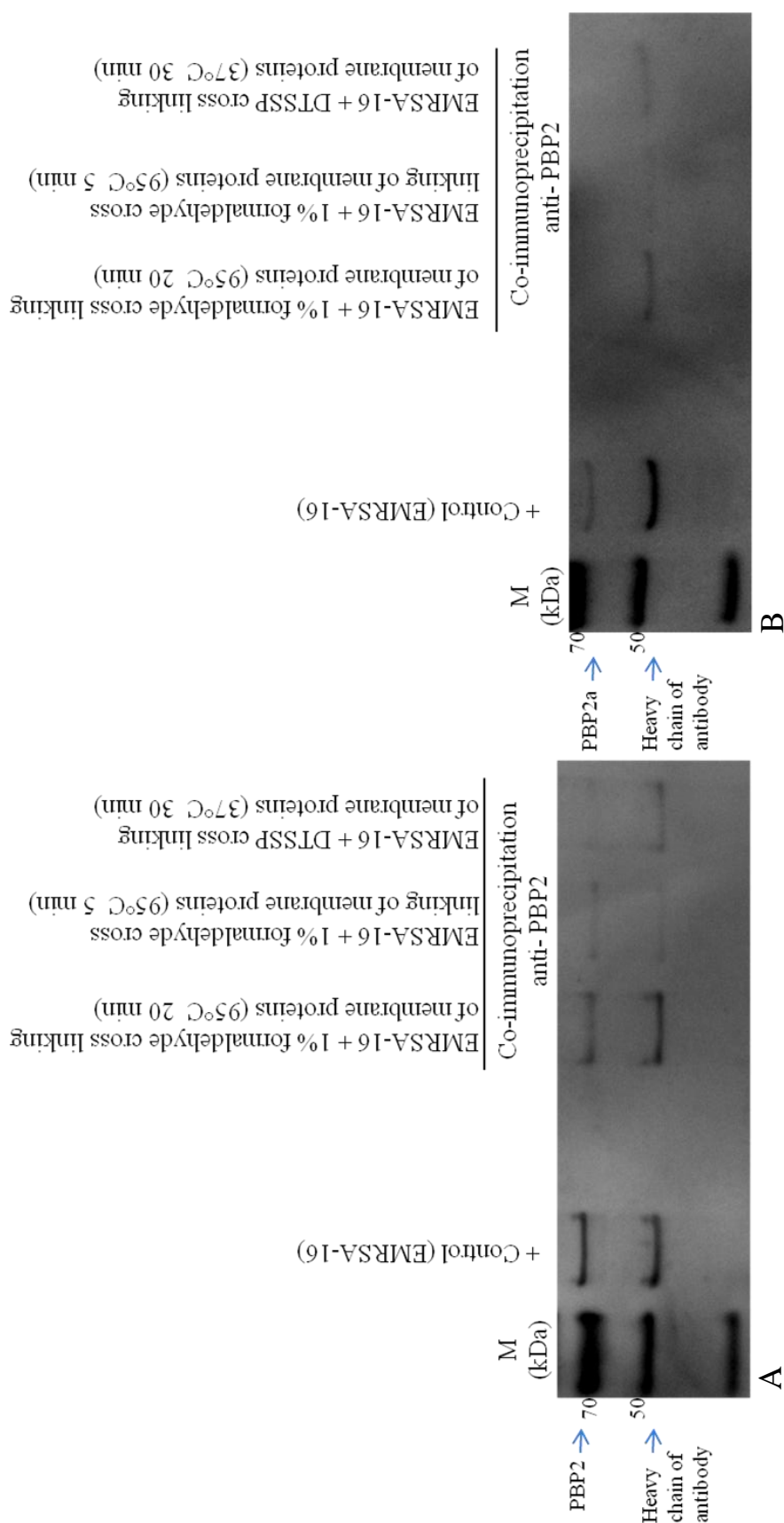


Figure 2-11 Anti-PBP2 Ab co-immunoprecipitation of cross-linked EMRSA-16 membrane proteins solubilised with surfactant Triton X-100. Enriched proteins were separated by SDS-PAGE and Western blots probed with (A) anti-PBP2 and (B) anti-PBP2a antiserum. PBP2a was not found complexed with PBP2

2.5 Discussion

PBP2 and PBP2a are essential for division of MRSA cells in the presence of β -lactam agents. PBP2 and PBP2a are class A and class B PBPs, respectively, and probably cooperate within a multi-enzyme complex (Pinho *et al.*, 2001b). There have been several studies in other bacterial species that provide evidence for interactions between class A and class B PBPs. Examples include *Haemophilus influenza* (Alaadini and Day, 1999) and *B. subtilis* (Simon and Day, 2000). These studies employed protein cross-linking to establish the presence of PBP complexes. Alaadini and Day (1999) used a cyanogen cross-linker specific for salt bridges to identify two multi-enzyme PBP complexes of PBPs by chromatographic profiling of PBPs labelled with dansyl-penicillin, which reacts with primary amino groups in aromatic amines to emit a fluorescent signal. Following cross-linking, two prominent peaks of approximately 400 and 600 kDa molecular weight replaced the seven initial PBP peaks, indicating the presence of complexes following cross-linking. The same cross-linker was used in a study by Simon and Day (2000) to identify covalently-linked PBP complexes in *B. subtilis*.

In *S. aureus*, Pinho *et al.* (2001b) speculated that PBP2 and PBP2a form a complex in MRSA. Inactivation of the PBP2 TGase domain resulted in loss of β -lactam resistance, demonstrating that this domain is absolutely required for expression of the resistant phenotype and was indicative of an interaction between the PBP2 TGase and the PBP2a TPase domains. A second study by Pinho and Errington (2005) went one step further to show that PBP2 localisation to the site of division at the septum is dependent on the interaction with non-acylated PBP2a in the presence of oxacillin. PBP2 required substrate availability (D-Ala-D-Ala) for correct localisation, which is blocked in the presence of oxacillin, leading to dispersal of PBP2 throughout the cell membrane. However, in the presence of PBP2a, normal localisation of PBP2 at the septum was observed, suggesting substrate binding to PBP2a. This observation implies that PBP2 and PBP2a form a multi-enzyme complex in the presence of β -lactams, both for cooperation of TPase and TGase domains as well as functional localisation dependent on substrate recognition (Pinho and Errington, 2005). In order to probe for hypothetical PBP2/PBP2a complexes and determine if ECg disrupts complex formation, oxacillin induction of complex formation was necessary. As discussed, previous PBP complex

research indicated that cross-linking was desirable to facilitate co-immunoprecipitation and capture of the unstable complex (Pinho and Errington, 2005).

ECg causes for an initial delay of the lag phase of EMRSA-16 growth, most probably due to the cells adjusting to the intercalation of ECg into the cell walls as cells first display a less fluid cell wall following one hour as the cells overcompensate followed by a more fluid cell wall (Palacios *et al.*, 2014). The MIC of EMRSA-16 to 12.5 mg/L ECg is 128 mg/L (data not shown); however, at concentrations of 12.5 and 25 mg/L in 2% NaCl (CLSI guidelines for β -lactam resistance), MICs of oxacillin dropped below 0.5 and <0.06 mg/L for the two respective ECg concentrations, consistent with previous data from Stapleton *et al.* (2004). An ECg concentration of 12.5 mg/L was employed in all subsequent work. The impact of oxacillin on ECg-grown cells was not instantaneous and I therefore allowed at least 10 min exposure to the antibiotic prior to the collection of cells. As PBP2/PBP2a complexes only form in the presence of β -lactams (Pinho and Errington, 2005); 10 min exposure to the antibiotic should induce complex formation and allow its capture and analysis.

The morphology of EMRSA-16 cells exposed to ECg confirmed the observations of Bernal *et al.* (2009). Clumping was evident and cells appeared slightly larger with a rougher surface compared to controls but, orthogonal division planes, characteristic of bacteria grown in standard media, were clearly observed (Figure 2-12).

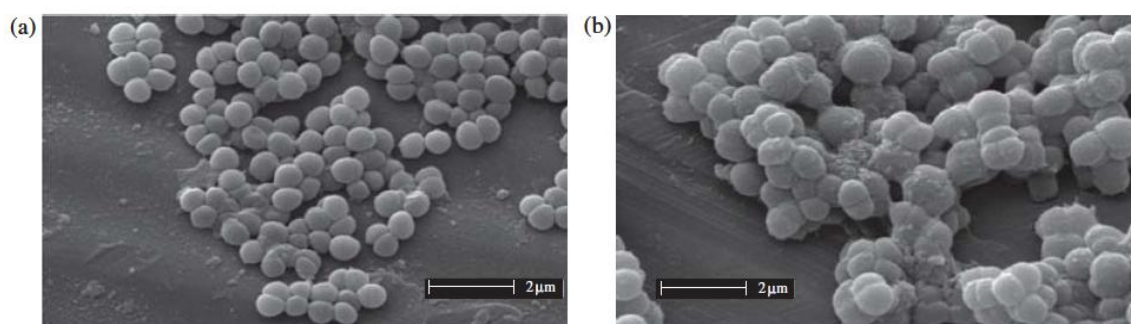


Figure 2-12 SEM of (a) EMRSA-16 and (b) ECg-exposed EMRSA-16 cells grown to mid-log phase (from Bernal *et al.*, 2009)

In a study by Bernal *et al.* (2010) demonstrated that ECg caused delocalisation of PBP2 from the septum; these investigators suggested that this was due to either disruption of the PBP2/PBP2a complex or dislocation of the division septum, resulting in dispersed

PG synthesis. The data showed that nascent PG synthesis was evident at the division septum in ECg treated cells, indicating that the latter is not the case. Previous studies have shown that PBP2 localises within a ring structure (two fluorescent dots) around the future division plane and, as the septum closes, the ring forms a border across the cell corresponding to the established division septum (Figure 2-13).

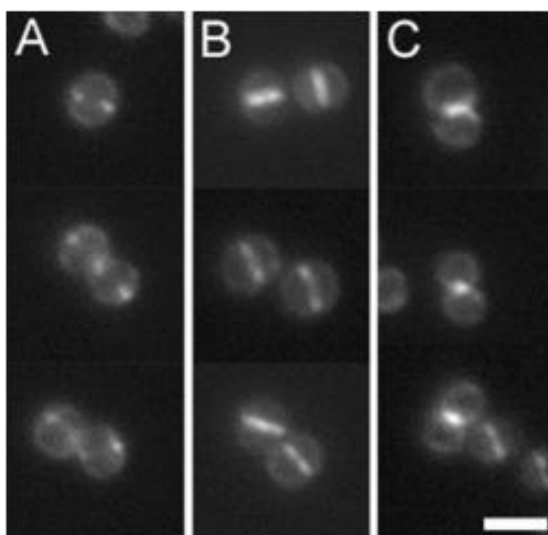


Figure 2-13 Fluorescence imaging of GFP-PBP2 localising PBP2 during cell division in RNpPBP2-31. Initially, (A) two spots are visible corresponding to localisation of PBP2 to the ring surrounding the future division site and (B) a border at mid-cell that appears as the septum closes across the disc containing co-localised PBP2; (C) the process continues as daughter cells are formed. Scale bar: 2 μ M (from Pinho and Errington, 2005).

A similar phenomenon is observed with EMRSA-16 grown in medium containing ECg (Figure 2-8) suggesting that cellular division is not disrupted at the septum by ECg. Taken together with data from Bernal *et al.* (2010) this observation suggests at least partial displacement of PBP2/PBP2a components of the division complex.

Two-hybrid or affinity enrichment methods are frequently used to investigate protein-protein interactions. The two-hybrid system is prone to false positives and does not take into account temporal and local separations within cells. Affinity enrichment frequently results in failure to detect weak interactions due to stringent washing or false positives due to employment of less stringent conditions. Another method widely used in this context is epitope tagging but is limited to investigation of stable complexes. A promising technique for the study of weak and/or transient protein-protein interactions is the use of cross-linkers to fix proteins in close proximity to each other. DTSSP is a soluble, reversible cross-linker with a 12 Å spacer arm that reacts with primary amines.

This reagent has been used to detect interactions between PBP1B and PBP3 in *E. coli* with data confirmed by two-hybrid methodology (Bertsche *et al.*, 2006). Thus, proteins were cross-linked with DTSSP and solubilised with Triton X-100 prior to co-immunoprecipitation. An alternative cross-linker, formaldehyde, was also used to cross-link proteins within whole cells prior to isolation of membranes and solubilisation of membrane proteins. Formaldehyde has a spacer arm of 2.3 - 2.7 Å and represents an alternative to DTSSP (Vasilescu *et al.*, 2004). Formaldehyde is used for histological fixation and at low concentrations (0.5 - 2%) with short fixation times (5 - 30 min) can be used for investigation of protein-protein interactions (Hall and Struhl, 2002). Formaldehyde readily penetrates cells due to its low molecular mass and charge characteristics, is stable (Vasilescu *et al.*, 2004) and inactivates enzymes, “freezing” cells to give a snapshot of interactions at time of addition. However, use of DTSSP and formaldehyde did not lead to the co-purification of PBP2 and PBP2a from Triton X-100 solubilised membranes. One explanation for the capture of PBP2/PBP2a complexes unsuccessful with DTSSP cross-linking was because the cross-linker was added prior to extraction of the proteins.

In summary, I adjusted procedures to optimise the number of viable cells likely to express PBP2/PBP2a complexes. Exposure of EMRSA-16 to ECg reduced β -lactam resistance and altered cell morphology but did not disrupt nascent PG synthesis. The surfactant Triton X-100 was not suitable for solubilisation of detectable PBP2/PBP2a multi-enzyme complexes in EMRSA-16 cells. These results accord with previously published data.

CHAPTER THREE

3. SMALPS: METHOD DEVELOPMENT

3.1 Introduction

3.1.1 Membrane protein solubilisation

Membrane proteins play a fundamental role in cellular processes and are important targets for drugs. They are embedded in a mosaic lipid bilayer, a complex, heterogeneous and dynamic environment that limits standard biophysical techniques for structural and functional studies (Seddon *et al.*, 2004). They are not soluble in aqueous milieu, requiring synthetic systems for extraction. Membrane proteins belong to two classes, peripheral and integral (Luckey, 2008). Peripheral proteins may be purified by exploiting changes in ionic strength or pH, whereas removal of integral proteins from bilayers requires physical disruption of the membrane with chemical agents such as surfactants (Luckey, 2008). The major disadvantage in the use of traditional surfactants for solubilisation of membrane proteins is the fundamental difference between the native environment of the protein, the dynamic cell membrane and a micellar environment (London and Khorana, 1982).

Native biological membranes consist of bilayer and non-bilayer lipids that aid the stabilisation of membrane proteins, creating lateral pressure and curvature (Lee, 2003). Synthetic lipids may support the investigation of membrane proteins by mimicking their native membrane environment (Botelho *et al.*, 2002); and solubilisation methods have been developed in which lipids are employed along with surfactants. However, the presence of surfactants remains a limiting factor as they strip away lipids surrounding the embedded proteins, altering the protein environment (Rajesh *et al.*, 2011).

There are three forms of lipids; lipid bilayers, annular lipids and lipid co-factors, which in sum play a role in maintaining membrane proteins in their native state (Luckey, 2008). The lipid bilayer provides lateral pressure on the proteins and affects protein folding (Lee, 2003; Seddon *et al.*, 2008). Annular lipids encircle the proteins and influence function; lipid co-factors are found tightly bound between protein subunits and are likely to be involved in protein function (Luckey, 2008). The addition of synthetic lipids during solubilisation of membrane proteins mimics the native membrane environment, reflecting their functions as discussed above. The absence of bound lipids and reduced lateral pressure as a consequence of surfactant solubilisation

drastically hinders investigation of the functional state of proteins and this is almost certainly the case for the PBP2/PBP2a complex.

Hydrophobically associating polymer systems provide one potential solution for membrane protein solubilisation in which protein-protein and protein-lipid interactions are maintained. Several polymer systems have been developed and were described in section 1.6; these include amphipols and SMA. Amphipols are amphipathic polymers with a hydrophilic backbone and grafted hydrophobic side chains (Seddon *et al.*, 2004). Membrane proteins are stabilised in a semi-native state in amphipols but initial surfactant protein extraction is required, limiting their use (Popot, 2010). On the other hand, the amphipathic polymer SMA has shown great potential for the study of membrane proteins, both for extraction and for down-stream investigations (Knowles *et al.*, 2009). SMA is the primary focus of the work in this chapter and has been applied to the study of the PBP2/PBP2a complex.

3.1.2 Solubilisation of membrane proteins with SMA co-polymer

SMA may be used to solubilise membrane proteins in a semi-native environment; the co-polymer consists of alternating styrene and maleic units (Tonge, 2006) (Figure 1-16). The styrene pendant groups provide the hydrophobic moiety and together with maleic acid form a hypercoiling polymer that self assembles to form nanostructures (SMALPs) in the presence of lipids and/or proteins (Tonge and Tighe, 2001). The structure dissociates at pH 4 due to ionization of the maleic group and re-associates at a pH above 6.5 (Figure 3-1).

Malvern Cosmesceutics initially developed the polymer as a delivery method for hydrophobic agents using a styrene: maleic acid ratio of 3:1 (Knowles *et al.*, 2009). SMA has also been used at a ratio of 1:1 in de-pigmentation and anti-aging cosmetic products as well as in cosmetics to protect skin from UV radiation and sunburns (Tonge, 2006).

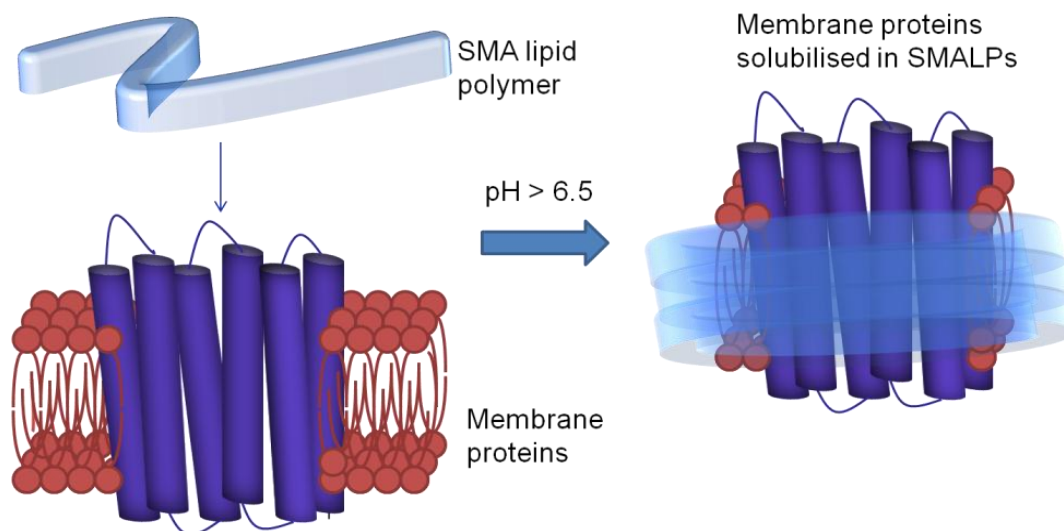


Figure 3-1 Formation of SMALP nanostructure around an integral membrane protein and associated lipids in an environment above pH 6.5

The polymer has a transparent appearance with high heat resistance and dimensional stability and solubilises proteins in alkaline solutions due to the reactivity of the anhydride group in the maleic acid/anhydride component (Tonge, 2006). Knowles *et al.* (2009) integrated recombinant PagP (8 stranded β -barrel) and bacteriorhodopsin (bR) (7 transmembrane α -helices) within SMALPs with radii of 9.0 ± 1.1 nm as determined by dynamic light scattering (DLS), which increased to 11.2 ± 1.4 nm after PagP incorporation (Knowles *et al.*, 2009). Circular dichroism (CD) and nuclear magnetic resonance (NMR) indicated correct folding of PagP and 90% greater stability compared to surfactant-solubilised PagP (Knowles *et al.*, 2009).

Biophysical investigation of SMALPs, or ‘lipodisqs’, revealed a close association between SMA and DMPC lipids (Orwick *et al.*, 2012). SMALPs extended lateral pressure on lipid tails without perturbing the core (Orwick *et al.*, 2012). The diameter of empty SMALPs determined by DLS was 12 nm, 3 nm greater than reported by Knowles *et al.* (2009). This work indicates that SMALPs may vary in diameter and membrane proteins solubilised within the SMALPs remain correctly folded, active and thermostable, providing a new avenue for the study of membrane proteins and protein complexes.

Another approach for measuring cell size and complexity is the use of flow cytometry. The method was first used in microbiological assays in 1977 for the separation of bacterial cells (Bailey *et al.*, 1977; Paau *et al.*, 1977). It was used to study cell numbers, cell size, membrane potential and fluorescence staining (Steen, 2000). More recently, flow cytometry has been employed to investigate smaller particles approximately 100 nm in size through use of fluorescence triggers (van der Vlist *et al.*, 2012).

Flow cytometry measures the light scattering signal and fluorescence emission of cells or particles in suspension as a single particle passes through the beam of light emitted from a laser (Figure 3-2).

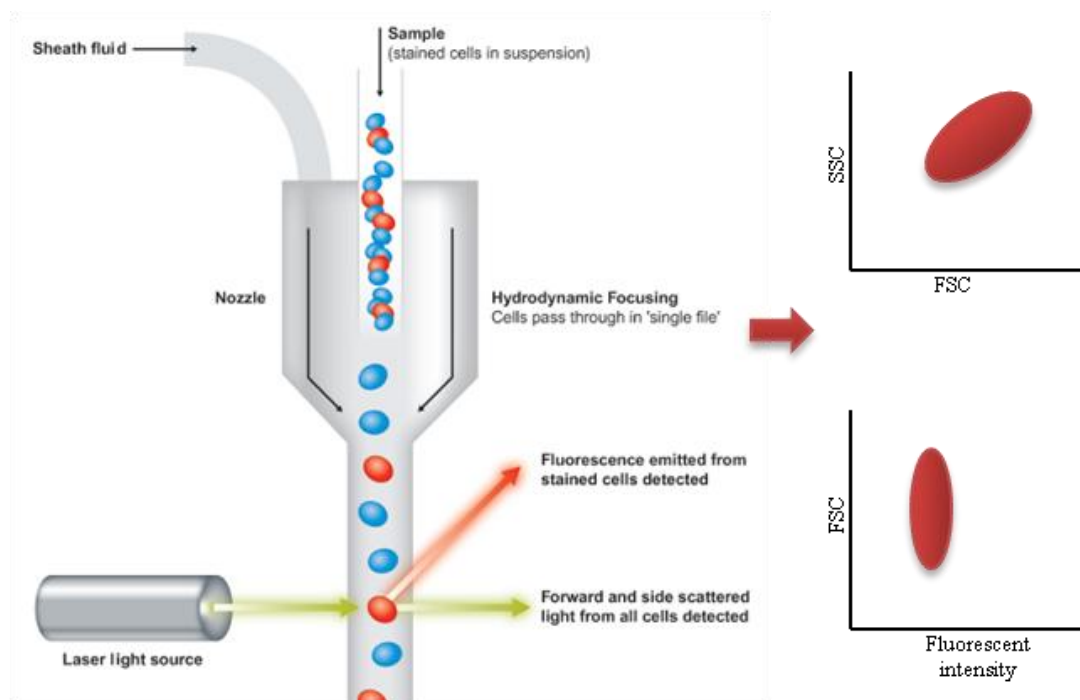


Figure 3-2 Cells and/or particles analysed by flow cytometry. Particles pass through the beam of light emitted by the laser and are scattered according to cell size (forward scatter (FSC)) or complexity (side scatter (SSC)). A second parameter, the addition of fluorescent signals, can be detected. Two-parameter dot plots of FSC vs. SSC or fluorescent signal vs. light-scattering parameters can be created from the data. Adapted from abcam, flow cytometry guide

Cells or particles are detected by FSC, which is associated with size; SSC is correlated with particle complexity. Two-parameter dot plots of FSC vs. SSC indicate changes in population size and complexity. Further two-parameter dot plots of a light scatter parameter (FSC or SSC) and fluorescence emission can be used to control for fluorescence emission. Bi-variant fluorescent plots can be used for determination of two

fluorescence parameters simultaneously from one sample (Radcliff and Jaroszeski, 1998).

Utilising SMA, I developed a method for the solubilisation of MRSA membrane proteins from whole cells in order to capture and solubilise the native PBP2/PBP2a complex; I also investigated the capacity of ECg to physically disrupt the complex.

3.2 Material and methods

3.2.1 Bacterial strains and reagents

MRSA strain COL (BB568) was provided by Brigitte Berger-Bächi, University of Zurich, Switzerland. COL lacks chromosomal or plasmid-born regulatory elements that control transcription of *mecA*, resulting in constitutive expression of PBP2a. Strain SH1000 was Hydrolysed SMA polymer was supplied by Timothy Dafforn, Birmingham University; the polymer contained styrene and maleic acid in a ratio of 2:1. 1,2-dimyristoyl-sn-glycerol-3-phosphocoline (DMPC) was purchased from Avanti Polar Lipids, Inc. (Alabaster, Alabama, USA).

3.2.2 Cell preparation

3.2.2.1 Membranes

EMRSA-16 protoplasts were prepared using a modification of the methods described by Kaback (1971) and Chopra *et al.* (1974). EMRSA-16 was grown as described in Chapter 2; PBP2a was induced with 4 mg/L oxacillin, cells harvested by centrifugation (5000 g, 4 °C, 10 min) and washed twice with PBS. The cell pellet was suspended in digestion buffer (20% (w/v) sucrose, 0.05 M Tris-HCl, 0.145 M NaCl, pH 7.6) to a final concentration of 40-50 mg/mL wet weight. The cell wall was digested with 20 µg of the glycine-glycine endopeptidase lysostaphin (Sigma) in the presence of 25 µg DNase I for 45 min at 37 °C. Protease inhibitor (Roche Complete Mini, EDTA-free) was then added to a final concentration of 10 mM and incubation continued for 15 min. Bacterial membranes were collected by centrifugation (20,000 rpm; 15 min; 4 °C).

3.2.2.2 Whole cells

Cells was grown in MHB as described in section 3.2.2.1; the PBP2/PBP2a complex was induced with 4 mg/L oxacillin for 10 min. Alternatively, cells were grown in MHB supplemented with 0.125 mg/L oxacillin. COL cells did not require oxacillin induction; however, the same procedure was performed for consistency. The cell pellet was suspended in 3 mL digestion buffer.

3.2.2.3 Preparation of hydrolysed SMA

A 5 % (w/v) stock of SMA polymer was prepared in 1.0 M sodium hydroxide by reflux for 2 h followed by 48 h incubation at 4 °C. Samples were dialysed extensively in 50 mM Tris pH 8 to remove traces of sodium hydroxide. The structure of the lyophilised product was determined by Fourier transform infrared spectroscopy.

3.2.2.4 SMALP solubilisation of DMPC lipids

Hydrolysed SMA was added to 3 mL of digestion buffer at a 2.5% (v/v) concentration, and DMPC lipids added to give a final concentration of 0.5 - 1% and incubated for 1 h at 37 °C. The solution was sonicated for 1 min (15 sec on, 20 sec off; 4 μ amplitude) to produce small unilamellar vesicles and incubated for 14 - 16 h at 37 °C with constant shaking. DMPC SMALPs were collected by ultracentrifugation at 100,000 g 1 h at 37 °C; supernatant contained the SMALPs.

3.2.3 Solubilisation of membrane proteins from membranes

To solubilise membrane proteins from MRSA protoplasts, the same methodology as for DMPC lipids was used with slight alterations. SMA was added at a 2.5% concentration to the membrane sample of cells described in section 3.2.2.1. Additional DMPC lipids were added at a 0.5 - 1% concentration to stabilise the membrane proteins within the SMALPs. The membrane and SMALPs solution was sonicated, incubated overnight and collected by ultracentrifugation as described in section 3.2.2.4.

3.2.4 Solubilisation of membrane proteins from whole cells

Initially the protoplast method described in section 3.2.2.1 was adapted for the use of SMALPs with whole cells, following the preparation of whole cells as described in section 3.2.2.2. The cell wall (from 2 L culture) was digested with 80 μ g lysostaphin in the presence of 25 μ g DNase I and 1 x HALT (protease and phosphatase inhibitor, Sigma) for 10 min at 37 °C in digestion buffer to a final volume of 3 ml. SMA (2.5%) was added for a further 50 min. A growth curve was constructed to determine the optimum lysostaphin incubation period prior to the addition of SMA. Following incubation, the SMALP solution was sonicated (section 3.2.2.4). The SMALPs were

collected through ultracentrifugation and the supernatant containing the SMALPs removed for further investigation.

3.2.5 Optimisation steps of SMALPs solubilisation method

The impact of oxacillin induction, temperature, lysostaphin digestion and sonication of SMALPs was determined. Cells were induced with oxacillin from onset of growth with 0.5, 0.25 and 0.125 mg/L oxacillin. Following collection of the cells and suspension of the cell pellet in digestion buffer, membrane proteins were solubilised with SMA at 37 °C and 4 °C. For lysostaphin digestion three different conditions were used; addition of lysostaphin for 10 min followed by SMA for 50 min, SMA directly added to the cells for 1 h at 37 °C without lysostaphin, and finally SMA and lysostaphin added simultaneously for 1 h. After SMALP solubilisation, SMALPs were either sonicated prior to collection, or directly collected by ultracentrifugation.

3.2.6 Optimised SMALPs method

A culture was grown to mid-log together with 0.125 mg/L oxacillin. The cells were harvested through centrifugation and the cell pellet suspended in 3 mL digestion buffer; incubated with 80 µg lysostaphin in the presence of 25 µg DNase I and 1x HALT for 10 min at 37 °C followed by the addition of SMA (2.5%) for 50 min. The SMALPs were collected through ultracentrifugation and the supernatant containing the SMALPs removed for further investigation by SDS-PAGE and Western blot.

3.2.6.1 Tricine SDS-PAGE

N-[2-hydroxy-1,1-bis(hydroxymethyl) ethyl] glycine (Tricine) modification to 1D SDS-PAGE was used to avoid aggregation of membrane proteins as described by Schägger and von Jagow (1987). Samples were added to an equal amount of double-strength Tricine sample buffer (900 mM Tris-HCl, 24% (v/v) glycerol, 4% (w/v) SDS, 0.0005% (w/v) Coomassie blue, 0.0004% (w/v) phenol red, pH 6.8) supplemented with 5% (v/v) β-mercaptoethanol for 15 min at 37 °C. Samples in Tricine sample buffer were loaded on to a 10% Tricine-SDS gel (Table 3-1), which separates proteins over the range 1-100 kDa.

Table 3-1 Components of Tricine-SDS-PAGE for one gel

10% resolving gel (volumes)	Components	4% stacking gel (volumes)
1.75 mL	H ₂ O	1.95 mL
2.5 mL	3M Tris-HCl/SDS, pH 8.45	0.775 mL
2.5 mL	29:1% acrylamide: bis-acrylamide	0.4 mL
0.75 mL	100% glycerol	-
7 µL	30% APS	7 µL
7 µL	TEMED	7 µL

Anode buffer (0.2 M Tris-HCl, pH 8.9) and cathode buffer (0.1 M Tris-HCl, 0.1 M Tricine, 0.1 M SDS, pH 8.25) were added to the tank as the lower and upper electrode buffers and Tricine-SDS gels run at 30 V until the samples entered the resolving matrix and the remainder of the run performed at 100 V. Protein bands were visualised with Coomassie brilliant blue or silver stain, or transferred to a membrane by Western blotting for protein identification. Gels were scanned using a Molecular Imager FX and examined using Quantity One Advanced software.

3.2.7 Imaging of SMALPs

3.2.7.1 Transmission electron microscopy (TEM)

Dilutions (1, 1:10, 1:100) of SMALPs in wash buffer (50 mM Tris-HCl, 300 mM NaCl, pH 8.0) were mounted onto a Cu grid and washed twice with the same buffer. A drop of 2% uranyl acetate was added and the images visualised with a CM 120 Bio-Twin transmission electron microscope (Philips Electron Optics) operated at 120 kV. I was assisted in this procedure by David McCarthy (UCL School of Pharmacy) and images analysed using ATM software. Bacteria were also visualised during the solubilisation process; prior to lysostaphin digestion of the bacterial culture, following the addition of lysostaphin for 10 min, and following 50 min incubation with SMA after lysostaphin digestion.

3.2.7.2 SEM

SMALPs were freeze-dried overnight. Gold-coated samples were prepared under vacuum and images collected with a FEI XL30 scanning electron microscope (Philips Electron Optics) with assistance from David McCarthy.

3.2.7.3 Confocal fluorescence microscopy

In order to co-localise PBPs and SMA lipids, confocal microscopy was used to detect the fluorescence emission of fluorescently labelled samples. PBPs were labelled with Bocillin FL (Sigma) and the membranes/SMA labelled with Nile Red dye (Molecular Probes) with excitation and emission wavelengths of 485/530 and 552/636 nm respectively. Nile Red is a fluorescent lipid probe that does not fluoresce in water and polar solvents but undergoes large absorption and emission shifts in non-polar environments that are greater for lipids than proteins (Greenspan and Fowler, 1985).

SMALP (20 μ L; approx 500 μ g protein) were incubated with 0.8 μ L Bocillin FL for 30 min at 30 °C prior to placing the sample onto a poly-L-lysine slide. Subsequently, 2 μ L of 1 mM Nile red dye (final concentration 2 μ M) was added and the mixture incubated for 15 min at RT. The slide was washed twice in wash buffer and dried overnight at RT. Either one drop of vectashield hard set mounting medium or 20 μ L 0.1% agarose was applied to the sample prior to mounting the cover-slip. The samples were examined by confocal fluorescence microscopy.

3.2.8 Size distribution of SMALPs

3.2.8.1 Dynamic light scattering (DLS)

The molecular size distribution of SMALPs was measured by DLS with a Zetasizer Nano ZS (Malvern, Worcestershire, UK). DLS measures the fluctuation of scattering intensity, with the fluctuations dependent on the diffusion coefficient of the molecule, which in turn is dependent on the size of the molecule. As intensity is proportional to mass, the sensitivity is relatively high; however, DLS assumes that molecules are spherical, which may not be the case with SMALP molecules. Thus, approximations are made with respect to hydrodynamic diameter measurement (Malvern).

SMALPs (1 mL) were placed in a disposable polystyrene cuvette (Semi-micro PS) (Fischer Scientific Inc.) and equilibrated at 25 °C for 5 min. Size was determined in triplicate with 16 measurements per sample and data analysed with the Malvern DLS software.

3.2.8.2 Flow cytometry

Flow cytometry was used to investigate changes in FSC and SSC of EMRSA-16 SMALPs when EMRSA-16 cells were exposed to ECg before membrane protein solubilisation. A reduction in size may be indicative of membrane protein complex disruption. The size and complexity of SMALPs were determined with a MACS quant flow cytometer (Miltenyi Biotec Ltd.). SMALPs were suspended in digestion buffer in 1:100 dilutions and 500 µL stained with 60 µM Nile Red probe in the dark for 30 min prior to flow cytometry analysis. Samples were gated for B2 (361V); the red fluorescent channel (trigger 3.0) (250V FSC and 400V SSC) and subsequently back-gated for SSC and FSC. Twenty thousand events were measured for each sample and data analysed using the MACS Quantify™ Software (Miltenyi).

3.3 Results

3.3.1 Membrane proteins from protoplasts solubilised in SMALPs

Membrane proteins from EMRSA-16 and ECg-exposed cells were solubilised with SMA after enzymatic lysis of the cell wall with lysostaphin. Efficiency of solubilisation compared with surfactant-extracted proteins were compared by SDS-PAGE. More proteins were revealed by silver stain compared to Coomassie-stained gels (Figure 3-3).

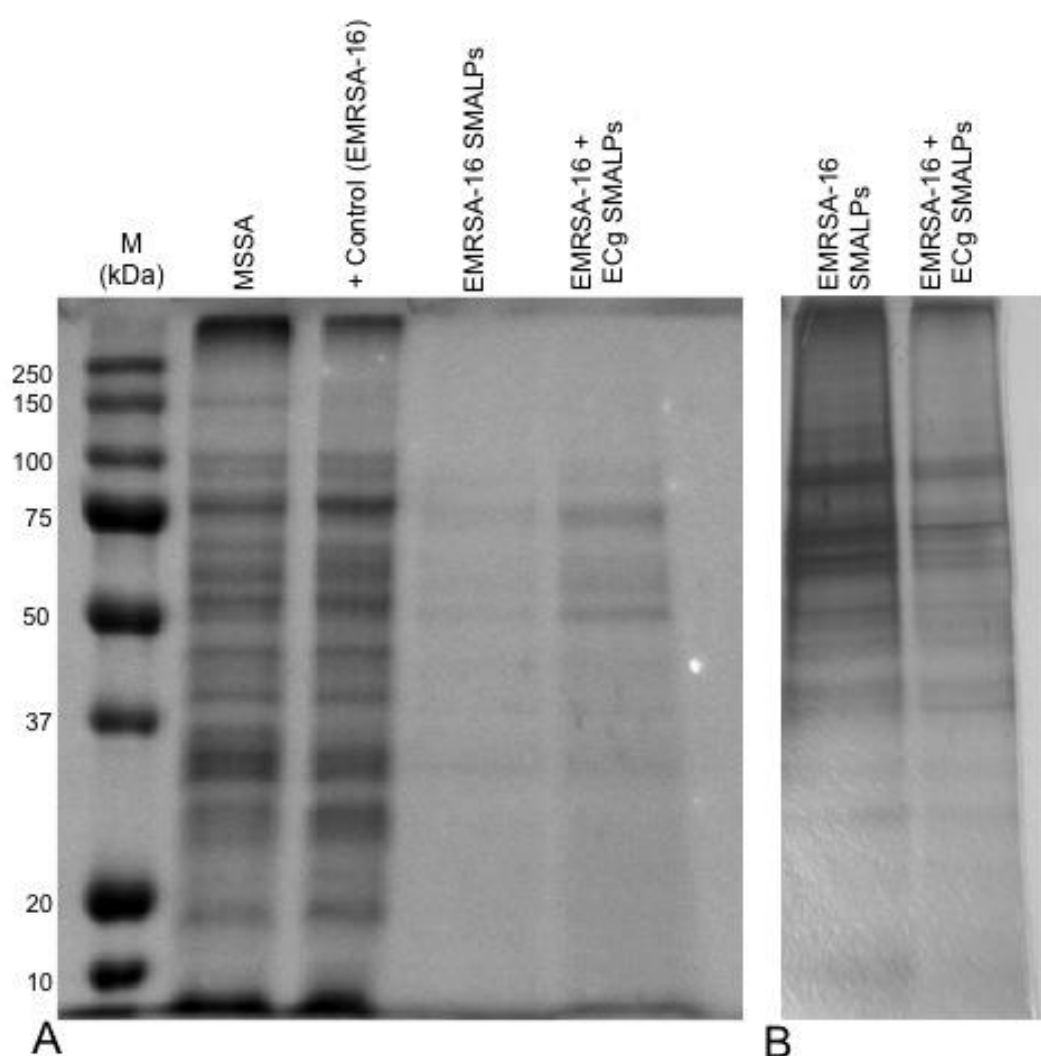


Figure 3-3 SDS-PAGE of membrane proteins stained with (A) Coomassie brilliant blue or (B) silver stain. MSSA and EMRSA-16 surfactant-solubilised proteins were separated in the gels along with SMALP-solubilised membrane proteins from EMRSA-16 and ECg-exposed EMRSA-16

Membrane protein bands are generally broader than water-soluble proteins and often stain poorly with Coomassie (Schägger, 2006). To overcome this, SMALP preparations were concentrated (Figure 3-4), as detection of low abundance PBP2/PBP2a complexes will require high initial membrane protein concentrations.

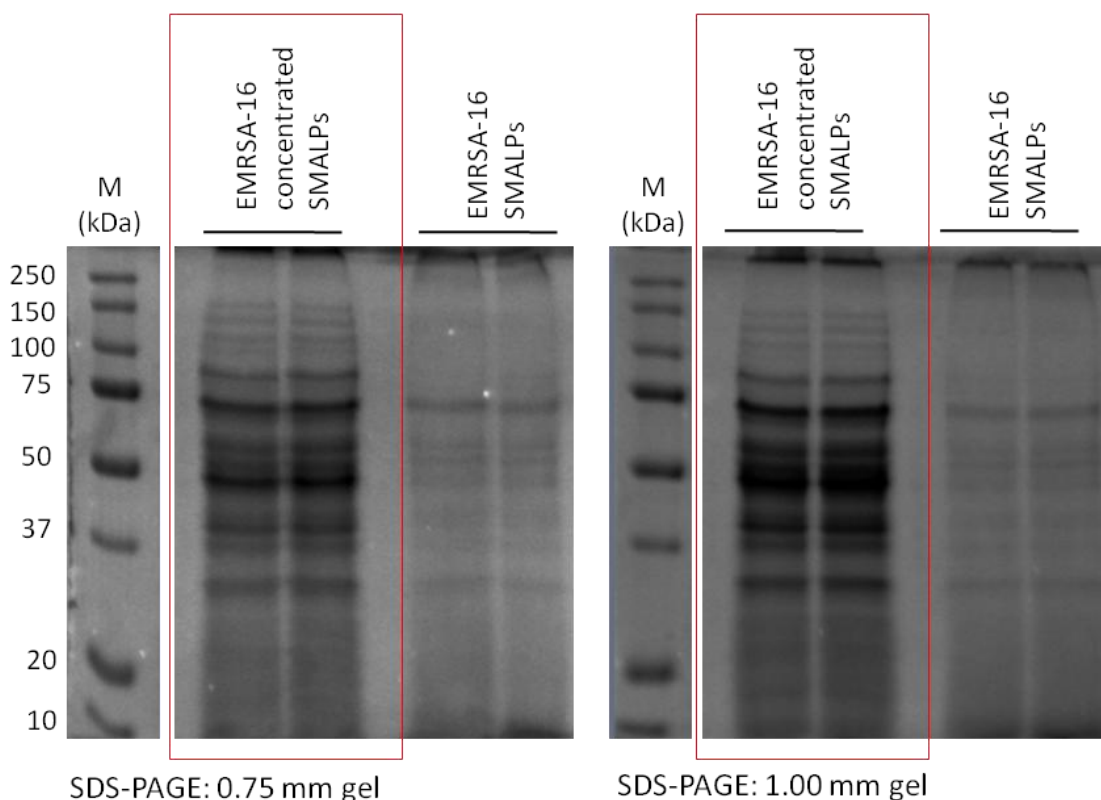


Figure 3-5 EMRSA-16 membrane proteins solubilised in SMALPs. Samples were concentrated using 10,000 molecular weight cut-off Vivaspins to 25 mg/mL, samples run on a 0.75 mm and 1.00 mm 10% SDS-PAGE and stained with silver stain. Red boxes indicated the SMALP samples (concentrated) that were used for future experiments

SMALP samples were concentrated to a final concentration of 25 mg/mL as determined by Nanodrop A280 absorbance assay. Equal amounts of EMRSA-16 and ECg-exposed EMRSA-16 solubilised membrane proteins were added to capacity of a 0.75 mm and a 1.00 mm gel. The most intense bands were found with EMRSA-16 SMALPs run in a 1.00 mm gel. There was a general decrease in band intensities in both gels of proteins from ECg-exposed EMRSA-16 cells compared to controls.

Protein-containing SMALPs were also separated using Tricine-SDS-PAGE, suitable for the separation of proteins in the range 1-100 kDa; the proteins of interest, PBP2, and PBP2a, have molecular weights of 80 and 78 kDa respectively. Tricine migrates faster

than glycine and tricine gels tolerate overloading, which is beneficial for detection of low abundance membrane proteins (Schägger and von Jagow, 1987). Further, it is not necessary to boil samples to achieve separation of individual proteins (Schägger, 2006), avoiding the irreversible aggregation that commonly occurs with SDS; samples are held at 37 °C for 30 min (Schägger, 2006). Cultures (1 L) of EMRSA-16 grown to mid-logarithmic phase with and without ECg yielded approximately 3.5 g (wet weight) of cells. Following solubilisation of membrane proteins from protoplasts in SMALPs, both concentrated and non-concentrated SMALPs were separated on Tricine-SDS-PAGE gels and Western blots probed for proteins of interest (Figure 3-5).

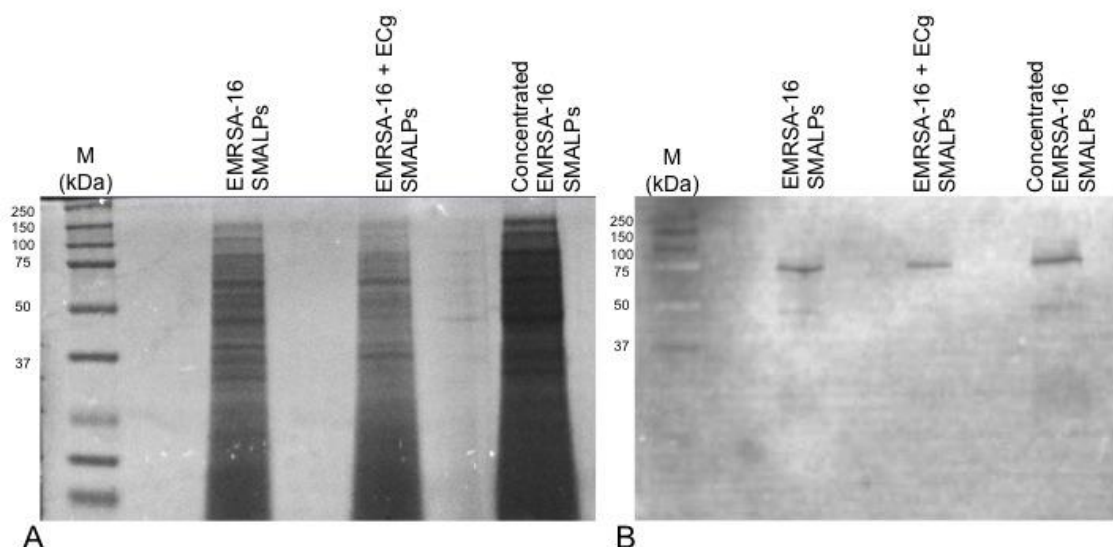


Figure 3-5 (A) Tricine-SDS-PAGE and (B) Western blot using anti-PBP2 Ab of EMRSA-16 and ECg-exposed EMRSA-16 membrane proteins extracted from protoplasts with SMA. A protein-enriched EMRSA-16 SMALP sample was also examined

No protein aggregation was observed in Tricine-SDS-PAGE gels and PBP2 was identified by Western blotting, following the modified protein denaturation method. SMALP samples were also probed in Western blots with PBP2a and FtsZ antiserum; both proteins were readily detected (Figure 3-6).

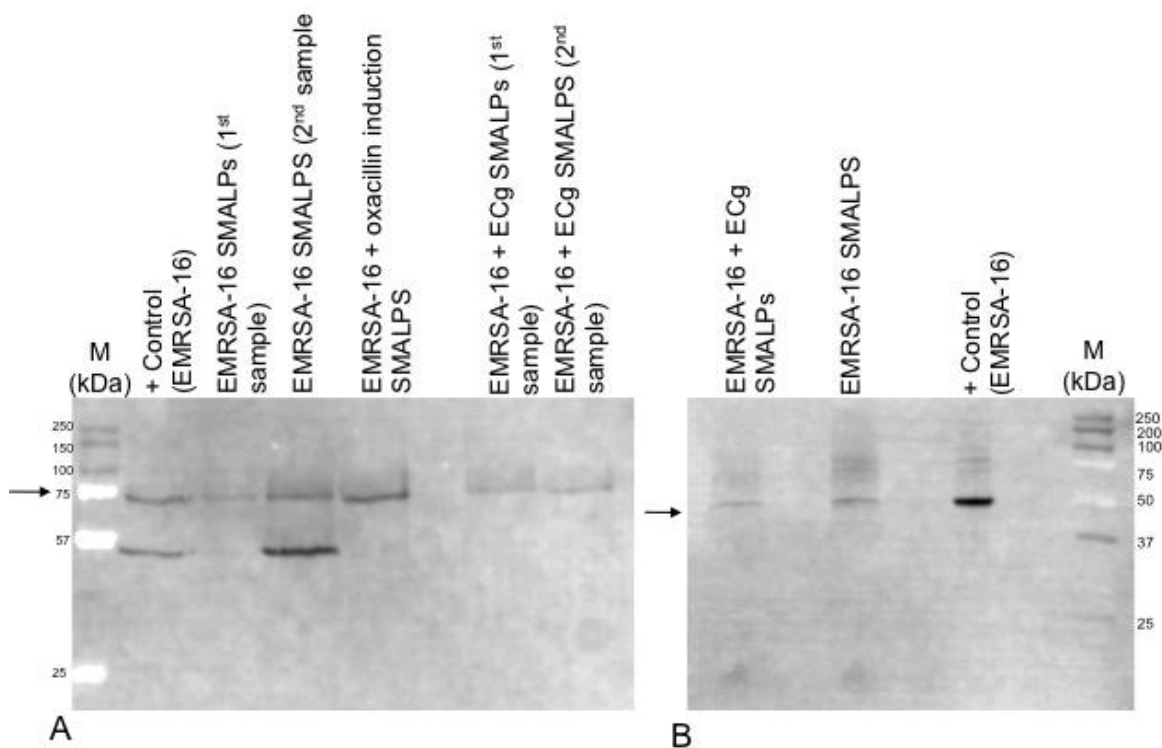


Figure 3-6 Western blot with (A) anti-PBP2a and (B) anti-FtsZ antiserum of EMRSA-16 and ECg-exposed SMALPs. Arrows indicate proteins of interest. Triton X-100 solubilised EMRSA-16 membrane proteins are also shown

A single band (~50 kDa) representing FtsZ was detected along with an additional band that is probably attributable to Ab binding to protein A. The molecular mass (~75 kDa) of the PBP2a band was marginally lower than predicted (78 kDa).

3.3.2 Solubilisation of membrane proteins from intact cells

To investigate the effect of ECg exposure on the PBP2/PBP2a complex, a method was developed to closely represent the native environment. Initially, protoplasts from viable bacteria were used as a source for extraction of membrane proteins with SMA. However whole cells were subsequently utilised in order to minimise disruption to membrane architecture prior to solubilisation by SMA; in particular, removal of the cell wall may disrupt the anchored septal divisome complex (Pinho and Errington, 2003).

3.3.2.1 Enzymatic disruption of the cell wall

Initially, one-litre batches were grown to mid-logarithmic phase, collected by centrifugation and SMA added together with DNase I (experiment 1; in table 3-2). SMALPs were collected and the hydrodynamic diameter determined by DLS.

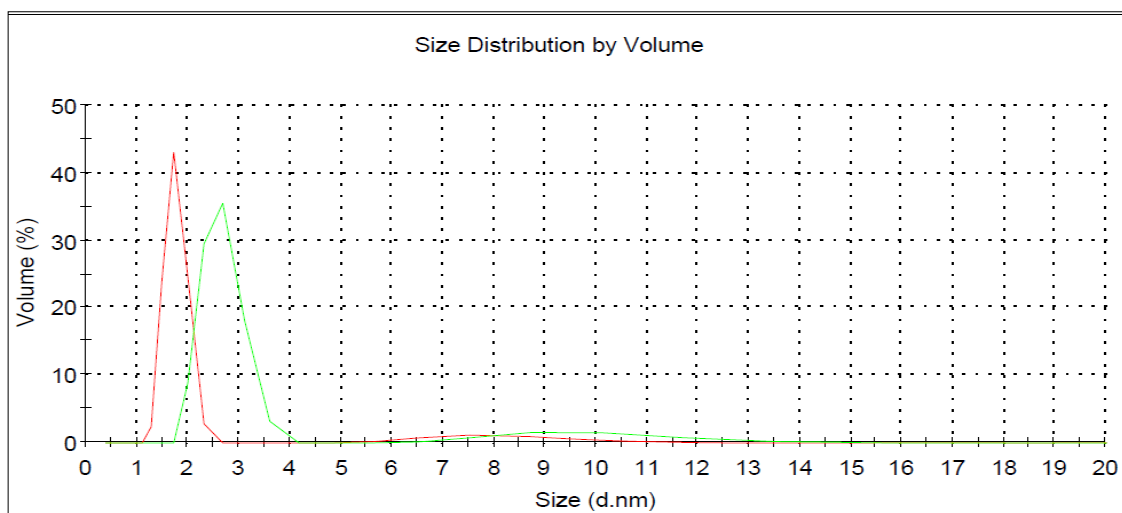


Figure 3-7 Distribution of the hydrodynamic diameter determined by DLS of SMALPs from (red) EMRSA-16 and (green) ECg-exposed EMRSA-16 SMALPs. Lysostaphin was not employed for this experiment; SMALPs collected by centrifugation

Knowles *et al.* (2009) showed that the mean diameter of SMALPs incorporating a single PagP protein molecule was 11.2 ± 1.4 nm. In the current study, SMALPs obtained by addition of SMA to intact cells exhibited diameters of approximately 2.8 nm for EMRSA-16 and 1.8 nm for ECg-exposed EMRSA-16 SMALPs (Figure 3-7). In experiment 1, only low concentrations of protein were captured by SMA from EMRSA-16 bacteria and only faint protein bands were detected following SMA extraction of ECg-exposed bacteria (Figure 3-8a). A blue smear accompanied the protein bands at the bottom of the Tricine-SDS-PAGE, corresponding to smearing of the SMA polymer as visualised in figure 3-8b. Consequently, in further experiments, 80 μ g lysostaphin was added to whole cells for 10 min at 37 °C prior to addition of SMA to aid access of SMA to the proteins.

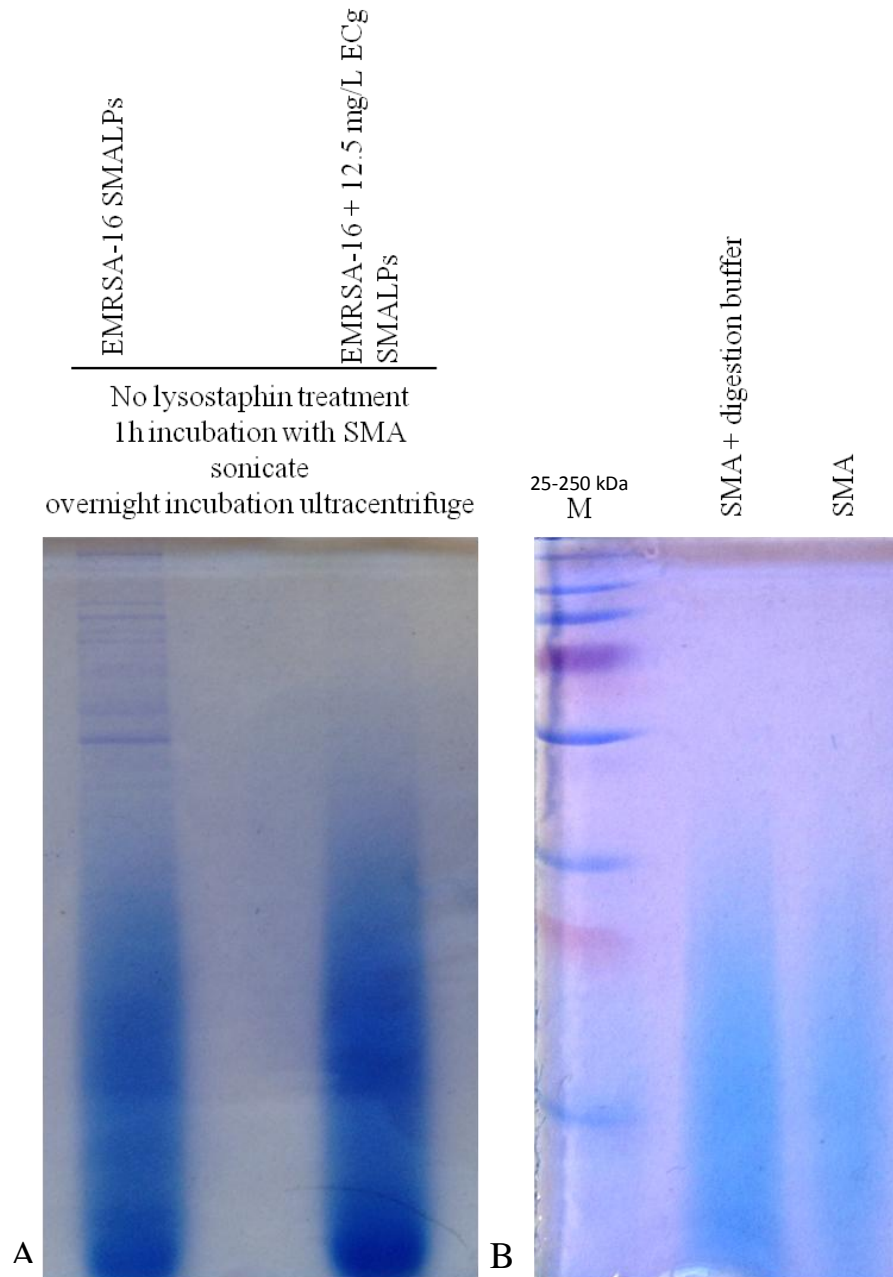


Figure 3-8 (A) Coomassie brilliant blue-stained Tricine-SDS-PAGE of total protein of EMRSA-16 and ECg exposed EMRSA-16 solubilised in SMALPs. Washed cell pellets were suspended in digestion buffer and SMA for 1 h at 37 °C, no lysostaphin. SMALPs were then sonicated and incubated overnight at 37 °C. (B) SMA with and without digestion buffer; Tricine-SDS-PAGE gel stained with Coomassie brilliant blue

Mean SMALP size distribution was 13 nm for EMRSA-16 and 8 nm for ECg-exposed EMRSA-16 (Figure 3-9).

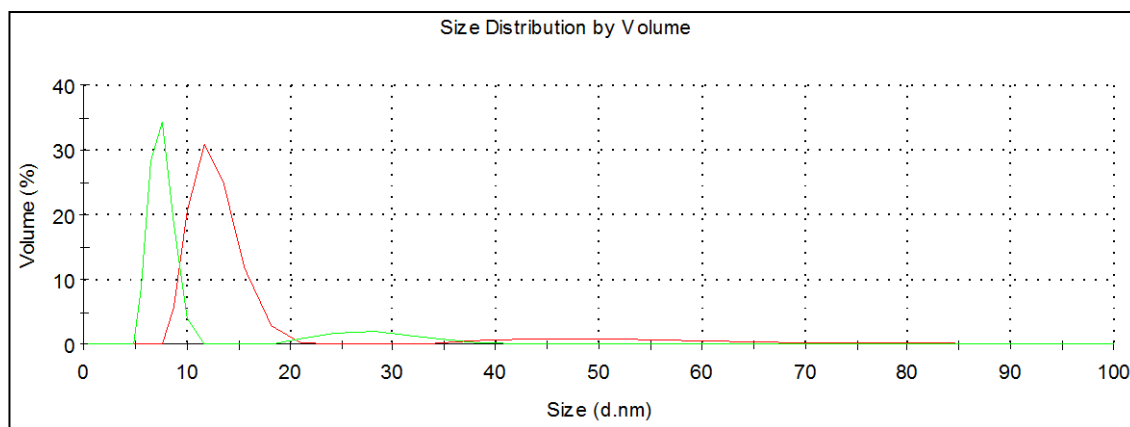


Figure 3-9 Hydrodynamic diameter of SMALPs from (red) EMRSA-16 and (green) ECg-exposed EMRSA-16 determined by DLS; lysostaphin was added to the preparations for 10 min followed by addition of SMA for 50 min

TEM images of EMRSA-16 (± 12.5 mg/L ECg) and COL were examined before and after 10 min exposure to lysostaphin and following exposure to SMA for 50 min. There was little apparent cell disruption of EMRSA-16 (Figure 3-11) or COL (Figure 3-14) after 10 min exposure to lysostaphin, although some damage to cell walls was evident at higher magnification disruption (Figure 3-12). Images for ECg-exposed EMRSA-16 were comparable, but the images were sometimes difficult to interpret due to accumulation of electron-opaque cell debris (Figure 3-13).

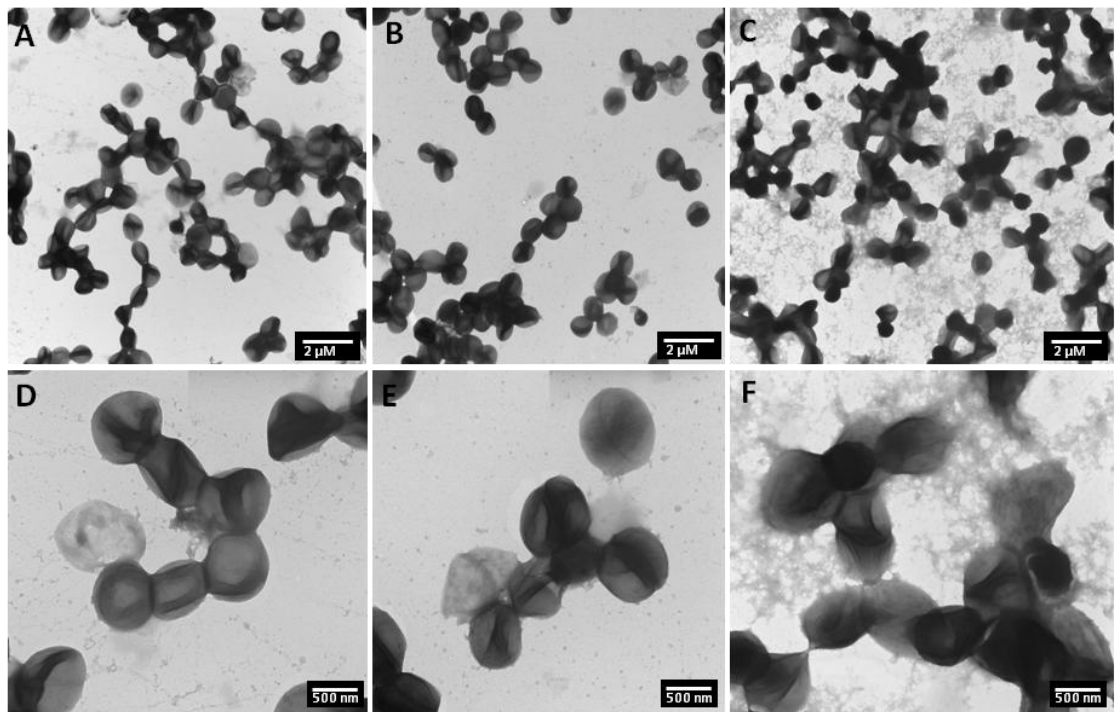


Figure 3-10 TEM of A-C: low magnification and D-F: high magnification, of (A, D) EMRSA-16 in digestion buffer, (B, E) digested with lysostaphin for 10 min, and (C, F) 50 min after addition of SMA

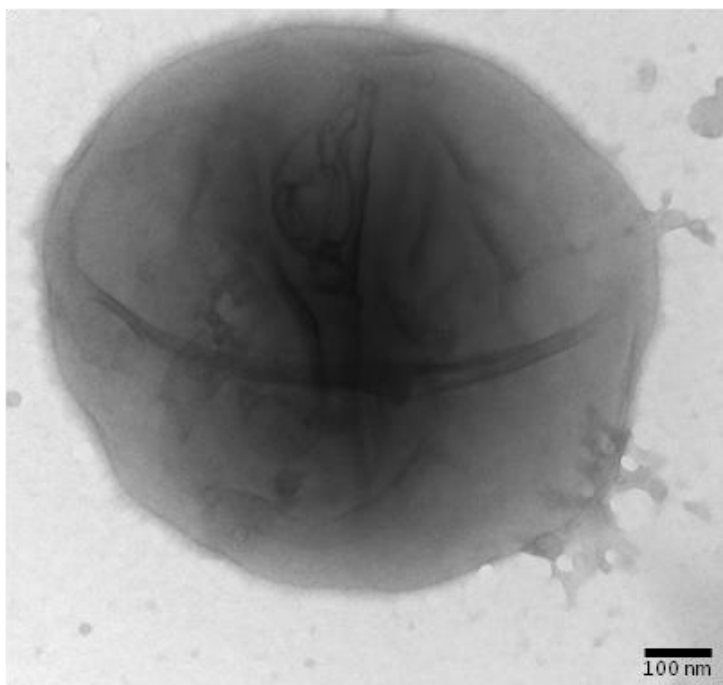


Figure 3-11 TEM (930000x magnification) of an EMRSA-16 cells after 10 min exposure to lysostaphin

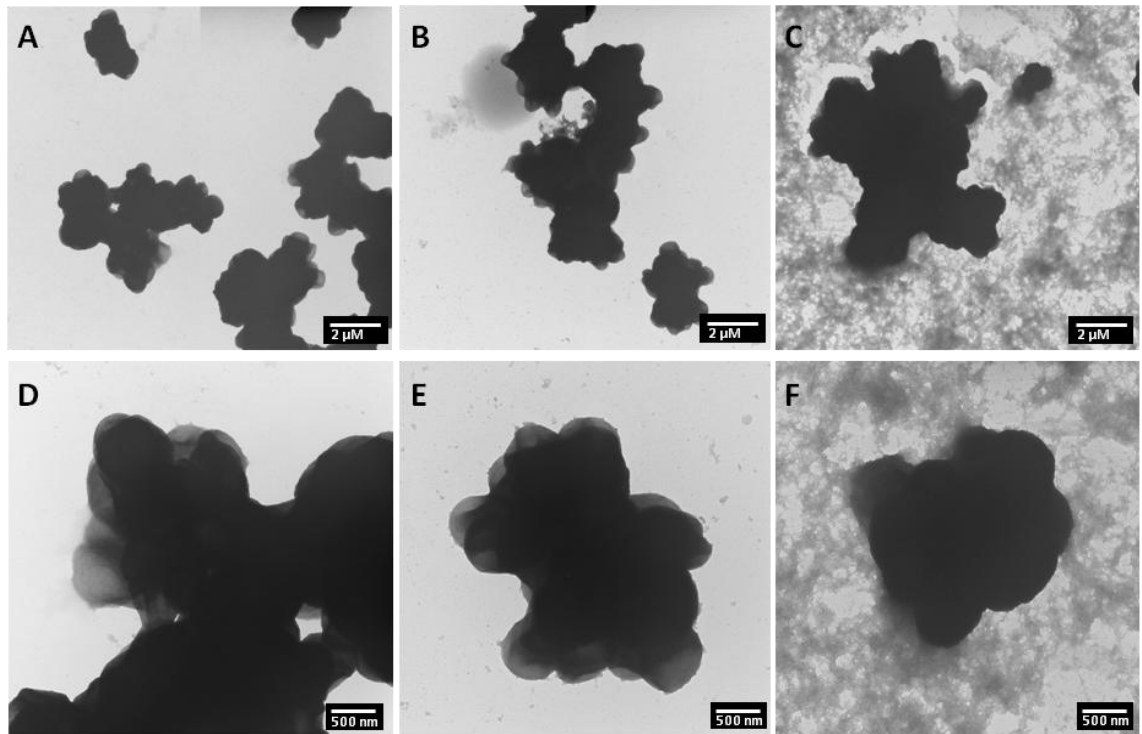


Figure 3-12 TEM of A-C: low magnification and D-F: high magnification, of ECg-exposed EMRSA-16 cells in (A, D) digestion buffer, (B, E) digested with lysostaphin for 10 min, and (C, F) after addition of SMA and incubation for 50 min

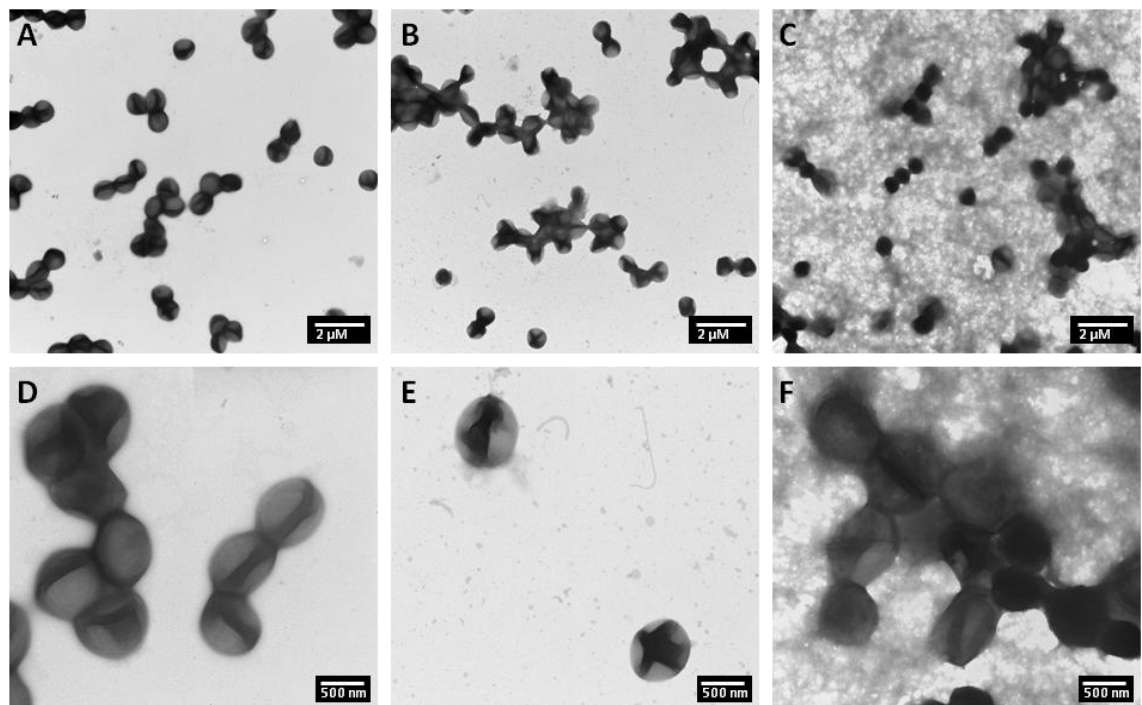


Figure 3-13 TEM of A-C: low magnification and D-F: high magnification, of COL (A, D) in digestion buffer, (B, E) digested with lysostaphin for 10 min, and (C, F) after addition of SMA and incubation for 50 min

Exposure to lysostaphin (10 min) followed by addition of SMA and incubation for a further 50 min led to further cell disruption and the appearance of large amounts of cell debris (Figure 3-10, figure 3-12 and figure 3-13). At 65000x magnification, formation of SMALPs could be detected at this point (Figure 3-14).

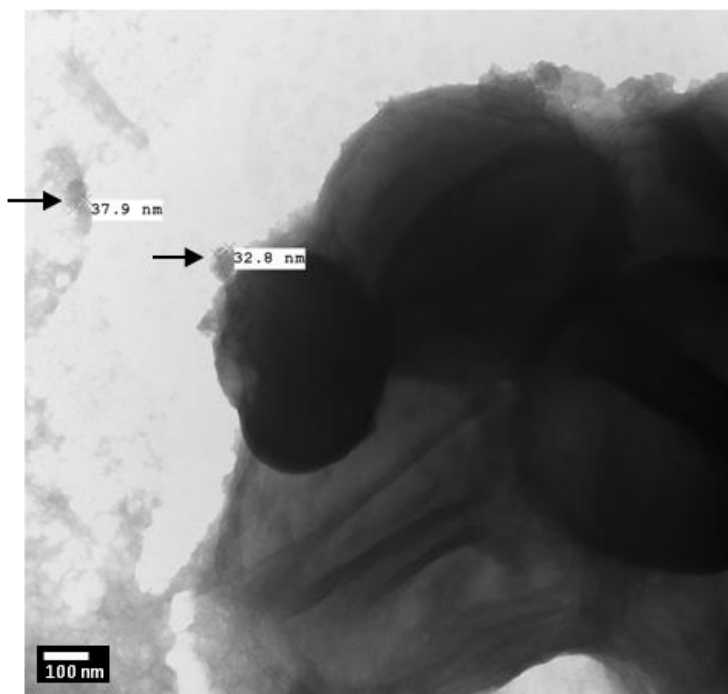


Figure 3-14 TEM (65000x magnification) of an EMRSA-16 after 10 min lysostaphin digestion followed by addition of SMA and incubation for 50 min. Two SMALPs (37.9 nm and 32.8 nm) can be seen

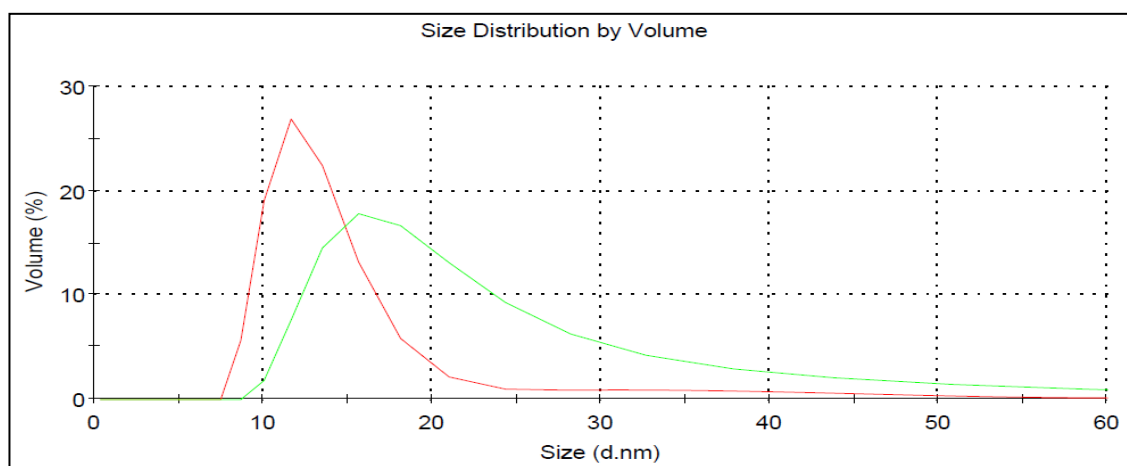


Figure 3-15 Hydrodynamic diameter, determined by DLS, of SMALPs from EMRSA-16 following (red) concomitant addition of SMA, lysostaphin and DNaseI and incubation for 60 min in comparison to (green) SMALPs obtained by addition of lysostaphin and DNaseI (10 min) followed by addition of SMA and incubation for a further 50 min

In a further series of experiments, lysostaphin and SMA were added together and the mixture incubated for 60 min; smaller nanoparticles were obtained (Figure 3-15).

3.3.2.2 Overnight incubation of SMALPs

Following solubilisation of membrane proteins with SMA, SMALPs were sonicated and incubated with agitation at 37 °C for 14 - 16 h prior to collection by ultracentrifugation (Experiment 2, in table 3-2). Size distribution of SMALPs from EMRSA-16 (Figure 3-16) and ECg-exposed EMRSA-16 (Figure 3-17), determined by DLS, indicated that this modification produced particles with increased hydrodynamic diameter.

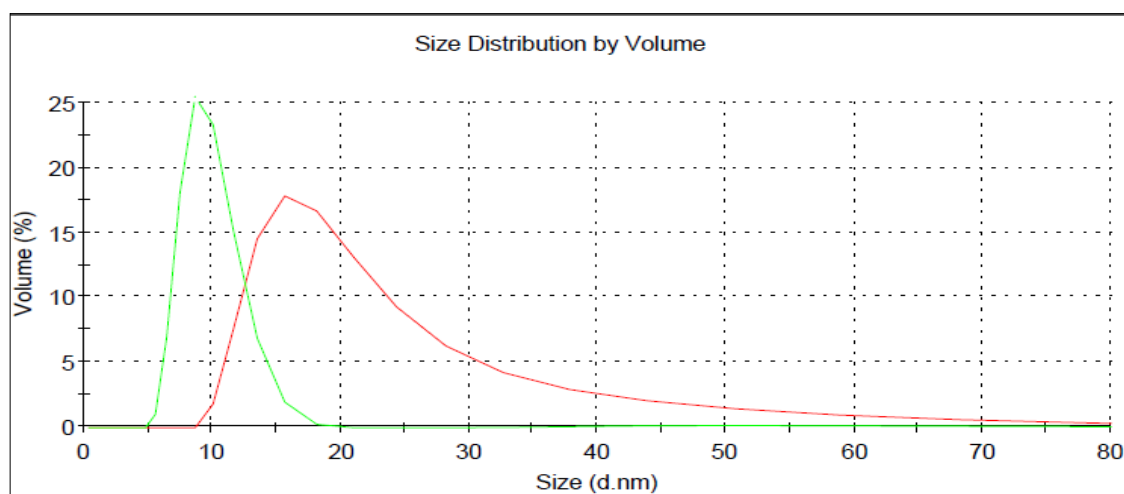


Figure 3-16 Hydrodynamic diameter of EMRSA-16 SMALPs with the (red) presence or (green) absence of 14 - 16 h incubation of SMALPs at 37 °C with agitation prior to collection, measured by DLS

The mean diameter ($n=3$) of EMRSA-16 and EMRSA-16 membrane protein SMALPs exposed to 12.5 mg/L ECg without 14 - 16 h incubation were 20.06 ± 2.28 nm and 14.32 ± 1.48 nm respectively. The DLS images displayed are a representation of one of the DLS data indicating an increase in average SMALPs sizes following 14 – 16 h incubation. There was a variation in sizes measured, however the trend in the increase in size remained the same. Stronger total protein bands were detected by Tricine-SDS-PAGE Membrane proteins of SMALPs derived from ECg-exposed and control cells were subjected to Tricine-SDS-PAGE, with a stronger total protein bands detected with the exclusion of overnight incubation (Figure 3-18). Transfer of hydrophobic membrane proteins from the gel can be achieved with this system through use of high-ionic

strength buffers, low voltage and extended transfer time (Schägger and von Jagow, 1987; Schägger, 2006).

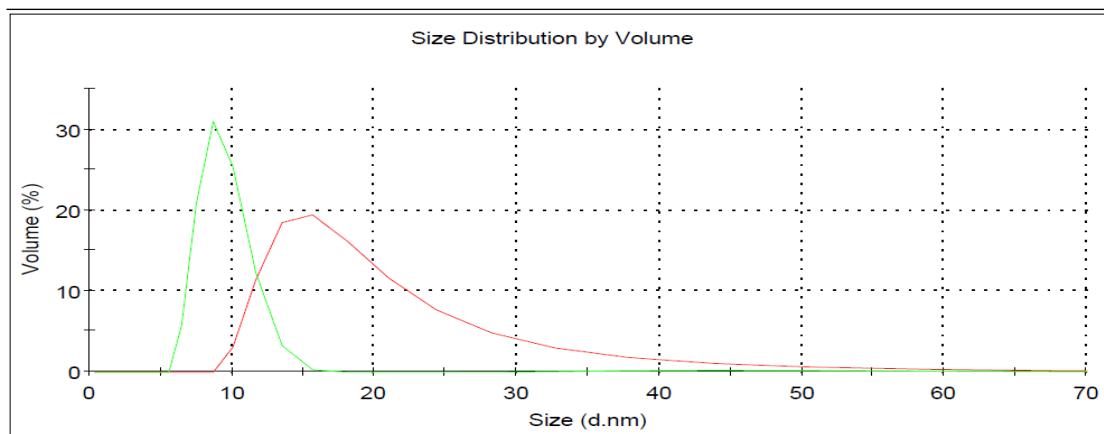


Figure 3-17 Hydrodynamic diameter of ECg-exposed EMRSA-16 SMALPs (red) with or (green) without 14-16 h incubation at 37 °C with agitation prior to collection as measured by DLS

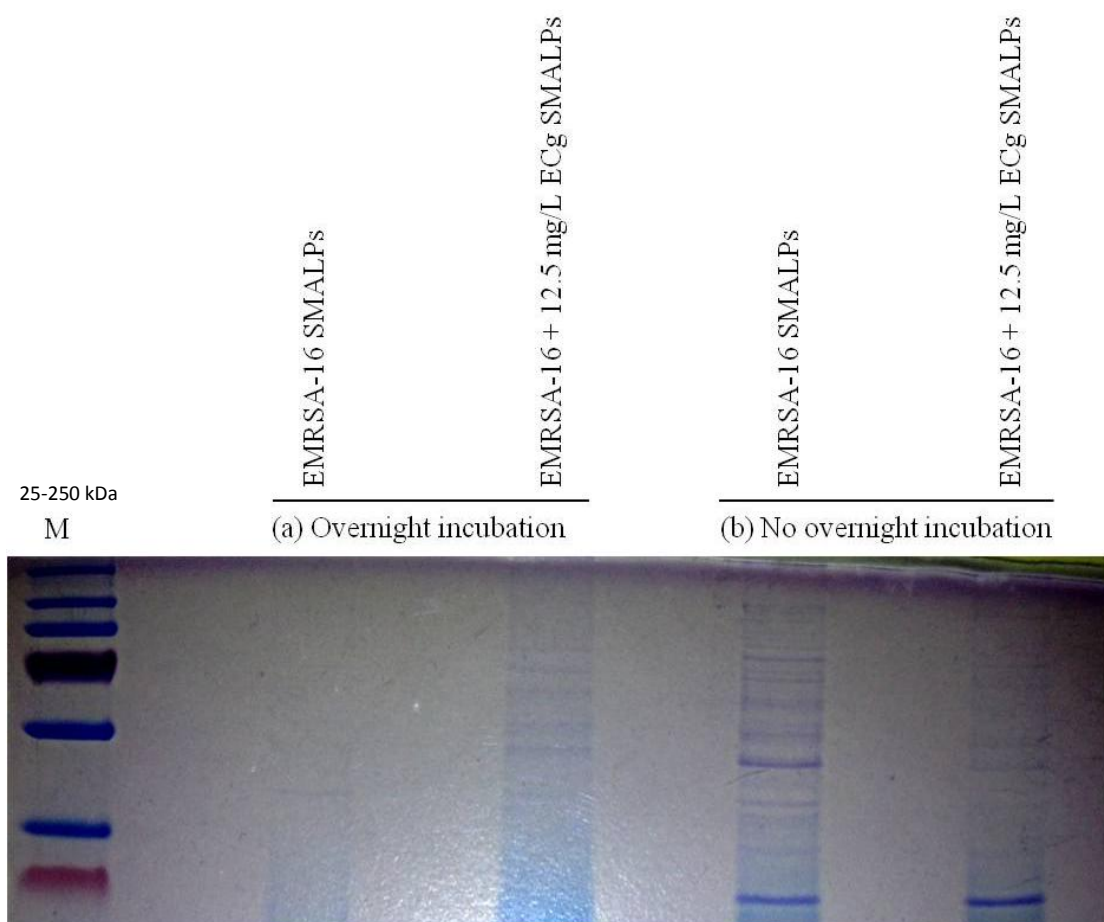


Figure 3-18 Tricine-SDS-PAGE of total protein from EMRSA-16 and ECg-exposed cells solubilised in SMALPs. Lysostaphin and SMA were added and bacteria incubated for 1 h at 37

°C. SMALPs were then sonicated and either (a) incubated overnight (14 - 16 h) at 37 °C or (b) processed without overnight incubation

3.3.2.3 Sonication

After solubilisation of membrane proteins with SMA, the nanoparticles were dispersed with a probe tip sonicator prior to SMALP collection. Sonication enables reformation of vesicles by insertion of energy. This step could lead to disruption of the PBP2/PBP2a complex. Sonication of SMALPs containing EMRSA-16 membrane proteins generated smaller nanoparticles compared to SMALPs prepared without sonication (Figure 3-19). Sonication had no impact on the membrane protein profile of EMRSA-16 (Figure 3-20).

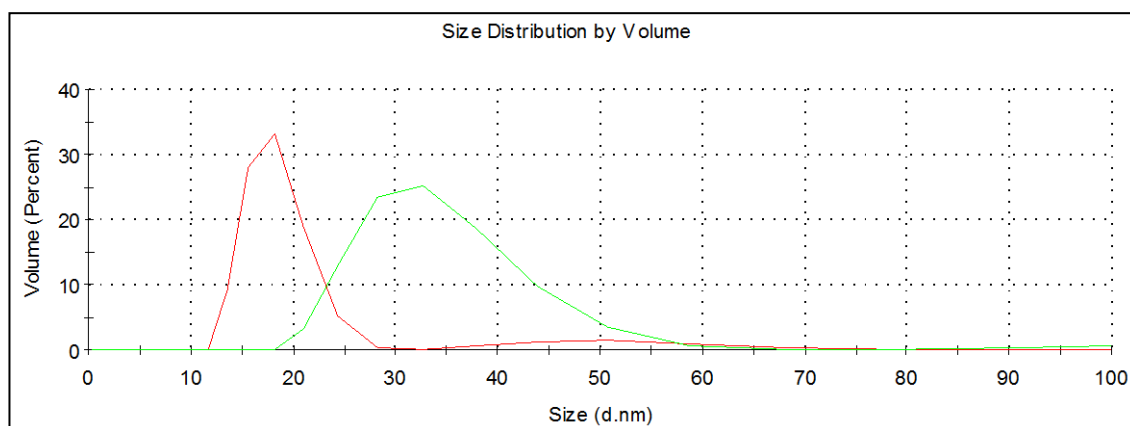


Figure 3-19 Size distribution (hydrodynamic diameter) of EMRSA-16 SMALPs (red) after sonication prior to collection by ultracentrifugation, or (green) without sonication; measured by DLS

Total SMALP proteins captured and investigated by Tricine-SDS-PAGE and Coomassie staining showed a lack of a visible difference in membrane protein band intensity following SMALP solubilisation with and without sonication (figure 3-21).

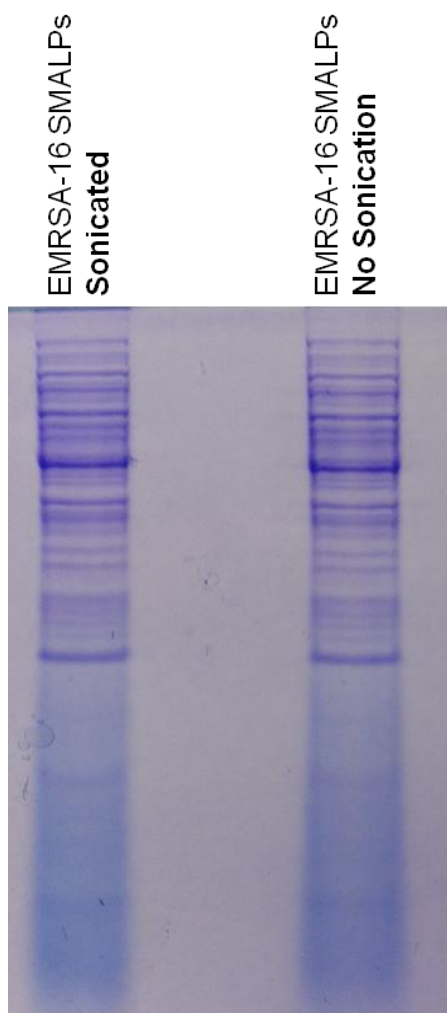


Figure 3-20 Tricine-SDS-PAGE of total membrane proteins from EMRSA-16 solubilised in SMALPs. Washed cell pellets were suspended in digestion buffer and digested with lysostaphin (10 min) prior to addition of SMA (50 min). Subsequently SMALPs were sonicated or not

3.3.2.4 The effect of temperature on SMALP development

SMA solubilisation of EMRSA-16 membrane proteins was investigated at 4 °C and 37 °C. A significant decrease in size distribution was observed when SMALPs were formed at 4 °C compared to 37 °C (Figure 3-21). The same held true for ECg exposed EMRSA-16 SMALPs (data not shown).

The optimisation steps for the development of the SMALPs procedure adopted in this study are shown in table 3-2 along with comments comparing methods. The optimal method (Experiment 9, in table 3-2) was employed to probe for the PBP2/PBP2a complex in EMRSA-16 and to investigate the effect of ECg on the integrity of the complex.

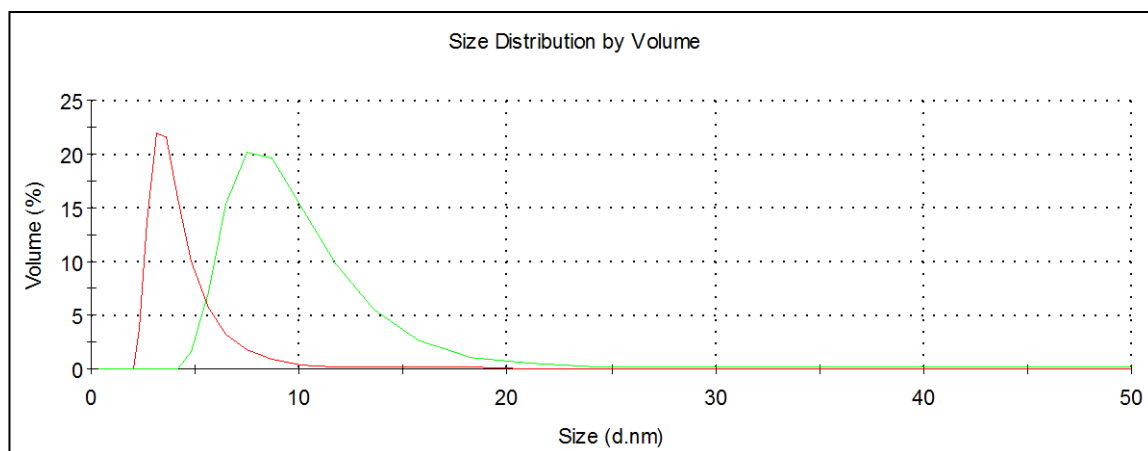


Figure 3-21 The hydrodynamic diameter of EMRSA-16 SMALPs formed at (red) 4 °C and (green) 37 °C before sonication and ultracentrifugation as determined by DLS

Table 3-2 Optimisation of the SMALPs procedure for solubilisation of MRSA membrane proteins

Exp. #	Condition for BP2-PBP2a induction with oxacillin	Lysostaphin cell wall digestion	Sonicate	Overnight incubation at 37 °C	Collect SMALPs 100,000 x g	Comments
1	10 min at mid-log with 4 mg/L		✓	✓	✓	Does not work for ECg treated
2	10 min at mid-log with 4 mg/L	✓(A)	✓	✓	✓	Initial size distribution
3	10 min at mid-log with 4 mg/L	✓(A)	✓		✓	3>2 size distribution DLS for EMRSA-16
4	10 min at mid-log with 4 mg/L	✓(B)	✓	✓	✓	4>2 size distribution DLS for EMRSA-16
5	4 h from beginning with 0.125 mg/L	✓(A)	✓	✓	✓	6>5>2: Better SDS-PAGE outcome than 2. Worse DLS than 6
6	4 h from beginning with 0.125 mg/L	✓(B)	✓	✓	✓	6>5, a better size distribution with overnight
7	4 h from beginning with 0.125 mg/L	✓(A)	✓		✓	7>8 Better DLS distribution without overnight
8	4 h from beginning with 0.125 mg/L	✓(B)	✓		✓	7>8>6 Better protein SDS-PAGE than 6
9	4 h from beginning with 0.125 mg/L	✓(A)			✓	9>7 DLS size distribution

(A) 10 min lysostaphin solubilisation of cell wall prior to addition of SMA for a further 50 min

(B) Lysostaphin and SMA added and incubated for 60 min

* Optimised procedure for membrane protein solubilisation in MRSA with SMALPs

3.3.3 Optimal SMALP conditions

A two litre culture of EMRSA-16 (± 12.5 mg/L ECg) containing 0.125 mg/L oxacillin was grown to mid-logarithmic phase at 37 °C. Cells were collected by centrifugation and the pellet suspended in digestion buffer containing 80 μ g lysostaphin and DNaseI for 10 min at 37 °C prior to the addition of 2.5% SMA. SMA was added and the mixture incubated for 50 min; SMALPs were collected by ultracentrifugation.

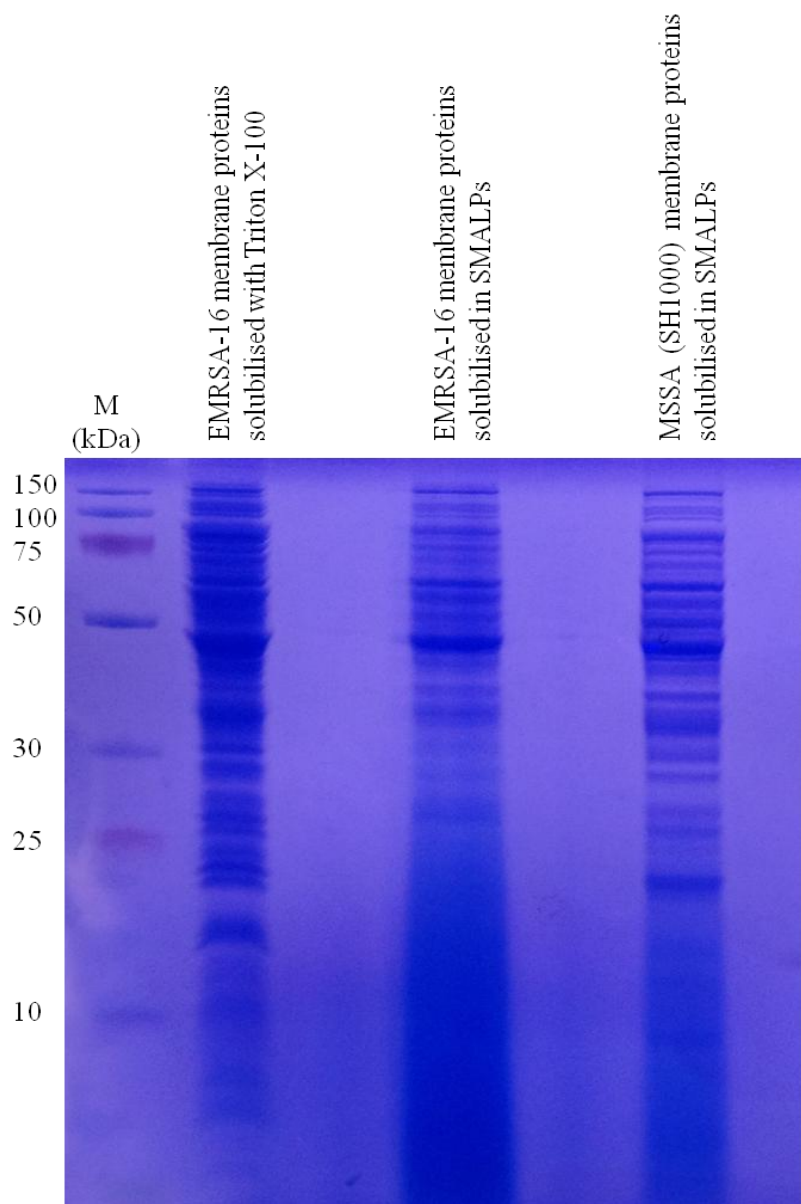


Figure 3-22 Tricine SDS-PAGE of EMRSA-16 and SH1000 membrane proteins solubilised with Triton X-100 or SMA. Proteins were resolved in a 10% Tricine-SDS-PAGE gel

In order to evaluate the enhanced efficacy of SMA solubilisation compared to surfactant solubilisation, equal amounts of membrane protein preparations from a 400 mL culture (EMRSA-16 and SH1000) were solubilised with Triton X-100 or SMA. After concentration of the samples, equal amounts were separated by Tricine-SDS-PAGE (Figure 3-22). Fewer proteins with decreased band intensity were found after SMA solubilisation as compared to surfactant extraction.

3.3.3.1 Examination of size distribution of SMALPs by TEM

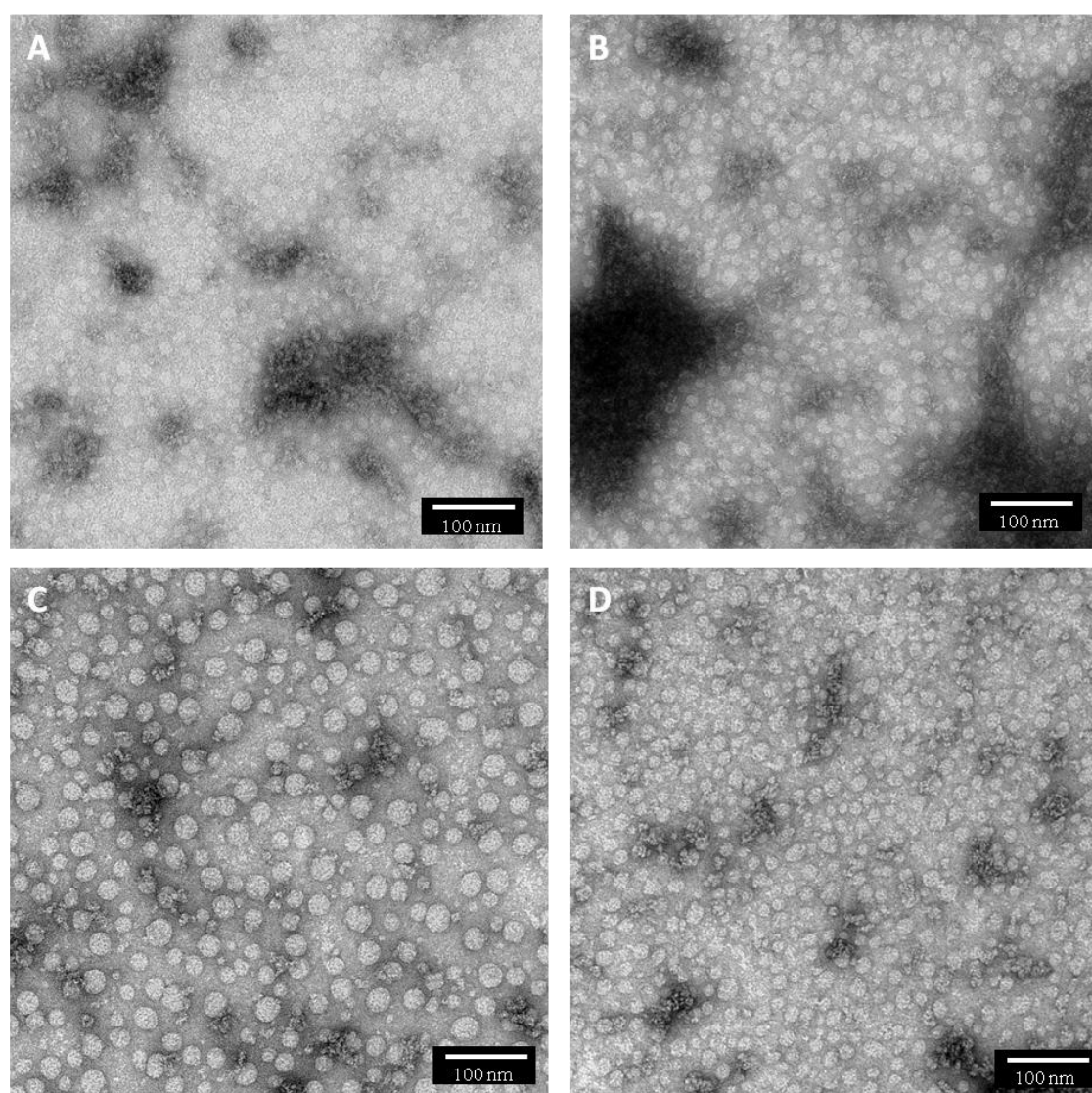
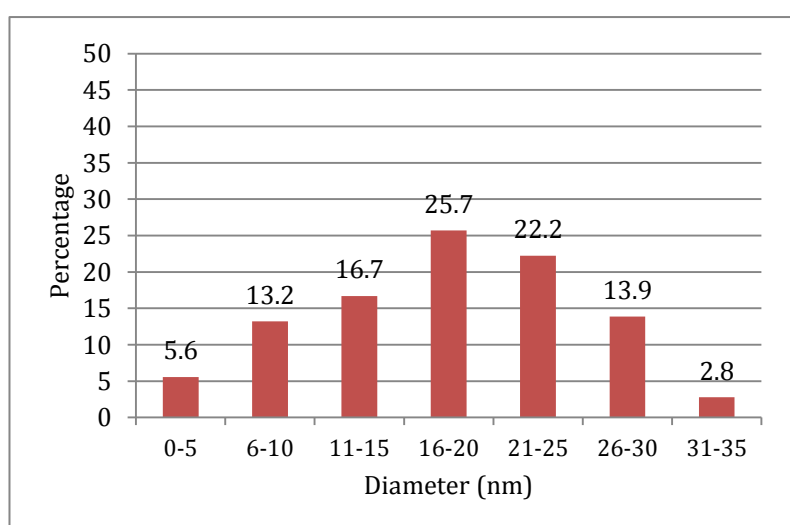


Figure 3-23 TEM images of (A) DMPC lipids solubilised within SMALPs and (B) SH1000 (C) EMRSA-16 and (D) ECg exposed EMRSA-16 membrane proteins solubilised in SMALPs

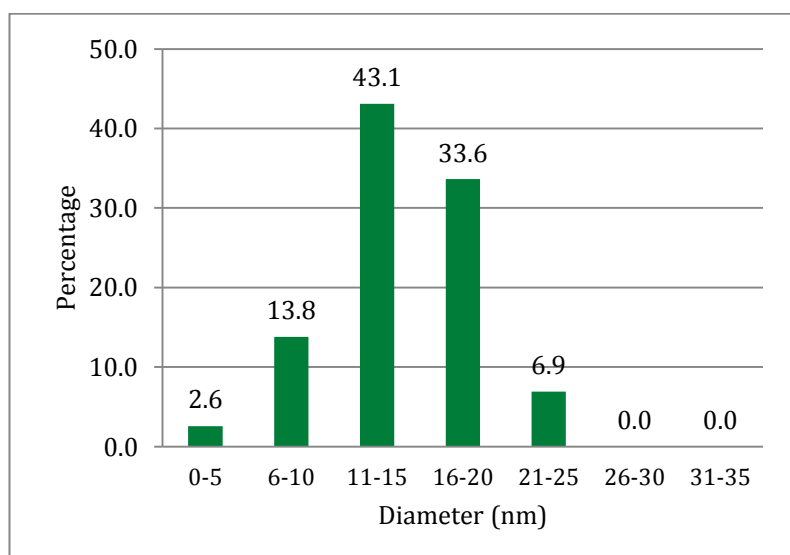
SMA-derived nanoparticles from SH1000, EMRSA-16 and ECg-exposed EMRSA-16 were examined by TEM; homogeneous preparations were noted for each sample (Figure

3-23). Mean diameters were determined from the micrographs: DMPC lipid SMALPs (12 ± 2 nm) (Figure 3-23a) < SH1000 (18 ± 3 nm) (Figure 3-23b) < EMRSA-16 SMALPs (24 ± 4 nm) (Figure 3-23c) ($n=75$ for all). A decrease was observed following exposure of EMRSA-16 to ECg (17 ± 4 nm) (Figure 3-23d).

A large proportion of EMRSA-16 SMALPs sized in the range 16-20 nm (25.7%), whereas ECg exposed EMRSA-16 SMALPs were smaller (11-15 nm; 43.1%) (Figure 3-24). It was not possible to meaningfully resolve SMALPs by SEM due to their nanoparticulate nature.



A



B

Figure 3-24 TEM size distribution of SMALPs of (A) EMRSA-16 membrane protein SMALPs and (B) ECg exposed EMRSA-16 membrane protein SMALPs

3.3.3.2 Examination of size distribution of SMALPs by DLS and flow cytometry

The diameter distribution of EMRSA-16 and ECg-exposed EMRSA-16 SMALPs utilising DLS method 9 showed a shift to smaller particles (mean measurements (n=3); 14.22 nm to 11.50) following exposure to ECg. SMA and digestion buffer SMALPs measured 1.33 nm (Figure 3-25). Again there was variation in DLS sizes measured, with the mean stated above, however every experiment showed the same trend with a shift in the size following ECg exposure.

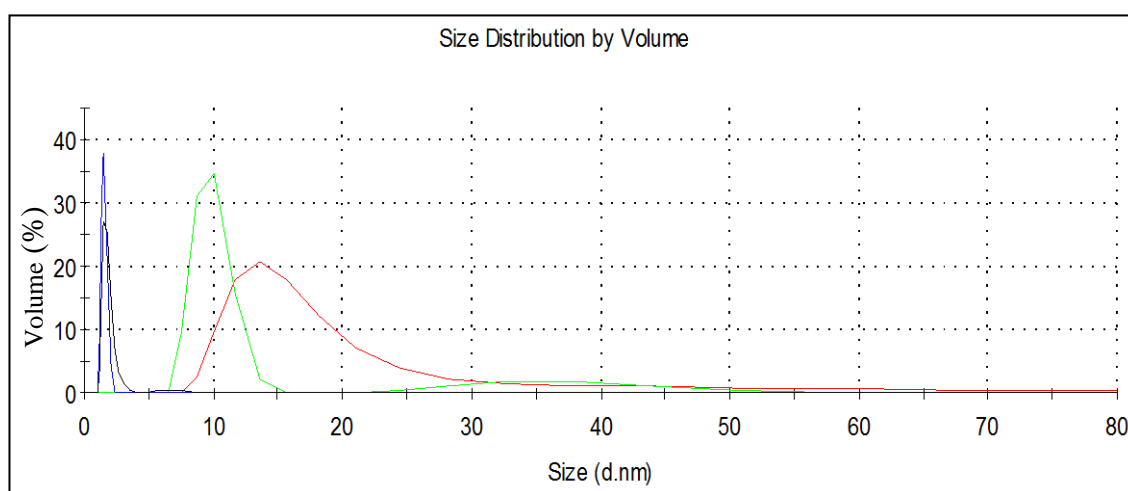


Figure 3-25 Hydrodynamic diameter of (red) EMRSA-16 and (green) ECg-exposed EMRSA-16 SMALPs; (blue) digestion buffer and (black) SMA, measured by DLS

This shift in size distribution due to ECg exposure was also observed for the COL MRSA isolate. An overlap in size distribution was observed between COL and EMRSA-16 SMALPs grown in the presence and absence of ECg as is shown in figure 3-26 as a representative of one experiment on one day. Measurements were taken on 3 separate days and the mean displayed in figure 3-7.

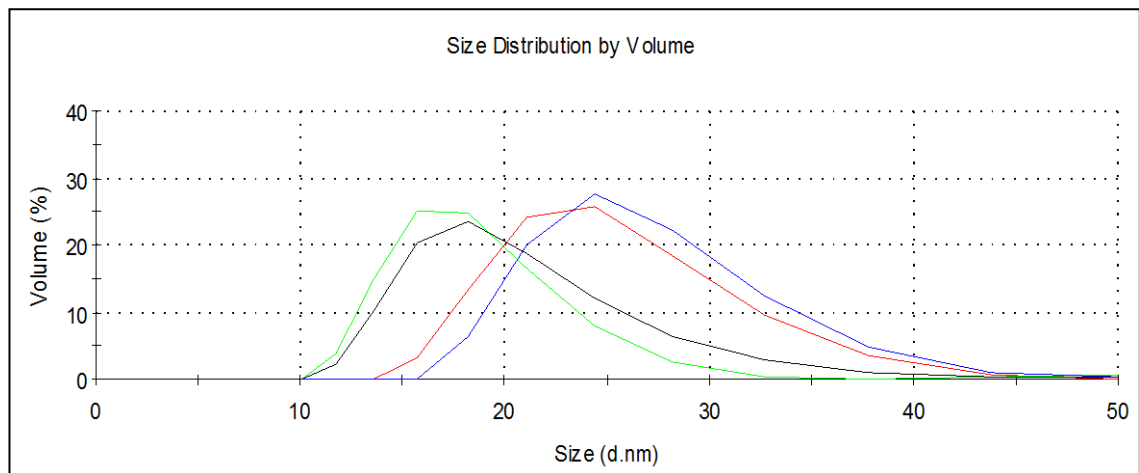
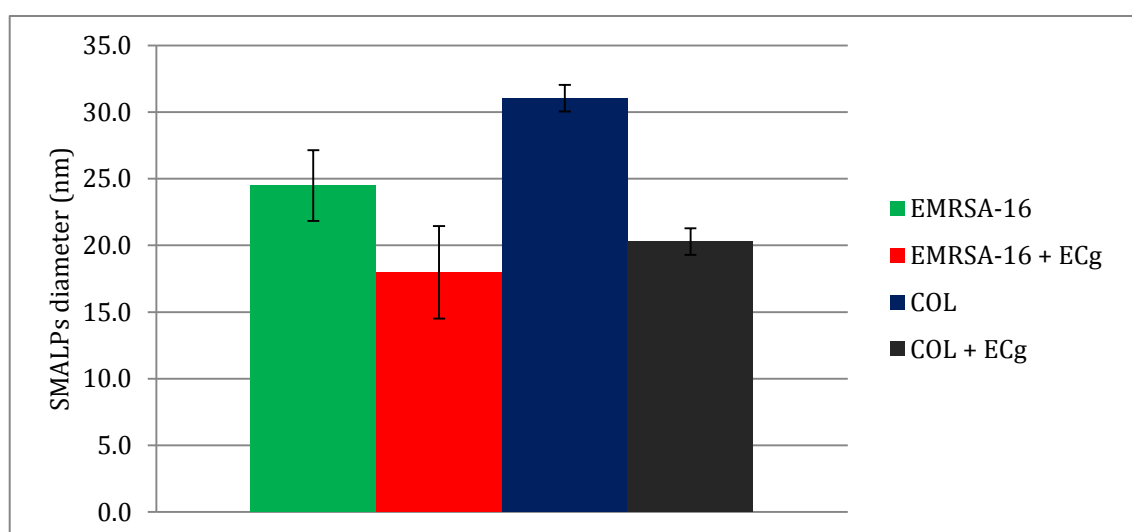


Figure 3-26 Size distribution (hydrodynamic diameter) of (red) EMRSA-16 and (green) ECg-exposed EMRSA-16 SMALPs; (blue) MRSA COL; (black) ECg-exposed COL determined by DLS. EMRSA-16 and COL SMALPs overlap in a size range from 15 to 45 nm and ECg-exposed SMALPs from 10 to 40 nm

Hydrodynamic diameters of EMRSA-16 and COL SMALPs were determined as 26.8 ± 1.72 nm and 31.0 ± 3.44 nm respectively. ECg-exposed EMRSA-16 SMALPs measured 18.0 ± 3.47 nm and COL SMALPs exposed to ECg measured 20.3 ± 5.33 nm (Figure 3-27). All samples had a high polydispersity index (0.60 - 0.89) indicative of the polydisperse SMALP diameters with a large standard deviation. Due to the preliminary nature of these experiments and with a variation in SMALP sizes observed on consequent days, the results obtained are an indication of a general reduction in SMALP sizes following ECg exposure as opposed to a definitive size difference.



The size distribution of SMALPs derived from SH1000 and EMRSA-16, determined by

Figure 3-27 Size distribution of SMALPs and impact of growth in ECg ($n=3$)

DLS also indicated a general decrease in SMALP sizes between EMRSA-16 membrane protein SMALPs and SH1000 (MSSA) membrane protein SMALPs (Figure 3-28).

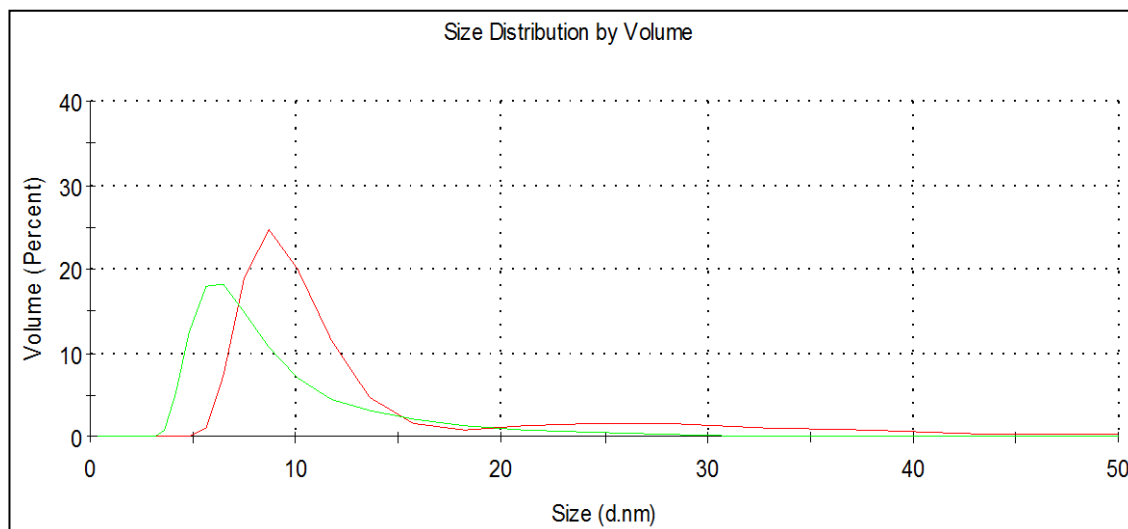


Figure 3-28 Hydrodynamic diameter of (red) EMRSA-16 and (green) SH1000 SMALPs determined by DLS

The decrease in overall SMALP diameter induced by exposure to ECg was also examined by flow cytometry. SMALPs were stained with Nile Red (60 μ M) to determine size (FSC) and complexity (SSC). Nile Red-labelled SMALPs from EMRSA-16 and ECg exposed EMRSA-16 could be readily resolved and were distinct from unstained SMALPs (Figure 3-29).

Twenty thousand events were collected while triggering for red fluorescence (B2; red fluorescent channel). The fluorescence of Nile Red-stained EMRSA-16 SMALPs was 11.04 AU compared to ECg-exposed EMRSA-16 SMALPs (10.73 AU). SSC of the SMALPs was similar for EMRSA-16 and ECg-exposed EMRSA-16 (56.59 AU and 56.77 AU respectively; Figure 3-30a).

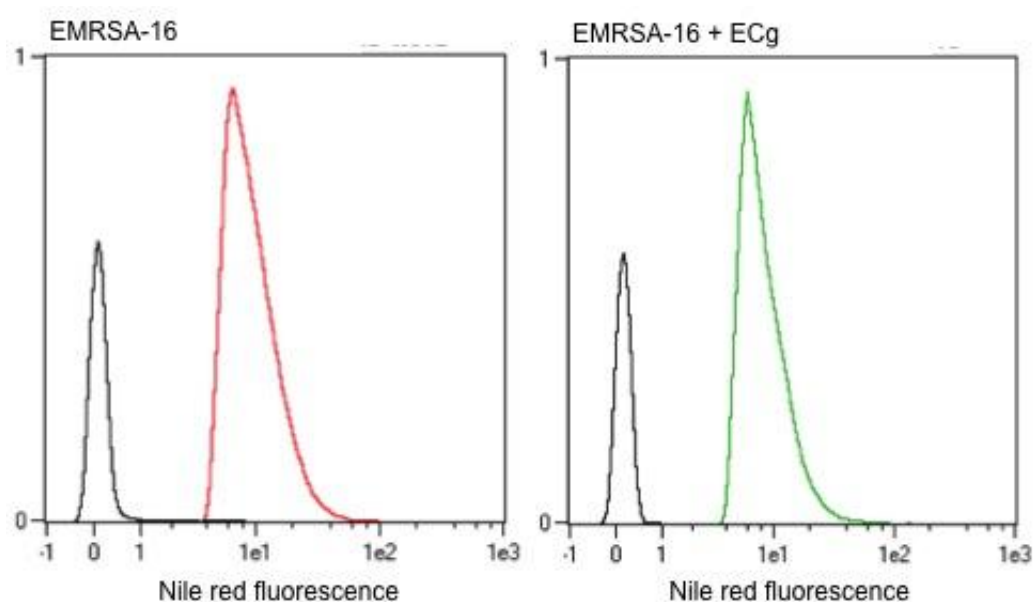


Figure 3-29 Fluorescence intensity of (red and green) 60 μ M Nile Red-staining for lipids in SMALPs compared to (black) non-fluorescence SMALPs. AU, arbitrary units

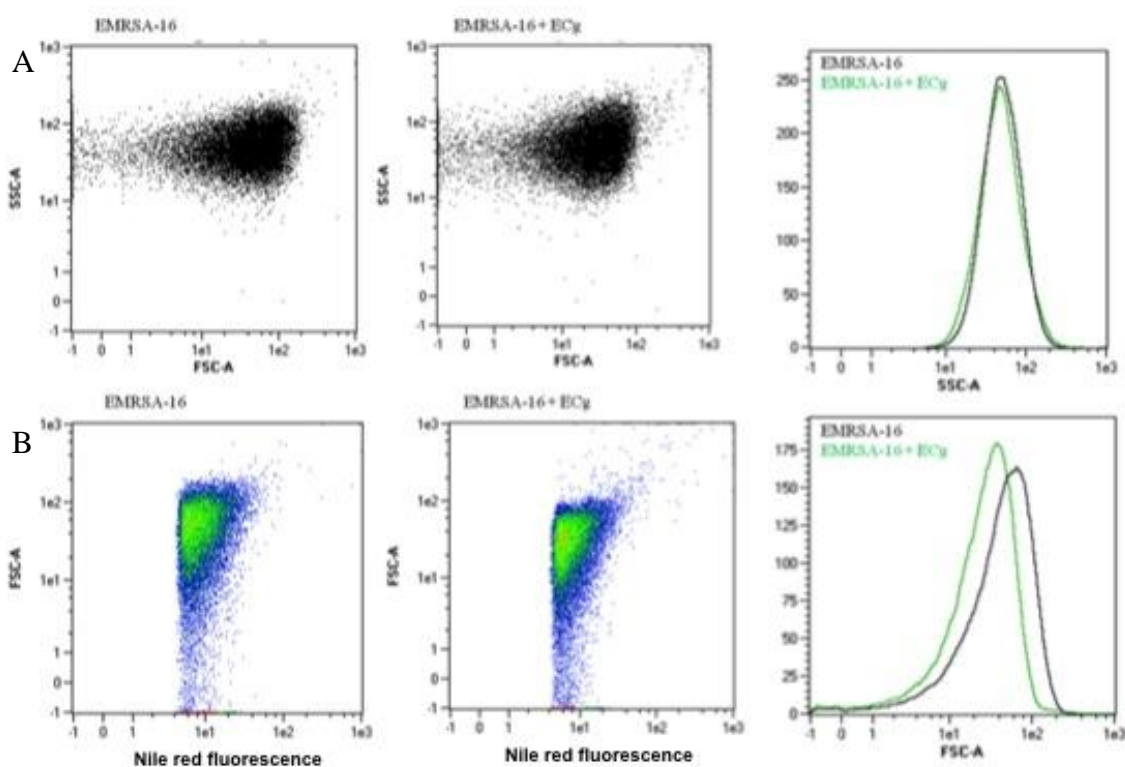


Figure 3-30 Flow cytometry of (A) EMRSA-16 and (B) ECg-exposed EMRSA-16 SMALPs (labelled with 60 μ M Nile Red); by size (FSC-A) and complexity (SSC-A)

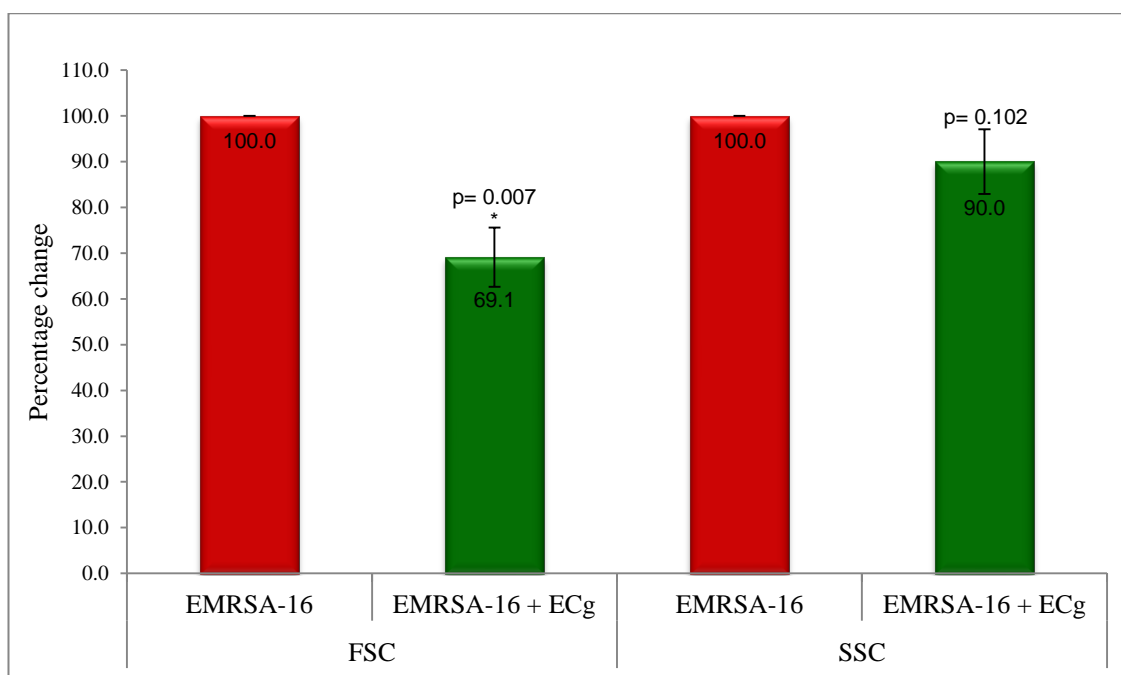
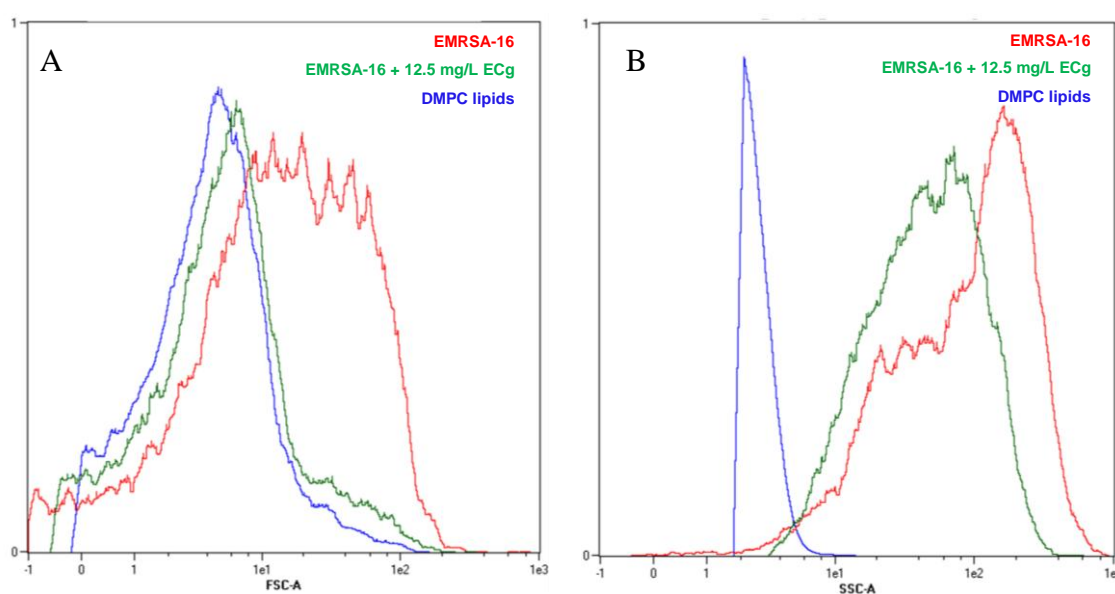


Figure 3-31 Change in FSC and SSC values determined by flow cytometry of EMRSA-16 SMALPs following exposure to ECg and incubation with 60 μ M Nile Red for 30 min ($n=3$)

In accord with TEM and DLS, an overall decrease ($p = 0.007$) in EMRSA-16 SMALP FSC was observed (46.05 to 32.31 AU) as a result of growth in the presence of ECg (Figure 3-30b). The reduction in size is shown in figure 3-30b. SMALPs derived from EMRSA-16 exhibited a 30.9% decrease in FSC and 10.0% decrease in SSC as a result of growth in ECg (Figure 3-31); a comparable decrease induced by ECg exposure was found with COL and complemented DLS (Figure 3-32c).



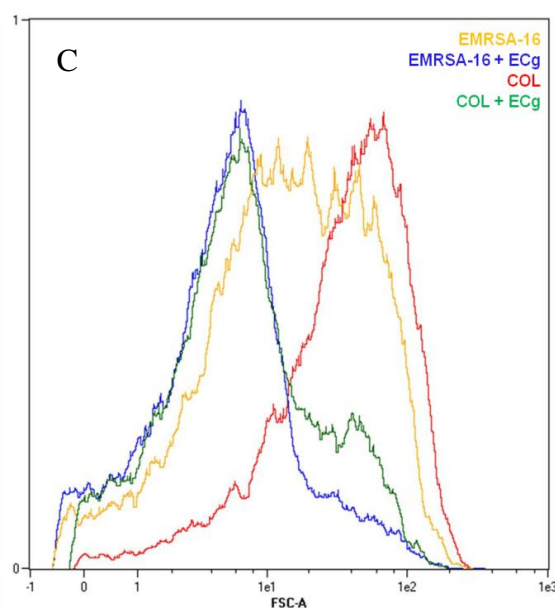


Figure 3-32 Single parameter histogram of light measurements of SMALP particles by flow cytometry stained with 60 μM Nile Red. (A) FSC-A and (B) SSC-A measurements of EMRSA-16, EMRSA-16 exposed to ECg and DMPC. (C) FSC-A of EMRSA-16, COL and ECg exposed SMALPs

3.3.3.3 Co-localisation of PBPs

After SMA solubilisation of membrane proteins, any co-localisation of PBPs and SMALP lipid was examined by confocal microscopy. PBPs and lipid were detected with bodipy FL and Nile Red. Co-localisation of these markers was observed (Figure 3-33).

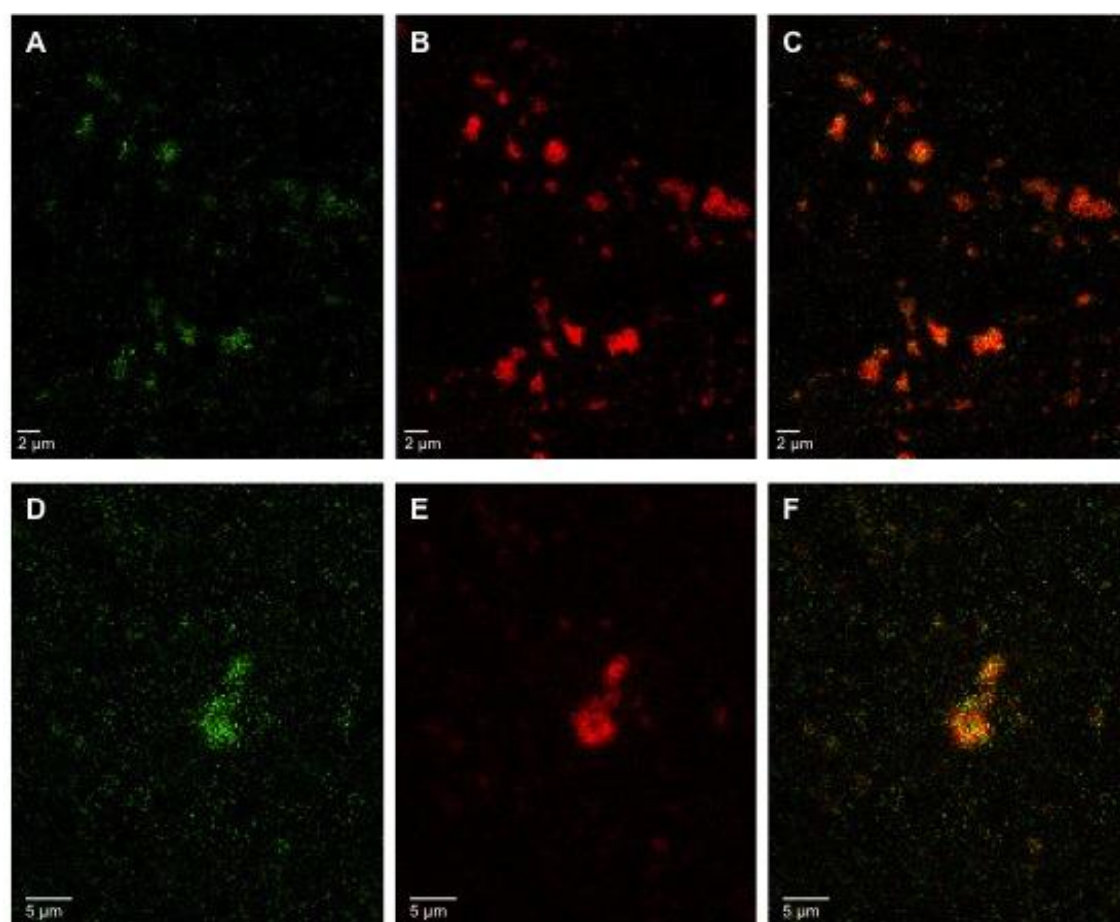


Figure 3-33 Confocal fluorescence microscopy of EMRSA-16 SMALPs labelled with (A and D) bocillin FL and (B and E) Nile Red detecting PBPs and lipid SMALPs. C and F are merged confocal images

3.4 Discussion

Knowles *et al.* (2009) demonstrated that recombinant bR and PagP were integrated into SMALPs to produce nanoparticles with a mean diameter of 11 nm. In the current study, a method was developed utilising SMA to solubilise membrane proteins directly from the cytoplasmic membrane following removal of the staphylococcal cell wall. SMALPs trapped membrane proteins that were amenable to investigation by SDS-PAGE and their protein content was low, necessitating concentration of the preparations prior to analysis. However, following successful protein solubilisation, further modifications were made to reduce the degree of disruption to the cell and internal environment prior to protein extraction in an attempt to maximise recovery.

A method was developed for the solubilisation of membrane proteins from whole cells. To allow access of SMA to the cytoplasmic membrane, it became apparent that lysostaphin was required to facilitate minimal degradation of the cell wall through cleavage of pentaglycine cross-bridges. Ten minutes incubation of cells with lysostaphin allowed minimal disruption of the cell wall for SMA to gain access to the membrane proteins. SMA solubilisation after incubation with lysostaphin resulted in SMALPs with a higher mean diameter, in comparison to preparations obtained when SMA and lysostaphin were employed together.

Jamshad *et al.* (personal communication) had employed an overnight incubation step at optimal temperature following SMA solubilisation in order to increase protein capture. In the current study, omission of the overnight incubation step resulted in SMALPs with a lower mean diameter; however, investigation of SMA-solubilised proteins showed that absence of the overnight step resulted in a larger number of protein bands (Figure 3-19) Therefore, overnight incubation was omitted to reduce the number of steps in the procedure and to reduce the potential for membrane protein complex disruption

A gentle sonication step introduced by Jamshad and co-workers to disperse SMALPs prior to collection by ultracentrifugation was also found to be unnecessary for solubilisation of staphylococcal membrane proteins. Sonication disrupts vesicles and subsequent vesicle reformation may result in damage and/or disruption of macromolecules, as demonstrated for fragmentation of DNA (Sambrook and Russell,

2006a). The sonication step could, therefore, result in disruption of PBP2/PBP2a complexes and possible denaturation of proteins. Analysis of the size distribution of SMALPs without omission of the sonication step produced particles with higher mean diameter and more extensive size distribution (Figure 3-19). In this comparison, there was no decrease in protein band intensity, providing justification for omission of the sonication step.

The optimised method for SMA solubilisation of membrane proteins from intact cells encompassed a two litre culture volume, SMALP collection at 37 °C and the modifications described above (Table 3-2, experiment 9). For reasons of scale and economy, in particular the cost of lysostaphin, cultures larger than two litre could not be employed. Key elements of the method employed are as follows;

-
- ❖ Large starting culture (2 L)
 - ❖ Suspension of cell pellet in 20% (w/v) sucrose to stabilise membrane proteins
 - ❖ Digestion of cell wall with lysostaphin for 10 min prior to addition of SMA
 - ❖ SMA solubilisation at 37 °C
 - ❖ Collection of SMALPs at 100,000 g for 1 h
 - ❖ Concentration of SMALP samples to 1 ml with Vivaspin columns at 4 °C
 - ❖ Analysis of membrane proteins using Tricine-SDS-PAGE
 - ❖ Denaturation of proteins at 37 °C for 30 min prior to gel electrophoresis
-

Knowles *et al.* (2009) and Orwick *et al.* (2012) visualised SMALPs by negative stain TEM (Figure 3-14). SMALPs obtained in their studies were not uniformly cylindrical in nature and there was some variation in size. The size of SMALPs derived from DMPC were approximately 9 nm in diameter whereas SMALPs containing PagP or bR were ~10.2 nm in diameter (Knowles *et al.*, 2009; Orwick *et al.*, 2012).

EMRSA-16 membrane proteins solubilised by SMA displayed a denser and higher resolution surface of SMALPs compared to SMALPs by Orwick *et al.* (2012) with an average size range between 16 and 20 nm (Figure 3-24a). Their mean diameters were 5-9 nm greater than those of Knowles *et al.* (2009) and this may be due to encapsulation of protein complexes rather than molecules of one protein species.

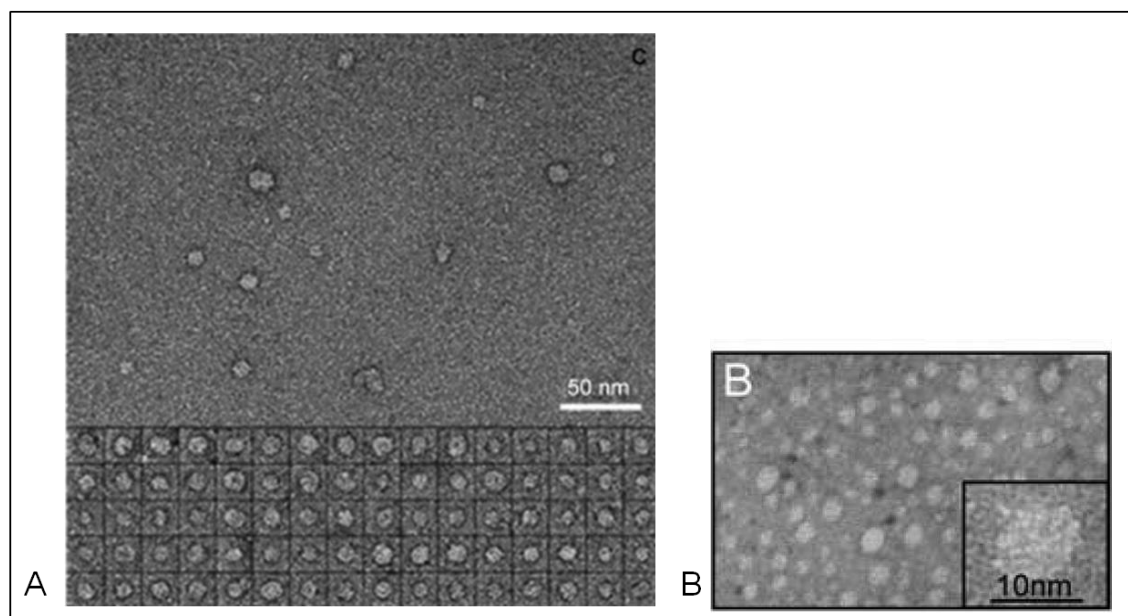


Figure 3-34 TEM of uranyl acetate stained preparations of (A) DMPC SMALPs (also termed lipodisks) from Orwick *et al.* (2012) and (B) SMALPs containing PagP or bR with the insert showing a single SMALP particle (Knowles *et al.*, 2009)

After exposure of EMRSA-16 to ECg, average size diameters fell within 11 - 15 nm (Figure 3-24b), representing an overall size decrease compared to unexposed EMRSA-16 SMALPs. The size range of the ECg-exposed SMALPs may be comparable to that of particles containing single protein species and this may reflect disruption of protein complexes following exposure to ECg.

Similar size distribution data was observed using DLS, with reductions in diameter after exposure of EMRSA-16 to ECg. Due to the preliminary nature of these experiments and that a difference in SMALP sizes was observed on consequent days, at this stage, the data is indicative of an overall reduction in SMALP sizes following ECg exposure. The dimensions measured by DLS were also greater than those obtained by TEM and could be due to the fact that DLS determinations take into account the hydrodynamic diameter of particles. DLS measures the hydrodynamic diameter of a hypothetical hard spheres that diffuses in the same manner as the SMALPs; TEM shows that these nanoparticles are not perfectly spherical and measurement of the hydrated/solvated particle results in an overestimation of true particle size (Malvern). In practice, intensity distributions determined by DLS are converted to volume distribution using Mie theory to compare relative proportions of SMALP preparations dependent on volume rather than scatter.

Flow cytometry, was also employed to compare EMRSA-16 and ECg-exposed EMRSA-16 membrane protein SMALPs. An overall reduction ($p = 0.007$) in size (FSC) was found when EMRSA-16 cells were exposed to ECg. This data accords with changes in the dimensions of SMALPs measured by TEM and DLS. Due to their small size, SEM images and SSC measurements determined by flow cytometry did not provide significant findings.

After SMA solubilisation of EMRSA-16 membrane proteins to form approximately spherical particles, PBPs co-localised with SMALP lipids. Previous work by Jorge *et al.* (2011) localised PBPs within *S. aureus* cells labelled with bocillin FL. Atilano *et al.* (2010) also demonstrated that the membrane dye Nile Red can be used to visualise *S. aureus* membranes. In the current study, Nile Red and bocillin FL were combined in order to examine the propensity for co-localisation of lipids together with PBPs to take place within SMALPs. PBPs and lipids could be co-localised in SMALPs derived from EMRSA-16 and ECg-exposed EMRSA-16 when confocal microscopy was employed together with bocillin FL (PBPs) and Nile Red (SMALPS) fluorescent staining. The particles were too small to allow for resolution of structural detail. These data provide some evidence that PBPs, including PBP2/PBP2a complexes, were successfully incorporated within SMALPs.

CHAPTER FOUR

4. EFFECT OF EXPOSURE TO ECG ON THE PBP2/PBP2A COMPLEX

4.1 Introduction

Following solubilisation of EMRSA-16 membrane proteins with SMA and co-localisation of PBPs and SMALP nanoparticles, the integrity of the PBP2/PBP2a complex was investigated.

Immunoprecipitation, co-immunoprecipitation and Ab affinity chromatography are key tools for the investigation of single proteins and protein-protein interactions (Qoronfleh *et al.*, 2003). Immunoprecipitation is a immunochemical technique for antigen characterisation, molecular weight determination, rates of synthesis or degradation, posttranslational modifications and interactions with proteins, nucleic acids or ligands (Williams, 2000). On the other hand, co-immunoprecipitation and Ab affinity chromatography are commonly employed to study *in vivo* protein interactions and to identify interacting protein partners (Yamauchi *et al.*, 1995) and receptor-ligand (Shi *et al.*, 2000) and enzyme-substrate (Honda *et al.*, 1997) interactions in suspension (Sambrook and Russell, 2006b). These procedures are limited by the availability of high affinity Abs and the capacity to detect physiological levels of the target protein (Ransone, 1995). Ab affinity chromatography is dependent on the chemical binding or coupling of the affinity ligand (e.g. Ab) to a solid, chromatographic matrix (stationary phase); the target proteins and protein partners in solution (mobile phase) interact with the ligand (Urh *et al.*, 2009). Unbound proteins are removed by washing and the target proteins recovered (Urh *et al.*). Co-immunoprecipitation, in similar fashion to Ab affinity chromatography, involves the capture and detection of a specific protein with a ligand of choice along with additional proteins in the complex independent on whether they are bound directly or indirectly (Yang *et al.*, 2008). If a suitable Ab is available, co-immunoprecipitation and Ab affinity chromatography more rapidly detect protein interactions than other commonly used methods such as epitope tagging and glutathione s-transferase (GST) pull down (Yang *et al.*, 2008).

Epitope tagging of proteins (e.g. His₆ or calmodulin binding peptides), enables rapid and reliable procedures for the study of protein-protein interaction, as genetic tagging is usually more straightforward than raising a high quality Ab (Yang *et al.*, 2008). Protein complexes are purified in gentle conditions with a commercial kit and bait proteins over-expressed to compensate for the low abundance of some proteins. However, the

addition of a tag may compromise protein folding, function or protein-protein binding; this may limit its use for the study of PBP2/PBP2a complexes (Yang *et al.*, 2008).

GST pull down assays are primarily employed to identify interacting partners of a known protein or to confirm protein-protein interactions observed using two hybrid-systems (Ren *et al.*, 2003). GST-protein fusions are expressed in *E. coli*, immobilised on a solid support (e.g. glutathione sepharose beads) and interacting proteins pulled down with the GST-tagged protein (Yang *et al.*, 2008). A frequent shortcoming of the method is the inability to over-express all proteins in soluble form in *E. coli*. Further, the fusion proteins often lack posttranslational modifications required for interactions with other proteins.

In this chapter, Ab affinity chromatography and co-immunoprecipitation were employed to investigate potential interactions between SMA-solubilised PBP2 and PBP2a from EMRSA-16, together with the impact of exposure of the bacteria to ECg (Figure 4-1).

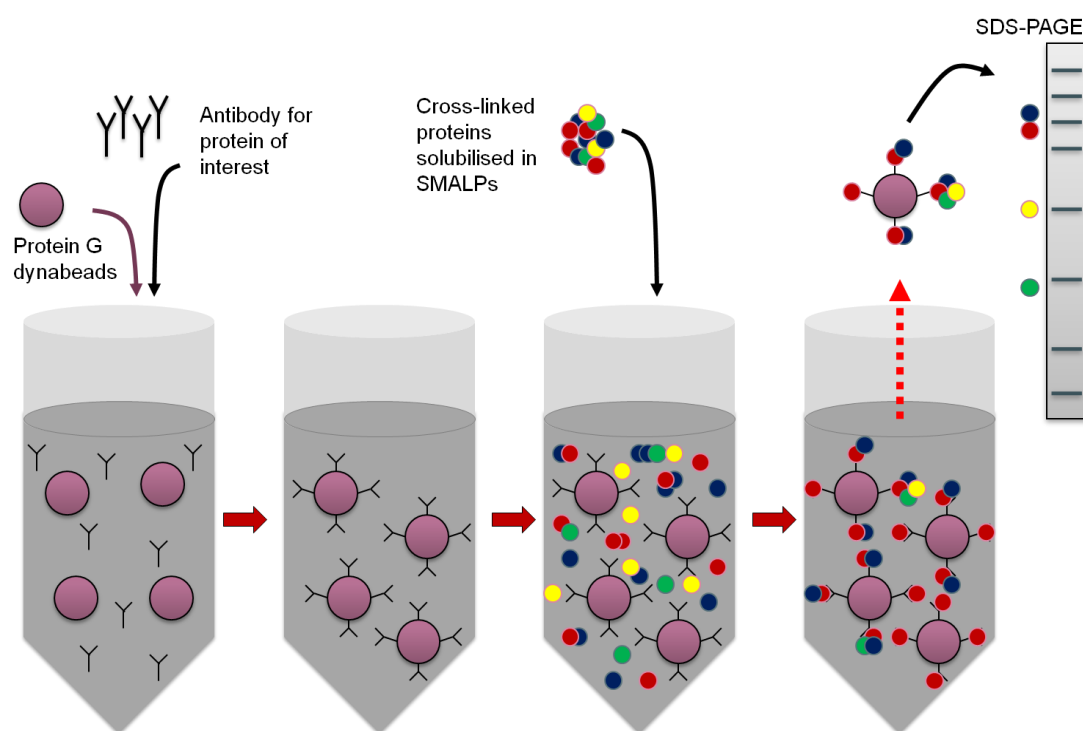


Figure 4-1 Co-immunoprecipitation for protein-protein interactions

Abs for the proteins of interest were bound to an immobilised protein G matrix. The suitability of protein A or G matrices is dependent upon the source and class of the Ab used; protein A is generally less expensive but protein G binds to a wider range of Abs,

including those from mice and rabbits. Membrane proteins solubilised with SMA were cross-linked and probed for the presence of PBP2/PBP2a complexes with Ab-protein G solution (Qoronfleh *et al.*, 2003). Proteins interacting with Ab-protein G were precipitated from the matrix and examined by SDS-PAGE (Figure 4-1); interacting protein partners are then detected by Western blotting or flow cytometry (Qoronfleh *et al.*, 2003).

Western blotting (Figure 4-2) is essential for the discrimination of PBP2 (80 kDa) and PBP2a (78 kDa). This method can also identify other proteins that interact *in situ* with PBP2 and PBP2a. If PBP2 and PBP2a form a physical complex, both proteins will be found in co-immunoprecipitation eluents following individual Western blotting (Figure 4-3). This procedure could be confounded by low abundance partner proteins, present in concentrations below the threshold of detection.

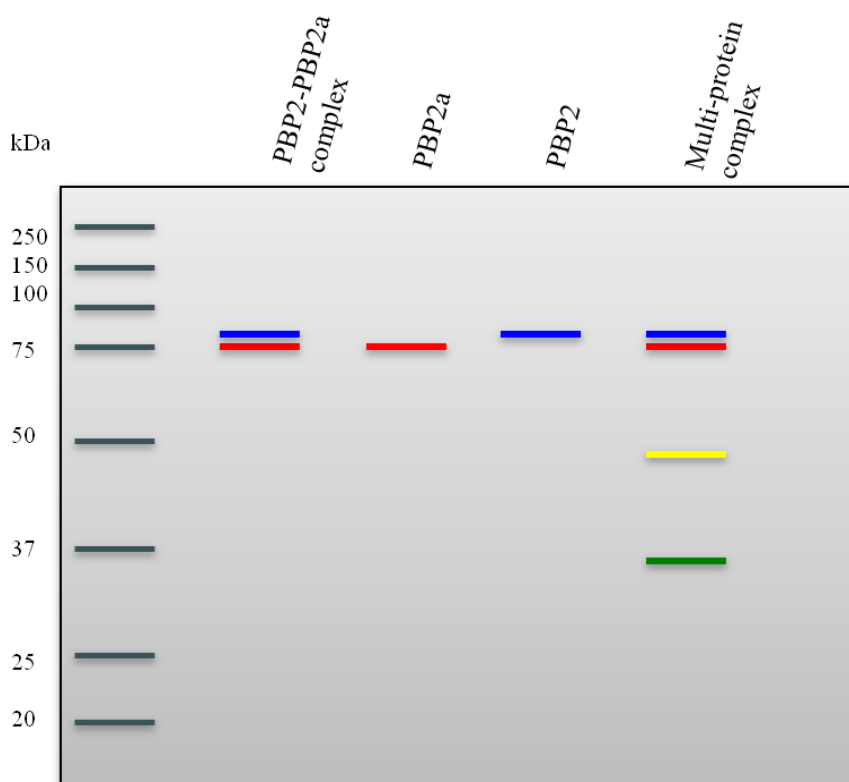


Figure 4-2 Gel mapping of PBP2, PBP2a, PBP2/PBP2a complexes and multi-protein complexes

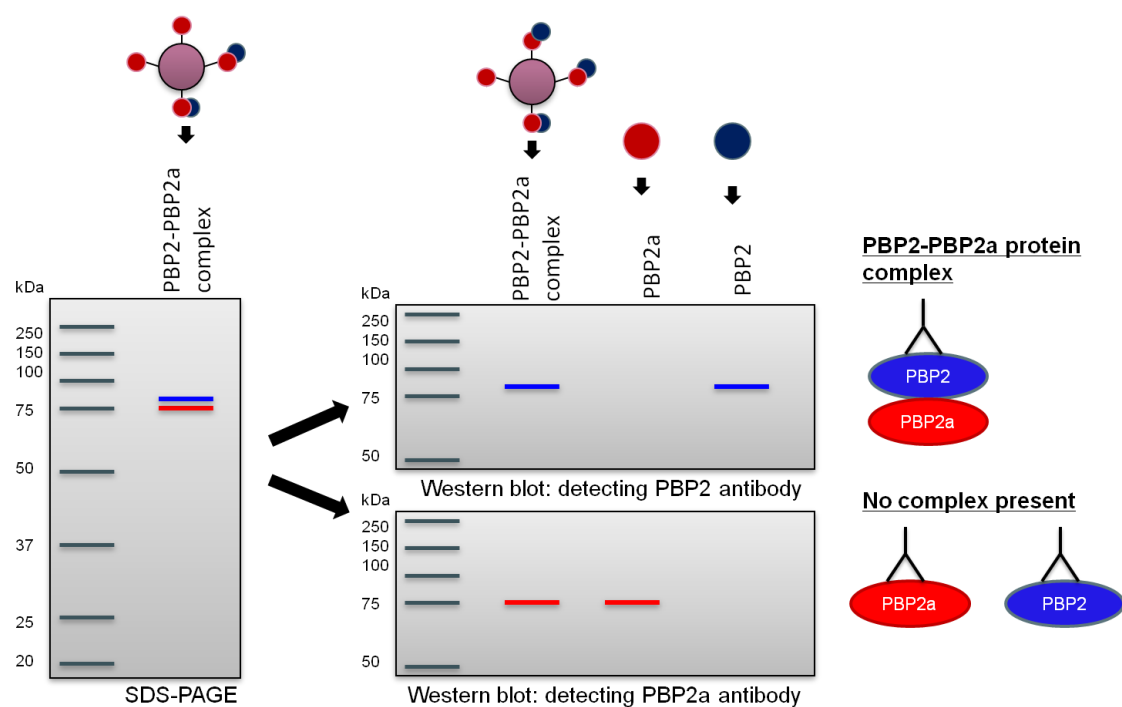


Figure 4-3 Predicted Western blots for individual or complexed proteins captured by SMALPs and purified by co-immunoprecipitation

4.2 Materials and methods

4.2.1 Bacterial strains and reagents

Polyclonal rabbit anti-PBP2a serum was produced and purchased from BioServ (Sheffield University, UK). Rabbit anti-FtsZ Ab was donated by Jeff Errington (Newcastle University, UK).

4.2.2 Anti-PBP2a polyclonal Ab affinity purification

Rabbit anti-PBP2a serum was produced commercially by BioServ with 2 mg/mL purified PBP2a protein supplied by David Roper (University of Warwick). Abs from 600 μ L antiserum was purified utilising a protein G HP SpinTrap column (GE Healthcare Life Sciences); the column contained protein G Sepharose with a high affinity for the IgG Fc region. Column storage solution was removed by centrifugation (100 g, 1 min, 4 °C) and columns washed three times with 400 μ L Tris-buffer saline (TBS) (50 mM Tris, 150 mM NaCl, pH 7.5). After column equilibration, 600 μ L of anti-PBP2a serum was incubated with the protein G agarose for 5 min at 4 °C with agitation. The protein G-IgG complex was washed five times with 400 μ L TBS. Purified anti-PBP2a IgG was then eluted from the affinity matrix with 400 μ L 0.1 M citrate (pH 2 - 3) by centrifugation at 70 g; 30 μ L 1 M Tris-HCl pH 9.0 added to restore the pH to physiological levels.

4.2.3 Cross-linking of proteins in SMALPs

DTSSP was dissolved to 10 mM in 500 μ L of concentrated SMALP solution (~25 mg/mL) and the mixture incubated at 4 °C for 30 min. The cross-linking reaction was quenched as described in section 2.3.8.1. Prior to loading the protein sample onto an SDS-PAGE, the cross-linker was cleaved with 5 % β -mercaptoethanol (Sigma) in Tricine sample buffer.

4.2.4 Protein pull down assays for complex identification

Ab affinity chromatography and co-immunoprecipitation were employed with Abs for PBP2 and PBP2a. Samples were normalised to equal concentrations of protein SMALPs (~25 mg/mL). Equal amounts (~500 μ L) were added to all affinity matrix-Ab solutions,

equivalent amounts of eluent (8 - 10 μ L) separated with 2-3 SDS-PAGEs and proteins identified by Western blotting.

The bicinchoninic acid method, a modification of the Lowry method (Smith *et al.*, 1985), and the Bradford assay could not be employed for the quantification of protein within particles due to the presence of SMA polymer and lipids, which caused SMALP precipitation and aggregation. Instead, the Nanodrop A_{280} absorbance assay was employed, with an absorbance maximum in the near-UV (280 nm) due to the aromatic amino acids tyrosine and tryptophan (Nelson and Cox, 2000; Hunte *et al.*, 2003). Protein content of SMALPs (2 mL) was determined in this assay at 280 nm (A_{280}) in triplicate, with A_{260}/A_{280} also measured. Values with a A_{260}/A_{280} ratio of <0.5 were included to minimise nucleic acid contamination error (Atiken and Learmonth, 2002). Protein concentrations were measured in mg/mL.

4.2.4.1 Ab affinity chromatography

Protein G HP spintrap columns with a Sepharose matrix of 6% highly cross-linked agarose with 2 mg protein G/mL medium were used. The storage solution (20% ethanol) was removed by centrifugation (150 g, 1 min) and the columns washed three times with 400 μ L of TBS to equilibrate the matrix. Two hundred μ L of Ab (anti-PBP2, -PBP2a or -FtsZ) solution (0.5 - 1.0 mg/mL Ab in TBS) was added to the columns, which were incubated at RT for 1 h with gentle agitation. Excess unbound Ab was removed by centrifugation and the matrix washed with 400 μ L TBS. Cross-linked SMALPs were added to the columns (maximum volume 500 μ L). The spin columns were placed on a shaker and incubated at 4 $^{\circ}$ C for 1 h. The protein-IgG complex bound to the matrix was washed five times with TBS. The IgG-protein complexes were eluted with 100 μ L 0.1 M glycine (pH 2.5), centrifuged for 1 min (1000 g, 4 $^{\circ}$ C) and the pH restored as described in section 4.2.2.

4.2.4.2 Co-immunoprecipitation

The Dynabead protein G immunoprecipitation kit (Life Technology Ltd.) was utilised. Dynabeads suspended in PBS + 0.09% (w/v) sodium azide were homogenously distributed through pipetting and 50 μ L Dynabeads transferred to one Eppendorf tube for each co-immunoprecipitation assay. Tubes were placed on a magnet and the

supernatant removed. The Dynabeads were suspended in 200 μ L Ab binding and wash buffer containing 8-10 μ g of either anti-PBP2 or anti-PBP2a Ab. The Dynabead-Ab solution was incubated for 1 h at RT with agitation, the Dynabead-Ab complex collected and washed with 200 μ L Ab binding and wash buffer. Cross-linked SMALPs (~500 μ L) were added to the Dynabeads and incubated for 2 h at 4 °C with agitation. The Dynabead-Ab-protein complex was washed three times in 200 μ L wash buffer, the Ab-protein complex eluted with 20 μ L of elution buffer and the pH restored to physiological levels as mentioned in section 4.2.2.

Conditions for elution of precipitated proteins from the affinity matrix often result in release of the Ab, contaminating the sample and leading to background noise that can interfere with the detection of protein bands (Yang *et al.*, 2008). Ab in solution was coupled to the affinity matrix with dimethyl pimelimidate x 2HCl (DMP), a water-soluble and membrane-permeable homo-bifunctional imidoester cross-linker (Deleault *et al.*, 2005). The Dynabead-Ab complex was washed twice with 1 mL 0.2 M triethanolamine (pH 8.2), suspended in 1 mL 20 mM DMP in 0.2 M triethanolamine (pH 8.2) and incubated at 20 °C for 30 min with gentle agitation. After removal of the Dynabead-Ab complex with a magnet, the beads were suspended in 1 mL 50 mM Tris (pH 7.5) and incubated for 15 min at RT. The supernatant was discarded and the cross-linked Dynabeads washed three times with 1 mL PBS (0.01 - 0.1% Tween-20). After cross-linking, SMALPs (~500 μ L) were added to the beads and the co-immunoprecipitation procedure continued as described previously.

4.2.5 Identification of protein complexes

4.2.5.1 1D SDS-PAGE

Samples were normalised using the A₂₈₀ absorbance assay prior to protein pull down and equal amounts of eluent in 2x sample buffer added to each 10% SDS-PAGE (25 μ L) or 10% Tricine-SDS-PAGE (15 μ L) slot. Proteins were transferred to a membrane by Western blotting for protein identification.

4.2.5.2 Western blotting

Western blotting was undertaken as described in section 2.3.1.0 Equivalent volumes of eluent were run on separate SDS-PAGEs resulting in two or three separate Western blots to identify PBP2, PBP2a and FtsZ in co-immunoprecipitation eluents. Transfer was performed at 100 V (Constant V) for 1 h at RT followed by membrane blocking for 1 h at RT with agitation using 40 mL Western blotting solution. Membranes were then incubated with primary Ab (anti-PBP2, -PBP2a or -FtsZ) in 30 mL Western blotting solution at optimised concentration for detection and incubated overnight at 4 °C with agitation. Dilutions for primary Ab were 1:500, 1:10,000 and 1:10,000 for anti-PBP2, -PBP2a and -FtsZ respectively. Membranes were washed four times for 5 min with 40 mL tris buffer saline with tween 20 (TBST) followed by incubation with secondary HRP-conjugated monoclonal Ab at 1: 10,000 dilution in 20 mL Western blotting solution for 1 h at RT. After four washes of 5 min each with TBST, protein bands were detected with TMB or supersignal West pico chemiluminescent substrate (Thermo Scientific). For chemiluminescent detection, 2 mL of luminol enhancer solution was mixed with 2 mL of stable peroxidase solution and the membrane submerged in the solution in the dark for 5 min with gentle agitation. Protein bands were visualised with a Molecular Imager Gel Doc XR (Bio-Rad).

4.2.5.3 2D gel electrophoresis

SMALPs (125 µL; 25 mg/L) were rehydrated overnight at RT on 7 cm IPG ReadyStrips pH 7 - 10 (Bio-Rad). Isoelectric focusing of proteins was undertaken using Protean IEF Cell (Bio-Rad) at 20 °C with an accumulated total of 10,000 V-h and a final voltage of 4000 V. Focused strips were stored at -80 °C prior to 2D SDS-PAGE. For 2D separation, IPG strips were equilibrated in buffer (6M Urea, 2% SDS, 0.05 M Tris-HCl pH 8.8, 20% glycerol) containing 1% Dithiothreitol (DTT) (Sigma) for 15 min and then in the same buffer containing 2.5% iodoacetamide (Sigma) and no DTT for 15 min. Strips were transferred to a 10% Tris-SDS-PAGE gel, electrophoresed at 110 V (constant V) for 80 min and protein bands visualised with silver stain.

4.2.5.4 Flow cytometry

Proteins recovered by co-immunoprecipitation were detected with the primary and secondary fluorescence-conjugated Abs described above by flow cytometry in a MACS Quant[®] Analyser (Miltenyi Biotec Ltd.). Primary Abs were mouse anti-PBP2a and rabbit anti-PBP2. Co-immunoprecipitation eluents (5 μ L) were suspended in 495 μ L digestion buffer, labelled with primary anti-PBP2 (1:500) or PBP2a (1:10,000) Ab for 1 h at RT with gentle agitation. After, they were incubated with 1:10,000 dilution fluorescein-isothiocyanate (FITC) conjugated secondary Ab (goat anti-rabbit and rabbit anti-mouse) and 60 μ L Nile Red for 30 min in the dark. Twenty thousand Nile Red fluorescence events were gated (B2, trigger 3.0) as described in section 3. Co-immunoprecipitation eluents of SMALPs enriched with anti-PBP2 Ab were probed for PBP2a in the B3 green fluorescent channel (330V, trigger 2.0) after back gating of the 20,000 Nile Red events. Eluents from co-immunoprecipitation with anti-PBP2a Ab were probed in the same manner for PBP2. Data was analysed using the MACS Quantify[™] Software (Miltenyi Biotec Ltd.).

4.3 Results

Expression of PBP2a and PBP2 by EMRSA-16 was investigated following exposure to ECg (12.5 and 25 mg/L); membrane proteins solubilised in SMALPs. A decrease in both PBP2a and PBP2 expression was observed following growth in 25 mg/L ECg (Figure 4-4) and was subject to limits of detection of the Western blotting procedure and the specificity and sensitivity of the Ab used.

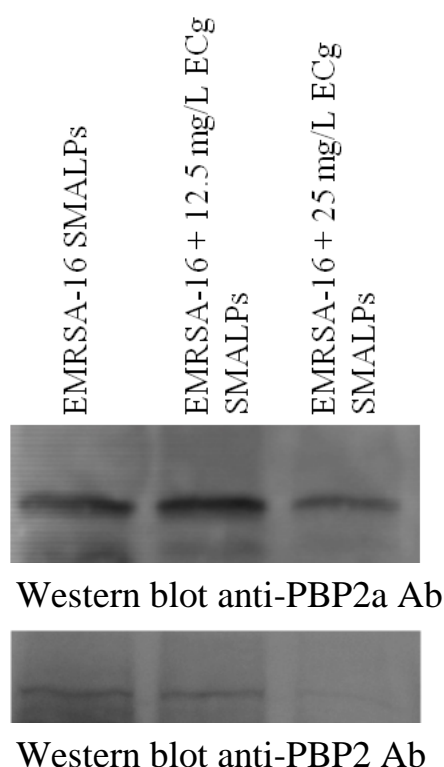


Figure 4-4 Detection in SMALPs of PBP2a and PBP2 from EMRSA-16 after growth in ECg

Membrane proteins solubilised in SMALPs were separated with 2D gel electrophoresis using IPG strips focusing over the pH range 7-10. Some protein spots from EMRSA-16 SMALPs were detected but gels of proteins from bacteria exposed to ECg showed a high degree of “smearing” (data not shown).

4.3.1 Protein complexes

4.3.1.1 FtsZ/PBP2/PBP2a

The PBP2/PBP2a complex was initially isolated along with the FtsZ division anchor; employing anti-FtsZ Ab affinity chromatography and interacting protein partners detected with anti-PBP2, -PBP2a and -FtsZ Ab (Figure 4-5).

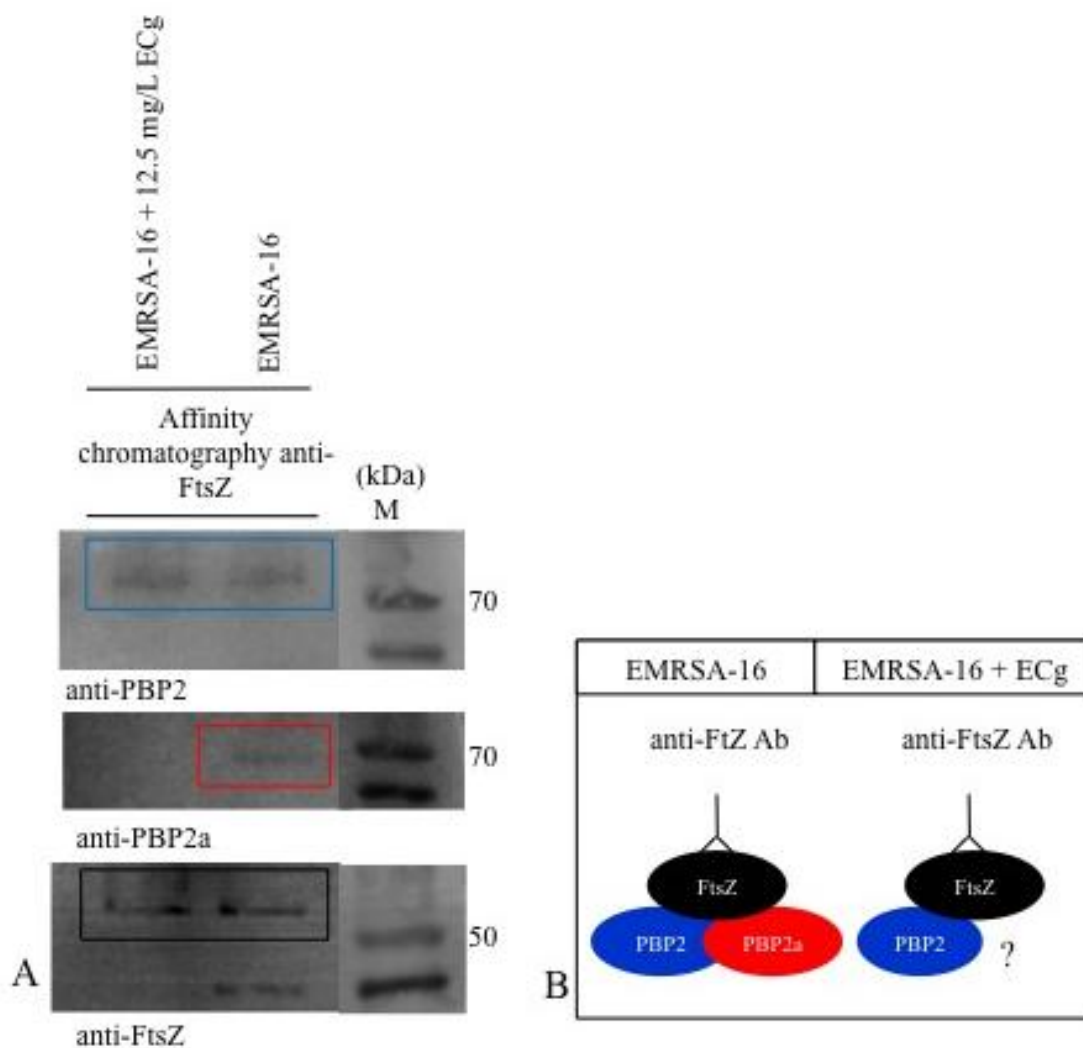


Figure 4-5 (A) Western blot and (B) schematic of the anti-FtsZ affinity chromatography eluent showing the presence of FtsZ/PBP2/PBP2a and FtsZ/PBP2 complexes in EMRSA-16 and ECg exposed SMALPs. The colour of the boxes corresponds to the protein colour in the schematic

PBP2a was not detected together with FtsZ/PBP2 in EMRSA-16-derived SMALPS after exposure of bacteria to 12.5 mg/L ECg. FtsZ/PBP2/PBP2a complexes were not detected using anti-PBP2 and PBP2a Ab as the affinity ligand (data not shown), in all likelihood due to the sensitivity of the detection method and the affinity of the Ab used.

To minimise ligand Ab leaching from the support matrix during protein pull down, the anti-FtsZ Ab was cross-linked to the protein G matrix with DMP and compared to Ab captured in non-covalent fashion by protein G. A more prominent FtsZ band was observed without DMP cross-linking in both SDS-PAGE gels (Figure 4-6a) and Western blots (Figure 4-6b).

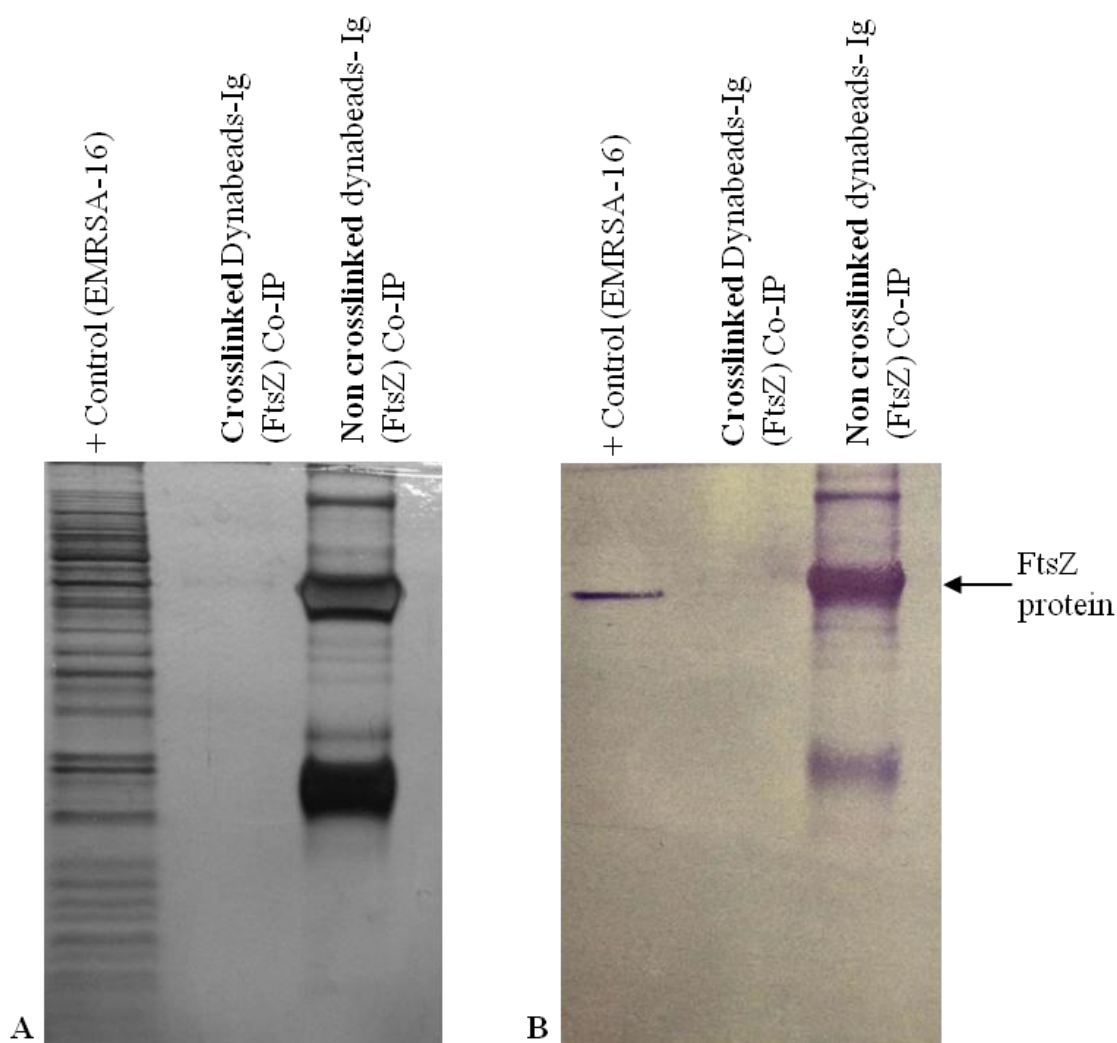


Figure 4-6 (A) Tricine-SDS-PAGE (silver stain) and (B) anti-FtsZ Ab Western blot of purified FtsZ from EMRSA-16 SMALPs; chemical cross-linking is compared to the conventional methodology

4.3.1.2 PBP2/PBP2a complexes

A culture volume of 500 mL was used for investigation of PBP2/PBP2a complexes by Ab affinity chromatography, employing anti-PBP2 and anti-PBP2a Ab as the affinity ligands. PBP2/PBP2a complexes were detected in control EMRSA-16 SMALPs (Figure 4-7). Proteins were precipitated with anti-PBP2 polyclonal Ab and detected with anti-

PBP2 (polyclonal) and anti-PBP2a (monoclonal) Ab. Complexes were not detected in ECg-exposed cells or when anti-PBP2a Ab was employed as the affinity ligand (Figure 4-7). Comparatively, the complex was investigated with surfactant solubilisation, complexes were not evident after solubilisation of EMRSA-16 membrane proteins with Triton X-100, although both PBP2 and PBP2a were detected, as described in section 2 (Figure 2-10), indicating the enhanced capacity of the SMALP solubilisation method for complex extraction.

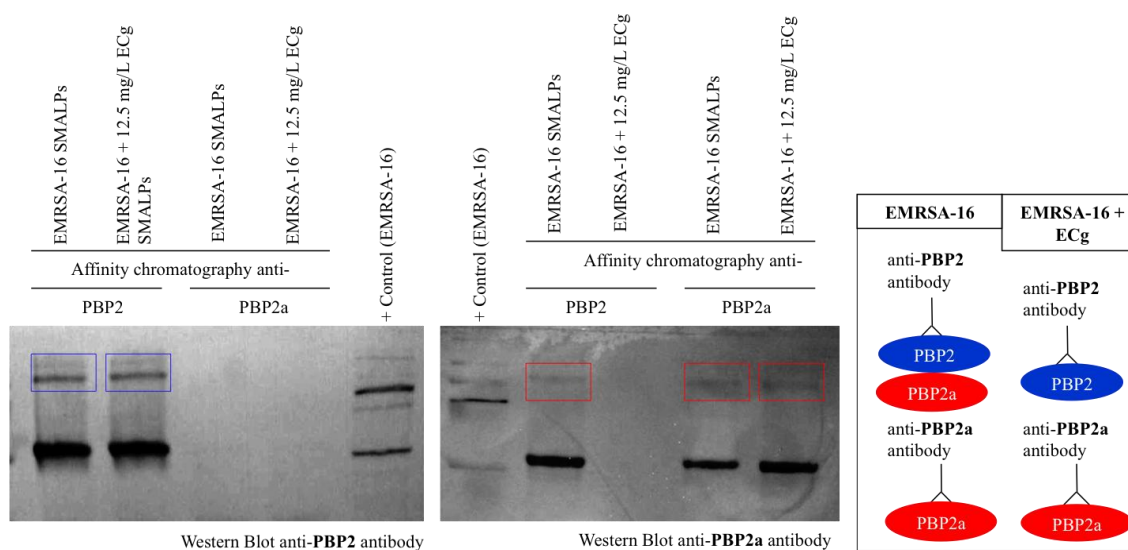


Figure 4-7 Western blot detection of PBP2 and PBP2a interacting proteins following affinity chromatography with (A) anti-PBP2 and (B) anti-PBP2a Ab. The PBP2/PBP2a complexes were detected in EMRSA-16 SMALPs. The colour of the boxes corresponds to the protein colour in the schematic

PBP2/PBP2a complexes could also be recovered from MRSA COL strain (Figure 4-8). PBP2/PBP2a complexes were only detected in Western blots when anti-PBP2a Ab was employed as the affinity ligand. More sensitive methods of detection of protein bands in Western blots were therefore investigated; TMB and chemiluminescence substrates for HRP. Co-immunoprecipitated PBP2 yielded a stronger band following chemiluminescence detection in this manner (Figure 4-9).

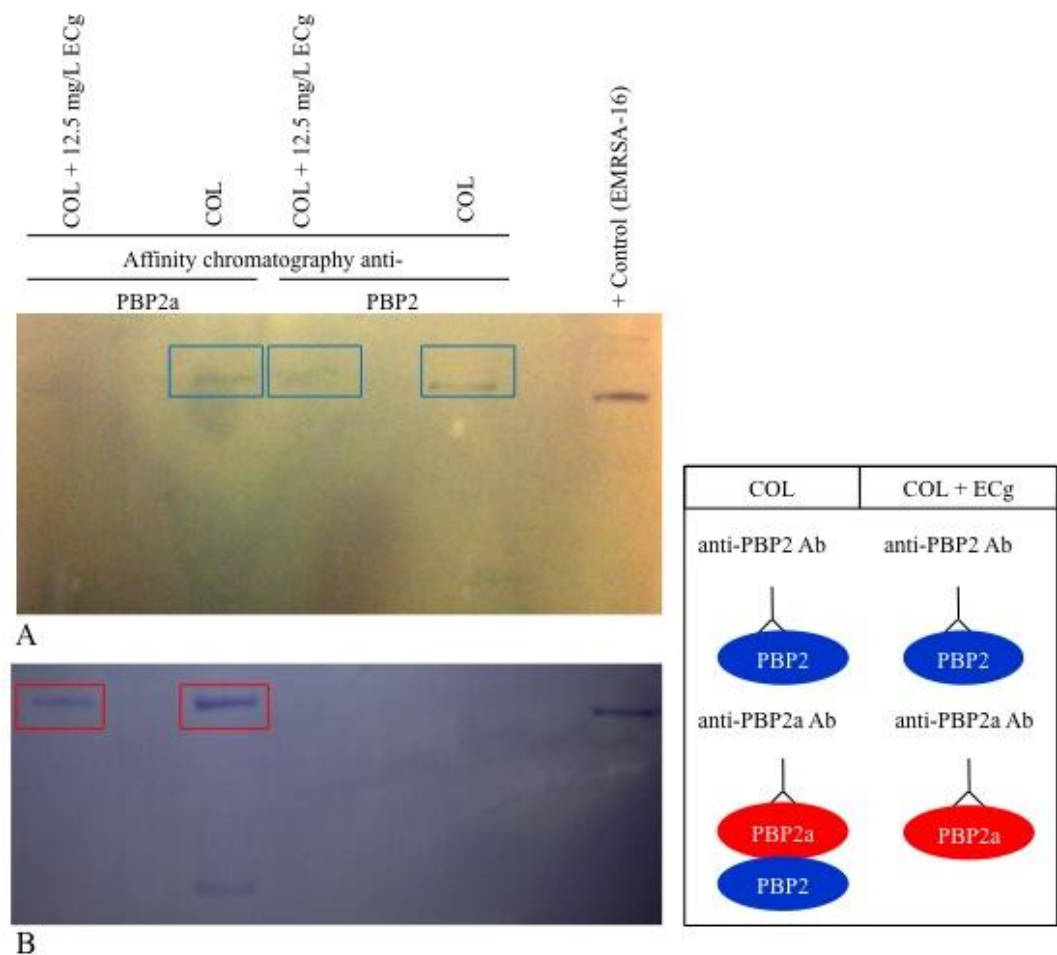


Figure 4-8 Western blot of affinity chromatography eluents from assays utilising (A) anti-PBP2 and (B) -PBP2a Ab. PBP2/PBP2a complexes were observed in COL SMALPs

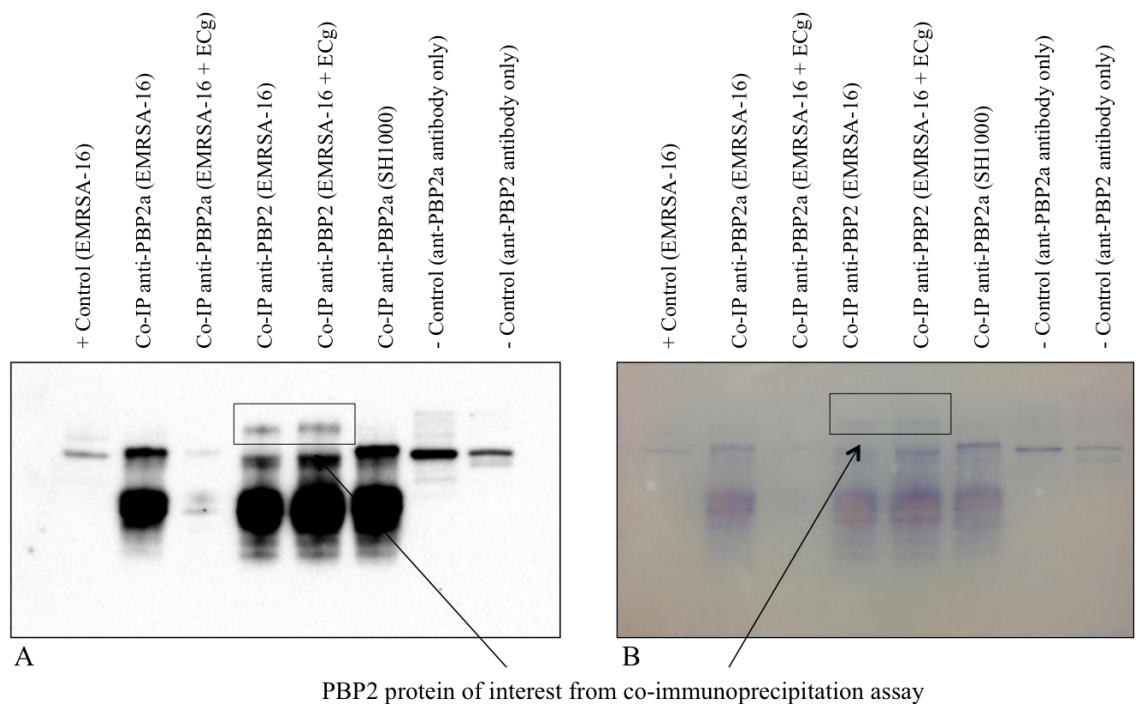


Figure 4-9 Detection of PBP2 in Western blots from co-immunoprecipitation eluents with anti-PBP2 Ab (A) super signal West pico chemiluminescence or (B) TMB detection. The box indicates the position of PBP2 protein of two samples of EMRSA-16 membrane proteins solubilised in SMALPs

A reduction in PBP2 and PBP2/PBP2a complexes was observed following ECg exposure, likely to be indicative of a degree of complex disruption. However the data is still very preliminary and variations in the level of detection of the complex was seen as can be seen when comparing figure 4-10 and 4-11. Also an accurate comparison of data between samples could only be inferred due to the low sensitivity of the functional normalisation method used (A_{280}). The heavy chain of the anti-PBP2 and PBP2a Ab precipitated from the affinity matrix during co-immunoprecipitation in all samples, indicating that co-immunoprecipitation was mediated through Ab binding (Figure 4-10).

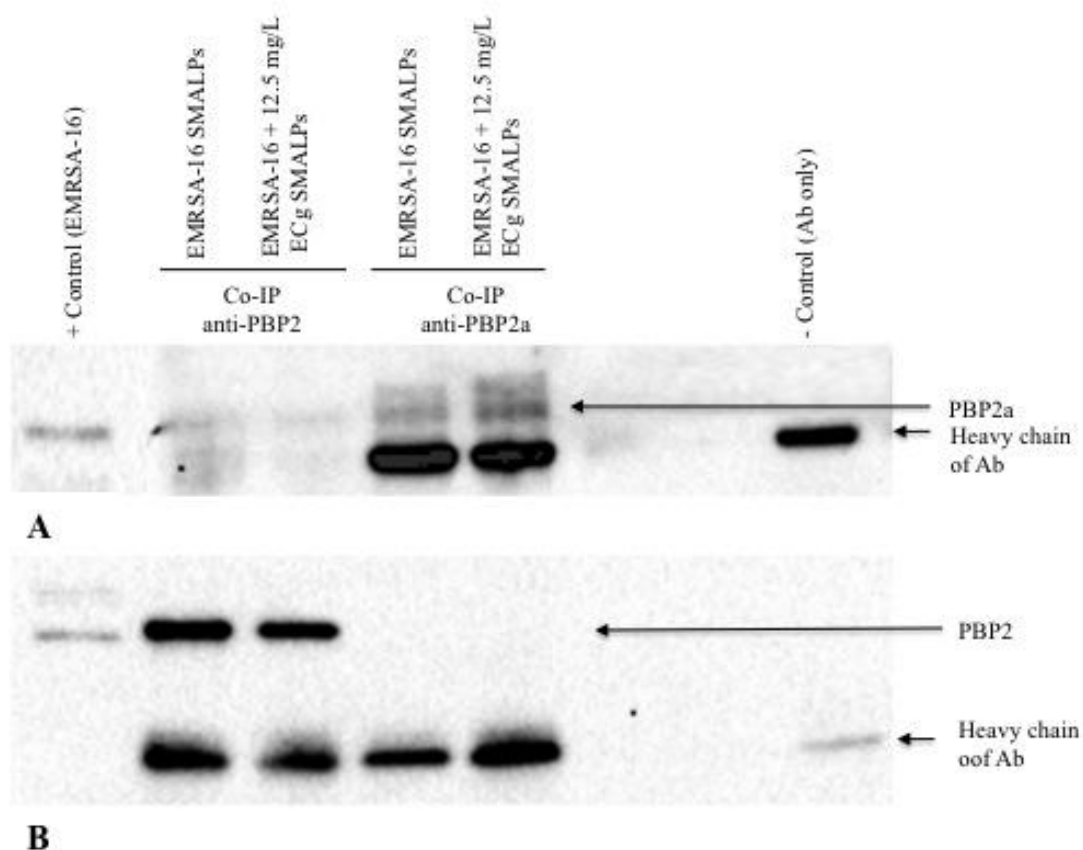


Figure 4-10 Western blots employing (A) anti-PBP2a and (B) anti PBP2 Ab of co-immunoprecipitation eluents from SMALPs recovered with anti-PBP2 and -PBP2a Abs. Protein bands detected by chemiluminescence

PBP2/PBP2a complexes were also detected by Western blotting after purification of SMALPs with anti-PBP2 Ab (Figure 4-11); inferring a partial complex disruption after ECg exposure (12.5 mg/L). Precipitation of Ab heavy chains from Dynabeads was

detected in all samples in the anti-PBP2 Western blot. Variations in levels of PBP2/PBP2a complex detection following ECg exposure varied to lack of a complex or lower levels of protein complex bands being detected. This stems from the preliminary nature of these results and further investigation is needed.

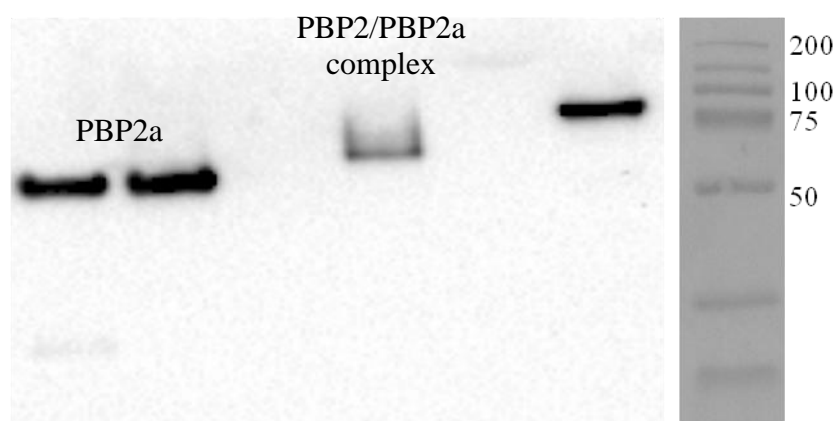
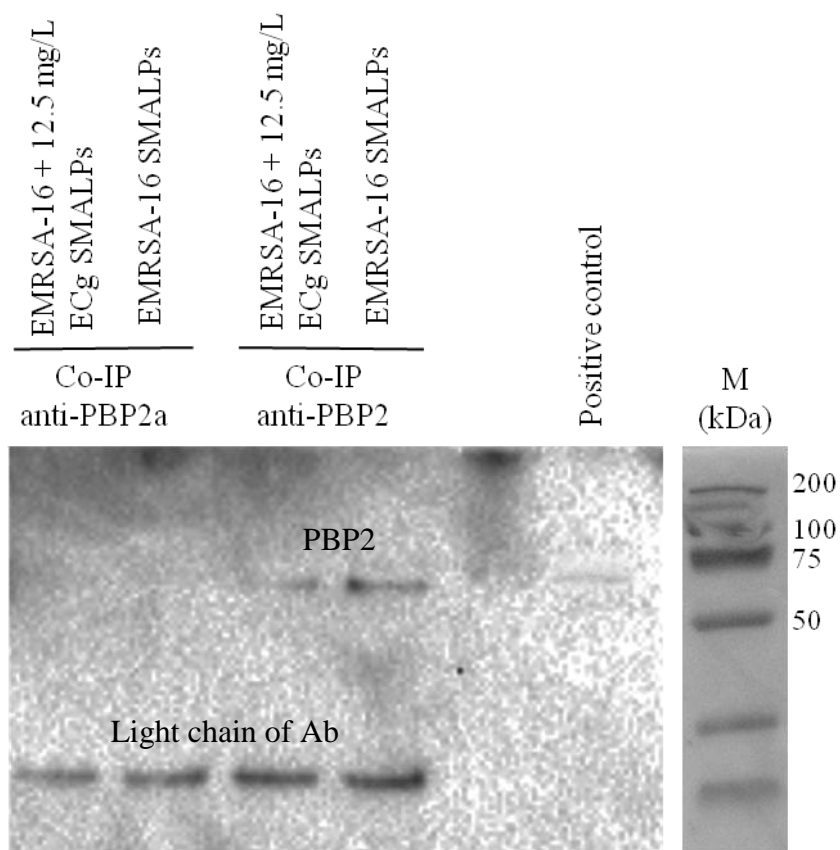


Figure 4-11 Detection of PBP2 and PBP2a in EMRSA-16 and ECg-exposed EMRSA-16 SMALPs following co-immunoprecipitation with anti-PBP2 and -PBP2a Ab. Protein bands detected by chemiluminescence

Subsequently, a native gel was employed to probe for PBP2/PBP2a complexes in COL. A higher molecular weight band than the proteins of interest in the Western blot following co-immunoprecipitation was detected, indicative of the PBP2/PBP2a complex. This band was also found in blots of proteins from SMALPs obtained from ECg-exposed cells when probed with anti-PBP2a Ab (Figure 4-12). A native gel is more sensitive to membrane protein complex detection as the proteins are not denatured. This data indicates a base level of PBP2/PBP2a complexes still present following ECg exposure, which is below of the level of detection of denaturing SDS-PAGEs. The heavy chain of the co-immunoprecipitation Ab was detected in all samples.

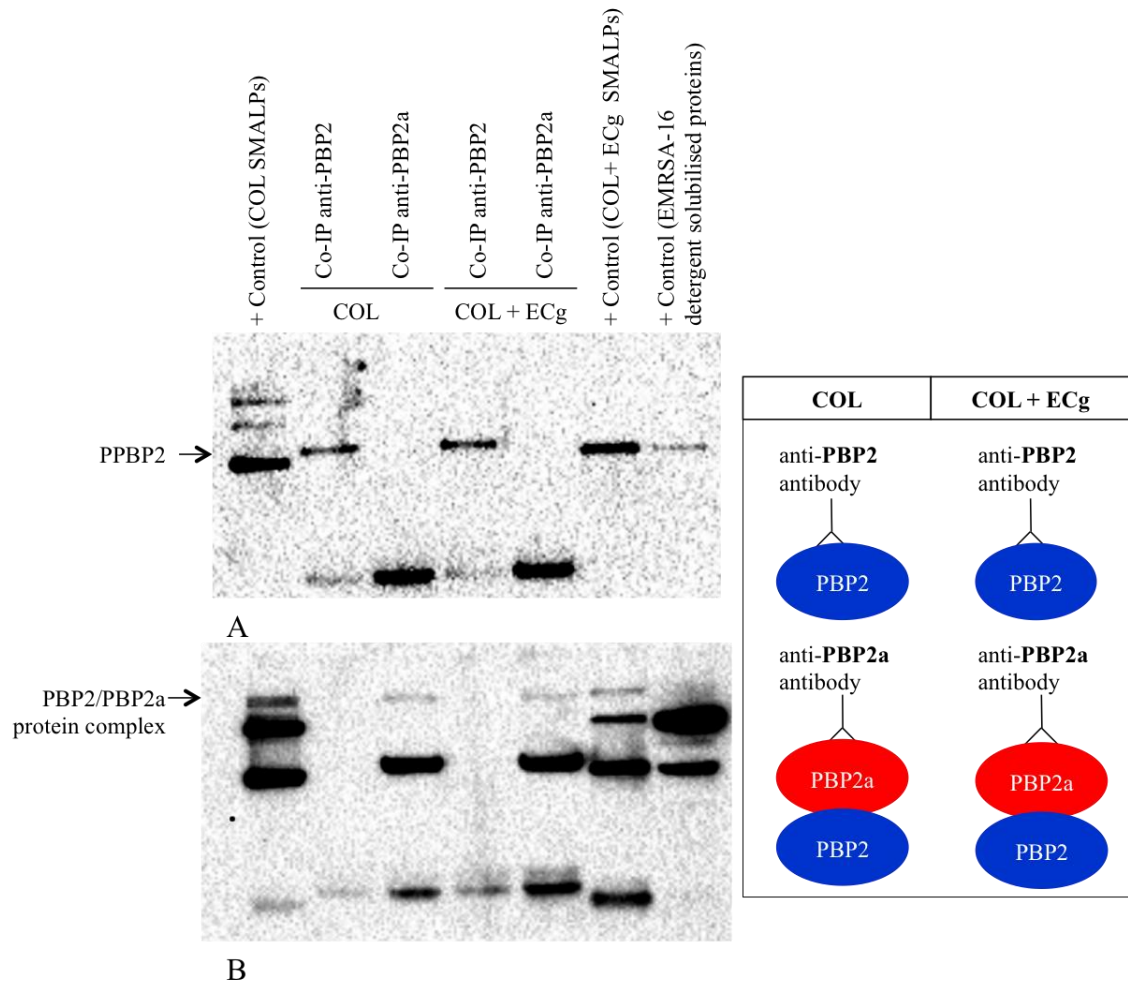


Figure 4-12 Western blots with anti- (A) PBP2 and (B) PBP2a Ab of SMALPs from COL and ECg-exposed COL co-immunoprecipitation eluents using anti-PBP2 and anti-PBP2a Ab. Samples were run on a Tricine-SDS-PAGE under native conditions. The PBP2/PBP2a complex was detected in COL and ECg-exposed COL SMALPs

Purified polyclonal rabbit anti-PBP2a and polyclonal rabbit anti-PBP2 Abs were used to probe gels under denaturing SDS-PAGE conditions for the presence of PBP2/PBP2a complexes. PBP2/PBP2a complexes were observed in EMRSA-16 membrane protein SMALPs when employing both Abs as co-immunoprecipitation ligands (Figure 4-13), however the complexes were not found in ECg-exposed SMALPs (data not shown).

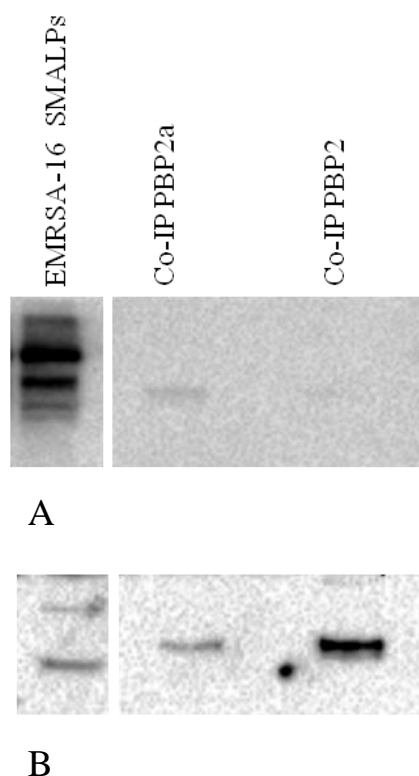


Figure 4-13 Western blots with polyclonal (A) anti-PBP2a and (B) anti-PBP2 Ab of co-immunoprecipitation eluents from EMRSA-16 SMALPs. Protein bands detected with chemiluminescence

4.3.2 Complex detection by flow cytometry

Co-immunoprecipitation eluents were analysed by flow cytometry to investigate the association between PBP2 and PBP2a embedded within SMALPs. Samples (labelled with 60 μ M Nile Red) were gated for 20,000 SMALP fluorescence events and the fluorescence intensity of the FITC-labelled PBP component (either PBP2 or 2a) quantified in the green fluorescence channel (Figure 4-14).

As shown in Figure 4-14a, PBP2/PBP2a complexes were purified within SMALPs using anti-PBP2a Abs and then probed with anti-PBP2 and FITC-conjugated secondary Ab. A 1.63 ± 0.18 fold decrease in fluorescence was observed following ECg exposure

(Figure 4-15). When anti-PBP2 Abs were used to purify SMALPs from ECg-exposed bacteria (Figure 4-14b) and gels probed with anti-PBP2a Ab, a 1.33 ± 0.14 fold reduction was found (Figure 4-16).

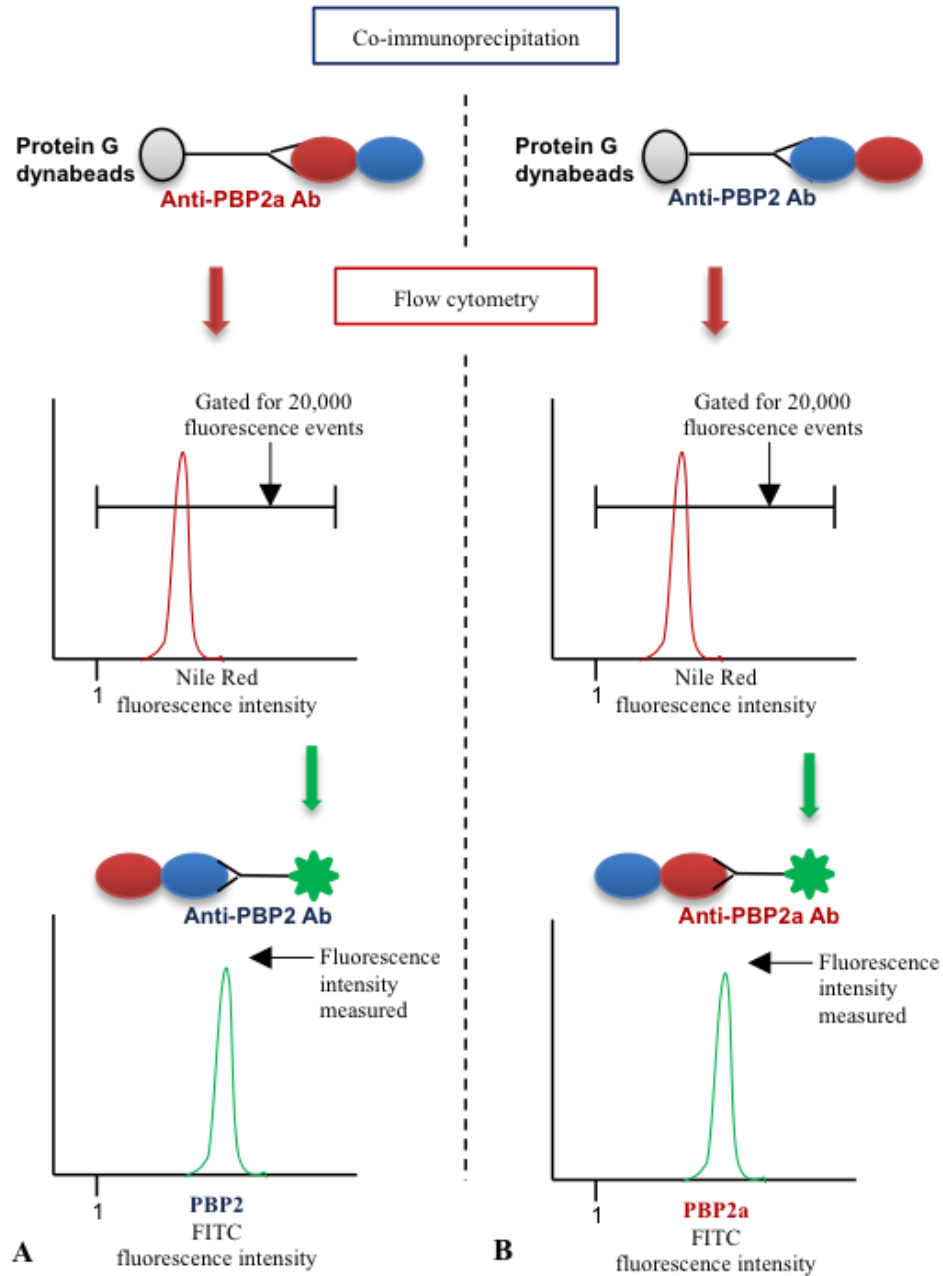


Figure 4-14 Flow cytometry for detection of PBP2/PBP2a complexes after co-immunoprecipitation of SMALPs with (A) anti-PBP2a or (B) anti-PBP2 Abs. Eluent was labelled with (A) anti-PBP2 or (B) anti-PBP2 Ab and a fluorescent secondary Ab. The eluent was gated for 20,000 Nile Red events and the fluorescence intensity of the secondary Ab conjugated to FITC measured (AU)

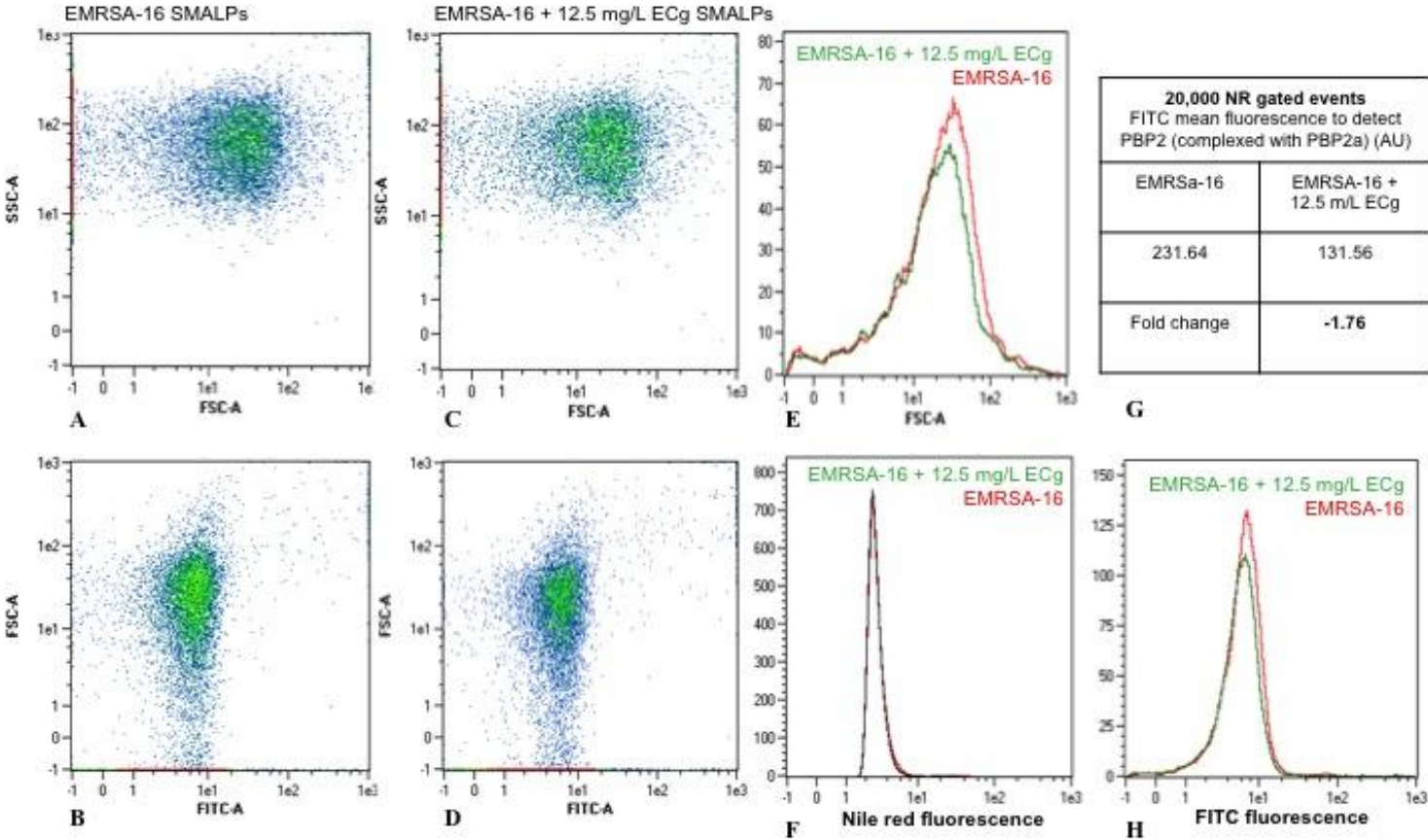


Figure 4-15 Co-immunoprecipitation eluents of SMALPs obtained from (A) EMRSA-16 and (C) ECg-exposed EMRSA-16 by precipitation with anti-PBP2a Ab were gated for 20,000 Nile Red events and (E) the FSC change determined. After fluorescence labelling of the partner protein in the complex (PBP2) with secondary FITC conjugated Ab, the fluorescence intensity was determined for SMALPs from (B) EMRSA-16 and (D) ECg-exposed EMRSA-16. Changes in fluorescence intensity are shown (G & H). F shows the fluorescence intensity of Nile Red labelled SMALPs. Values in AU

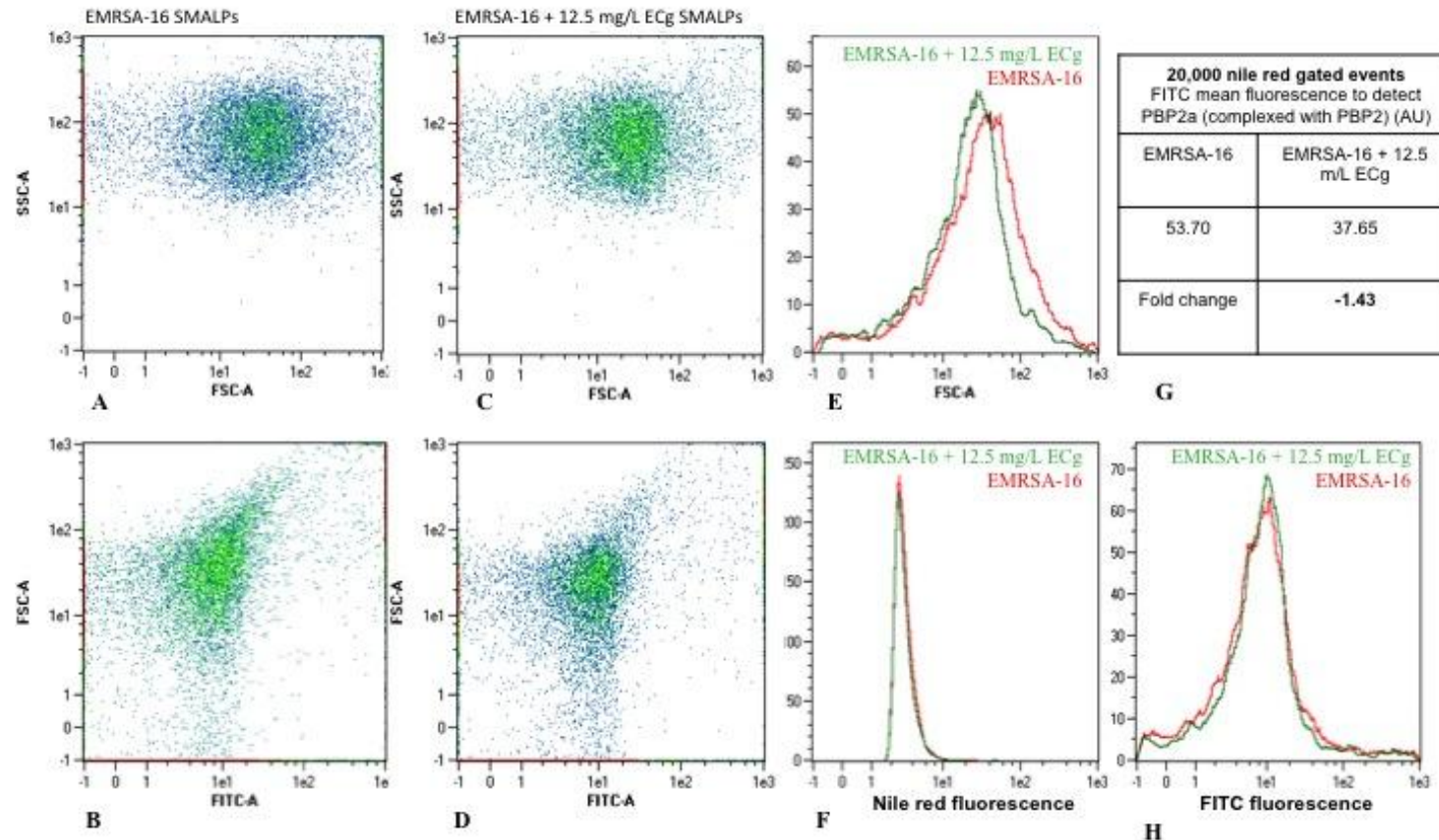


Figure 4-16 Co-immunoprecipitation eluents of SMALPs from (A) EMRSA-16 and (C) ECg-exposed EMRSA-16 SMALPs after purification with anti-PBP2 Ab were gated for 20,000 Nile Red events and (E) FSC changes determined. After fluorescence labelling of the partner protein in the complex (PBP2a) with secondary FITC conjugated Ab, the fluorescence intensity of FITC was determined for (B) EMRSA-16 and (D) ECg-exposed EMRSA-16. Changes in fluorescence intensity are shown (G & H). F shows the fluorescence intensity of Nile Red labelled SMALPs. Values in AU

Flow cytometry data from duplicate experiments are shown in table 4-1.

Table 4-1 *Changes in fluorescence intensity (AU) of PBP2 and PBP2a after exposure of EMRSA-16 to ECg, co-immunoprecipitation and flow cytometry*

PBP2/PBP2a content of SMALPs normalised to 20,000 Nile Red gated events		
	Scenario A Co-immunoprecipitation PBP2a FITC PBP2	Scenario B Co-immunoprecipitation PBP2 FITC PBP2a
Experiment 1	-1.43	-1.76
Experiment 2	-1.23	-1.50
Mean-fold change	-1.33 ± 0.14	-1.63 ± 0.18

Flow cytometry data was also normalised to the FITC fluorescence of the recovery protein (PBP2a in scenario A and PBP2 in scenario B; figure 4-15). In A (Figure 4-15a), a 1.18 fold decrease was observed and, in B, 1.89 (Figure 4-15b). Although the values obtained are dependent on the normalisation method employed and the specificity of the Abs, a reduction in the relative number of PBP2/PBP2a complexes was determined by flow cytometry after exposure of bacteria to ECg. However, further investigation is needed as the data is still very preliminary at this point.

4.4 Discussion

In 1961, an MRSA isolate was recovered; its β -lactam resistance was independent of penicillinase activity, as had been observed previously (Jevons, 1961). Rather it possessed intrinsic resistance to β -lactam antibiotics (Dyke *et al.*, 1966; Seligman and Hewitt, 1966). Brown and Reynolds (1980) investigated the presence of a novel low-affinity PBP (PBP2a) confirming, at least in part, the intrinsic resistance observed. It was hypothesised that the PBPs in MRSA may act together in a manner similar to the multi-enzyme complex involved in cell wall biosynthesis in *E. coli* (Höltje, 1996); the proteins were later identified as PBP1b and PBP3 (Bertsche *et al.*, 2006).

Pinho *et al.* (2001a) recognised that intrinsic methicillin resistance is dependent on co-operation between native PBP2 and acquired PBP2a. In *pbp2* mutant MRSA cells, PBP2a was shown to replace essential functions of PBP2 in the absence of β -lactam antibiotics, but not in the presence of the antibiotic (Pinho *et al.*, 2001b). Following MRSA exposure to β -lactam agents, the TPase function of PBP2 is abrogated by β -lactam acylation; acquired PBP2a substitutes this function and in co-operation with the TGase domain of PBP2 maintains cell wall synthesis (Fuda *et al.*, 2004). In this study I have demonstrated for the first time that PBP2 and PBP2a form a physical complex in an epidemic MRSA strain, EMRSA-16 and I observed that exposure to ECg disrupts the integrity of the complex, at least in part, which may contribute to re-sensitisation to β -lactam agents.

The PBP2/PBP2a complex was identified by membrane protein solubilisation in SMALPs. Subsequently, proteins were cross-linked and the complex purified by Ab affinity chromatography and co-immunoprecipitation; the individual components were identified by Western blotting and flow cytometry. Previous studies to identify the direct or indirect function and interaction of PBP2 and PBP2a primarily investigated recombinant proteins in a non-native system, resulting in an unfavourable environment for complex formation. In contrast, the work presented in this chapter employed a method that confers a semi-native environment for the capture of membrane protein complexes from whole cells.

Initially, PBP2/PBP2a complexes were identified with FtsZ, the cytoplasmic divisome anchor at the septum (Figure 4-5); the two proteins were recovered after probing for FtsZ with anti-FtsZ polyclonal Ab and the protein constituents identified by Western blotting (anti-PBP2, -PBP2a and -FtsZ Abs). Equivalent data was not obtained when anti-PBP2 or -PBP2a Abs were used as affinity ligands. FtsZ is a highly abundant, constitutively expressed protein (Lu *et al.*, 1998) conserved across bacterial species (Margolin, 2000; Lock and Harry, 2008). *E. coli* has approximately 15,000 FtsZ monomers per cell and this number remains constant throughout the cell cycle (Rueda *et al.*, 2003). Its constitutive expression and relatively high abundance can in part explain recovery of FtsZ/PBP2/PBP2a complexes with a polyclonal anti-FtsZ Ab.

To address low abundance of the target proteins, a two litre starting culture was used in order to enable detection of the complex by Tricine-SDS-PAGE and Western blotting. PBP2/PBP2a complexes were identified in EMRSA-16 (Figure 4-5) and COL (Figure 4-8). In EMRSA-16, complexes were initially identified when co-immunoprecipitation was performed with polyclonal anti-PBP2 Ab as the affinity ligand; they could not be recovered with monoclonal anti-PBP2a Ab as the ligand, which was also examined. On the other hand, with the COL strain, in which PBP2a is constitutively expressed, the complex was isolated with monoclonal anti-PBP2a Ab and identified in Tricine-SDS-PAGE gels run under both denaturing (Figure 4-8) and non-denaturing (figure 4-12) conditions. There was a variation in levels of PBP2/PBP2a complex disruption detected from one experiment to the next due to the preliminary nature of the data. A reduction in protein bands was always detected following ECg exposure, however the degree of reduction varied. Further investigation is needed as well as a larger starting volume to examine further the disruption of the complex with ECg.

Polyclonal Abs recognise multiple epitopes on a single antigen, which can amplify the signal of the target protein, in this case the target protein purified through co-immunoprecipitation, allowing for enhanced detection of low abundance proteins (Abcam). In contrast, monoclonal Abs, although more specific, detect a single epitope on an antigen, limiting detection if the protein binding site is sheltered or altered (Abcam). ECg may have the capacity to induce small conformational changes on the target proteins; thus, polyclonal Abs should prove superior for detection of proteins, although non-specific binding and false positives are more common. Subsequently, a

polyclonal anti-PBP2a Ab was made to probe for the complex. Anti-PBP2a serum was affinity-purified, as the serum contained a heterogeneous population of Abs with diverse affinities (data not shown).

Following the optimisation steps shown below, PBP2/PBP2a complexes were identified in EMRSA-16 cells with both anti-PBP2 and PBP2a polyclonal Abs for purification and detection (Figure 4-13):

-
- ❖ Cross-linked membrane proteins with DTSSP
 - ❖ Incubated Ab with Dynabeads for 30 min (RT) followed by incubation of SMALPs with Dynabead-Ab complex for 1 h (4 °C)
 - ❖ Performed co-immunoprecipitation, SDS-PAGE and Western blot transfer on same day
 - ❖ Employed Tricine-SDS PAGE for protein separation
 - ❖ Denatured proteins prior to SDS-PAGE at 30°C for 30 min
 - ❖ Incubated Western blot with primary Ab overnight (4 °C) and the secondary Ab for 2 h (RT)
 - ❖ Detected protein band with chemiluminescence
-

The capacity of ECg to uncouple PBP2/PBP2a in MRSA was investigated. Polyphenols have been shown to affect division proteins in *E. coli*, a bacterium commonly used to study prokaryotic cell division, with polyphenols in curcumin de-stabilising FtsZ (Rai *et al.*, 2008). Further, carboxybiphenylindole, an inhibitor of the interaction between FtsZ and ZipA in *E. coli*, was also identified (Sutherland *et al.*, 2003). I hypothesised that similar effects occur for ECg with the PBP2/PBP2a complex in MRSA. Previous studies of MRSA exposure to ECg identified phenotypic changes indicative of partial disruption of the complex (Stapleton *et al.*, 2007; Bernal *et al.*, 2010). Bernal *et al.* (2010) speculated incomplete uncoupling of the complex, as PBP2 was partially displaced from the FtsZ bound division septum. In the current study, I observed that PBP2a was displaced from the FtsZ/PBP2 components of the division complex and I have speculated that, although PBP2 is displaced from the septum, sufficient numbers of PBP2 molecules remain coupled to FtsZ to enable detection by Ab affinity chromatography and Western blotting. On the other hand, PBP2a was uncoupled from the complex at higher rate, limiting its detection. Bernal *et al.* (2010) did not localise PBP2a in the cell following ECg exposure. In summary, the results presented in this chapter, combined with previous observations, indicate that both PBP2 and PBP2a are

partially displaced from the FtsZ-anchored division septum during cell division of MRSA in the presence of ECg, restricting cell wall biogenesis and leading to a re-sensitisation to β -lactam antibiotics.

ECg exposure did not alter the expression of PBP2 and PBP2a at 12.5 mg/L, but did so at 25 mg/L. Thus, changes observed with 12.5 mg/L ECg exposure are primarily dependent on displacement of the complex rather than a decrease in abundance of the complex constituents. In both EMRSA-16 and COL, disruption of PBP2/PBP2a complexes was inferred following purification of the complex with polyclonal anti-PBP2 Ab. However variation in the level disruption of the complex was observed stemming from the preliminary nature of the data, and further investigation is needed. Using a more sensitive Western blot detection method involving chemiluminescence, sufficient resolution was achieved to indicate displacement of the complex by ECg (figure 4-11). No cross-reactivity was observed (data not shown) as a consequence of differences in Ab source (rabbit: PBP2, mouse: PBP2a).

Due to working at the limit of detection of Western blots, a native gel was employed to investigate the degree of displacement of PBP2/PBP2a complexes following ECg exposure. The native gel indicated an incomplete uncoupling of the complex (Figure 4-13). These results were subsequently confirmed by flow cytometry (Figure 4-15 and 4-16). A direct comparison between PBP2 and PBP2a expression from the flow cytometry data was limited due to the nature of the Abs used; polyclonal and monoclonal. Thus, the same Ab conditions were used to evaluate the complex content between EMRSA-16 and ECg-exposed EMRSA. After co-immunoprecipitation of complexes with anti-PBP2a Ab and detection with anti-PBP2 Ab, a 1.63 ± 0.18 fold decrease in complex recovery was observed following ECg exposure. Purification with anti-PBP2 Ab and detection with anti-PBP2a Ab showed a 1.33 ± 0.14 fold decrease. These results suggest an overall decrease in the abundance of PBP2/PBP2a complexes induced by ECg, indicating a partial uncoupling of the complex in accord with native gel observations. A second normalisation was applied to the flow cytometry data; normalising to the total abundance of protein 1 in the complex rather than to 20,000 SMALP events. A 1.18 (co-immunoprecipitation: PBP2a, flow cytometry: PBP2) and 1.89 (co-immunoprecipitation: PBP2, flow cytometry: PBP2a) fold decrease was observed following ECg exposure. In summary, the flow cytometry results, regardless of the

normalisation method used, infer a decrease in the number of PBP2/PBP2a complexes recovered following ECg exposure.

The data presented in this chapter contain two limitations; first, the normalisation method used for protein content quantification within SMALPs. The A_{280} absorbance assay was employed as the BCA and Bradford methods could not be used due to SMALP precipitation and aggregation in the reagents. This allowed for direct comparison intra-sample, but only an inferred comparison inter-sample due to the possibility of measurement error resulting from contamination. The same observation was made in a study by Lin (2011). To reduce this error, absorbance readings were only utilised if the ratio 260 nm/280 nm was <0.5 ; this limited nucleic acid contamination. For future studies, the CBQCA protein quantification kit should be used, as employed by Lin (2011), where SMA and lipid interference did not occur. A second limitation involved the limit of detection of Western blotting and the availability of high quality Ab. However, the combined results presented in this chapter indicate that ECg, at least in part, uncouples PBP2/PBP2a resistance complexes in MRSA. Complex disruption undoubtedly plays a major role in the multifactorial impact of ECg on the re-sensitisation of MRSA to β -lactam agents.

-
- ❖ The SMALPs solubilisation method was successfully employed to isolate protein complexes.
 - ❖ The FtsZ/PBP2/PBP2a protein complex was identified, and it was inferred that PBP2a is partially displaced from the complex following EMRSA-16 exposure to 12.5 mg/L ECg.
 - ❖ The PBP2/PBP2a protein complex was identified and partial displacement of the complex was observed following ECg exposure.
-

CHAPTER FIVE

5. EFFECT OF EXPOSURE TO ECG ON OTHER PBPS

5.1 Introduction

Increasing evidence indicates that PBP2a is not the sole resistance determinant for β -lactam resistance in MRSA (Memmi *et al.*, 2008). Additional PBPs, in particular PBP4, have been shown to play a key role in β -lactam resistance in CA-MRSA strains (Memmi *et al.*, 2008). PBP4, is a LMW PBP, and the only type-5 PBP that is not a strict DD-carboxypeptidase; instead it catalyses TPase reactions and is involved in secondary cross-linking of the highly cross-linked *S. aureus* PG (Matsushashi *et al.*, 1979). The cooperative function of PBP4 and PBP2 is critical for resistance (Memmi *et al.*, 2008), along with the vital cooperation between PBP2 and PBP2a (Pinho *et al.*, 2001a). In a study by Leski and Tomasz (2005), inactivation of *pbpD*, the structural gene for PBP4, resulted in a reduction from 45% to 22% of highly cross-linked components of the muropeptides. In CA-MRSA, loss of PBP4 also impacts on PBP2 transcription following exposure of cells to oxacillin, leading to a decrease in PG cross-linking. The same phenomenon was not observed with HA-MRSA COL (Memmi *et al.*, 2008).

Additional resistance determinants that have been described include auxiliary gene products involved in cell division. In particular genes involved in PG metabolism (associated with *femABCD*) (de Lencastre and Tomasz, 1994), synthesis, including *murE* (Gardete *et al.*, 2004) and *murF* (Sobral *et al.*, 2003), and *vraSR*, encoding a two-component stress stimulon involved in PG regulation (Kuroda *et al.*, 2003).

As the effect of ECg on the susceptibility of EMRSA-16 to β -lactam agents is multifactorial (section 1.5), leading to a phenotypic alteration of the cell, it is possible that the other resistance determinants described above are also affected. Regarding expression of PBPs, ECg elicits an indirect effect but does not bind to these proteins (Bernal *et al.*, 2010). ECg exposure led to reduced expression of PBP1 and PBP3 and de-localised PBP2 from the division septum. (Bernal *et al.*, 2010) Further, a 5-10% reduction in PG cross-linking was observed, which may be attributed to a change in PBP2 and/or PBP4, as they are required for primary and secondary cross-linking of the PG respectively (Stapleton *et al.*, 2007).

In this chapter the inhibition of specific PBPs and the effect of ECg exposure on this inhibition was investigated. Four β -lactam agents were chosen, following a study by

Dumitrescu *et al.* (2011), that selectively bind to the PBPs of interest: imipenem (PBP1) (Yang *et al.*, 1995), cefotaxime (PBP2) (Georgopapadakou *et al.*, 1986), cefaclor (PBP3) (Georgopapadakou *et al.*, 1982), and ceftiofur (PBP4) (Curtis *et al.*, 1980). Vital PBPs involved in the ECg-mediated re-sensitisation of MRSA to β -lactam agents were revealed and further investigated.

5.2 Materials and methods

5.2.1 Bacterial strains and reagents

EMRSA-16 and exposure to 12.5 mg/L ECg were employed. Cefaclore and cefotaxime were purchased from Envo Life Sciences (Farmingdale, NY, USA), and imipenem and cefoxitin from Sigma. Rabbit anti-PBP4 Ab was a gift from Mariana G. Pinho (Universidade Nova de Lisboa, Portugal).

5.2.2 MICs of PBP inhibition by β -lactam agents

The susceptibility of EMRSA-16 and ECg-exposed cells to cefaclore, cefotaxime, imipenem and cefoxitin was determined by the CLSI microbroth dilution method described in section 2.3.3. All MICs were performed at 37 °C for 14 - 16 h in MHB supplemented with 2% NaCl.

5.2.3 Detection of PBP2/PBP4 complexes

The PBP2/PBP4 complex were investigated with SMALPs (section 3) derived from 2 L cultures grown in MHB supplemented with 0.125 mg/L oxacillin at 37 °C; 8 - 10 μ g of anti-PBP2 Ab was used to purify PBP2/PBP4 complexes from the SMALPs with protein G Dynabeads, following the method described in section 4.2.4.2, after DTSSP cross-linking. All steps were performed at 4 °C apart from initial attachment of the Ab to the protein G matrix, which was performed at RT.

5.2.4 Analysis of protein complexes with 1D Tricine-SDS-PAGE and Western blotting

A 1 mm thick Tricine-SDS-PAGE followed by Western blotting was utilised as described in section 4.2.5.1 and 4.2.5.2. A 1:200 dilution of primary anti-PBP4 Ab, and 1:500 of anti-PBP2 Ab were used together with a 1:10,000 dilution of the secondary Ab, HRP-conjugated goat anti-rabbit IgG (Sigma). PBP2 and PBP4 expression in SMALP-derived nanoparticles was also investigated.

5.3 Results

MICs of the four β -lactam agents (imipenem, cefotaxime, cefaclore and ceftiofur) for EMRSA-16 and EMRSA-16 exposed to ECg are shown in table 5-1.

Table 5-1 EMRSA-16 MICs of four β -lactam agents with selective binding to PBPs 1-4

EMRSA-16 MIC (mg/L)							
Imipenem *(PBP1)		Cefotaxime *(PBP2)		Cefaclore *(PBP3)		Ceftiofur *(PBP4)	
-	12.5 mg/L ECg	-	12.5 mg/L ECg	-	12.5 mg/L ECg	-	12.5 mg/L ECg
16	0.25	1024	256	512	256	256	4
n=3		n=4		n=4		n=4	

* PBP selectivity of β -lactam agents from Dumitrescu *et al.* (2011)

A 12-fold decrease in MICs following ECg exposure was observed for imipenem (16 to 0.25 mg/L) and ceftiofur (256 to 4 mg/L). On the other hand, a 4-fold and 2-fold decrease was noted for cefotaxime (1024 to 256 mg/L) and cefaclore (512 to 256 mg/L) respectively.

As I found a significant reduction in MICs of β -lactam agents that bind selectively to PBP1 and PBP4 after ECg exposure, PBP4 was further investigated. PBP4 is required for highly cross-linked PG, of which a 5 - 10% reduction is observed in ECg exposed cells. Memmi *et al.* (2008) determined that PBP4 co-operates with PBP2, either in complex or indirectly. Therefore, EMRSA-16 was examined for the presence of PBP2/PBP4 complexes after co-immunoprecipitation as described in section 4; the effect of ECg on the complex was also investigated.

Initially, expression of individual proteins was investigated by Tricine-SDS-PAGE and Western blotting (Figure 5-1). A decrease in PBP4 (~50 kDa) band intensity was observed following ECg exposure. However, this was not the case for PBP2 (~76 kDa). In subsequent gels, a minor reduction in PBP2 was observed, as is evident from Figure 5-1.

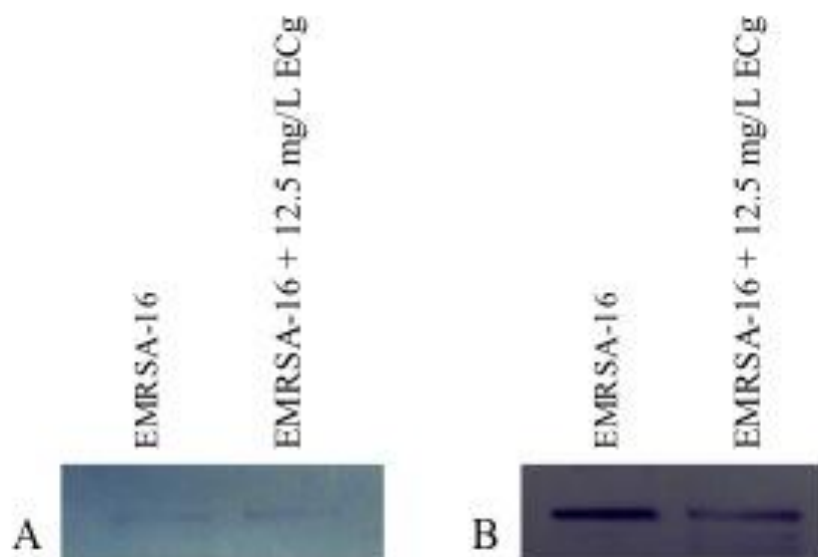


Figure 5-1 Western blot of protein expression of (A) PBP2 and (B) PBP4 by EMRSA-16 and ECg-exposed cells

Subsequently, PBP2/PBP4 complexes were identified by anti-PBP2 Ab co-immunoprecipitation and the protein constituents identified with anti-PBP2 and -PBP4 Abs (Figure 5-2). The heavy chains of the PBP2 Ab, which leached from the protein G affinity matrix, were detected in all samples, indicating that co-immunoprecipitation was effective.

PBP2/PBP4 complexes were identified in SMALPs from both EMRSA-16 and ECg-exposed bacteria; a small decrease in PBP2 was observed. Protein bands were detected by chemiluminescence detection of HRP-conjugated secondary Ab.

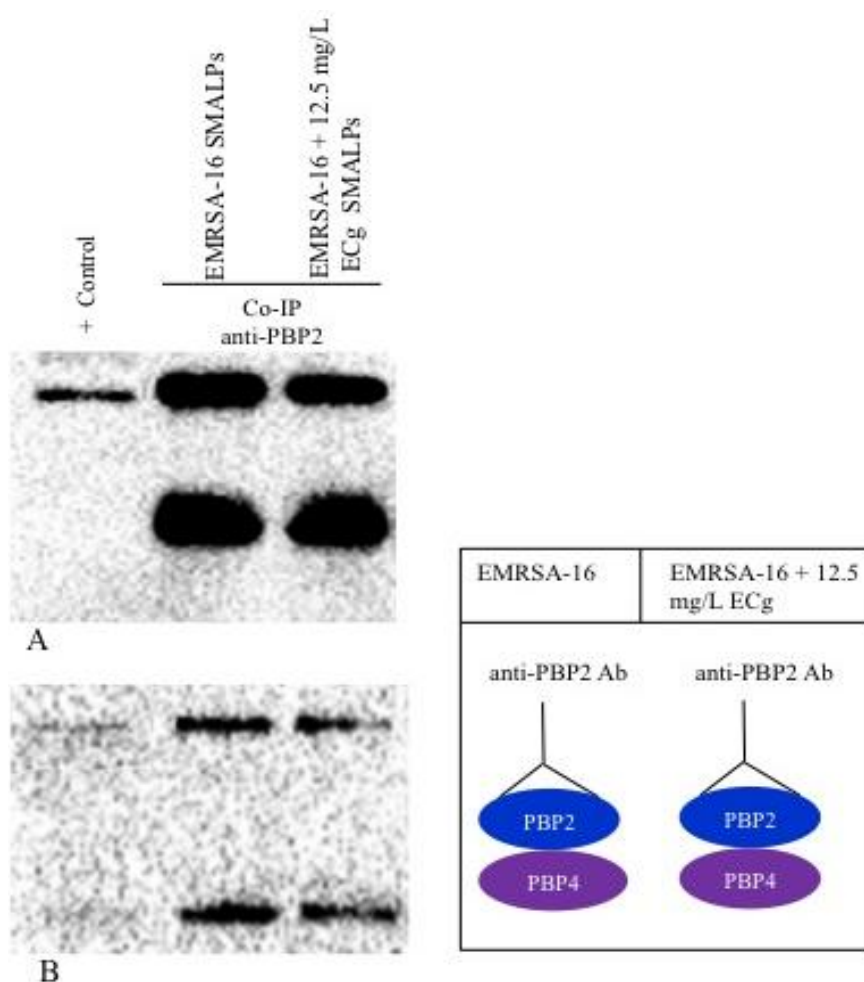


Figure 5-2 Detection of PBP2/PBP4 complexes by Western blot with (A) anti-PBP2 and (B) anti-PBP4 Ab using co-immunoprecipitation (affinity ligand: anti-PBP2 Ab) eluent of EMRSA-16 and ECg SMALPs. Proteins detected by chemiluminescence

5.4 Discussion

Evidence for the involvement of additional β -lactam resistance determinants in MRSA has recently increased, in particular to support the role of the non-essential LMW PBP4 as a resistance determinant (Chambers *et al.*, 1994); in this study, over-expression of the protein led to increased β -lactam resistance (Henze and Berger-Bächi, 1996). Further work has identified the essential role of PBP2 together with PBP4 for highly cross-linked PG, a characteristic of *S. aureus* (Memmi *et al.*, 2008).

The susceptibility of EMRSA-16 and ECg-exposed EMRSA-16 to β -lactam agents that bind selectively and irreversibly to PBPs 1, 2, 3 and 4 was investigated. ECg had an impact on beta-lactam inhibitor MICs specific for PBP1 and PBP4. PBP1 is an essential PBP in *S. aureus* and is involved in septum formation and cell separation during cell division (Pereira *et al.*, 2007; Atilano *et al.*, 2010). On the other hand, PBP4 is nonessential and is involved in secondary cross-linking. A decrease in cross-linking has been previously observed in ECg-exposed EMRSA-16 cells (Stapleton *et al.*, 2007). The hypersensitivity of EMRSA-16 to cefoxitin, which irreversibly binds to PBP4, was further investigated.

Leski and Tomasz (2005) identified that suboptimal levels of PBP2 function in a ZOX3 *S. aureus* strain resulted in hypersensitivity to cefoxitin. This was also observed after ECg exposure of EMRSA-16 in the current study. PBP2 is affected by ECg, as it is partially displaced from the division septum during cell division (Bernal *et al.*, 2010), and I have provided further evidence for the partial disruption of PBP2/PBP2a complexes (section 4). When EMRSA-16 cells were exposed to ECg, a 12-fold decrease in cefoxitin susceptibility was observed, which may be explained through a functional change of PBP2, leading to suboptimal activity. Alternatively, there may be an alteration in its co-operative functionality with PBP4, and this hypothesis was subsequently examined.

Priliminary data suggests the PBP2/PBP4 complexes were detected. Although the MICs of PBP4 indicated that it may play a role in ECg-mediated sensitisation to β -lactam agents, through a possible conformational change, a significant decrease in PBP2/PBP4 complexes was not observed.

The results do not indicate disruption of PBP2/PBP4 complexes in ECg-mediated re-sensitisation to β -lactam agents.

-
- ❖ PBP1 and more significantly PBP4 were shown to play an important role in ECg sensitisation of MRSA to β -lactam agents

 - ❖ PBP2/PBP4 complexes were found in EMRSA-16, although a significant reduction in the number of complexes was not observed following ECg exposure as indicated by preliminary SMALPs investigation
-

CHAPTER SIX

6. GENERAL DISCUSSION

This thesis describes the use of surfactants for the solubilisation of membrane proteins and the development of a novel method for the isolation of membrane proteins in a semi-native environment. The experimental sections described the development of the method, its application for the isolation of the resistance complex from MRSA and an evaluation of the effect of ECg exposure on the integrity of the complex. At this point the data is still very preliminary in its nature, and further investigation is needed. This chapter will provide an overview of the results as well as a more in depth discussion of the use of ECg, in combination with currently ineffective β -lactams, as a novel therapeutic approach against MRSA infections, by modulation of the bacterial phenotype and disruption of the resistance mechanism. Suggestions for future investigation of both the application of the method for MRSA membrane proteins and the use of ECg as a potential combinatorial therapy are also included.

The first membrane protein structure, the *Rhodospseudomonas viridis* photosynthetic reaction centre, was published in 1985 (Deisenhofer *et al.*). However, since then the study of these cellular constituents has been limited by the inability to produce high yields of functional proteins and their complexes. Thus, membrane proteins only account for less than one percent of the sequences deposited into protein data banks (White, 2004). The relatively small number of studies of the structure and function of membrane proteins stems primarily from the lack of a universal protocol for the solubilisation of these proteins from their native environment while maintaining their native structure and function (Mackenzie, 2006; Moore *et al.*, 2008, Langosch and Arkin, 2009).

Membrane proteins constitute 30% of the proteome of *Homo sapiens*, *E. coli* and *Saccharomyces cerevisiae*; however, very little is known of their structure and function within the membrane bilayer (Seddon *et al.*, 2004). This has limited the study of bacterial membrane proteins as potential targets for novel antibacterial agents (Seddon *et al.*, 2004)

Recent advances, including the use of liposomes, amphipols, nanodiscs and bicelles, have aided the study of membrane proteins. However, methods based on these reagents have major limitations, primarily the requirement for membrane protein extraction with surfactants. Thus it is imperative to develop novel methods for protein extraction in a

native-like environment without the use of surfactants that are compatible with downstream experiments.

The use of SMA for the surfactant-free solubilisation of membrane proteins in a native-like environment represents a novel method to address the limitations of previous studies. This method has already been used for the isolation of the abundant bacterial proteins PagP and bR (Knowles *et al.*, 2009). In my work, a method was developed for the isolation of membrane protein complexes within SMALPs from whole cells, which may pave the way for future studies of membrane protein complex in a more natural environment. The isolation of membrane proteins in SMALPs limits the disruption of native protein interactions, both stable and transient. The method was applied to the investigation of the mechanism of action of ECg, a constituent of the green tea plant *C. sinensis*, for the modification of MRSA resistant phenotypes based primarily on the membrane protein complex PBP2/PBP2a.

The antibacterial properties of green tea and specifically the green tea catechin ECg have been widely documented. However, the mechanism of action in relation to abrogation of the β -lactam resistance of MRSA is only partially understood. The effect of ECg on MRSA is believed to be multifactorial, as described in chapter one. Intercalation of ECg into the *S. aureus* bilayer causes a reduction in membrane fluidity followed by an increase in fluidity as the cell responds by incorporation of a higher proportion of branched chain fatty moieties into membrane phospholipids and tighter acyl chain packing (Bernal *et al.*, 2009; 2010). The membrane bilayer asymmetry remains unaltered (H. Rosado and P.W. Taylor unpublished observation). Intercalation of ECg also affects the membrane-anchored protein MprF, which is responsible for the attachment of lysine residues to phosphatidylglycerol and the subsequent translocation of positively charged lysophosphotidyl glycerol to the outer leaflet of the membrane (Ernst *et al.*, 2009). There is a large reduction in the levels of lysophosphotidyl glycerol in ECg-exposed MRSA (Bernal *et al.*, 2010). Taken together, these observations suggest that a more fluid and negatively charged MRSA membrane may alter the environment of the membrane proteins, including those involved in cell wall synthesis.

In this study, the mechanism of action of ECg on the MRSA division complex PBP2/PBP2a was assessed. The use of SMALPs enabled the isolation of PBP2 and

PBP2a together with other proteins. SMA was also used to investigate if ECg uncouples additional associated proteins (PBP4 and FtsZ).

After exposure to 12.5 mg/L ECg, PBP2/PBP2a complexes were partially uncoupled and there was a partial displacement of PBP2a from the septum anchor complex FtsZ/PBP2/PBP2a. The degree of displacement of the complex varied between strains and between experimental days stemming back to the preliminary nature of the experiments. However, these results suggest that β -lactam agents and ECg may work in tandem on distinct bacterial targets. β -lactam agents target and irreversibly acylate PBP2, whereas ECg induces reconfiguration of the membrane (Palacios *et al.*, 2014), leading to partial uncoupling of FtsZ/PBP2/PBP2a and PBP2/PBP2a complexes. As a consequence, PBP2a is no longer able to compensate for the loss of the PBP2 TPase activity following its acylation by β -lactam agents; this event results in cell death. ECg, in combination with β -lactams, may represent a novel therapeutic approach for the treatment of MRSA infections by modulation of resistance to β -lactam agents.

The data presented in this thesis, utilising the novel SMALP solubilisation method, should enable further investigation of the MRSA divisome. The high quality of the anti-FtsZ Ab together with the relative abundance of this scaffold protein emphasise the attraction of this protein as the best target for SMALP extraction of the divisome complex. Although the capacity of SMALP to extract complex protein assemblages has not been explored in this study, it is possible that the polymer may capture the entire divisome comprising FtsZ and the partner proteins FtsA/FtsL, SepF, EzrA, GpsB, DivIC/DivID and PBP1/PBP2/PBP3/PBP4. The assemblage could be purified by co-immunoprecipitation with FtsZ Ab and other components subsequently identified by Western blotting. Another protein that could be exploited for protein pull down is EzrA, a membrane anchor that serves a similar role to FtsZ but is membrane-embedded rather than located in the cytoplasm. Thus, SMALP solubilisation may facilitate the identification of novel membrane protein interacting partners both in MRSA and other Gram-positive and Gram-negative bacteria and may aid the identification of novel therapeutic targets.

Antibiotic resistance is a major health threat and constitutes an important agenda on a national and international scale. Increases in the frequency of isolation of community

and hospital-acquired resistant bacteria such as staphylococci, enterococci, gonococci, enterobacteriae, *Pseudomonas* and *Acinetobacter* species and MDR *M. tuberculosis* have received much recent attention (Carlet *et al.*, 2011; Gagliotti *et al.*, 2011; Piddock, 2012). In the USA, in FY 2011 - 2012, approximately 2 million infections were caused by drug resistant bacteria, with 23,000 attributed deaths and an extra 20 billion US dollars in health care costs (CDC, 2013). Of these infections, approximately 90,000 were caused by MRSA, resulting in 11,285 deaths annually (CDC, 2013). In Europe, MDR resistant bacteria caused 400,000 infections in 2007, resulting in 25,000 deaths and 1.5 million euro in extra hospital costs and productivity losses (ECDC and EMEA, 2009).

There has been a steady decrease in the incidence of MRSA infections in recent years in the wealthier European countries such as Germany, France and UK due to the implementation of control programs; however, they remain a serious health threat, as the percentage of infections reported in European Union/European Economic Area (EU/EEA) by the ECDC in 2012 is 17.8% (EARS-Net, 2013). As is evident from figure 6-1, 7/30 reporting countries still have an infection rate of >25% and an uneven distribution is seen throughout EU/EEA, with the majority of the highest percentages reported by Southern European countries such as Portugal and Greece (EARS-Net, 2013).

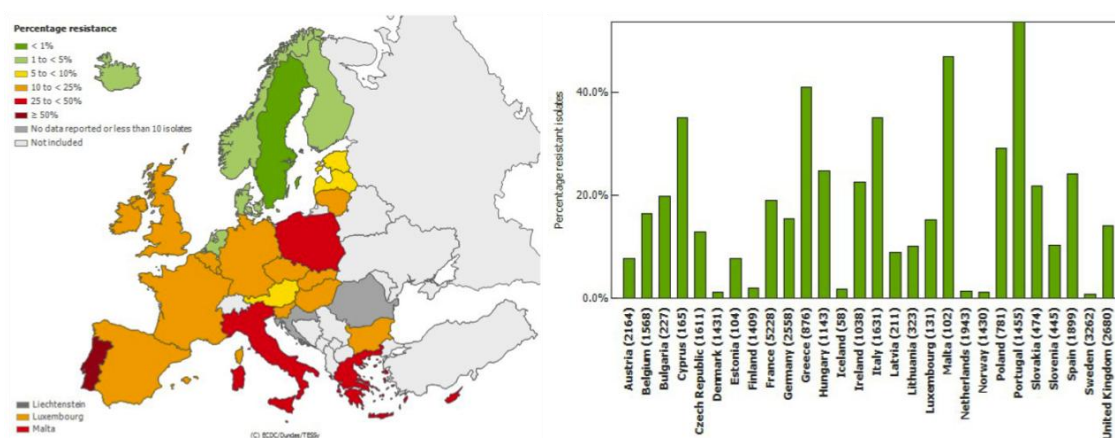


Figure 6-1 Proportion of MRSA cases in EU/EEU countries in 2012 surveyed by the European Antimicrobial Resistance Surveillance Network (EARS-Net)

The EU/EEA has also seen a rise in antibiotic resistance and MDR resistance in Gram-negative bacteria, such as extended β -lactamase-producing *E. coli*, carbapenem resistant Enterobacteriaceae and the emergence and spread of the New Delhi metallo- β -lactamase 1 (EARS-Net, 2013).

The above paragraphs highlight that urgent action is needed against the threat of antibiotic resistance, which has been reiterated by the CDC;

“Antimicrobial resistance is one of our most serious health threats...the loss of effective antibiotics will undermine our ability to fight infectious diseases and manage the infectious complications common in vulnerable patients undergoing chemotherapy for cancer, dialysis for renal failure, and surgery, especially organ transplantation, for which the ability to treat secondary infections is crucial” (CDC, 2013).

Without effective antibiotics, infection-related mortality rates could return to those of the early 20th century prior to the golden era of antibiotics. In response, combating antibiotic resistance has become a global agenda; Antibiotic Awareness days have been organised annually in Europe and Canada and alliances such as the EARS-Net and the Transatlantic Task for Antimicrobial Resistance have also been established (WHO, 2013). In the UK, antibiotic resistance is a priority, with a cross-governmental strategy launched in 2013 (Howard *et al.*, 2013). One of the key elements on the health initiatives agenda is ‘the development of new drugs and better funding of research in antimicrobial resistance’ (Howard *et al.*, 2013). However, the antibiotic pipeline is drying up, with antibiotic development less favourable to pharmaceutical companies due to the expense of this time-consuming process. In 2008, 167 new drug candidates were discovered, of which only 15 portrayed a novel mechanism of action for potential treatment of MDR infections (ECDC and EMEA, 2009). Thus, the lack of a surge in new antibiotics has prompted research into alternative approaches, including new preventative vaccines and new therapeutic interventions such as the use of bacteriophages (Hanlon, 2007), antimicrobial peptides (Eckert, 2011) and anti-toxins (Hotchkiss and Opal, 2010) as well as combination therapy including antibiotics and/or natural products (Geddes *et al.*, 2007).

Traditional antibiotic therapy exposes bacteria to selective pressure and may lead to the evolution of new resistance mechanisms required for survival (Figure 6-2a). In addition, the use of drug combinations, such as suflamethoxazole-trimethoprim with rifampicin for the treatment of MRSA, rather than monotherapy, have shown to have superior efficacy against MDR bacteria (Yamaoka, 2007). A further example is the use of clavulanic acid, a β -lactamase inhibitor discovered in 1981 (Geddes *et al.*), which is still used today in combination with β -lactam agents. However, resistance has also emerged against these combination therapies (Entenza *et al.*, 2010).

An alternative approach to combination therapy is the use of natural compounds and secondary metabolites (phytochemicals) derived from plants in combination with conventional antibiotics. These include tannins, alkaloids, terpenoids and polyphenols, which are effective against both Gram-positive and Gram-negative bacteria (Cowan, 1999; Tegos *et al.*, 2002; Soe *et al.*, 2010).

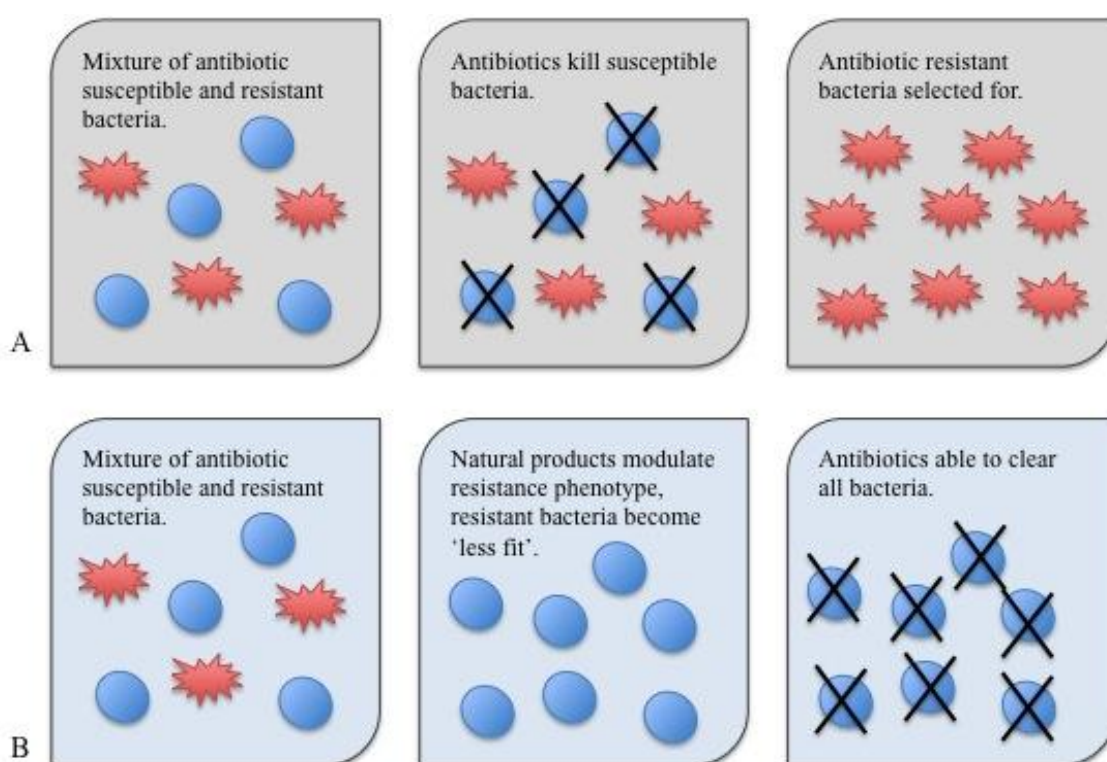


Figure 6-2 Modulation of bacterial resistance phenotype by natural products. A) Classic scenario selecting for antibiotic resistant bacteria as a consequence of treatment with antibiotics. B) Novel therapeutic approach using natural products to modulate the resistance phenotype, resulting in 'less fit' bacteria that are cleared by the host or become susceptible to previously ineffective antibiotics

In general, the MICs of such phytochemicals are higher (100 – 500 mg/L) than conventional antibiotics and they are therefore not as effective in monotherapy. However, in combination they can potentiate the activity of antibiotics by increasing their efficacy (Tegos *et al.*, 2002). Examples include the synergism of piperine with ciprofloxacin (Khan *et al.*, 2006) and ethyl gallate with fusidic acid (Soe *et al.*, 2010) for the treatment of MRSA infections. Several phytochemicals also have the capacity to modulate or modify complex bacterial resistance phenotypes resulting in ‘less fit’ bacteria, allowing previously ineffective antibiotics or the host’s immune system to clear the infection (Figure 6-2b) (Taylor, 2013).

Natural compounds have been shown to modify bacterial resistance mechanisms, including inhibition of efflux pumps (Sudano Roccaro *et al.*, 2004), down-regulation of resistance virulence factors and gene expression (Lee *et al.*, 2009), as well as the inhibition of antibiotic modifying enzymes (Zhao *et al.*, 2001). Pertinent to the treatment of MRSA infections, a study by Smith *et al.* (2007) showed inhibition of the NorA efflux pump, responsible for the influx of broad-spectrum antibiotics including fluoroquinolones, by a phenolic totarol from *Chamaecyparis nootkatensis*. Reversal of oxacillin resistance in MRSA has been reported after use of the antibiotic in combination with manuka honey (Jenkins and Cooper, 2012), *Salvia miltiorrhiza* (red sage) (Lee *et al.*, 2007), *Glycyrrhiza uralensis* (Chinese liquorice) (Lee *et al.*, 2009) and *C. sinensis* (Stapleton *et al.*, 2004). In a study by Jenkins and Cooper (2012), a 10% (v/v) solution of manuka honey reversed oxacillin resistance in EMRSA-15; at sub-inhibitory concentrations there was a three-fold down-regulation of *mecR1*, which encodes the two-component system regulating PBP2a expression. Studies by Lee *et al.* (2007; 2009) with *Salvia miltiorrhiza* and *Glycyrrhiza uralensis* reported a re-sensitisation of MRSA to oxacillin following exposure to the hexane fraction from both natural products. The mechanism of action of the *Salvia miltiorrhiza* hexane fraction was inhibition of expression of *mecA*, *mecR1* and *femA* (Lee *et al.*, 2007). A further re-sensitisation of MRSA to oxacillin using ECg, a polyphenol catechin found in *C. sinensis*, has been described in previous publications and in this thesis.

As mentioned previously, ECg intercalates into the cytoplasmic membrane and re-sensitises MRSA to β -lactam agents through a multi-factorial process that includes the partial displacement of PBP2/PBP2a complexes. Furthermore, interactions between

ECg and the MRSA cytoplasmic membrane can be enhanced by structural modification of the compound (Figure 6-3) (data not presented in this thesis); the analogues show equal or greater antibacterial activity which may be indicative of a further modification of the MRSA resistance complex (Anderson *et al.*, 2011).

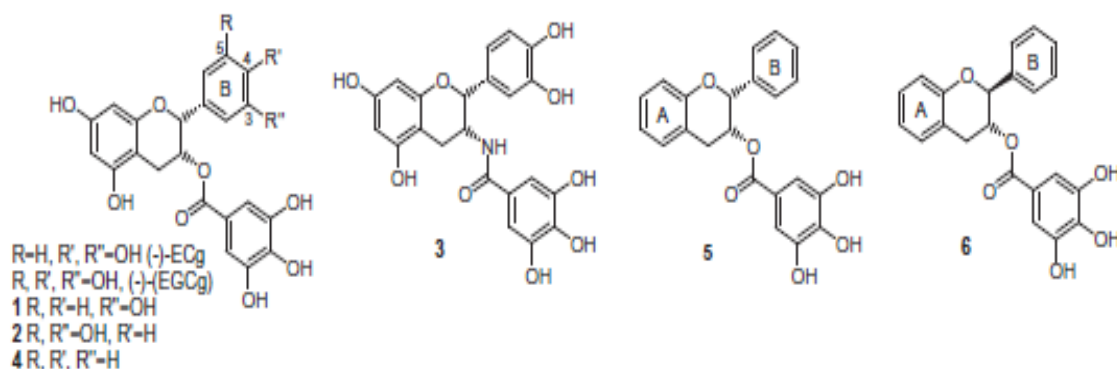


Figure 6-3 Structures of (-)-ECg, (-)-EGCg and analogues 1-6 synthesised by Anderson *et al.* (2011)

Chemical modification of the ester bond as well as the hydroxylation of the B-ring are important in the synthesis of more stable compounds with greater affinity for the cytoplasmic membrane (Anderson *et al.*, 2011). *In vivo* studies have shown that ECg rapidly degrades to inactive products because of the presence of esterase-susceptible linkage groups. The presence of an amide bond in analogue 3 (Figure 6-3) in place of an ester linkage resulted in a more stable compound. Furthermore, intercalation of ECg into the bilayer is believed to be due to its hydrophobicity, with this compound penetrating further into the membrane bilayer compared to EGCg (Caturla *et al.*, 2002). It was hypothesised that analogues with a reduction in the hydroxylation of the B-ring would penetrate deeper into the membrane due to their increased lipophilic nature, resulting in increased antimicrobial activity (Anderson *et al.*, 2005a).

Analogues 1 and 2, with a mono-hydroxylated 3-hydroxy and a di-hydroxylated 3,5-dihydroxy B ring respectively (Figure 6-3), showed equivocal anti-staphylococcal activity compared to ECg (MIC 128 mg/L) and an equal re-sensitisation of MRSA to oxacillin (MIC 1 mg/L) following exposure to 12.5 mg/L of the natural compound. For synthesis of analogue 4, all hydroxyls were removed from the B-ring; this compound displayed greater anti-staphylococcal activity (MIC 64 mg/L) and further re-sensitised

MRSA to oxacillin (MIC 0.25 mg/L) without increased bacteriostatic or bactericidal effects as was observed for analogues 5 and 6 (MIC <0.25 mg/L).

From the above observations, analogue 4 containing an amide bond for further stability (Anderson *et al.*, 2011), may represent a promising modifying agent for treatment of MRSA infections due to its enhanced anti-staphylococcal activity in combination with β -lactams and negligible bacteriostatic and bactericidal properties. This is an important factor for development of resistance modifying agents to combat the rise in antibiotic resistance. The mechanism of action of these analogues is currently under evaluation; use of SMALP solubilisation in combination with co-immunoprecipitation may shed light on the degree of displacement of PBP2/PBP2a complexes, in particular following exposure to analogue 4. Future *in vivo* testing for assessment of the stability and bioavailability of these analogues is required for assessment of their potential as therapeutics.

There is a need for a paradigm shift for treatment of bacterial infections to counteract increased antibiotic resistance and the lack of new antibiotics in pharmaceutical company pipelines. A change in the use of conventional antibiotics with more emphasis on combination therapy, which benefits from synergy between natural secondary metabolites and currently ineffective antibiotics, is one possible approach. The results presented here indicate that ECg and its analogues have the potential to be used in combination with first and second-generation β -lactam agents, modifying the MRSA resistance mechanism and providing opportunities for the treatment or prevention of community and hospital-acquired infections.

LIST OF PUBLICATIONS, PRESENTATIONS AND AWARDS

Publications

1. Anderson, J. C., McCarthy, R. A., **Paulin, S.** and Taylor, P. W. 2011. Anti-staphylococcal activity and β -lactam resistance attenuating capacity of structural analogues of (-)-epicatechin gallate. *Bioorganic and Medicinal Chemistry Letters*, 21, 6996-7000.
2. **Paulin, S.**, Jamshad, M., Dafforn, T. R., Garcia-Lara, J., Foster, S. J., Galley, N. F., Roper, D. I., Rosado, H., Taylor, P.W. 2013. Surfactant-free purification of membrane protein complexes from bacteria: application to the staphylococcal penicillin-binding protein complex PBP2/PBP2a. Accepted for publication in June, 2014 (*Nanotechnology*).

Presentations

1. **Paulin, S.**, Jamshad, M., Dafforn, T.M. and Taylor, P.W. (2012). Identification of the multi-enzyme division complex in methicillin resistant *Staphylococcus aureus* and the effect of (-)-epicatechin gallate on the complex. Poster Presentation. UCL School of Pharmacy Research Day. 21st September 2012.
2. **Paulin S.**, Jamshad M., Dafforn T.M., Roper D.I. and Taylor P.W. (2013). Identification of the PBP2-PBP2a division complex in methicillin resistant *Staphylococcus aureus* and the effect of (-)-epicatechin gallate on the complex. Poster presentation. UCL Graduate School Poster Competition. February 2013.
3. **Paulin S.**, Jamshad M., Dafforn T.M. and Taylor P.W. (2013). Impact of (-)-epicatechin gallate on the PBP2-PBP2a division complex in methicillin resistant *Staphylococcus aureus*. Oral Presentation. UCL School of Pharmacy Research Day. April 2013.
4. **Paulin S.**, Jamshad M., Dafforn T.M., Roper D.I. and Taylor P.W. (2013). Impact of epicatechin gallate on the structural integrity of the PBP2-PBP2a division complex in methicillin resistant *Staphylococcus aureus*. Poster presentation. American Society of Microbiology, 113th General Meeting. May 2013.
5. **Paulin S.**, Jamshad M., Rosado, H., Dafforn T.M., Roper D.I. Foster S.J. and Taylor P.W. (2013). Epicatechin gallate disrupts the structural integrity of the PBP2-PBP2a division complex in methicillin resistant *Staphylococcus aureus*. Poster presentation at UCL Faculty of Life Sciences Research Day, London, September 2013.

Awards

1. Best poster presentation at the UCL School of Pharmacy PhD Research Day, London, September 2012.
2. Successful grant application for £500.00 from the UCL Graduate School Student Conference Fund to attend the ASM general meeting in Denver in May 2013.
3. Best lecture award at the UCL School of Pharmacy PhD Research Day, London, April 2013.
4. Best poster award at the UCL Faculty of Life Sciences Research Day, London, September 2013.

REFERENCES

- ABCAM. *Polyclonal and monoclonal: A comparison* [Online]. Available: <http://www.abcam.com/index.html?pageconfig=resource&rid=11269&pid=11287> [Accessed 18 October 2013].
- ABRAHAM, E. P. & CHAIN, E. 1940. An enzyme from bacteria able to destroy penicillin. *Rev Infect Dis*, 10, 677-8.
- ABRAHAM, E. P., CHAIN, E., FLETCHER, C. M., GARDNER, A. D., HEATLEY, N. G., JENNINGS, M. A. & FLOREY, H. W. 1941. Further observations on penicillin. *Lancet*, 238, 177-189.
- ABRAHAM, J. J. 1948. Some account of the history of the treatment of syphilis. *Br J Vener Dis*, 24, 153-61.
- ADAMS, D. W. & ERRINGTON, J. 2009. Bacterial cell division: assembly, maintenance and disassembly of the Z ring. *Nat Rev Microbiol*, 7, 642-653.
- ADHAMI, V. M., AHMAD, N. & MUKHTAR, H. 2003. Molecular targets for green tea in prostate cancer prevention. *J Nutr*, 133, 2417S-2424S.
- ALAEDINI, A. & DAY, R. A. 1999. Identification of two penicillin-binding multienzyme complexes in *Haemophilus influenzae*. *Biochem Biophys Res Commun*, 264, 191-5.
- ANDERSON, J. C., HEADLEY, C., STAPLETON, P. D. & TAYLOR, P. W. 2005a. Asymmetric total synthesis of B-ring modified (-)-epicatechin gallate analogues and their modulation of beta-lactam resistance in *Staphylococcus aureus*. *Tetrahedron*, 61, 7703-7711.
- ANDERSON, J. C., HEADLEY, C., STAPLETON, P. D. & TAYLOR, P. W. 2005b. Synthesis and antibacterial activity of hydrolytically stable (-)-epicatechin gallate analogues for the modulation of beta-lactam resistance in *Staphylococcus aureus*. *Bioorg Med Chem Lett*, 15, 2633-2635.
- ANDERSON, J. C., MCCARTHY, R. A., PAULIN, S. & TAYLOR, P. W. 2011. Anti-staphylococcal activity and β -lactam resistance attenuating capacity of structural analogues of (-)-epicatechin gallate. *Bioorganic & Med Chem Lett*, 21, 6996-7000.
- ATIKEN, A. & LEARMONTH, M. 2002. Protein determination by UV. *The protein protocols handbook*. 2nd ed.: Humana Press.
- ATILANO, M. L., PEREIRA, P. M., YATES, J., REED, P., VEIGA, H., PINHO, M. G. & FILIPE, S. R. 2010. Teichoic acids are temporal and spatial regulators of peptidoglycan cross-linking in *Staphylococcus aureus*. *Proc Natl Acad Sci U S A*, 107, 18991-6.
- BACCANARI, D. P. & KUYPER, L. F. 1993. Basis of selectivity of antibacterial diaminopyrimidines. *J Chemother*, 5, 393-9.
- BAILEY, J. E., FAZEL-MAKJLESSI, J., MCQUITTY, D. N., LEE, Y. N., ALLRED, J. C. & ORO, J. A. 1977. Characterization of bacterial growth by means of flow microfluorometry. *Science*, 198, 1175-6.
- BARRETEAU, H., KOVAC, A., BONIFACE, A., SOVA, M., GOBEC, S. & BLANOT, D. 2008. Cytoplasmic steps of peptidoglycan biosynthesis. *FEMS Microbiol Rev*, 32, 168-207.
- BAYBURT, T. H. & SLIGAR, S. G. 2002. Single-molecule height measurements on microsomal cytochrome P450 in nanometer-scale phospholipid bilayer disks. *Proc Natl Acad Sci U S A*, 99, 6725-30.
- BENNETT, K. L., KUSSMANN, M., BJÖRK, P., GODZWON, M., MIKKELSEN, M., SØRENSEN, P. & ROEPSTORFF, P. 2000. Chemical cross-linking with thiol-cleavable reagents combined with differential mass spectrometric peptide

- mapping-a novel approach to assess intermolecular protein contacts. *Protein Sci*, 9, 1503-18.
- BERA, A., HERBERT, S., JAKOB, A., VOLLMER, W. & GÖTZ, F. 2005. Why are pathogenic staphylococci so lysozyme resistant? The peptidoglycan O-acetyltransferase OatA is the major determinant for lysozyme resistance of *Staphylococcus aureus*. *Mol Microbiol*, 55, 778-87.
- BERGER-BACHI, B. 2002. Resistance mechanisms of Gram-positive bacteria. *Int J Med Microbiol*, 292, 8.
- BERGER-BÄCHI, B. & ROHRER, S. 2002. Factors influencing methicillin resistance in staphylococci. *Arch Microbiol*, 178, 165-71.
- BERNAL, P., LEMAIRE, S., PINHO, M. G., MOBASHERY, S., HINDS, J. & TAYLOR, P. W. 2010. Insertion of epicatechin gallate into the cytoplasmic membrane of methicillin-resistant *Staphylococcus aureus* disrupts penicillin-binding protein (PBP) 2a-mediated beta-lactam resistance by delocalizing PBP2. *J Biol Chem*, 285, 13.
- BERNAL, P., ZLOH, M. & TAYLOR, P. W. 2009. Disruption of D-alanyl esterification of *Staphylococcus aureus* cell wall teichoic acid by the beta-lactam resistance modifier (-)-epicatechin gallate. *J Antimicrob Chemo*, 63, 1156-1162.
- BERTSCHE, U., KAST, T., WOLF, B., FRAIPONT, C., AARSMAN, M. E., KANNENBERG, K., VON RECHENBERG, M., NGUYEN-DISTÈCHE, M., DEN BLAAUWEN, T., HÖLTJE, J. V. & VOLLMER, W. 2006. Interaction between two murein (peptidoglycan) synthases, PBP3 and PBP1B, in *Escherichia coli*. *Mol Microbiol*, 61, 675-90.
- BETONI, J. E., MANTOVANI, R. P., BARBOSA, L. N., DI STASI, L. C. & FERNANDES JUNIOR, A. 2006. Synergism between plant extract and antimicrobial drugs used on *Staphylococcus aureus* diseases. *Mem Inst Oswaldo Cruz*, 101, 387-90.
- BIGELOW, R. L. & CARDELLI, J. A. 2006. The green tea catechins, (-)-epigallocatechin-3-gallate (EGCG) and (-)-epicatechin-3-gallate (ECG), inhibit HGF/Met signaling in immortalized and tumorigenic breast epithelial cells. *Oncogene*, 25, 1922-30.
- BOHACH, G. A. & FOSTER, T. A. 1999. *Staphylococcus aureus* exotoxins. In: FISCHETTI, V. A., NOVICK, R. P., FERRETTI, J. J. & J.I., R. (eds.) *Gram positive bacterial pathogens*. Washington, D.C., USA: American Society for Microbiology.
- BORCH, J. & HAMANN, T. 2009. The nanodisc: a novel tool for membrane protein studies. *Biol Chem*, 390, 805-14.
- BOTELHO, A. V., GIBSON, N. J., THURMOND, R. L., WANG, Y. & BROWN, M. F. 2002. Conformational energetics of rhodopsin modulated by nonlamellar-forming lipids. *Biochem*, 41, 6354-68.
- BOYCE, J. M., COOKSON, B., CHRISTIANSEN, K., HORI, S., VUOPIO-VARKILA, J., KOCAGÖZ, S., OZTOP, A. Y., VANDENBROUCKE-GRAULS, C. M., HARBARTH, S. & PITTET, D. 2005. Methicillin-resistant *Staphylococcus aureus*. *Lancet Infect Dis*, 5, 653-63.
- BROWN, D. F. & REYNOLDS, P. E. 1980. Intrinsic resistance to beta-lactam antibiotics in *Staphylococcus aureus*. *FEBS Lett*, 122, 275-8.
- BUSH, K. 1989. Characterization of beta-lactamases. *Antimicrob Agents Chemother*, 33, 259-63.
- BUSH, K. 2013. Introduction to antimicrobial therapeutics reviews: the bacterial cell wall as an antimicrobial target. *Ann N Y Acad Sci*, 1277, v-vii.
- BUSH, K., COURVALIN, P., DANTAS, G., DAVIES, J., EISENSTEIN, B., HUOVINEN, P., JACOBY, G. A., KISHONY, R., KREISWIRTH, B. N.,

- KUTTER, E., LERNER, S. A., LEVY, S., LEWIS, K., LOMOVSKAYA, O., MILLER, J. H., MOBASHERY, S., PIDDOCK, L. J., PROJAN, S., THOMAS, C. M., TOMASZ, A., TULKENS, P. M., WALSH, T. R., WATSON, J. D., WITKOWSKI, J., WITTE, W., WRIGHT, G., YEH, P. & ZGURSKAYA, H. I. 2011. Tackling antibiotic resistance. *Nat Rev Microbiol*, 9, 894-6.
- CARLET, J., COLLIGNON, P., GOLDMANN, D., GOOSSENS, H., GYSSENS, I. C., HARBARTH, S., JARLIER, V., LEVY, S. B., N'DOYE, B., PITTET, D., RICHTMANN, R., SETO, W. H., VAN DER MEER, J. W. & VOSS, A. 2011. Society's failure to protect a precious resource: antibiotics. *Lancet*, 378, 369-71.
- CARLETON, H. A., DIEP, B. A., CHARLEBOIS, E. D., SENSABAUGH, G. F. & PERDREAU-REMINGTON, F. 2004. Community-adapted methicillin-resistant *Staphylococcus aureus* (MRSA): population dynamics of an expanding community reservoir of MRSA. *J Infect Dis*, 190, 1730-8.
- CARPENTER, C. F. & CHAMBERS, H. F. 2004. Daptomycin: another novel agent for treating infections due to drug-resistant gram-positive pathogens. *Clin Infect Dis*, 38, 994-1000.
- CATURLA, N., VERA-SAMPER, E., VILLALAIN, J., MATEO, C. R. & MICOL, V. 2002. The relationship between the antioxidant and the antibacterial properties of galloylated catechins and the structure of phospholipid model membranes. *Free Rad Biol Med*, 34, 648-662.
- CDC 2002. *Staphylococcus aureus* resistant to vancomycin-United States, 2002. *MMWR Morb Mortal Wkly Rep*, 51, 565-7.
- CDC. 2013. *Threat report 2013* [Online]. Available: <http://www.cdc.gov/drugresistance/threat-report-2013/> [Accessed 24th November 2013].
- CHAMBERS, H. F. 1988. Methicillin-resistant *Staphylococci*. *Clin Microbiol Rev*, 1, 173-186.
- CHAMBERS, H. F. 2003. Solving staphylococcal resistance to beta-lactams. *Trends Microbiol*, 11, 145-148.
- CHAMBERS, H. F. & DELEO, F. R. 2009. Waves of resistance: *Staphylococcus aureus* in the antibiotic era. *Nat Rev Microbiol*, 7, 629-641.
- CHAMBERS, H. F., SACHDEVA, M. J. & HACKBARTH, C. J. 1994. Kinetics of penicillin binding to penicillin-binding proteins of *Staphylococcus aureus*. *Biochem J*, 301 (Pt 1), 139-44.
- CHEN, L., LEE, M. J., LI, H. & YANG, C. S. 1997. Absorption, distribution, elimination of tea polyphenols in rats. *Drug Metab Dispos*, 25, 1045-50.
- CHEN, Z., ZHU, Q. Y., TSANG, D. & HUANG, Y. 2001. Degradation of green tea catechins in tea drinks. *J Agric Food Chem*, 49, 477-82.
- CHEUNG, A. L., EBERHARDT, K. J., CHUNG, E., YEAMAN, M. R., SULLAM, P. M., RAMOS, M. & BAYER, A. S. 1994. Diminished virulence of a sar-/agr-mutant of *Staphylococcus aureus* in the rabbit model of endocarditis. *J Clin Invest*, 94, 1815-22.
- CHO, Y. S., SCHILLER, N. L. & OH, K. H. 2008. Antibacterial effects of green tea polyphenols on clinical isolates of methicillin-resistant *Staphylococcus aureus*. *Curr Microbiol*, 57, 542-546.
- CHOPRA, I. 1985. Mode of action of the tetracyclines and the nature of bacterial resistance to them. In: HLAVKA, J. & BOOTHE, J. (eds.) *Handbook of experimental pharmacology*. Berlin, Germany: Springer-Verlag KG.
- CHOPRA, I., LACEY, R. W. & CONNOLLY, J. 1974. Biochemical and genetic basis of tetracycline resistance in *Staphylococcus aureus*. *Antimicrob Agents Chemother*, 6, 397-404.

- CLAESSEN, D., EMMINS, R., HAMOEN, L. W., DANIEL, R. A., ERRINGTON, J. & EDWARDS, D. H. 2008. Control of the cell elongation-division cycle by shuttling of PBP1 protein in *Bacillus subtilis*. *Mol Microbiol*, 68, 1029-46.
- CLARDY, J., FISCHBACH, M. A. & CURRIE, C. R. 2009. The natural history of antibiotics. *Curr Biol*, 19, R437-41.
- CLINICAL AND LABORATORY STANDARDS INSTITUTE (CLSI) (2008). Document M31-A3. Performance Standards for Antimicrobial Disk and Dilution Susceptibility Tests for Bacteria Isolated from Animals, Approved Standard, Third Edition. CLSI, 940 West Valley Road, Suite 1400, Wayne, Pennsylvania 19087-1898, USA
- COWAN, M. M. 1999. Plant products as antimicrobial agents. *Clin Microbiol Rev*, 12, 564-82.
- CURTIS, N. A. C., HAYES, M. V., WYKE, A. W. & WARD, B. 1980. A mutant of *Staphylococcus aureus* H lacking penicillin-binding protein 4 and transpeptidase activity *in vitro*. *FEMS Microbiol Lett*, 9, 263-266.
- DAVIES, J. & DAVIES, D. 2010. Origins and evolution of antibiotic resistance. *Microbiol Mol Biol Rev*, 74, 417-33.
- DE LENCASTRE, H. & TOMASZ, A. 1994. Reassessment of the number of auxiliary genes essential for expression of high-level methicillin resistance in *Staphylococcus aureus*. *Antimicrob Agents Chemother*, 38, 2590-8.
- DEBNATH, D. K., BASAIAWMOIT, R. V., NIELSEN, K. L. & OTZEN, D. E. 2011. The role of membrane properties in Mistic folding and dimerisation. *Protein Eng Des Sel*, 24, 89-97.
- DEISENHOFER, J., EPP, O., MIKI, K., HUBER, R. & MICHEL, H. 1985. Structure of the protein subunits in the photosynthetic reaction centre of *Rhodospseudomonas viridis* at 3Å resolution. *Nat*, 318, 618-24.
- DELEAULT, N. R., GEOGHEGAN, J. C., NISHINA, K., KASCSAK, R., WILLIAMSON, R. A. & SUPATTAPONE, S. 2005. Protease-resistant prion protein amplification reconstituted with partially purified substrates and synthetic polyanions. *J Biol Chem*, 280, 26873-9.
- DENYER, S. P., HODGES, N., GORMAN, S. P. & GILMORE, B. F. (eds.) 2011. *Hugo & Russell's Pharmaceutical Microbiology*, Oxford: Blackwell Publishing Ltd.
- DEURENBERG, R. H. & STOBBERINGH, E. E. 2008. The evolution of *Staphylococcus aureus*. *Infect Gen Evol*, 8, 747-763.
- DEURENBERG, R. H., VINK, C., KALENIC, S., FRIEDRICH, A. W., BRUGGEMAN, C. A. & STOBBERINGH, E. E. 2007. The molecular evolution of methicillin-resistant *Staphylococcus aureus*. *Clin Microbiol Infect*, 13, 222-35.
- DIXON, R. A. 2001. Natural products and plant disease resistance. *Nature*, 411, 843-7.
- DRAWZ, S. M. & BONOMO, R. A. 2010. Three decades of beta-lactamase inhibitors. *Clin Microbiol Rev*, 23, 160-201.
- DUMITRESCU, O., CHOUDHURY, P., BOISSET, S., BADIOU, C., BES, M., BENITO, Y., WOLZ, C., VANDENESCH, F., ETIENNE, J., CHEUNG, A. L., BOWDEN, M. G. & LINA, G. 2011. Beta-lactams interfering with PBP1 induce Panton-Valentine leukocidin expression by triggering sarA and rot global regulators of *Staphylococcus aureus*. *Antimicrob Agents Chemother*, 55, 3261-71.
- DYKE, K. G., JEVONS, M. P. & PARKER, M. T. 1966. Penicillinase production and intrinsic resistance to penicillins in *Staphylococcus aureus*. *Lancet*, 1, 835-8.

- EARS-NET. *Antimicrobial resistance interactive database* [Online]. Available: http://www.ecdc.europa.eu/en/healthtopics/antimicrobial_resistance/database/Pages/database.aspx [Accessed 25th November 2013].
- EARS-NET 2013. Antimicrobial resistance surveillance in Europe 2012. Stockholm: ECDC.
- ECDC & EMEA 2009. ECDC/EMA joint technical report. The bacterial challenge: time to react. Stockholm: ECDC.
- ECKERT, R. 2011. Road to clinical efficacy: challenges and novel strategies for antimicrobial peptide development. *Future Microbiol*, 6, 635-51.
- EDWARDS, D. I. 1980. Mechanisms of selective toxicity of metronidazole and other nitroimidazole drugs. *Br J Vener Dis*, 56, 285-90.
- EHRlich, P. & SHIGA, K. 1904. *Berlin Klin Wochenschrift*, 20, 329-362.
- ELLINGTON, M. J., HOPE, R., LIVERMORE, D. M., KEARNS, A. M., HENDERSON, K., COOKSON, B. D., PEARSON, A. & JOHNSON, A. P. 2010. Decline of EMRSA-16 amongst methicillin-resistant *Staphylococcus aureus* causing bacteraemias in the UK between 2001 and 2007. *J Antimicrob Chemother*, 65, 446-8.
- ENTENZA, J. M., GIDDEY, M., VOUILAMOZ, J. & MOREILLON, P. 2010. *In vitro* prevention of the emergence of daptomycin resistance in *Staphylococcus aureus* and enterococci following combination with amoxicillin/clavulanic acid or ampicillin. *Int J Antimicrob Agents*, 35, 451-6.
- ERICKSON, H. P., ANDERSON, D. E. & OSAWA, M. 2010. FtsZ in bacterial cytokinesis: cytoskeleton and force generator all in one. *Microbiol Mol Biol Rev*, 74, 504-28.
- ERNST, C. M., STAUBITZ, P., MISHRA, N. N., YANG, S. J., HORNIG, G., KALBACHER, H., BAYER, A. S., KRAUS, D. & PESCHEL, A. 2009. The bacterial defensin resistance protein MprF consists of separable domains for lipid lysinylation and antimicrobial peptide repulsion. *PLoS Pathog*, 5, e1000660.
- ERRINGTON, J., DANIEL, R. A. & SCHEFFERS, D.-J. 2003. Cytokinesis in bacteria. *Microbiol Mol Biol Rev*, 67, 52-65.
- FASSINA, G., BUFFA, A., BENELLI, R., VARNIER, O. E., NOONAN, D. M. & ALBINI, A. 2002. Polyphenolic antioxidant (-)-epigallocatechin-3-gallate from green tea as a candidate anti-HIV agent. *AIDS*, 16, 939-41.
- FLEMING, A. 1929. On the antibacterial action of cultures of a penicillium, with special reference to their use in the isolation of *B. influenzae*. *Br J Exp Pathol*, 10, 226-236.
- FLOSS, H. G. & YU, T. W. 2005. Rifamycin-mode of action, resistance, and biosynthesis. *Chem Rev*, 105, 621-32.
- FORREST, D. 1985. *The World Trade: A Survey of the Production, Distribution and Consumption of Tea*, Cambridge, UK, Woodhead-Faulkner Publishers, Limited.
- FOSTER, T. 1996. *Staphylococcus*. In: BARON, S. (ed.) *Medical Microbiology*. 4th ed. Galveston, Texas: University of Texas Medical Branch at Galveston.
- FOSTER, T. J. 2005. Immune evasion by Staphylococci. *Nat Rev Microbiol*, 3, 948-958.
- FUDA, C., SUVOROV, M., VAKULENKO, S. B. & MOBASHERY, S. 2004. The basis for resistance to beta-lactam antibiotics by penicillin-binding protein 2a of methicillin-resistant *Staphylococcus aureus*. *J Biol Chem*, 279, 40802-40806.
- GAGLIOTTI, C., BALODE, A., BAQUERO, F., DEGENER, J., GRUNDMANN, H., GÜR, D., JARLIER, V., KAHLMEIER, G., MONEN, J., MONNET, D. L., ROSSOLINI, G. M., SUETENS, C., WEIST, K., HEUER, O. & AMR), E.-N. P. D. S. C. P. F. 2011. *Escherichia coli* and *Staphylococcus aureus*: bad news and

- good news from the European Antimicrobial Resistance Surveillance Network (EARS-Net, formerly EARSS), 2002 to 2009. *Euro Surveill*, 16.
- GALLAGHER, S. R. 2006. One-dimensional SDS gel electrophoresis of proteins. *Curr Protoc Immunol*, Chapter 8, Unit 8.4.
- GAO, Y. T., MCLAUGHLIN, J. K., BLOT, W. J., JI, B. T., DAI, Q. & FRAUMENI, J. F. 1994. Reduced risk of esophageal cancer associated with green tea consumption. *J Natl Cancer Inst*, 86, 855-8.
- GARDETE, S., LUDOVICE, A. M., SOBRAL, R. G., FILIPE, S. R., DE LENCASTRE, H. & TOMASZ, A. 2004. Role of murE in the expression of beta-lactam antibiotic resistance in *Staphylococcus aureus*. *J Bacteriol*, 186, 1705-13.
- GEDDES, A. M., KLUGMAN, K. P. & ROLINSON, G. N. 2007. Introduction: historical perspective and development of amoxicillin/clavulanate. *Int J Antimicrob Agents*, 30 Suppl 2, S109-12.
- GEORGOPAPADAKOU, N. H., DIX, B. A. & MAURIZ, Y. R. 1986. Possible physiological functions of penicillin-binding proteins in *Staphylococcus aureus*. *Antimicrob Agents Chemother*, 29, 333-6.
- GEORGOPAPADAKOU, N. H., SMITH, S. A. & BONNER, D. P. 1982. Penicillin-binding proteins in a *Staphylococcus aureus* strain resistant to specific beta-lactam antibiotics. *Antimicrob Agents Chemother*, 22, 172-5.
- GERACI, J. E. & HERMANS, P. E. 1983. Vancomycin. *Mayo Clin Proc*, 58, 88-91.
- GHUYSEN, J. M. 1991. Serine beta-lactamases and penicillin-binding proteins. *Annu Rev Microbiol*, 45, 37-67.
- GIBBONS, S. 2004. Anti-staphylococcal plant natural products. *Nat Prod Rep*, 21, 263-77.
- GIESBRECHT, P., KERSTEN, T., MAIDHOF, H. & WECKE, J. 1998. Staphylococcal cell wall: morphogenesis and fatal variations in the presence of penicillin. *Microbiol Mol Biol Rev*, 62, 1371-1414.
- GILLET, Y., ISSARTEL, B., VANHEMS, P., FOURNET, J. C., LINA, G., BES, M., VANDENESCH, F., PIÉMONT, Y., BROUSSE, N., FLORET, D. & ETIENNE, J. 2002. Association between *Staphylococcus aureus* strains carrying gene for Panton-Valentine leukocidin and highly lethal necrotising pneumonia in young immunocompetent patients. *Lancet*, 359, 753-9.
- GLAUERT, A. M. & THORNLEY, M. J. 1969. The topography of the bacterial cell wall. *Annu Rev Microbiol*, 23, 159-98.
- GOERING, R. V., DOCKRELL, H. M., ZUCKERMAN, M., ROITT, I. M. & CHIODINI, P. L. 2013. *Mim's Medical Microbiology*, Philadelphia, PA, Elsevier Saunders.
- GOFFIN, C. & GHUYSEN, J. M. 1998. Multimodular penicillin-binding proteins: an enigmatic family of orthologs and paralogs. *Microbiol Mol Biol Rev*, 62, 1079-1093.
- GORDON, R. J. & LOWY, F. D. 2008. Pathogenesis of methicillin-resistant *Staphylococcus aureus* infection. *Clin Infect Dis*, 46 Suppl 5, S350-9.
- GRAHAM, H. N. 1992. Green tea composition, consumption, and polyphenol chemistry. *Prev Med*, 21, 334-50.
- GREENSPAN, P. & FOWLER, S. D. 1985. Spectrofluorometric studies of the lipid probe, Nile red. *J Lipid Res*, 26, 781-9.
- GREENWOOD, D., FINCH, R., DAVEY, P. & WILCOX, M. (eds.) 2007a. *Antimicrobial Chemotherapy*, New York, NY: Oxford University Press Inc.
- GREENWOOD, D., SLACK, R., PEUTHERE, J. & BARER, M. (eds.) 2007b. *Medical Microbiology*, Philadelphia, PA: Elsevier Limited.

- GUO, Q., ZHAO, B., SHEN, S., HOU, J., HU, J. & XIN, W. 1999. ESR study on the structure-antioxidant activity relationship of tea catechins and their epimers. *Biochim Biophys Acta*, 1427, 13-23.
- GUPTA, S., AHMAD, N., NIEMINEN, A. L. & MUKHTAR, H. 2000. Growth inhibition, cell-cycle dysregulation, and induction of apoptosis by green tea constituent (-)-epigallocatechin-3-gallate in androgen-sensitive and androgen-insensitive human prostate carcinoma cells. *Toxicol Appl Pharmacol*, 164, 82-90.
- GÜNDOĞDU, M. E., KAWAI, Y., PAVLENOVA, N., OGASAWARA, N., ERRINGTON, J., SCHEFFERS, D. J. & HAMOEN, L. W. 2011. Large ring polymers align FtsZ polymers for normal septum formation. *EMBO J*, 30, 617-26.
- HAHN, F., WISSEMAN, C. & HOPPS, H. 1954. Mode of action of chloramphenicol, II. Inhibition of bacterial D-polypeptide formation by an L-stereoisomer of chloramphenicol. *J Bacteriol*, 67, 674-679.
- HALL, D. B. & STRUHL, K. 2002. The VP16 activation domain interacts with multiple transcriptional components as determined by protein-protein cross-linking *in vivo*. *J Biol Chem*, 277, 46043-50.
- HAMILTON-MILLER, J. M. 1995. Antimicrobial properties of tea (*Camellia sinensis*). *Antimicrob Agents Chemother*, 39, 2375-7.
- HANLON, G. W. 2007. Bacteriophages: an appraisal of their role in the treatment of bacterial infections. *Int J Antimicrob Agents*, 30, 118-28.
- HARRISON, E. M., PATERSON, G. K., HOLDEN, M. T., LARSEN, J., STEGGER, M., LARSEN, A. R., PETERSEN, A., SKOV, R. L., CHRISTENSEN, J. M., BAK ZEUTHEN, A., HELTBERG, O., HARRIS, S. R., ZADOKS, R. N., PARKHILL, J., PEACOCK, S. J. & HOLMES, M. A. 2013. Whole genome sequencing identifies zoonotic transmission of MRSA isolates with the novel *mecA* homologue *mecC*. *EMBO Mol Med*, 5, 509-15.
- HASHIMOTO, T., KUMAZAWA, S., NANJO, F., HARA, Y. & NAKAYAMA, T. 1999. Interaction of tea catechins with lipid bilayers investigated with liposome systems. *Biosci Biotechnol Biochem*, 63, 2252-2255.
- HAYDEN, M. K., REZAI, K., HAYES, R. A., LOLANS, K., QUINN, J. P. & WEINSTEIN, R. A. 2005. Development of daptomycin resistance *in vivo* in methicillin-resistant *Staphylococcus aureus*. *J Clin Microbiol*, 43, 5285-7.
- HEESEMAN, J. 1993. Mechanisms of resistance to beta-lactam antibiotics. *Infect*, 21 Suppl 1, S4-9.
- HELENIUS, A. & SIMONS, K. 1975. Solubilization of membranes by detergents. *Biochim Biophys Acta*, 415, 29-79.
- HENNING, S. M., FAJARDO-LIRA, C., LEE, H. W., YOUSSEFIAN, A. A., GO, V. L. & HEBER, D. 2003. Catechin content of 18 teas and a green tea extract supplement correlates with the antioxidant capacity. *Nutr Cancer*, 45, 226-35.
- HENZE, U. U. & BERGER-BÄCHI, B. 1996. Penicillin-binding protein 4 overproduction increases beta-lactam resistance in *Staphylococcus aureus*. *Antimicrob Agents Chemother*, 40, 2121-5.
- HIRASAWA, M. & TAKADA, K. 2004. Multiple effects of green tea catechin on the antifungal activity of antimycotics against *Candida albicans*. *J Antimicrob Chemother*, 53, 225-9.
- HOBSON, D. 1954. Activity of erythromycin against *Staphylococcus aureus*. *Br Med J*, 1, 236-9.
- HONDA, R., TANAKA, H. & YASUDA, H. 1997. Oncoprotein MDM2 is a ubiquitin ligase E3 for tumor suppressor p53. *FEBS Lett*, 420, 25-7.

- HONG, M., ZHANG, Y. & HU, F. 2011. Membrane protein structure and dynamics from NMR spectroscopy. *Annu Rev Phys Chem*.
- HOOVER, D. C. 1993. Quinolone mode of action--new aspects. *Drugs*, 45 Suppl 3, 8-14.
- HOPWOOD, D. 2007. A call to arms. *Nat Rev Drug Discov*, 6, 8-12.
- HOTCHKISS, R. S. & OPAL, S. 2010. Immunotherapy for sepsis--a new approach against an ancient foe. *N Engl J Med*, 363, 87-9.
- HOWARD, S. J., CATCHPOLE, M., WATSON, J. & DAVIES, S. C. 2013. Antibiotic resistance: global response needed. *Lancet Infect Dis*, 13, 1001-3.
- HPA June 2011. Summary points on meticillin resistant *Staphylococcus aureus* (MRSA) bacteraemia. London: Health Protection Agency.
- HPA. Sept 2009. *Healthcare-associated infections in England: 2008-2009 report* [Online]. London: Health Protection Agency. Available: http://www.hpa.org.uk/web/HPAwebFile/HPAweb_C/1252326222452.
- HUBSCHER, J., JANSEN, A., KOTTE, O., SCHAFER, J., MAJCHERCZYK, P. A., HARRIS, L. G., BIERBAUM, G., HEINEMANN, M. & BERGER-BACHI, B. 2007. Living with an imperfect cell wall: compensation of femAB inactivation in *Staphylococcus aureus*. *BMC Genomics*, 8, 307.
- HUNTE, C., JAGOW, G. J. & SCHAGGER, H. 2003. Membrane protein purification and crystallization. *A practical guide*. London: Academic Press.
- HÖLTJE, J. V. 1996. A hypothetical holoenzyme involved in the replication of the murein sacculus of *Escherichia coli*. *Microbiol*, 142 (Pt 8), 1911-8.
- JAMSHAD, M., LIN, Y.-P., KNOWLES, T. J., PARSLow, R. A., HARRIS, C., WHEATLEY, M., POYNER, D. R., BILL, R. M., THOMAS, O. R., OVERDUIN, M. & DAFFORN, T. R. 2011. Surfactant-free purification of membrane proteins with intact native membrane environment. *Biochem. Soc. Trans.*, 39, 813.
- JENKINS, R. E. & COOPER, R. 2012. Synergy between oxacillin and manuka honey sensitizes methicillin-resistant *Staphylococcus aureus* to oxacillin. *J Antimicrob Chemother*, 67, 1405-7.
- JEVONS, M. 1961. *Brit Med J*, 1, 124-125.
- JOHNSON, A. P. 2011. Methicillin-resistant *Staphylococcus aureus*: the European landscape. *J Antimicrob Chem*, 66, iv43-iv48.
- JOHNSON, A. P., AUCKEN, H. M., CAVENDISH, S., GANNER, M., WALE, M. C., WARNER, M., LIVERMORE, D. M., COOKSON, B. D. & PARTICIPANTS, U. E. 2001. Dominance of EMRSA-15 and -16 among MRSA causing nosocomial bacteraemia in the UK: analysis of isolates from the European Antimicrobial Resistance Surveillance System (EARSS). *J Antimicrob Chemother*, 48, 143-4.
- JORGE, A. M., HOICZYK, E., GOMES, J. P. & PINHO, M. G. 2011. EzrA contributes to the regulation of cell size in *Staphylococcus aureus*. *PLoS ONE*, 6, e27542.
- KABACK, H. R. 1971. Bacterial membranes. In: JAKOBY, W. B. (ed.) *Methods in enzymology*. New York: Academic Press Inc.
- KAHAN, J. S., KAHAN, F. M., GOEGELMAN, R., CURRIE, S. A., JACKSON, M., STAPLEY, E. O., MILLER, T. W., MILLER, A. K., HENDLIN, D., MOCHALES, S., HERNANDEZ, S., WOODRUFF, H. B. & BIRNBAUM, J. 1979. Thienamycin, a new beta-lactam antibiotic. I. Discovery, taxonomy, isolation and physical properties. *J Antibiot (Tokyo)*, 32, 1-12.
- KAWAI, Y. & OGASAWARA, N. 2006. *Bacillus subtilis* EzrA and FtsL synergistically regulate FtsZ ring dynamics during cell division. *Microbiol*, 152, 1129-41.

- KELLY, J. A., DIDEBERG, O., CHARLIER, P., WERY, J. P., LIBERT, M., MOEWS, P. C., KNOX, J. R., DUEZ, C., FRAIPONT, C. & JORIS, B. 1986. On the origin of bacterial resistance to penicillin: comparison of a beta-lactamase and a penicillin target. *Science*, 231, 1429-31.
- KHAN, I. A., MIRZA, Z. M., KUMAR, A., VERMA, V. & QAZI, G. N. 2006. Piperine, a phytochemical potentiator of ciprofloxacin against *Staphylococcus aureus*. *Antimicrob Agents Chemother*, 50, 810-2.
- KIRKPATRICK, C. L. & VIOLLIER, P. H. 2011. News to the Z-ring. *Curr Opin Microbiol*, 14, 691-7.
- KNOWLES, T. J., FINKA, R., SMITH, C., LIN, Y.-P., DAFFORN, T. & OVERDUIN, M. 2009. Membrane proteins solubilized intact in lipid containing nanoparticles bounded by styrene maleic acid copolymer. *J Am Chem Soc*, 131, 7484-7485.
- KURIEN, B. T. & SCOFIELD, R. H. 2006. Western blotting. *Methods*, 38, 283-93.
- KURIYAMA, S., SHIMAZU, T., OHMORI, K., KIKUCHI, N., NAKAYA, N., NISHINO, Y., TSUBONO, Y. & TSUJI, I. 2006. Green tea consumption and mortality due to cardiovascular disease, cancer, and all causes in Japan: the Ohsaki study. *JAMA*, 296, 1255-65.
- KURODA, M., KURODA, H., OSHIMA, T., TAKEUCHI, F., MORI, H. & HIRAMATSU, K. 2003. Two-component system VraSR positively modulates the regulation of cell-wall biosynthesis pathway in *Staphylococcus aureus*. *Mol Microbiol*, 49, 807-21.
- KÖCK, R., BECKER, K., COOKSON, B., VAN GEMERT-PIJNEN, J. E., HARBARTH, S., KLUYTMANS, J., MIELKE, M., PETERS, G., SKOV, R. L., STRUELENS, M. J., TACCONELLI, E., NAVARRO TORNÉ, A., WITTE, W. & FRIEDRICH, A. W. 2010. Methicillin-resistant *Staphylococcus aureus* (MRSA): burden of disease and control challenges in Europe. *Euro Surveill*, 15, 19688.
- LANCINI, G., PARENTI, F. & GALLO, G. G. 1995. *Antibiotics a multidisciplinary approach*, New York, NY, Plenum Press.
- LANGLEY-EVANS, S. C. 2000. Antioxidant potential of green and black tea determined using the ferric reducing power (FRAP) assay. *Int J Food Sci Nutr*, 51, 181-8.
- LANGOSCH, D. & ARKIN, I. T. 2009. Interaction and conformational dynamics of membrane-spanning protein helices. *Protein Sci*, 18, 1343-58.
- LEE, A. G. 2003. Lipid-protein interactions in biological membranes: a structural perspective. *Biochim Biophys Acta*, 1612, 1-40.
- LEE, A. G. 2005. How lipids and proteins interact in a membrane: a molecular approach. *Mol Biosyst*, 1, 203-12.
- LEE, J. W., JI, Y. J., LEE, S. O. & LEE, I. S. 2007. Effect of *Salvia miltiorrhiza* bunge on antimicrobial activity and resistant gene regulation against methicillin-resistant *Staphylococcus aureus* (MRSA). *J Microbiol*, 45, 350-7.
- LEE, J. W., JI, Y. J., YU, M. H., BO, M. H., SEO, H. J., LEE, S. P. & LEE, I. S. 2009. Antimicrobial effect and resistant regulation of *Glycyrrhiza uralensis* on methicillin-resistant *Staphylococcus aureus*. *Nat Prod Res*, 23, 101-11.
- LESHER, G. Y., FROELICH, E. J., GRUETT, M. D., BAILEY, J. H. & BRUNDAGE, R. P. 1962. 1,8-Naphthyridine derivative. A new class of chemotherapeutic agents. *J Med Pharm Chem*, 91, 1063-5.
- LESKI, T. A. & TOMASZ, A. 2005. Role of penicillin-binding protein 2 (PBP2) in the antibiotic susceptibility and cell wall-linking of *Staphylococcus aureus*: evidence for the cooperative functioning of PBP2, PBP4, and PBP2a. *J Bacteriol*, 187, 1815-1824.

- LIANG, X., YU, C., SUN, J., LIU, H., LANDWEHR, C., HOLMES, D. & JI, Y. 2006. Inactivation of a two-component signal transduction system, SaeRS, eliminates adherence and attenuates virulence of *Staphylococcus aureus*. *Infect Immun*, 74, 4655-65.
- LIM, D. & STRYNADKA, N. C. J. 2002. Structural basis for the beta-lactam resistance of PBP2a from methicillin-resistant *Staphylococcus aureus*. *Nat Struc Biol*, 9, 870-876.
- LIN, Y.-P. 2011. *Over-expression and biophysical characterisation of membrane proteins solubilised in a styrene maleic acid polymer*. Doctor of Philosophy, University of Birmingham.
- LIN, Y. S., TSAI, Y. J., TSAY, J. S. & LIN, J. K. 2003. Factors affecting the levels of tea polyphenols and caffeine in tea leaves. *J Agric Food Chem*, 51, 1864-73.
- LIU, C., BAYER, A., COSGROVE, S. E., DAUM, R. S., FRIDKIN, S. K., GORWITZ, R. J., KAPLAN, S. L., KARCHMER, A. W., LEVINE, D. P., MURRAY, B. E., RYBACK, M. J., TALAN, A. & CHAMBERS, H. F. 2011. Clinical practice guidelines by the infectious diseases society of America for the treatment of methicillin-resistant *Staphylococcus aureus* infections in adults and children. *Clin Infect Dis*, 52, 1-38.
- LIU, X., LI, J., WANG, Y., LI, T., ZHAO, J. & ZHANG, C. 2013. Green tea polyphenols function as prooxidants to inhibit *Pseudomonas aeruginosa* and induce the expression of oxidative stress-related genes. *Folia Microbiol*, 58, 211-7.
- LIVNEH, E. & FISHMAN, D. D. 1997. Linking protein kinase C to cell-cycle control. *Eur J Biochem*, 248, 1-9.
- LLARRULL, L. I., FISHER, J. F. & MOBASHERY, S. 2009. Molecular basis and phenotype of methicillin resistance in *Staphylococcus aureus* and insights into new beta-lactams that meet the challenge. *Antimicrob Agents Chemother*, 53, 4051-63.
- LLARRULL, L. I., TESTERO, S. A., FISHER, J. F. & MOBASHERY, S. 2010. The future of the beta-lactams. *Curr Opin Microbiol*, 13, 551-557.
- LOCK, R. L. & HARRY, E. J. 2008. Cell-division inhibitors: new insights for future antibiotics. *Nat Rev Drug Discov*, 7, 324-38.
- LONDON, E. & KHORANA, H. G. 1982. Denaturation and renaturation of bacteriorhodopsin in detergents and lipid-detergent mixtures. *J Biol Chem*, 257, 7003-11.
- LOVERING, A. L., DE CASTRO, L. H., LIM, D. & STRYNADKA, N. C. 2007. Structural insight into the transglycosylation step of bacterial cell-wall biosynthesis. *Science*, 315, 1402-5.
- LU, C., STRICKER, J. & ERICKSON, H. P. 1998. FtsZ from *Escherichia coli*, *Azotobacter vinelandii*, and *Thermotoga maritima*-quantitation, GTP hydrolysis, and assembly. *Cell Motil Cytoskeleton*, 40, 71-86.
- LU, G., XIAO, H., YOU, H., LIN, Y., JIN, H., SNAGASKI, B. & YANG, C. S. 2008. Synergistic inhibition of lung tumorigenesis by a combination of green tea polyphenols and atorvastatin. *Clin Cancer Res*, 14, 4981-8.
- LU, H., MENG, X. & YANG, C. S. 2003. Enzymology of methylation of tea catechins and inhibition of catechol-O-methyltransferase by (-)-epigallocatechin gallate. *Drug Metab Dispos*, 31, 572-9.
- LUCKEY, M. 2008. *Membrane structural biology: with biochemical and physical foundation*, New York, USA, Cambridge University Press.
- LUONG, T. T., NEWELL, S. W. & LEE, C. Y. 2003. Mgr, a novel global regulator in *Staphylococcus aureus*. *J Bacteriol*, 185, 3703-10.

- LUZZATTO, L., APIRION, D. & SCHLESSINGER, D. 1968. Mechanism of action of streptomycin in *E. coli*: interruption of the ribosome cycle at the initiation of protein synthesis. *Proc Natl Acad Sci U S A*, 60, 873-80.
- MACCABE, A. F. & GOULD, J. C. 1956. The epidemiology of an erythromycin resistant *Staphylococcus*. *Scott Med J*, 1, 223-6.
- MACKENZIE, K. R. 2006. Folding and stability of alpha-helical integral membrane proteins. *Chem Rev*, 106, 1931-77.
- MAIDHOF, H., REINICKE, B., BLÜMEL, P., BERGER-BÄCHI, B. & LABISCHINSKI, H. 1991. femA, which encodes a factor essential for expression of methicillin resistance, affects glycine content of peptidoglycan in methicillin-resistant and methicillin-susceptible *Staphylococcus aureus* strains. *J Bacteriol*, 173, 3507-13.
- MALVERN. *Dynamic Light Scattering DLS* [Online]. Malvern Instruments Ltd. Available: http://www.malvern.com/labeng/technology/dynamic_light_scattering/dynamic_light_scattering.htm [Accessed 2nd September 2013].
- MANACH, C. & DONOVAN, J. L. 2004. Pharmacokinetics and metabolism of dietary flavonoids in humans. *Free Radic Res*, 38, 771-85.
- MARGOLIN, W. 2000. Themes and variations in prokaryotic cell division. *FEMS Microbiol Rev*, 24, 531-48.
- MARGOLIN, W. 2009. Sculpting the Bacterial Cell. *Current Biology*, 19, R812-R822.
- MATSUHASHI, M., TAMAKI, S., CURTIS, S. J. & STROMINGER, J. L. 1979. Mutational evidence for identity of penicillin-binding protein 5 in *Escherichia coli* with the major D-alanine carboxypeptidase IA activity. *J Bacteriol*, 137, 644-7.
- MCCALLUM, N., BERGER-BÄCHI, B. & SENN, M. M. 2010. Regulation of antibiotic resistance in *Staphylococcus aureus*. *Int J Med Microbiol*, 300, 118-29.
- MCCULLOUGH, J. L. & MAREN, T. H. 1973. Inhibition of dihydropteroate synthetase from *Escherichia coli* by sulfones and sulfonamides. *Antimicrob Agents Chemother*, 3, 665-9.
- MCKAY, D. L. & BLUMBERG, J. B. 2002. The role of tea in human health: an update. *J Am Coll Nutr*, 21, 1-13.
- MCMANUS, M. C. 1997. Mechanisms of bacterial resistance to antimicrobial agents. *Am J Health Syst Pharm*, 54, 1420-33; quiz 1444-6.
- MEERAN, S. M., AKHTAR, S. & KATIIYAR, S. K. 2009. Inhibition of UVB-induced skin tumor development by drinking green tea polyphenols is mediated through DNA repair and subsequent inhibition of inflammation. *J Invest Dermatol*, 129, 1258-70.
- MEMMI, G., FILIPE, S. R., PINHO, M. G., FU, Z. & CHEUNG, A. 2008. *Staphylococcus aureus* PBP4 is essential for beta-lactam resistance in community-acquired methicillin-resistant strains. *Antimicrob Agents Chemo*, 52, 3955-3966.
- MICHALOPOULOS, A. & FALAGAS, M. E. 2008. Colistin and polymyxin B in critical care. *Crit Care Clin*, 24, 377-91, x.
- MINODA, K., ICHIKAWA, T., KATSUMATA, T., ONOBORI, K.-I., MORI, T., SIZUKI, Y., ISHII, T. & NAKAYAMA, T. 2010. Influence of the galloyl moiety in tea catechins on binding affinity for human serum albumin. *J Nutr Sci Vitaminol*, 56, 331-334.
- MOHAMED, A. A., ALI, S. I. & EL-BAZ, F. K. 2013. Antioxidant and antibacterial activities of crude extracts and essential oils of *Syzygium cumini* leaves. *PLoS One*, 8, e60269.

- MOHAMMADI, T., VAN DAM, V., SIJBRANDI, R., VERNET, T., ZAPUN, A., BOUHSS, A., DIEPEVEEN-DE BRUIN, M., NGUYEN-DISTECHE, M., DE KRUIJFF, B. & BREUKINK, E. 2011. Identification of FtsW as a transporter of lipid-linked cell wall precursors across the membrane. *EMBO J*, 30, 1425-32.
- MOORE, D. T., BERGER, B. W. & DEGRADO, W. F. 2008. Protein-protein interactions in the membrane: sequence, structural, and biological motifs. *Structure*, 16, 991-1001.
- MORELL, E. A. & BALKIN, D. M. 2010. Methicillin-resistant *Staphylococcus aureus*: a pervasive pathogen highlights the need for new antimicrobial development. *Yale J Biol Med*, 83, 223-33.
- MOUBARECK, C., MEZIANE-CHERIF, D., COURVALIN, P. & PÉRICHON, B. 2009. VanA-type *Staphylococcus aureus* strain VRSA-7 is partially dependent on vancomycin for growth. *Antimicrob Agents Chemother*, 53, 3657-63.
- MURRAY, T., POPHAM, D. L. & SETLOW, P. 1997. Identification and characterization of *pbpA* encoding *Bacillus subtilis* penicillin-binding protein 2A. *J Bacteriol*, 179, 3021-9.
- MÜLLER, V. S., JUNGBLUT, P. R., MEYER, T. F. & HUNKE, S. 2011. Membrane-SPINE: an improved method to identify protein-protein interaction partners of membrane proteins *in vivo*. *Proteomics*, 11, 2124-8.
- MÜNCH, D., ROEMER, T., LEE, S. H., ENGESER, M., SAHL, H. G. & SCHNEIDER, T. 2012. Identification and *in vitro* analysis of the GatD/MurT enzyme-complex catalyzing lipid II amidation in *Staphylococcus aureus*. *PLoS Pathog*, 8, e1002509.
- NAKACHI, K., MATSUYAMA, S., MIYAKE, S., SUGANUMA, M. & IMAI, K. 2000. Preventive effects of drinking green tea on cancer and cardiovascular disease: epidemiological evidence for multiple targeting prevention. *Biofactors*, 13, 49-54.
- NAVRATNA, V., NADIG, S., SOOD, V., PRASAD, K., ARAKERE, G. & GOPAL, B. 2010. Molecular basis for the role of *Staphylococcus aureus* penicillin binding protein 4 in antimicrobial resistance. *J Bacteriol*, 192, 134-44.
- NAZ, R., BANO, A. & ILYAS, N. 2012. Antimicrobial potential of *Ricinus communis* leaf extracts in different solvents against pathogenic bacterial and fungal strains. *Asian Pac J Trop Biomed*, 2, 944-7.
- NELSON, D. & COX, M. 2000. *Lehninger principle of biochemistry*, New York, Worth.
- NEWTON, B. 1956. The properties and mode of action of the polymyxins. *J Bacteriol Rev*, 20, 14-27.
- NOBELPRIZE.ORG. 2013. *The Nobel Prize in Physiology or Medicine 1945* [Online]. Nobel Media AB. [Accessed 12 October 2013].
- OKUSHIO, K., MATSUMOTO, N., KOHRI, T., SUZUKI, M., NANJO, F. & HARA, Y. 1996. Absorption of tea catechins into rat portal vein. *Biol Pharm Bull*, 19, 326-9.
- ORWICK, M. C., JUDGE, P. J., PROCEK, J., LINDHOLM, L., GRAZIADEI, A., ENGEL, A., GRÖBNER, G. & WATTS, A. 2012. Detergent-free formation and physicochemical characterization of nanosized lipid-polymer complexes: Lipodisq. *Angew Chem Int Ed Engl*, 51, 4653-7.
- PAAU, A. S., COWLES, J. R. & ORO, J. 1977. Flow-microfluorometric analysis of *Escherichia coli*, *Rhizobium meliloti*, and *Rhizobium japonicum* at different stages of the growth cycle. *Can J Microbiol*, 23, 1165-9.
- PADDON, C. J., WESTFALL, P. J., PITERA, D. J., BENJAMIN, K., FISHER, K., MCPHEE, D., LEAVELL, M. D., TAI, A., MAIN, A., ENG, D., POLICHUK, D. R., TEOH, K. H., REED, D. W., TREYNOR, T., LENIHAN, J., FLECK, M.,

- BAJAD, S., DANG, G., DENGROVE, D., DIOLA, D., DORIN, G., ELLENS, K. W., FICKES, S., GALAZZO, J., GAUCHER, S. P., GEISTLINGER, T., HENRY, R., HEPP, M., HORNING, T., IQBAL, T., JIANG, H., KIZER, L., LIEU, B., MELIS, D., MOSS, N., REGENTIN, R., SECREST, S., TSURUTA, H., VAZQUEZ, R., WESTBLADE, L. F., XU, L., YU, M., ZHANG, Y., ZHAO, L., LIEVENSE, J., COVELLO, P. S., KEASLING, J. D., REILING, K. K., RENNINGER, N. S. & NEWMAN, J. D. 2013. High-level semi-synthetic production of the potent antimalarial artemisinin. *Nature*, 496, 528-32.
- PEREIRA, S. F., HENRIQUES, A. O., PINHO, M. G., DE LENCASTRE, H. & TOMASZ, A. 2009. Evidence for a dual role of PBP1 in the cell division and cell separation of *Staphylococcus aureus*. *Mol Microbiol*, 72, 895-904.
- PEREIRA, S. F. F., HENRIQUES, A. O., PINHO, M. G., LENCASTRE, H. D. & TOMASZ, A. 2007. Role of PBP1 in cell division of *Staphylococcus aureus*. *J Bacteriol*, 189, 3525-3531.
- PICARD, M., DAHMANE, T., GARRIGOS, M., GAURON, C., GIUSTI, F., LE MAIRE, M., POPOT, J. L. & CHAMPEIL, P. 2006. Protective and inhibitory effects of various types of amphipols on the Ca^{2+} -ATPase from sarcoplasmic reticulum: a comparative study. *Biochem*, 45, 1861-9.
- PIDDOCK, L. J. 2012. The crisis of no new antibiotics-what is the way forward? *Lancet Infect Dis*, 12, 249-53.
- PINHO, M. G., DE LENCASTRE, H. & TOMASZ, A. 2001a. An acquired and a native penicillin-binding protein cooperate in building the cell wall of drug-resistant staphylococci. *Proc Natl Acad Sci U S A*, 98, 10886-91.
- PINHO, M. G. & ERRINGTON, J. 2003. Dispersed mode of *Staphylococcus aureus* cell wall synthesis in the absence of the division machinery. *Mol Microbiol*, 50, 871-81.
- PINHO, M. G. & ERRINGTON, J. 2005. Recruitment of penicillin-binding protein PBP2 to the division site of *Staphylococcus aureus* is dependent on its transpeptidation substrates. *Mol Microbiol*, 55, 799-807.
- PINHO, M. G., FILIPE, S. R., DE LENCASTRE, H. & TOMASZ, A. 2001b. Complementation of the essential peptidoglycan transpeptidase function of penicillin-binding protein 2 (PBP2) by the drug resistance protein PBP2A in *Staphylococcus aureus*. *J Bacteriol*, 183, 6525-6531.
- PINHO, M. G., LENCASTRE, H. D. & TOMASZ, A. 2000. Cloning, characterization, and inactivation of the gene *pbpC*, encoding penicillin-binding protein 3 of *Staphylococcus aureus*. *J Bacteriol*, 182, 1074-1082.
- POMPE, T., ZSCHOCHE, S., HEROLD, N., SALCHERT, K., GOUZY, M. F., SPERLING, C. & WERNER, C. 2003. Maleic anhydride copolymers--a versatile platform for molecular biosurface engineering. *Biomacromolecules*, 4, 1072-9.
- POPOT, J. L. 2010. Amphipols, nanodiscs, and fluorinated surfactants: three nonconventional approaches to studying membrane proteins in aqueous solutions. *Annu Rev Biochem*, 79, 737-75.
- PUCCI, M. J. & DOUGHERTY, T. J. 2002. Direct quantification of the numbers of individual penicillin-binding proteins per cell in *Staphylococcus aureus*. *J Bacteriol*, 184, 588-591.
- QANUNGO, S., DAS, M., HALDAR, S. & BASU, A. 2005. Epigallocatechin-3-gallate induces mitochondrial membrane depolarization and caspase-dependent apoptosis in pancreatic cancer cells. *Carcinogenesis*, 26, 958-67.
- QORONFLEH, M. W., REN, L., EMERY, D., PERR, M. & KABOORD, B. 2003. Use of immunomatrix methods to improve protein-protein interaction detection. *J Biomed Biotechnol*, 2003, 291-298.

- RADCLIFF, G. & JAROSZESKI, M. J. 1998. Basics of flow cytometry. *Methods Mol Biol*, 91, 1-24.
- RAI, D., SINGH, J. K., ROY, N. & PANDA, D. 2008. Curcumin inhibits FtsZ assembly: an attractive mechanism for its antibacterial activity. *Biochem J*, 410, 147-155.
- RAJESH, S., KNOWLES, T. & OVERDUIN, M. 2011. Production of membrane proteins without cells or detergents. *New Biotech*, 28, 250-254.
- RANSONE, L. J. 1995. Detection of protein-protein interactions by coimmunoprecipitation and dimerization. *Methods Enzymol*, 254, 491-7.
- REEVES, D. 1982. Sulphonamides and trimethoprim. *Lancet*, 2, 370-3.
- REN, L., CHANG, E., MAKKY, K., HAAS, A. L., KABOORD, B. & WALID QORONFLEH, M. 2003. Glutathione S-transferase pull-down assays using dehydrated immobilized glutathione resin. *Anal Biochem*, 322, 164-9.
- REYNOLDS, P. E. 1989. Structure, biochemistry and mechanism of action of glycopeptide antibiotics. *Eur J Clin Microbiol Infect Dis*, 8, 943-50.
- RICE-EVANS, C. A. & MILLER, N. J. 1996. Antioxidant activities of flavonoids as bioactive components of food. *Biochem Soc Trans*, 24, 790-5.
- ROHRER, S., EHLERT, K., TSCHIRSKE, M., LABISCHINSKI, H. & BERGER-BÄCHI, B. 1999. The essential *Staphylococcus aureus* gene *fmhB* is involved in the first step of peptidoglycan pentaglycine interpeptide formation. *Proc Natl Acad Sci U S A*, 96, 9351-6.
- RUEDA, S., VICENTE, M. & MINGORANCE, J. 2003. Concentration and assembly of the division ring proteins FtsZ, FtsA, and ZipA during the *Escherichia coli* cell cycle. *J Bacteriol*, 185, 3344-51.
- RUIZ, J. 2003. Mechanisms of resistance to quinolones: target alterations, decreased accumulation and DNA gyrase protection. *J Antimicrob Chemother*, 51, 1109-17.
- SALAH, N., MILLER, N. J., PAGANGA, G., TIJBURG, L., BOLWELL, G. P. & RICE-EVANS, C. 1995. Polyphenolic flavanols as scavengers of aqueous phase radicals and as chain-breaking antioxidants. *Arch Biochem Biophys*, 322, 339-46.
- SALEEM, M., NAZIR, M., ALI, M. S., HUSSAIN, H., LEE, Y. S., RIAZ, N. & JABBAR, A. 2010. Antimicrobial natural products: an update on future antibiotic drug candidates. *Nat Prod Rep*, 27, 238-54.
- SAMBROOK, J. & RUSSELL, D. W. 2006a. Fragmentation of DNA by sonication. *CSH Protoc*, 2006.
- SAMBROOK, J. & RUSSELL, D. W. 2006b. Identification of associated proteins by coimmunoprecipitation. *CSH Protoc*, 2006.
- SAMS-DODD, F. 2005. Target-based drug discovery: is something wrong? *Drug Discov Today*, 10, 139-47.
- SANDERS, C. R. & PROSSER, R. S. 1998. Bicelles: a model membrane system for all seasons? *Structure*, 6, 1227-34.
- SAUVAGE, E., KERFF, F., TERRAK, M., AYALA, J. A. & CHARLIER, P. 2008. The penicillin-binding proteins: structure and role in peptidoglycan biosynthesis. *FEMS Microbiol Rev*, 32, 234-258.
- SAÏD-SALIM, B., DUNMAN, P. M., MCALEESE, F. M., MACAPAGAL, D., MURPHY, E., MCNAMARA, P. J., ARVIDSON, S., FOSTER, T. J., PROJAN, S. J. & KREISWIRTH, B. N. 2003. Global regulation of *Staphylococcus aureus* genes by Rot. *J Bacteriol*, 185, 610-9.
- SCHATZ, A., BUGIE, E. & WAKSMAN, S. A. 1944. Streptomycin, a substance exhibiting antibiotic activity against gram-positive and gram-negative bacteria. *Exp Biol Med* 5, 66-69.

- SCHEFFERS, D. J. & PINHO, M. G. 2005. Bacterial cell wall synthesis: new insights from localization studies. *Microbiol Mol Biol Rev*, 69, 585-607.
- SCHIMERLIK, M. I. 2001. Overview of membrane protein solubilization. *Curr Protoc Neurosci*, Chapter 5, Unit 5.9.
- SCHLIEVERT, P. M., STRANDBERG, K. L., LIN, Y. C., PETERSON, M. L. & LEUNG, D. Y. 2010. Secreted virulence factor comparison between methicillin-resistant and methicillin-sensitive *Staphylococcus aureus*, and its relevance to atopic dermatitis. *J Allergy Clin Immunol*, 125, 39-49.
- SCHMID, E. E. 1971. The macrolide group of antibiotics. Mode of action. *Antibiot Chemother (1971)*, 17, 52-66.
- SCHNAPPINGER, D. & HILLEN, W. 1996. Tetracyclines: antibiotic action, uptake, and resistance mechanisms. *Arch Microbiol*, 165, 359-69.
- SCHNEIDER, T., SENN, M. M., BERGER-BÄCHI, B., TOSSI, A., SAHL, H. G. & WIEDEMANN, I. 2004. *In vitro* assembly of a complete, pentaglycine interpeptide bridge containing cell wall precursor (lipid II-Gly5) of *Staphylococcus aureus*. *Mol Microbiol*, 53, 675-85.
- SCHÄGGER, H. 2006. Tricine-SDS-PAGE. *Nat Prot*, 1, 16-22.
- SCHÄGGER, H. & VON JAGOW, G. 1987. Tricine-sodium dodecyl sulfate-polyacrylamide gel electrophoresis for the separation of proteins in the range from 1 to 100 kDa. *Anal Biochem*, 166, 368-79.
- SEDDON, A. M., CURNOW, P. & BOOTH, P. J. 2004. Membrane proteins, lipids and detergents: not just a soap opera. *Biochim Biophys Acta*, 1666, 105-17.
- SEDDON, A. M., LORCH, M., CES, O., TEMPLER, R. H., MACRAE, F. & BOOTH, P. J. 2008. Phosphatidylglycerol lipids enhance folding of an alpha helical membrane protein. *J Mol Biol*, 380, 548-56.
- SELIGMAN, S. & HEWITT, W. 1966. *Antimicrob Agents Chemother*, 387-391.
- SHAPIRO, A. L., VIÑUELA, E. & MAIZEL, J. V. 1967. Molecular weight estimation of polypeptide chains by electrophoresis in SDS-polyacrylamide gels. *Biochem Biophys Res Commun*, 28, 815-20.
- SHAW, A. W., MCLEAN, M. A. & SLIGAR, S. G. 2004. Phospholipid phase transitions in homogeneous nanometer scale bilayer discs. *FEBS Lett*, 556, 260-4.
- SHAW, D. 1998. Risks or remedies? Safety aspects of herbal remedies in the UK. *J R Soc Med*, 91, 294-6.
- SHI, Y., ULLRICH, S. J., ZHANG, J., CONNOLLY, K., GRZEGORZEWSKI, K. J., BARBER, M. C., WANG, W., WATHEN, K., HODGE, V., FISHER, C. L., OLSEN, H., RUBEN, S. M., KNYAZEY, I., CHO, Y. H., KAO, V., WILKINSON, K. A., CARRELL, J. A. & EBNER, R. 2000. A novel cytokine receptor-ligand pair. Identification, molecular characterization, and *in vivo* immunomodulatory activity. *J Biol Chem*, 275, 19167-76.
- SHORT, S. A. & WHITE, D. C. 1971. Metabolism of phosphatidylglycerol, lysylphosphatidylglycerol, and cardiolipin of *Staphylococcus aureus*. *J Bacteriol*, 108, 219-26.
- SIEPRAWSKA-LUPA, M., MYDEL, P., KRAWCZYK, K., WÓJCIK, K., PUKLO, M., LUPA, B., SUDER, P., SILBERRING, J., REED, M., POHL, J., SHAFER, W., MCALEESE, F., FOSTER, T., TRAVIS, J. & POTEMPA, J. 2004. Degradation of human antimicrobial peptide LL-37 by *Staphylococcus aureus*-derived proteinases. *Antimicrob Agents Chemother*, 48, 4673-9.
- SIERADZKI, K., PINHO, M. G. & TOMASZ, A. 1999. Inactivated pbp4 in highly glycopeptide-resistant laboratory mutants of *Staphylococcus aureus*. *J Biol Chem*, 274, 18942-6.

- SIES, H. 1991. Oxidative stress: from basic research to clinical application. *Am J Med*, 91, 31S-38S.
- SIMON, M. J. & DAY, R. A. 2000. Improved resolution of hydrophobic penicillin-binding proteins and their covalently linked complexes on a modified C18 reversed phase column. *Anal Lett*, 33, 861-867.
- SINGH, J. K., MAKDE, R. D., KUMAR, V. & PANDA, D. 2007. A membrane protein, EzrA, regulates assembly dynamics of FtsZ by interacting with the C-terminal tail of FtsZ. *Biochem*, 46, 11013-11022.
- SMITH, E. C., KAATZ, G. W., SEO, S. M., WAREHAM, N., WILLIAMSON, E. M. & GIBBONS, S. 2007. The phenolic diterpene totarol inhibits multidrug efflux pump activity in *Staphylococcus aureus*. *Antimicrob Agents Chemother*, 51, 4480-3.
- SMITH, P. K., KROHN, R. I., HERMANSON, G. T., MALLIA, A. K., GARTNER, F. H., PROVENZANO, M. D., FUJIMOTO, E. K., GOEKE, N. M., OLSON, B. J. & KLENK, D. C. 1985. Measurement of protein using bicinchoninic acid. *Anal Biochem*, 150, 76-85.
- SMITH, S. M. 2011. Strategies for the purification of membrane proteins. *Methods Mol Biol*, 681, 485-96.
- SOBRAL, R. G., LUDOVIC, A. M., GARDETE, S., TABELI, K., DE LENCASTRE, H. & TOMASZ, A. 2003. Normally functioning murF is essential for the optimal expression of methicillin resistance in *Staphylococcus aureus*. *Microb Drug Resist*, 9, 231-41.
- SOE, W. M., TZER PIN LIN, R., CHU SING LIM, L., SAKHARKAR, K. R. & SAKHARKAR, M. K. 2010. *In vitro* drug interactions of gallates with antibiotics in *Staphylococcus aureus*. *Front Biosci (Elite Ed.)*, 2, 668-72.
- SONG, J. M., LEE, K. H. & SEONG, B. L. 2005. Antiviral effect of catechins in green tea on influenza virus. *Antiviral Res*, 68, 66-74.
- SPEZIALE, P., PIETROCOLA, G., RINDI, S., PROVENZANO, M., PROVENZA, G., DI POTO, A., VISAI, L. & ARCIOLA, C. R. 2009. Structural and functional role of *Staphylococcus aureus* surface components recognizing adhesive matrix molecules of the host. *Future Microbiol*, 4, 1337-52.
- SPINELLA, F., ROSANÒ, L., DI CASTRO, V., DECANDIA, S., ALBINI, A., NICOTRA, M. R., NATALI, P. G. & BAGNATO, A. 2006. Green tea polyphenol epigallocatechin-3-gallate inhibits the endothelin axis and downstream signaling pathways in ovarian carcinoma. *Mol Cancer Ther*, 5, 1483-92.
- SPINK, W. W. & FERRIS, V. 1947. Penicillin-resistant staphylococci: mechanisms involved in the development of resistance. *J Clin Invest*, 26, 379-93.
- STAPLETON, P. D., SHAH, S., ANDERSON, J. C., HARA, Y., HAMILTON-MILLER, J. M. & TAYLOR, P. W. 2004. Modulation of beta-lactam resistance in *Staphylococcus aureus* by catechins and gallates. *Int J Antimicrob Agents*, 23, 462-7.
- STAPLETON, P. D., SHAH, S., EHLERT, K., HARA, Y. & TAYLOR, P. W. 2007. The beta-lactam-resistance modifier (-)-epicatechin gallate alters the architecture of the cell wall of *Staphylococcus aureus*. *Microbiol*, 153, 11.
- STAPLETON, P. D., SHAH, S., HARA, Y. & TAYLOR, P. W. 2006. Potentiation of Catechin Gallate-Mediated Sensitization of *Staphylococcus aureus* to Oxacillin by Nongalloylated Catechins. *Antimicrob Agents Chemother*, 50, 752-755.
- STAPLETON, P. D. & TAYLOR, P. W. 2002. Methicillin resistance in *Staphylococcus aureus* : mechanisms and modulation. *Sci Prog.*, 85, 57-72.

- STEELE, V. R., BOTTOMLEY, A. L., GARCIA-LARA, J., KASTURIARACHCHI, J. & FOSTER, S. J. 2011. Multiple essential roles for Ezra in cell division of *Staphylococcus aureus*. *Mol Microb*, 1365-2958.
- STEEN, H. B. 2000. Flow cytometry of bacteria: glimpses from the past with a view to the future. *J Microbiol Methods*, 42, 65-74.
- STEENBERGEN, J. N., ALDER, J., THORNE, G. M. & TALLY, F. P. 2005. Daptomycin: a lipopeptide antibiotic for the treatment of serious Gram-positive infections. *J Antimicrob Chemother*, 55, 283-8.
- STOICOV, C., SAFFARI, R. & HOUGHTON, J. 2009. Green tea inhibits *Helicobacter* growth *in vivo* and *in vitro*. *Int J Antimicrob Agents*, 33, 473-8.
- STRANDÉN, A. M., EHLERT, K., LABISCHINSKI, H. & BERGER-BÄCHI, B. 1997. Cell wall monoglycine cross-bridges and methicillin hypersusceptibility in a femAB null mutant of methicillin-resistant *Staphylococcus aureus*. *J Bacteriol*, 179, 9-16.
- SUDANO ROCCARO, A., BLANCO, A. R., GIULIANO, F., RUSCIANO, D. & ENEA, V. 2004. Epigallocatechin-gallate enhances the activity of tetracycline in staphylococci by inhibiting its efflux from bacterial cells. *Antimicrob Agents Chemother*, 48, 1968-73.
- SUGINO, A., HIGGINS, N. P., BROWN, P. O., PEEBLES, C. L. & COZZARELLI, N. R. 1978. Energy coupling in DNA gyrase and the mechanism of action of novobiocin. *Proc Natl Acad Sci U S A*, 75, 4838-42.
- SUNG, H., NAH, J., CHUN, S., PARK, H., YANG, S. E. & MIN, W. K. 2000. *In vivo* antioxidant effect of green tea. *Eur J Clin Nutr*, 54, 527-9.
- SUTHERLAND, A. G., ALVAREZ, J., DING, W., FOREMAN, K. W., KENNY, C. H., LABTHAVIKUL, P., MOSYAK, L., PETERSEN, P. J., RUSH, T. S., RUZIN, A., TSAO, D. H. & WHELESS, K. L. 2003. Structure-based design of carboxybiphenylindole inhibitors of the ZipA-FtsZ interaction. *Org Biomol Chem*, 1, 4138-40.
- SUTHERLAND, R. & ROLINSON, G. 1964. Activity of ampicillin *in vitro* compared with other antibiotics. *J Clin Pathol*, 17, 461-465.
- TAM, V. H., SCHILLING, A. N., VO, G., KABBARA, S., KWA, A. L., WIEDERHOLD, N. P. & LEWIS, R. E. 2005. Pharmacodynamics of polymyxin B against *Pseudomonas aeruginosa*. *Antimicrob Agents Chemother*, 49, 3624-30.
- TAN, C. M., THERIEN, A. G., LU, J., LEE, S. H., CARON, A., GILL, C. J., LEBEAU-JACOB, C., BENTON-PERDOMO, L., MONTEIRO, J. M., PEREIRA, P. M., ELSÉN, N. L., WU, J., DESCHAMPS, K., PETCU, M., WONG, S., DAIGNEAULT, E., KRAMER, S., LIANG, L., MAXWELL, E., CLAVEAU, D., VAILLANCOURT, J., SKOREY, K., TAM, J., WANG, H., MEREDITH, T. C., SILLAOTS, S., WANG-JARANTOW, L., RAMTOHUL, Y., LANGLOIS, E., LANDRY, F., REID, J. C., PARTHASARATHY, G., SHARMA, S., BARYSHNIKOVA, A., LUMB, K. J., PINHO, M. G., SOISSON, S. M. & ROEMER, T. 2012. Restoring methicillin-resistant *Staphylococcus aureus* susceptibility to beta-lactam antibiotics. *Sci Transl Med*, 4, 126ra35.
- TAYLOR, P. W. 2013. Alternative natural sources for a new generation of antibacterial agents. *Int J Antimicrob Agents*, 42, 195-201.
- TAYLOR, P. W., HAMILTON-MILLER, J. M. T. & STAPLETON, P. D. 2005. Antimicrobial properties of green tea catechins. *Food Sci Technol Bull.*, 2, 10.
- TEGOS, G., STERMITZ, F. R., LOMOVSKAYA, O. & LEWIS, K. 2002. Multidrug pump inhibitors uncover remarkable activity of plant antimicrobials. *Antimicrob Agents Chemother*, 46, 3133-41.

- TENOVER, F. C. 2006. Mechanisms of antimicrobial resistance in bacteria. *Am J Med*, 119, S3-10; discussion S62-70.
- TONGE, S. 2006. *The compositions compromising a lipid and copolymer styrene maleic acid*. UK patent application PCT/GB2006/050134.
- TONGE, S. R. & TIGHE, B. J. 2001. Responsive hydrophobically associating polymers: a review of structure and properties. *Adv Drug Deliv Rev*, 53, 109-22.
- TOWBIN, H., STAEBELIN, T. & GORDON, J. 1979. Electrophoretic transfer of proteins from polyacrylamide gels to nitrocellulose sheets: procedure and some applications. *Proc Natl Acad Sci U S A*, 76, 4350-4.
- TURNER, R. D., RATCLIFFE, E. C., WHEELER, R., GOLESTANIAN, R., HOBBS, J. K. & FOSTER, S. J. 2010. Peptidoglycan architecture can specify division planes in *Staphylococcus aureus*. *Nat Commun*, 1, 1-9.
- TZAGOLOFF, H. & NOVICK, R. 1977. Geometry of cell division in *Staphylococcus aureus*. *J Bacteriol*, 129, 343-50.
- URH, M., SIMPSON, D. & ZHAO, K. 2009. Affinity chromatography: general methods. *Methods Enzymol*, 463, 417-38.
- VAINIO, H. & HEMMINKI, K. 1989. Epidemiological and experimental applications to occupational cancer prevention. *J UOEH*, 11 Suppl, 323-45.
- VAN DER VLIST, E. J., NOLTE-T HOEN, E. N., STOORVOGEL, W., ARKESTEIJN, G. J. & WAUBEN, M. H. 2012. Fluorescent labeling of nano-sized vesicles released by cells and subsequent quantitative and qualitative analysis by high-resolution flow cytometry. *Nat Protoc*, 7, 1311-26.
- VAN JAGOW, G., LINK, T. & SCHAGER, H. 1994. Purification strategies for membrane proteins. In: VON JAGOW, G. & SCHAGER, H. (eds.) *A practical guide to membrane protein purification*. San Diego, USA: Academic.
- VASILESCU, J., GUO, X. & KAST, J. 2004. Identification of protein-protein interactions using *in vivo* cross-linking and mass spectrometry. *Proteomics*, 4, 3845-54.
- VOLLMER, W. 2006. The prokaryotic cytoskeleton: a putative target for inhibitors and antibiotics. *Appl Microbiol Biotechnol*, 73, 37-47.
- VON EIFF, C., BECKER, K., MACHKA, K., STAMMER, H. & PETERS, G. 2001. Nasal carriage as a source of *Staphylococcus aureus* bacteremia. *New Eng J Med*, 344, 11-16.
- VOYICH, J. M., BRAUGHTON, K. R., STURDEVANT, D. E., WHITNEY, A. R., SAÏD-SALIM, B., PORCELLA, S. F., LONG, R. D., DORWARD, D. W., GARDNER, D. J., KREISWIRTH, B. N., MUSSER, J. M. & DELEO, F. R. 2005. Insights into mechanisms used by *Staphylococcus aureus* to avoid destruction by human neutrophils. *J Immunol*, 175, 3907-19.
- WALEY, S. G. 1988. Beta-lactamases: a major cause of antibiotic resistance. *Sci Prog*, 72, 579-97.
- WANG, Y. & HO, C. T. 2009. Polyphenolic chemistry of tea and coffee: a century of progress. *J Agric Food Chem*, 57, 8109-14.
- WATKINS, R. R., DAVID, M. Z. & SALATA, R. A. 2012. Current concepts on the virulence mechanisms of methicillin-resistant *Staphylococcus aureus*. *J Med Microbiol*, 61, 1179-93.
- WHITE, S. H. 2004. The progress of membrane protein structure determination. *Protein Sci*, 13, 1948-9.
- WILKINSON, B. J. 1997. The staphylococci in human disease. In: CROSSLEY, K. B. & ARCHER, G. L. (eds.) *Biology*. New York, N.Y.: Churchill Livingstone.
- WILLEY, J. M., SHERWOOD, L. M. & WOOLVERTON, C. J. 2008. *Prescott, Harley, and Klein's Microbiology*, New York, NY, McGraw-Hill Companies, Inc.

- WILLIAMS, A. H. & GRÜNEBERG, R. N. 1984. Teicoplanin. *J Antimicrob Chemother*, 14, 441-5.
- WILLIAMS, N. E. 2000. Immunoprecipitation procedures. *Methods Cell Biol*, 62, 449-53.
- WISE, R., ANDREWS, J. & BEDFORD, K. 1978. *In vitro* study of clavulanic acid in combination with penicillin, amoxycillin, and carbenicillin. *Antimicrob Agents Chemother*, 13, 389-393.
- WORKE, E. 1957. Biochemistry of the bacterial cell wall. *Nature*, 179, 841-847.
- WHO. *Patient safety: facts and figures* [Online]. Available: <http://www.euro.who.int/en/what-we-do/health-topics/Health-systems/patient-safety/facts-and-figures> [Accessed 29th May 2013].
- WHO. *WHO mortality database* [Online]. Available: <http://www.who.int/topics/en/index.html> [Accessed 04/07/2013 2013].
- WHO. 2011. *World health day* [Online]. Available: <http://www.who.int/world-health-day/2011/en/> [Accessed 15 May 2013].
- WHO. 2013. *Antimicrobial resistance fact sheet 194* [Online]. Available: <http://www.who.int/mediacentre/factsheets/fs194/en/> [Accessed 25th November 2013].
- YAM, T. S., HAMILTON-MILLER, J. M. & SHAH, S. 1998. The effect of a component of tea (*Camellia sinensis*) on methicillin resistance, PBP2' synthesis, and beta-lactamase production in *Staphylococcus aureus*. *J Antimicrob Chemother*, 42, 211-6.
- YAMAOKA, T. 2007. The bactericidal effects of anti-MRSA agents with rifampicin and sulfamethoxazole-trimethoprim against intracellular phagocytized MRSA. *J Infect Chemother*, 13, 141-6.
- YAMAUCHI, J., KAZIRO, Y. & ITOH, H. 1995. Carboxyl terminal of G protein beta subunit is required for association with gamma subunit. *Biochem Biophys Res Commun*, 214, 694-700.
- YANG, W., STEEN, H. & FREEMAN, M. R. 2008. Proteomic approaches to the analysis of multiprotein signaling complexes. *Proteomics*, 8, 832-51.
- YANG, Y., BHACHECH, N. & BUSH, K. 1995. Biochemical comparison of imipenem, meropenem and biapenem: permeability, binding to penicillin-binding proteins, and stability to hydrolysis by beta-lactamases. *J Antimicrob Chemother*, 35, 75-84.
- YARWOOD, J. M. & SCHLIEVERT, P. M. 2003. Quorum sensing in *Staphylococcus* infections. *J Clin Invest*, 112, 1620-5.
- YOSHIDA, A., HIROOKA, Y., SUGATA, Y., NITTA, M., MANABE, T., IDO, S., MURAKAMI, K., SAHA, R. K., SUZUKI, T., OHSHIMA, M., ITOH, K., SHIMIZU, K., OKU, N., FURUTA, T., ASAKAWA, T., WAKIMOTO, T. & KAN, T. 2010. Concise synthesis of catechin probes enabling analysis and imaging of EGCg. *Chem Commun*, 47, 1794-1796.
- ZAPUN, A., CONTRERAS-MARTEL, C. & VERNET, T. 2008. Penicillin-binding proteins and beta-lactam resistance. *FEMS Microbiol Rev*, 32, 361-385.
- ZELLER, J. L., BURKE, A. E. & GLASS, R. M. 2007. JAMA patient page. MRSA infections. *JAMA*, 298, 1826.
- ZHAO, W. H., HU, Z. Q., OKUBO, S., HARA, Y. & SHIMAMURA, T. 2001. Mechanism of synergy between epigallocatechin gallate and beta-lactams against methicillin-resistant *Staphylococcus aureus*. *Antimicrob Agents Chemo*, 45, 1737-1742.
- ZHOU, Y., LAU, F. W., NAULI, S., YANG, D. & BOWIE, J. U. 2001. Inactivation mechanism of the membrane protein diacylglycerol kinase in detergent solution. *Protein Sci*, 10, 378-83.

- ZIGLAM, H. M., ELLIOTT, I., WILSON, V., HILL, K. & NATHWANI, D. 2005. Clinical audit of linezolid use in a large teaching hospital. *J Antimicrob Chemother*, 56, 423-6.